Conifer tree species differ in traits, growth, and drought resilience

Yanjun Song
宋彦君

PROPOSITIONS

1. Drought-resilient species are important for designing climate-smart forests, since high drought-resilience reduces tree mortality (this thesis).

2. In mild maritime conditions growth resilience to drought is explained by carbon-related leaf economic traits rather than by hydraulic-related stem traits (this thesis).

3. Asking what, how and why is the best approach to understand and do science.

4. The outcome of the peer reviewing process is highly random, as many journals have too little space and many reviewers and editors have too little time.

5. Happiness is the most important driver towards a successful scientific career.

6. The supervisors' way of thinking shapes the PhD students' way of thinking.

7. Paradoxically COVID reduces the speed of life and stress associated with travelling and commuting, but it increases the anxiety of human beings.

8. The working environment should guarantee a healthy work-life balance.

Propositions belonging to the thesis, entitled
Conifer tree species differ in traits, growth, and drought resilience

Yanjun Song
Wageningen, 11 November 2021

Conifer tree species differ in traits, growth, and drought resilience

Yanjun Song

Thesis committee

Promotors
Prof. Dr L. Poorter
Personal chair at Forest Ecology and Forest Management Group
Wageningen University & Research

Dr F. Sterck
Associate Professor, Forest Ecology and Forest Management Group
Wageningen University & Research

Other members

Prof. Dr W. Peters, Wageningen University & Research

Prof. Dr J. H. C. Cornelissen, Free University Amsterdam

Prof. Dr M. van der Maaten-Theunissen, Technische Universität Dresden, Germany

Dr J. L. Quero, University of Cordoba, Spain

This research was conducted under the auspices of the C.T. de Wit Graduate School for Production Ecology and Resource Conservation (PE&RC), the Netherlands.

Conifer tree species differ in traits, growth, and drought resilience

Yanjun Song

Thesis

submitted in fulfilment of the requirements for the degree of doctor
at Wageningen University
by the authority of the Rector Magnificus,
Prof. Dr A.P.J. Mol,
in the presence of the
Thesis Committee appointed by the Academic Board
to be defended in public
on Thursday 11 November 2021
at 11 a.m. in the Aula.

Yanjun Song
Conifer tree species differ in traits, growth, and drought resilience
176 pages.

PhD thesis, Wageningen University, Wageningen, the Netherlands (2021)
With references and English summary

ISBN : 978-94-6395-977-3
DOI : https://doi.org/10.18174/553576

Contents

CHAPTER 1

1

General introduction

1.1 Conifer species and climate change

Conifer species are woody cone-bearing gymnosperms belonging to a very old lineage originating >300 million years ago. They lived their golden era in the Mesozoic (250-65 million years ago) when they dominated together with the dinosaurs (Leslie *et al.*, 2012). Conifers went in decline during the Cenozoic (<65 million years ago) when flowering Angiosperms started to radiate, displacing conifers to sub-optimal, relatively cold, dry, or nutrient-poor habitats. Although the main conifer lineages are very old, recent genetic analysis shows that most conifer species developed only 2-3 million years ago, when the effect of climatic cooling and the ice ages was strongly felt in the Northern hemisphere. Conifers currently include 8 families and 615 species, dominating large areas of the globe (Farjon, 2010). They are not only widely distributed in the benign, temperate zone, but also in more extreme habitats such as cold boreal and dry Mediterranean zones (Farjon & Filer, 2013). Conifer species are therefore important for the global carbon pool, timber production, and provide habitat and food for many animals (Pan *et al.*, 2011; Hämäläinen *et al.*, 2018; Davies *et al.*, 2020).

Conifers have several unique features that make them relatively drought resistant. They normally possess narrow tracheids for water transport, pits with a special torus structure that connect neighboring tracheids and can increase hydraulic safety, and needle-like leaves that reduce water loss in dry habitats and are cold tolerant in winter (Egger *et al.*, 1996; Sperry *et al.*, 2006; Delzon *et al.*, 2010). Despite their known successful adaptations to dry conditions, increased drought events endanger tree growth and survival, leading to a large loss of productivity, forest carbon mitigation and future timber supply in temperate and boreal zones (Ciais *et al.*, 2005b; Nabuurs *et al.*, 2018; DeSoto *et al.*, 2020). Hence, It is important and timely to study how conifers respond to drought events and explore the underlying mechanisms. New insights are needed to explain how mechanisms contribute to reduced growth, resilience or increased mortality. This will allow to better predict the productivity, survival and carbon pool of conifer trees and temperate and boreal forests under climate change. Here I use a 50-year-old common garden experiment in the Netherlands to assess how 28 conifer species from the Northern hemisphere respond to climatic variation in terms of growth and drought resilience, and quantified multiple functional traits to explain the different responses of tree species.

1.2 Climatic drivers of growth variation

Climate change not only leads to extreme drought events, but also increased late spring frosts (Inouye, 2000). Climatic extremes such as cold winters, spring frosts and summer droughts may reduce species growth and productivity (D'Orangeville *et al.*, 2016; Vitasse *et al.*, 2019). Generally, spring frosts result in reduced stem growth due to the damaged leaves during

budbreak and leaf emergency (Vitra *et al.*, 2017). High winter temperature may however promote the growth of evergreen conifer species, since it allows for higher photosynthesis and advances the timing of stem cambial growth (Rahman *et al.*, 2020). In the summer, a high temperature in combination with low precipitation may lead to increased water shortage and reduce growth, except for extremely cold and humid areas where increased summer temperatures have a positive, rather than a negative effect on growth (Klesse *et al.*, 2018). Species growth sensitivity to climate therefore varies along climatic gradients, but such sensitivity can be confounded by site differences in, for example, climate and soil (Bose *et al.*, 2020). In my study I take advantage of a common garden experiment, which allows me to focus on species differences in growth responses to climate variation over time. Such studies are useful because they may help to select conifer species that can combine high productivity with high resilience, and thus cope with climate change.

1.3 Analyzing drought resilience

Drought and drought resilience

Global warming leads to an increase in the frequency and intensity of droughts. A drought is defined as a stochastic natural hazard due to an anomaly deficit of water(Lloyd-Hughes, 2014). It is difficult to quantify drought since drought periods differ in duration, frequency and severity (Zargar *et al.*, 2011; Gao *et al.*, 2018). The stem growth resilience of trees to drought is defined as the ability to maintain growth during the drought (resistance) and to regrow after a drought (recovery) (Depardieu *et al.*, 2020). Drought resilience thus consists of two underlying components; drought resistance and drought recovery (Lloret *et al.*, 2011). Species can thus be drought resilient in two contrasting ways: they either have a high resistance but low recovery or high recovery but low resistance (Gazol *et al.*, 2017). From this, a trade-off is expected between the resistance and recovery across resilient species. However, not all species may be resilient, since an increase in drought can lead to reduced growth and/or reduced recovery, and thus reducing species drought resilience (DeSoto *et al.*, 2020). Evaluating the influences of the different drought dimensions (e.g. timing, severity and length) on resilience is required to better predict the productivity and carbon storage in conifer forests in the future. In this thesis, I aim to quantify the effects of such drought dimensions on tree resilience of multiple species, which has rarely been done before.

Hydraulic traits

Tree hydraulics is fundamental to understand tree responses to drought, and has been received a lot of attention over recent years (e.g., Choat *et al.,* 2018 and Hammond *et al.,*

2019). Tree hydraulics refers to the traits regarding hydraulic architecture, i.e., the xylem structure that is responsible for the water transport in plants (Tyree & Ewers, 1991; Markesteijn *et al.*, 2011). Important hydraulic traits are the xylem specific hydraulic conductivity (Ks) and cavitation resistance, the xylem pressure when 50% of hydraulic conductivity is lost (P_{50}). Another hydraulic safety measure in the leaves is given by the minimum water potential (Ψ_{min}) that plants experience over the year in their habitat. Conceptually, the better proxy for hydraulic safety is given by the so-called hydraulic safety margin (HSM), which is the difference between Ψ_{min} and P_{50}. These hydraulic traits are not only considered predictors for drought resistance, but also for growth since water transport in the xylem will be impaired when leaf water potential falls below P_{50} or Ψ_{min} (Choat *et al.*, 2012). When trees avoid such hydraulic failure risks by closing their stomata, reducing water loss, then that also result in loss of carbon gain with potentially negative implications for growth (Poorter *et al.*, 2010).

HSM is expected to regulate drought resilience, including broadleaf and needleleaf trees (Anderegg, WR *et al.*, 2018). There are however only few studies that used hydraulic traits to directly predict the drought resilience of conifer species. One study found that P_{50} explained drought resistance of conifer species: species with more negative P_{50} were more drought resistant (Li *et al.*, 2020). However, another study quantified growth sensitivity with tree ring index to indicate drought tolerance and found that P_{50} was not related to drought resistance (D'Orangeville *et al.*, 2018). Thus, the role of hydraulic traits as drivers of drought resilience is still controversial and disputed. In addition, these studies have focused on broad-scale geographic patterns and species-level traits, and they used different methods for quantifying drought resilience, which makes it difficult to obtain a general conclusion. In addition, these contrasting results are possibly explained by mixing sites and species effects in different ways, since they focus on tree responses across climate gradients. Here we argue that a common garden experiment is important and timely to assess species difference in drought resilience and hydraulic traits, because environmental effects are controlled for. In my study, I will check whether hydraulic traits can predict species drought resilience for 20 conifer species in a common garden experiment.

1.4 The underlying hydraulic mechanisms

Conifer species with wide tracheids and wide pits that connect adjacent tracheids have a more efficient water transport (Woodruff *et al.*, 2008), but this may come at the cost of hydraulic safety (i.e., cavitation resistance) (Pittermann *et al.*, 2006a), since species with wide tracheids and pits are more vulnerable to freeze-thaw induced cavitation and drought-induced air seeding that leads to cavitation. The mechanisms of drought-induced cavitation resistance are

related to the structure of pits (Fig. 1.2d). Pits are membranes that occur in the cell walls of conduits, separating conduits and permitting water transport from one conduit to the next through the pit pore (i.e., aperture), but limiting the movement of gas and pathogens (Choat *et al.*, 2006). Compared to broadleaf species, conifer species usually have a unique pit structure, consisting of a lens-shaped impermeable torus that is suspended by a flexible margo. The flexible margo enables the torus to tightly seal the aperture against the pit border under tension, thus acting as a safety valve and avoiding the spread of drought-induced cavitation (Delzon *et al.*, 2010). P_{50} is most widely used to characterize the xylem vulnerability to cavitation of tree species because 50% loss of hydraulic conductivity may eventually result in tree death (Tyree & Ewers, 1991; Brodribb & Cochard, 2009; Gauthey *et al.*, 2020). A previous study found that high margo flexibility and torus overlap increased the valve effect and pit sealing. This valve effect was the best prediction for P_{50} of 40 conifers across a large area in North America, Europe and Australia that covered varying environmental conditions from wet to dry habitats (Delzon *et al.*, 2010). Hence, we lack studies that quantify and test for the combined effects of the pit and tracheid traits on species difference in hydraulic performance. Moreover, it is not yet clear whether there exists a trade-off between hydraulic efficiency and cavitation resistance (Larter *et al.*, 2017), because cavitation resistance may be mainly determined by pit sealing (Delzon *et al.*, 2010) whereas hydraulic efficiency is thought to be mainly determined by tracheid size and density (Sterck *et al.*, 2008).

1.5 Trait strategies and drought responses

Leaf and stem traits

Functional traits are defined as morphological, physiological, or phenological traits that impact tree species performance regarding growth, survival and reproduction (Violle *et al.*, 2007). Studying functional traits provides insights and allows more mechanistic predictions on how species may respond to climate change in terms of growth and survival (Sterck *et al.*, 2014). Although hydraulic stem traits are important, it is the hydraulic integration between leaf and stem traits that determine water transport, use and loss, and ultimately, carbon gain (Choat *et al.*, 2018). Functional traits are well known to predict tree species performance, and traits with divergent functions can be described as the plant economics spectrum (Reich, 2014). The leaf economics spectrum (LES) has been frequently used to reveal carbon balance components of plants (i.e., rapid carbon acqusition vs great carbon investment) (Wright *et al.*, 2004; Edwards *et al.*, 2014). The LES typically runs from a “live fast, die young” strategy (i.e., large specific leaf area, short leaf lifespan, high nutrient concentrations and photosynthetic rate) to “heavy-investment-with-long-time-to-obtain-returns” strategy (i.e, small specific leaf area, long leaf lifespan, low nutrient concentrations and photosynthetic rate). Similarly, there is also

empirical support for a wood economics spectrum with hydraulic traits that are related to plant growth and survival (Chave *et al.*, 2009; Poorter *et al.*, 2010).

The integration of leaf and stem traits is considered a good predictor for species whole-plant performance (Wright *et al.*, 2004; Chave *et al.*, 2009; Díaz *et al.*, 2016). The associations of leaf and stem traits have been studied in different biomes, and they seem to be more associated in temperate areas than in tropical and subtropical areas (Baraloto *et al.*, 2010; Kawai & Okada, 2019). However, these studies on multiple species (>10-20 species) focused on angiosperms, and comparisons are still scarce for conifer species. It thus remains unclear to what extent traits describing the function of different organs (e.g., leaf and stem) are coordinated and cause trade-offs across conifer species. Moreover, the implication of such spectra for whole-plant growth and survival of conifers remains an open question (Reich, 2014; Rosas Torrent, 2019).

Traits and tree strategies

A surge of trait-based approaches have been used to predict tree species growth and survival strategy, capturing core differences in the strategies plants use to acquire and invest resources (Westoby *et al.*, 2002; Chave *et al.*, 2009; Reich, 2014; Falster *et al.*, 2018). Traits related to fast carbon gain, water transport and soft tissue structure contribute to the more rapid growth of species (Reich, 2014). Specifically, leaves with high specific leaf area, stomatal conductance and nutrient concentrations, but low leaf dry matter content and short leaf lifespans may contribute to a higher growth rate (Sterck *et al.*, 2006; Kitajima & Poorter, 2010), since these traits reflect a high capacity of light capture, carbon assimilation, but at the cost of tissues construction. Stems with high hydraulic conductivity and softwood usually consist of large pits and tracheids, favoring high growth rates in conifer species but at the expense of drought tolerance (Pittermann *et al.*, 2006a; Chave *et al.*, 2009).

Yet, these studies predicted the growth potential in terms of carbon assimilation in leaves and the survival strategy in terms of xylem cavitation resistance. There are hardly studies that show how such traits simultaneously affect the stem growth of conifer species (Martínez-Vilalta *et al.*, 2010), and some of these generalizations may be premature. In addition, strong relationships between tissue traits and plant performance have been found for seedlings, but weaker relationships have been found for adult trees, probably because larger plants are more robust, and plant size overrules more subtle contributions of tissue traits (Poorter *et al.*, 2008). Dendrochronology provides an ideal tool to quantify both species growth potential and drought resilience and its two components drought resistance and recovery (Vitasse *et al.*, 2019). In this study, I aim to quantify multiple traits as well as stem growth potential and drought resilience to assess how these traits can explain species

differences in stem growth and resilience to drought. This is a first attempt to thus explain species growth performance from tree rings related to multiple traits (43) of 20 tree species responding to the same temporal climate variation. I can thus also test the prediction that species with trait values related to fast growth will be less tolerant to drought, since species maintain fast growth at the cost of hydraulic safety and tissue construction (Reich, 2014). This study can provide a solid foundation to use functional traits for understanding and modeling growth and survival across conifer species.

1.6 Objectives

This PhD thesis aims to understand the growth response of conifer tree species to climatic variation and drought, and explains the underlying mechanisms using functional traits. A 50-year-old common garden experiment was used, where 28 conifer species from the Northern hemisphere are growing under the same climatic and soil conditions. Such a common garden experiment is ideal to compare tree species, as it avoids the confounding effects of environment and acclimation.

1.7 Thesis outline

This thesis consists of six chapters, including a general introduction (Chapter 1), four main chapters (Chapter 2-5, Fig. 1.1, 1.2) and a general discussion (Chapter 6):

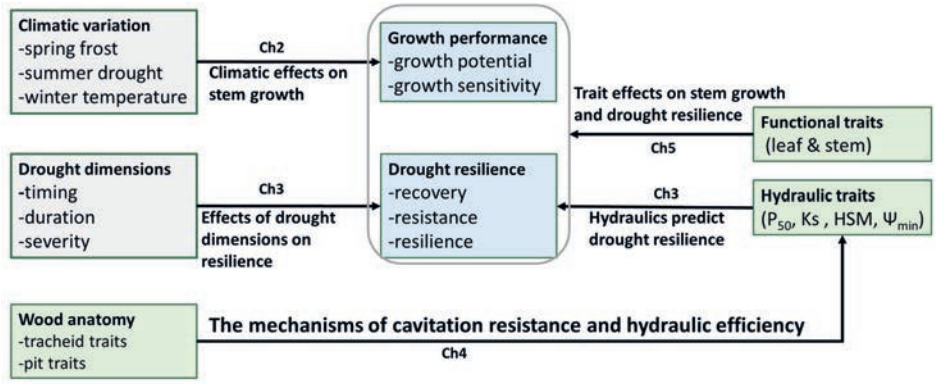

Fig. 1.1 The conceptual diagram of this thesis. It indicates the connections between the questions addressed in the different chapters: how climate affects stem growth (Ch2) and drought resilience (Ch3) and the underlying hydraulic mechanisms (Ch3 & Ch4), and how functional traits affect the growth and drought resilience of conifer species (Ch5). Climatic factors are shown in grey, stem growth and resilience are shown in light blue, and functional traits are shown in light green.

Chapter 2: Climatic effects on stem growth

This chapter addresses the questions how climatic variation affects the stem growth of conifer species, and to what extent the growth potential and sensitivity are phylogenetically controlled (Fig. 1.1,1.2a,b). Using a dendrochronological approach I quantified growth potential and growth sensitivity for 19 conifer species to climate variation over 44 years. I hypothesize that spring frosts, summer droughts and cold winters will reduce conifer species' growth because the late frosts can damage young leaves and buds, and the water deficits cause lower stomatal conductance. I also hypothesize that growth potential and sensitivity are weakly phylogenetically controlled because closely related conifer species are adapted to different habitats.

Chapter 3: Drought dimensions affect stem growth resilience

In this chapter I ask 1) how drought resistance and drought recovery affect drought resilience; 2) how multiple dimensions of droughts (i.e., timing, severity and duration) affect drought resistance and 3) whether hydraulic traits and growth potential can predict species drought resilience (Fig. 1.1,1.2b,c). To this end, I used a novel water-balance approach to quantify multiple dimensions of droughts and drought resilience components (resistance, recovery and resilience) for 11 identified drought years over the 44 years. I hypothesize that fast-growing species show stronger growth reductions in drought years (lower resistance) but also stronger recovery after drought years than slow-growing species. I also expect that high cavitation resistance ($|P_{50}|$) and hydraulic safety margins (HSM) favor high drought resistance because species will be more safe if their water potential during drought is far less than $|P_{50}|$ and if they can buffer drought better with high HSM. I also predict that high hydraulic conductivity increases growth and drought recovery because high conductivity contributes to high stomatal conductance, and hence high carbon assimilation.

Chapter 4: The mechanisms of cavitation resistance and hydraulic efficiency

This chapter addresses two questions, first how pit and tracheid traits determine hydraulic efficiency and cavitation resistance, and second whether there is a trade-off between hydraulic efficiency and cavitation resistance (Fig. 1.1,1.2d,e). I compare the hydraulic conductivity and cavitation resistance of 28 dominant conifer species originating from the Northern hemisphere that cover a broad range in phylogenetic and ecology diversity. I measured cavitation resistance, xylem-specific hydraulic conductivity, and wood anatomical traits in terms of pit and tracheids. I expect that hydraulic efficiency could be explained by thin cell walls, large pits and tracheids size; and that cavitation resistance would be explained by a

strong valve effect with high margo flexibility and torus overlap, because a strong valve effect could better seal the pit aperture during a drought-induced cavitation. From this, I predict that there is a trade-off between hydraulic efficiency and cavitation resistance .

Chapter 5: Traits effects on stem growth and drought resilience

Here, I aim to answer two questions: 1) how are functional traits associated with each other and 2) how do they predict the growth and drought resilience of conifer species? I measured 43 traits including leaf and stem traits (Fig. 1.1,1.2f), including traits related to leaf size and display, carbon assimilation, tissue toughness, wood anatomy, hydraulics and cavitation resistance, and pressure-volume traits. First, I predict that traits show a strategy spectrum running from conservative slow-growing species with dense tissues and high hydraulic safety to acquisitive fast-growing species with high hydraulic efficiency and carbon assimilation. Despite such trends across traits and functions, I expect that traits that are coupled to the same function are more closely correlated to one another than traits linked to other functions. Of all traits, I expect pit traits and hydraulic safety margin (HSM) to occupy the most central position in the trait network, because pit traits adjust hydraulic efficiency (via big pit aperture size) and safety (via big torus overlap due to small pit aperture size) and, hence, influence growth and survival. In addition, I predict that a larger HSM increases species ability to survive in a dry climate.

Chapter 6: General discussion

This chapter synthesizes the main results of my research and discusses how conifer tree species respond to climate change and to what extent this can be explained by species functional traits. Additionally, I provide guidelines for forest managers on how forests can be made future climate-proof, and I provide recommendations for future studies.

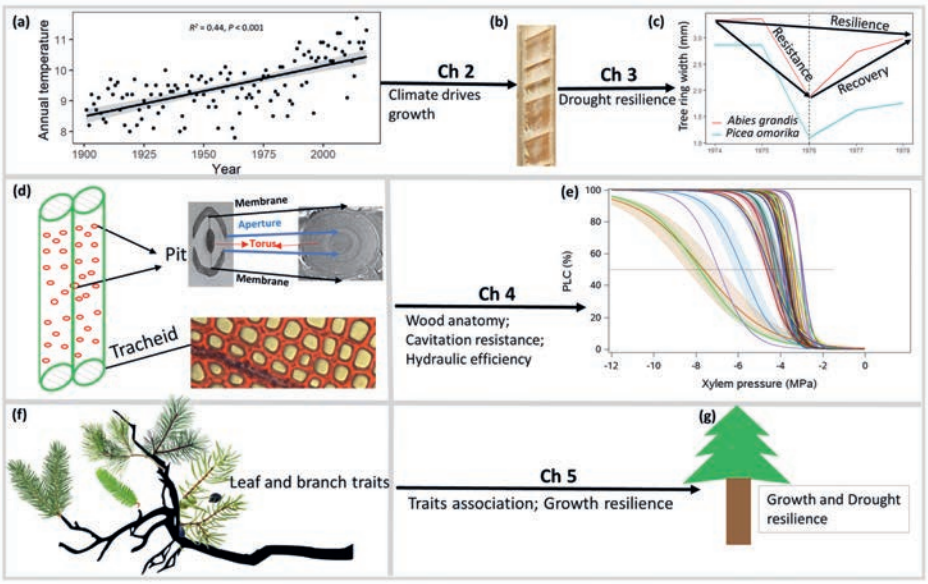

Fig. 1.2 Panel showing the concepts and framework used in this study: a) The global warming trend in the Netherlands, showing that the average annual temperature has increased from 8.7 degrees in 1900 to 11.3 degrees in 2018; b) A wood core showing annual variation in early-wood (white parts) and latewood (brown parts) of *Abies grandis* with productive years (bottom) and unproductive years (top); c) Drought resilience components consisting of resistance and recovery with the high-resilient *Abies grandis* (red) and low-resilient *Picea omorika* (blue); d) The wood anatomical structure of tracheids and pit consisting of a torus; e) Vulnerability curves indicating species difference in the percentage loss of hydraulic conductivity (PLC) with a different color; f). Leaf and stem traits collection; and g) Conifer tree with a good performance in terms of growth or survival.

1.8 Study site and species

This study is carried out in a common garden experiment, Schovenhorst (52.25° N, 5.63° E), Putten, the Netherlands (Fig. 1.3). The experiment was established in the 1960's to screen species for their potential timber productivity under maritime climatic conditions and relatively poor sandy soils that are typical for larger areas in the Netherlands. Over 30 conifer species from the Northern hemisphere were planted that had the potential to grow in the Netherlands. The species came from comparable climatic conditions as in the Netherlands (Willinge Gratama-Oudemans, 1992; de Lange & de Klein, 1998; Ellis *et al.*, 2004). The species were planted in monospecific stands to mimic natural growing conditions.

Research site. The research site has a mild maritime climate with an annual average precipitation of 830 mm y^{-1} and a mean temperature of 10.1 °C. The area is underlain by dry, loamy, sandy and nutrient-poor soils (Cornelissen *et al.,* 2012) with a low water retention capacity and a long-distance (>15 m) to the soil water table (TNO-NITG, 2020). Initially, over 30 species were selected from 3 different continents; North America, China, and Japan (Willinge Gratama-Oudemans, 1992). In this study I selected 28 conifer species from the Northern hemisphere and from different climatic origins (Fig. 1.4, 1.5; Table 1) covering a wide range of conifer species. The species covered diverse lineages, belonging to three different families, such as Pinaceae, Cupressaceae and Taxaceae. Most species were evergreen, with the exception of *Larix kaempferi*, and *Metasequoia glyptostroboides*. In 2017, the trees had attained an average stem diameter at breast height of 35.8 cm, which varied from 5.0 cm (*Taxus cuspidata*) to 86.3 cm (*Sequoiadendron giganteum*) across species.

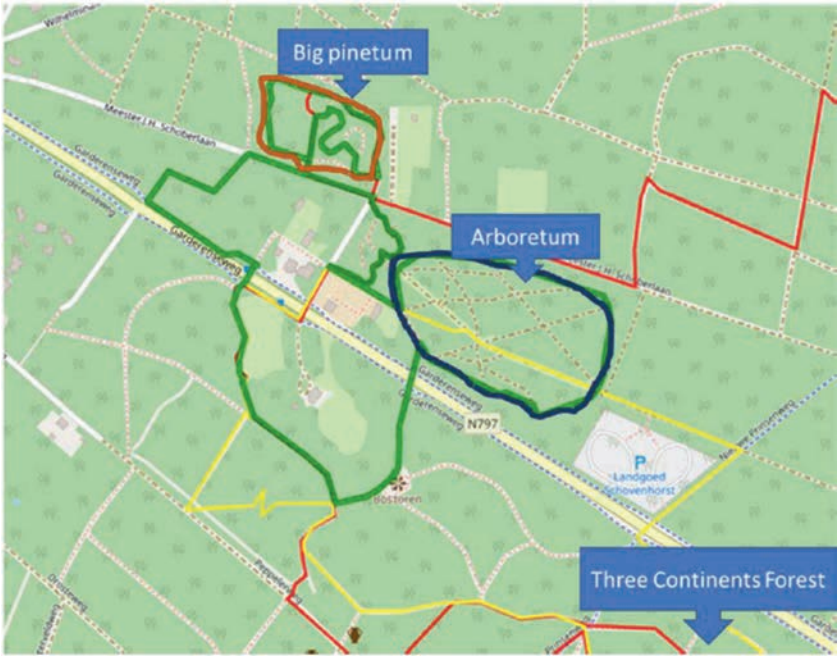

Fig. 1.3 The study area in Schovenhorst, Putten, the Netherlnads. Species were collected from three coniferous forest gardens, including Three Continents Forest, Arboretum and Big pinetum. These three coniferous forest gardens were established in 1848 to select high timber productivity of conifer species (Willinge Gratama-Oudemans, 1992) and the studied species were planted around the 1960's (Source: https://schovenhorst.nl/bomentuin/).

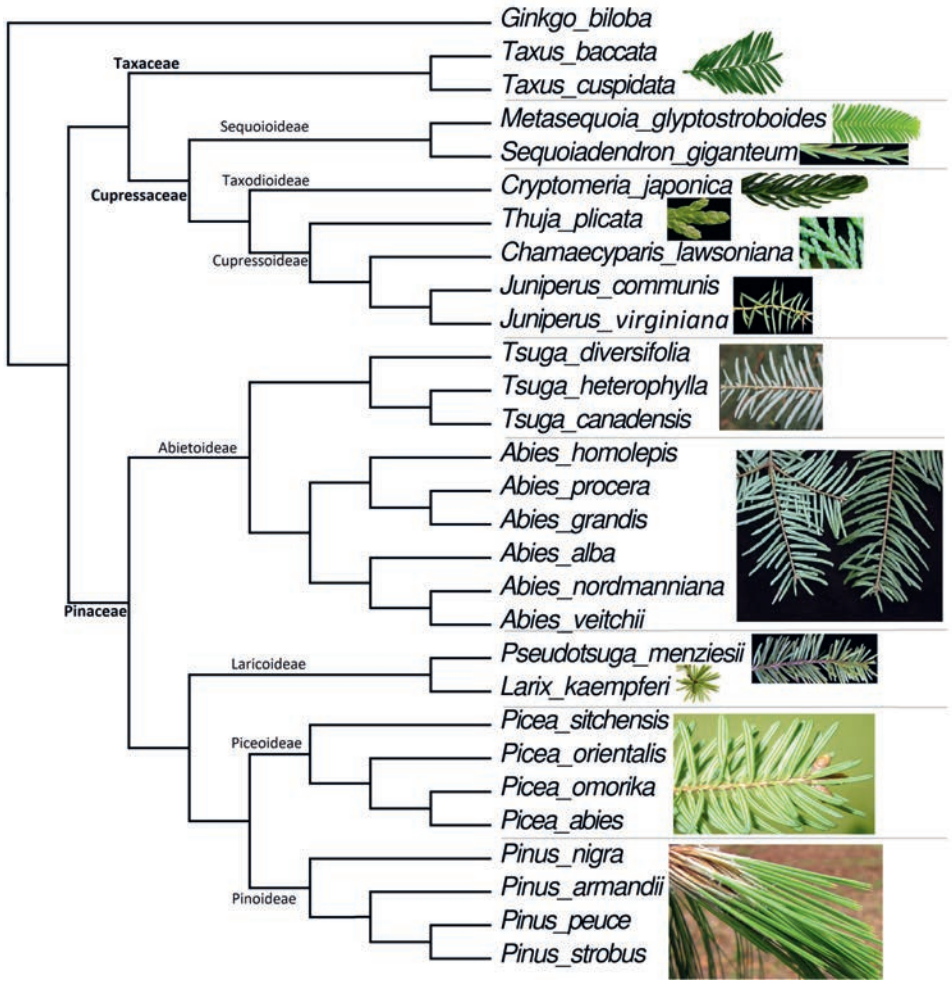

Fig. 1.4 The phylogenetic tree for 28 conifer species in this thesis. Family (in bold) and subfamily are shown. The appearance of the needles varies depending on the species or genera, reflecting the difference in growth and survival, such as drought-tolerant Cupressoideae with the scaled needles and fast-growing *Larix* and *Metasequoia* species with thin and relatively big leaves. The phylogenetic tree was built based on Zanne *et al.* (2014).

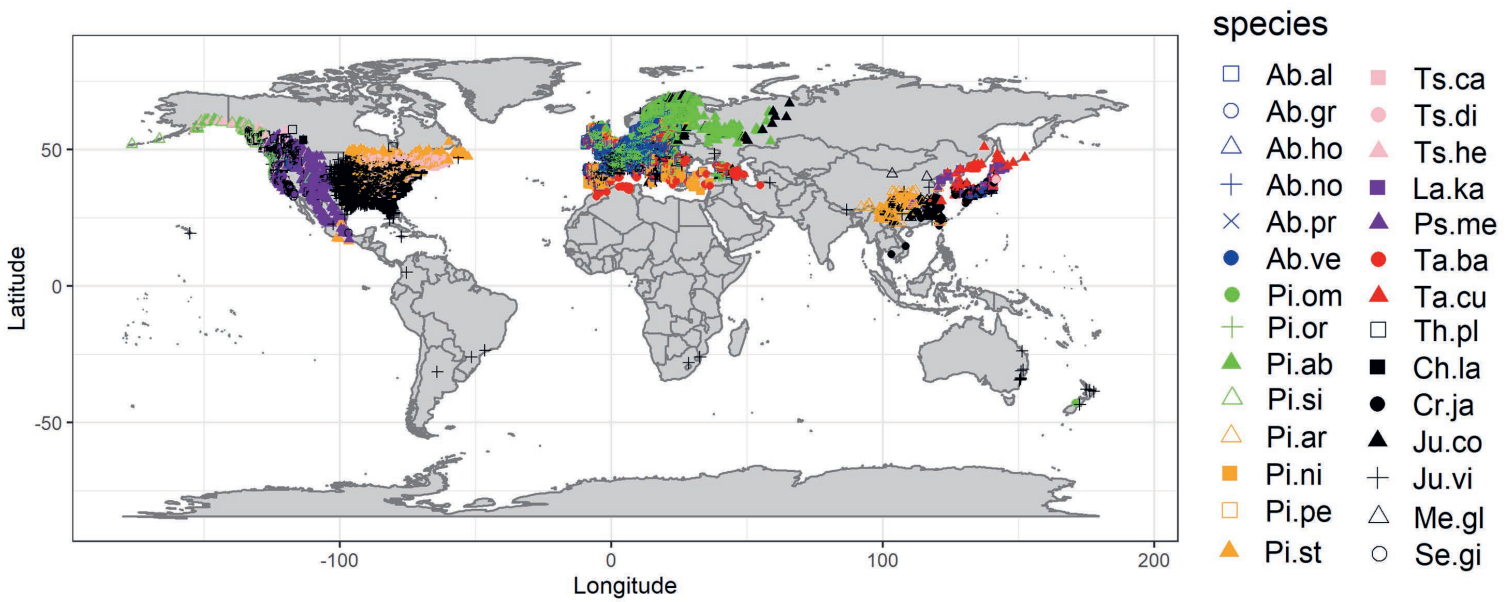

Fig. 1.5 The original distribution map for 28 conifer species in this thesis. Occurrence records were retrieved from Global Biodiversity Information Facility (GBIF: https://www.gbif.org/). For species abbreviations, see Table 1.

Table 1 Overview of 28 conifer species, abbreviations, distribution area and maximum height recorded in the world. For most species, the maximum height of was obtained from the monumental trees dataset (https://www.monumentaltrees.com/en/); *Taxus cuspidata* and *Tsuga diversifolia* were derived from obtained from Forest Garden Center (https://www.forestgardencentre.co.uk/).

Species	Family	Abbreviation	Distribution area	Maximum height
Abies alba	Pinaceae	Ab.al	Europe	60 m
Abies grandis	Pinaceae	Ab.gr	North America	64 m
Abies homolepis	Pinaceae	Ab.no	Japan	37 m
Abies nordmanniana	Pinaceae	Ab.no	Main land Asia and Japan	61 m
Abies procera	Pinaceae	Ab.pr	North America	56 m
Abies veitchii	Pinaceae	Ab.ve	Northern Honshu, Japan	32 m
Chamaecyparis lawsoniana	Cupressaceae	Ch.la	North America	82 m
Cryptomeria japonica	Cupressaceae	Cr.ja	Eastern Asia	45 m
Larix kaempferi	Pinaceae	La.ka	Eastern Asia	45 m
Metasequoia glyptostroboides	Cupressaceae	Me.gl	Main land Asia	42 m
Juniperus communis	Cupressaceae	Ju.co	Europe	17 m
Juniperus virginiana	Cupressaceae	Ju.vi	Europe	26 m
Picea abies	Pinaceae	Pi.ab	Europe	63 m
Picea orientalis	Pinaceae	Pi.or	Main land Asia	41 m
Picea omorika	Pinaceae	Pi.om	Europe	33 m
Picea sitchensis	Pinaceae	Pi.si	North America	84 m
Pinus armandii	Pinaceae	Pi.ar	Eastern Asia	26 m
Pinus nigra	Pinaceae	Pi.ni	South-Eastern Europe	47 m
Pinus peuce	Pinaceae	Pi.pe	Europe	36 m
Pinus strobus	Pinaceae	Pi.st	North America	58 m
Pseudotsuga menziesii	Pinaceae	Ps.me	North America	80 m
Sequoiadendron giganteum	Cupressaceae	Se.gi	North America	96 m
Taxus baccata	Taxaceae	Ta.ba	Europe	29 m
Taxus cuspidata	Taxaceae	Ta.cu	Mainland Asia	10 m
Thuja plicata	Cupressaceae	Th.pl	North America	56 m
Tsuga canadensis	Pinaceae	Ts.ca	North America	53 m
Tsuga diversifolia	Pinaceae	Ts.di	Japan	25 m
Tsuga heterophylla	Pinaceae	Ts.he	North America	83 m

CHAPTER 2

2

Growth of 19 conifer species is highly sensitive to winter warming, spring frost and summer drought

Song Y, Sass-Klaassen U, Sterck F, Goudzwaard L, Akhmetzyanov L, Poorter L (2021). Growth of 19 conifer species is highly sensitive to winter warming, spring frost and summer drought.
Annals of Botany, 128(5): 545-557, https://doi.org/10.1093/aob/mcab090

Abstract

- ***Background and Aims*** Conifers are key components of many temperate and boreal forests and are important for forestry, but species differences in stem growth responses to climate are still poorly understood and may hinder effective management of these forests in a warmer and drier future.
- ***Methods*** We studied 19 Northern hemisphere conifer species planted in a 50-year-old common garden experiment in the Netherlands to 1) assess the effect of temporal dynamics in climate on stem growth; 2) test for a possible positive relationship between the growth potential and climatic growth sensitivity across species, and 3) evaluate to what extent stem growth is controlled by phylogeny.
- ***Key results*** Eighty-nine percent of the species showed a significant reduction in stem growth to summer drought, 37% responded negatively to spring frost, 32% responded positively to higher winter temperatures. Species differed largely in their growth sensitivity to climatic variation and showed for example, a 4-fold difference in growth reduction to summer drought. Remarkably, we did not find a positive relationship between productivity and climatic sensitivity, but instead observed that some species combined a low growth sensitivity to summer drought with high growth potential. Both growth sensitivity to climate and growth potential were partly phylogenetically controlled.
- ***Conclusions*** A warmer and drier future climate is likely to reduce the productivity of most conifer species. We did not find a relationship between growth potential and growth sensitivity to climate; instead, some species combined high growth potential with low sensitivity to summer drought. This may help forest managers to select productive species that are able to cope with a warmer and drier future.

Key words: conifer species, growth potential, growth sensitivity, phylogeny, spring frost, summer drought, winter temperature

2.1 Introduction

Climate change leads to increased warming and an increased frequency of late spring frosts and summer droughts (Inouye, 2000; Hartmann, 2011), with potentially large repercussions for forest and tree productivity (Ciais *et al.*, 2005b; Gazol *et al.*, 2019). An improved understanding of how trees respond to long-term climatic variation may allow for a better understanding under what conditions forests are a net carbon source (Kurz *et al.*, 2008) or a carbon sink (Walker *et al.*, 2020). Here we focus on the effects of climate on stem growth of conifer species, which dominate large areas in cold boreal forests, temperate forests and dry Mediterranean forests (Farjon & Filer, 2013), and account for nearly one-third to the global forest carbon stock (Pan *et al.*, 2011).

2.1.1 Climate-growth relationships of conifer species

Dendrochronological studies provide a long-term perspective on how stem growth responds to climate (Fritts, 1976; Babst *et al.*, 2013; Charney *et al.*, 2016). Such growth responses for conifer species have been studied on a macro-scale across continents with climate gradients (Williams *et al.*, 2010; Klesse *et al.*, 2018). Winter temperature, spring frost and summer drought are primal factors to limit growth (D'Orangeville *et al.*, 2016; Camarero *et al.*, 2018; Vitasse *et al.*, 2019). Generally, in cold and mild areas, high temperatures in winter and early spring benefits evergreen conifer species' growth because species still maintain photosynthesis (Larcher, 2000). Warmer conditions during early spring and warming of frozen soils may lead to an earlier start of the growing season (Williams *et al.*, 2015; Harvey *et al.*, 2020), which increases the length of the growing season and tree growth. Yet, early warming and increased tree cambial and bud activity may also enhance the risk of damage by late spring frosts and, thus, reduced growth (Dy & Payette, 2007; Harvey *et al.*, 2020). In temperate regions, especially arid regions (Gazol *et al.*, 2018), high summer temperatures can lead to drought stress, reduced carbon gain, and an early cessation of the growing season (Ciais *et al.*, 2005a; Dietrich *et al.*, 2019). In contrast, in cold regions, higher summer temperatures may positively affect tree growth (Klesse *et al.*, 2018).

From these studies and others (Babst *et al.*, 2013; Bhuyan *et al.*, 2017; Montwé *et al.*, 2018), it is difficult to draw generalizations about differences in species-specific responses to climate, because different species are compared across different parts of the climatic gradient. Moreover, in general only one or a few conifer species have been included in these studies (Vitali *et al.*, 2017; Julio Camarero *et al.*, 2018; Klesse *et al.*, 2018). To better understand species differences in climatic response, long-term common garden experiments can control the potentially confounding effects of climatic or soil conditions on the growth of different tree species (cf. Huang *et al.*, 2017).

2.1.2 Relationship between growth sensitivity and potential

Growth sensitivity is defined as a large plastic response in growth in response to climatic variation (Klesse *et al.*, 2018). The climatic growth sensitivity varies across species because of differences in species traits. For examples, deep roots enable species to take up water from deeper soil layers during drought (Huang, 2000). Some traits may lead to fast growth and also high growth sensitivity. For example, species with wide tracheids have a high potentially growth rate, which normally comes at the cost of hydraulic safety because cheap light wood has a lower cell wall reinforcement (low thickness to span ratio) (Pittermann *et al.*, 2006b; Sperry *et al.*, 2006). Wide tracheids also allow for high hydraulic conductivity and, hence, high gas exchange, photosynthesis and growth rates (Chave *et al.*, 2009). Simultaneously, these species would also be sensitive to frost and drought, because increased conduit size increases species vulnerability to freezing- and drought-induced cavitation (Mayr *et al.*, 2006). However, few studies have directly evaluated these relationships between growth potential and growth sensitivity to climatic variation.

In this study, we compared stem-growth responses across 19 conifer species from the Northern hemisphere, which were planted in the late 1960s in a common garden experiment in the Netherlands. We used tree-ring analysis to evaluate how annual stem growth responded to variation in climate factors over 44 years. It is difficult to find common garden experiments old enough to assess species differences in long-term growth responses, as done here on 19 conifer species growing under Dutch maritime climate conditions.

First, we identified which climatic factors limit annual stem growth of the species in different months and seasons before and during the growing period. We hypothesize that growth of the 19 species is reduced by spring frosts and summer droughts (e.g., via high temperature and low precipitation) and sensitive to warm winters. Specifically, spring frost could limit growth because of freezing-induced cavitation, or damage to leaf and twig cambial activity (Begum *et al.*, 2010; Li *et al.*, 2013) which can delay the start of the growing season. Summer droughts reduce growth due to lower stomatal conductance reducing photosynthetic rates (McDowell *et al.*, 2008). Warm winters can lead to higher stem growth due to increased photosynthetic activity in warm areas (Fry & Phillips, 1977), but can also reduce the growth through increased respiration (Larsen *et al.*, 2007) or drought stress due to water deficit (DeSoto *et al.*, 2014).

Second, we quantified species differences in growth potential and related it to their growth sensitivity to climate variation. We predicted a positive relationship between stem growth potential and growth sensitivity to climate variation, because the traits that lead to high inherent growth rates, such as large cells with thin cell walls that facilitate high metabolic activity, may lead to a higher sensitivity (e.g., by a higher cavitation vulnerability) to extreme

climate events such as late spring frosts and summer droughts.

Third, we evaluated to what extent the growth sensitivity of species to climate factors is phylogenetically controlled. Given that closely related conifer species are adapted to different environmental conditions (Zanne *et al.*, 2014), we expect that growth potential and stem growth sensitivity to climate is only weakly phylogenetically controlled.

2.2 Material and methods

2.2.1 Study site

This study was carried out at Schovenhorst Estate (52.25 N, 5.63 E), east of Putten, the Netherlands. The elevation is approximately 30 m above sea level. The climate is characterized as a mild maritime climate with a mean annual temperature of 10.1 °C, maximum annual temperature of 13.5 °C, minimum annual temperature of 6.0 °C and a mean annual rainfall of 830 mm y^{-1} averaged over 44 years (1974-2017). Precipitation is quite evenly distributed across seasons (Fig. S2.1). Soils are derived from postglacial loamy sand deposits, forming well-drained and acidic (pH ~4) podzolic soils of generally low fertility (Cornelissen *et al.*, 2012; van der Wal *et al.*, 2016). The groundwater table is below 19.04 m and considered not accessible by trees (TNO-NITG, 2020).

2.2.2 Sample design and species selection

We used a long-term established common-garden experiment established between 1916 and 1974 (Table 2.1), which has advantages to assess the long-term climate-growth relationship, but has also short-coming such as no or limited control on the design of the experiment, e.g., blocks to correct for micro-site related differences, planting dates, plant density, etc. Yet from (limited) historical information and the actual situation, we can infer that trees have been planted in groups per species and with considerable distance to each other to exclude strong resource competition. The stands were never managed. Most species were planted in monospecific stands. This experiment was initially established to select non-native species with high timber production potential for the Netherlands, and only one native species was included (*Taxus baccata*) (Willinge Gratama-Oudemans, 1992). In our study, 19 coniferous species were selected, including genera and species originating from different biogeographic zones (Table 2.1). For each species, ten dominant and healthy individuals were selected that formed part of the canopy and hence could express their full growth potential.

Table 2.1 Overview of the 19 study species, their distribution area, the growth period considered, the average stem diameter at breast height (DBH) of the sampled trees (N=10 per species) in 2017/2018, and the mean basal area increment (BAI). The standard deviation is shown in parentheses. Mean basal area increment and standard deviation are calculated based on tree-ring data (Fig. S2.2). Distribution areas are derived from Farjon and Filer (2013).

Species	Distribution areas	Species abbreviations	Period considered	DBH (cm)	Mean BAI (cm^2 per year)
Abies alba	Europe	ABAL	1958-2018	46.9 (10.3)	29.5 (5.2)
Abies grandis	North America	ABGR	1940-2017	76.9 (8.7)	55.9 (6.1)
Abies veitchii	Northern Honshu, Japan	ABVE	1979-2018	27.1 (3.1)	12.6 (1.6)
Chamaecyparis lawsoniana	North America (USA)	CHLA	1911-2017	48.2 (9.6)	20.0 (2.4)
Cryptomeria japonica	Eastern Asia	CRJA	1969-2018	35.6 (6.2)	18.3 (1.9)
Larix kaempferi	Eastern Asia	LAKA	1945-2018	49.4 (6.8)	23.1 (3.2)
Pinus armandii	Eastern Asia	PIAR	1981-2018	24.0 (3.2)	10.9 (1.5)
Pinus nigra	South Eastern Europe	PINI	1945-2018	44.6 (6.5)	19.3 (1.5)
Picea abies	Europe	PIAB	1969-2018	43.4 (5.2)	27.7 (3.9)
Picea omorika	Europe	PIOM	1953-2018	30.9 (30.9)	13.7 (1.1)
Picea orientalis	Main land Asia	PIOR	1944-2017	47.7 (8.1)	23.8 (2.3)
Picea sitchensis	North America	PISI	1972-2018	44.5 (8.8)	34.8 (4.9)
Pseudotsuga menziesii	North America	PSEM	1916-2017	76.3 (10.1)	48.6 (4.3)
Taxus baccata	Europe	TABA	1957-2018	31.2 (9.9)	9.8 (1.6)
Taxus cuspidata	Main land Asia	TACU	1974-2018	14.8 (4.0)	3.9 (0.4)
Thuja plicata	North America	THPL	1942-2017	74.3 (12.7)	47.0 (5.9)
Tsuga canadensis	North America	TSCA	1972-2018	31.6 (4.8)	18.4 (2.1)
Tsuga diversifolia	Japan	TSDI	1972-2018	25.3 (3.6)	9.3 (1.7)
Tsuga heterophylla	North America	TSHE	1971-2017	53.2 (6.4)	42.6 (4.6)

2.2.3 Tree-ring analysis

To investigate stem growth rates and annual growth variation, we took two increment cores from each of the 10 selected individuals per species at two opposite sides at 1.3 m stem height using Haglof Pressler increment borers. All samples were cut with a microtome (Gärtner & Nievergelt, 2010) and sanded with progressively finer sandpaper (grain sizes from P600 to P1000, Fepa Abrasives) to improve the visibility of tree-ring boundaries. Flat surfaces were subsequently scanned with 2000 dpi using an Epson scanner (Epson 10000XL). Tree-ring width (TRW) was measured, and time series were cross-dated to assign a calendar year to each ring using CooRecorder and CDendro (v. 9.0, Cybis Electronik and Data AB, Sweden). Cross-dating was done by first matching the ring-width patterns of individual trees, and then different trees of the same species. To better detect the effect of climate on tree growth, we removed the confounding impact of tree age on ring-width. For each individual, tree ring-width series were detrended with the R '*dplR*' package (Bunn, 2008). We first fitted a cubic smoothing spline with a 50% frequency cutoff at 15 years. The standardization is crucial for assessing the climate-growth relationship, as it allows to remove all the low-frequency variation (i.e., non-climatic noise) (Cook *et al.*, 1990). We then divided the raw tree-ring width value with the

corresponding year's spline value, thus obtaining dimensionless ring-width index time series (TRI) per tree. Tree-ring index (TRI) chronologies were calculated for each species by averaging (biweight robust mean) the detrended individual time series of trees of the same species using the '*dplR*' package (Bunn, 2008). Chronology calculation strengthens the common climatic signal in the tree populations by at the same time dampening individual tree variation (Cook *et al.*, 1995). For more information about tree-ring characteristics, see Supplementary data Table S2.1.

2.2.4 Climate data from the Netherlands

To check how annual climate factors affected species growth, climate records were retrieved from the weather station "De Bilt", situated at approximately 45 km from the study site (KNMI, https://www.knmi.nl/home; https://www.knmi.nl/nederland-nu/klimatologie/daggegevens).

To evaluate how spring frost days affected stem growth, the number of spring frost days was defined as days where the minimum daily temperature dropped below 0°C (Chudnovskii, 1949; Gurskaya, 2014). Monthly frost days were then aggregated by counting the number of frost days per month. Because there were nearly no frost days recorded in May, we considered March and April for calculating spring frost days.

To assess the effects of summer droughts (i.e., water availability during summer) on the growth of the selected species, monthly data of mean temperature (°C) and total precipitation (mm per month) were downloaded (KNMI, https://www.knmi.nl/home). We also calculated potential evapotranspiration (PET, mm per month), and the standardized precipitation evapotranspiration index (SPEI) that is an indicator for the climate-water balance and a proxy for water availability (Vicente-Serrano *et al.*, 2010). For this calculation, we first calculated the potential evapotranspiration (PET, in mm) using the Thornthwaite method, which required monthly mean temperature and latitude (Thornthwaite, 1948). Next, we calculated SPEI based on precipitation (P) and PET, see Vicente-Serrano *et al.* (2010). The SPEI was a standardized index with an average value of 0 and a standard deviation of 1. SPEI can be calculated at different time scales. To focus on summer drought, we aggregated the climate-water balance based on a three months scale from June to August (Vicente-Serrano *et al.*, 2010). The SPEI was calculated using the R 'SPEI' package software (Beguería & Vicente-Serrano, 2013).

2.2.5 Data analysis

To analyse climate-growth relationships, the common period 1974 to 2017 was selected to compare the growth responses across species. Since *Pinus armandii* and *Abies veitchii* included individuals established after 1974, tree rings of these two species were analysed from 1981 to 2017 (Table 2.1). To avoid the inflation of significant correlations by calculating many

for a given question (Biondi, 1997), we used 1000 bootstrapped subsets for each species from the climate and tree-ring index data to calculate correlation coefficients between TRI chronologies and the monthly climatic factors. We will show such correlations with TRI with climate data from June in the year preceding the tree-ring formation until September in the year of tree-ring formation (Biondi & Waikul, 2004).

To evaluate and specify the growth sensitivity to different climate factors, we selected climate conditions from different seasons that were hypothesized to be growth-limiting, i.e., frost in spring (the number of frost days from March 1 to April 30), summer water availability (i.e., SPEI averaged from June 1 to August 31) and winter temperature (mean temperature from January 1 to March 31). Climate-growth analyses for the 19 species were carried out for the common period (1974-2017). The climatic effects on stem growth (i.e., tree-ring index) were assessed using a linear mixed model, with the averaged tree-ring width index from two cores per tree as the dependent variable, the interactions between seasonal climatic variables and species as fixed factors, and individuals as random factors. The Variance Inflation Factor (VIF) was <5 for all climatic factors, indicating that there were no collinearity problems with the predictor variables (Gould *et al.*, 2016). To compare the effect sizes, climatic data was standardized before analysis by subtracting the mean and dividing it by the standard deviation, which also improved the residuals' homogeneity and normality. To check the residuals' homogeneity and normality, residuals with Q-Q plot and frequency plot were produced (Supplementary data Fig. S2.2, S2.3). We used 7747 annual rings as data points rather than 8360 (44 years x 19 species x 10 trees) because parts of the cores were damaged for some individuals and outliers were removed. Regression coefficients were used to describe stem growth sensitivity of each species to four climate factors: spring frost, summer drought in the year of stem growth, summer drought in the year preceding growth and winter temperature, respectively. To obtain the proportional variance (R^2) explained by the multiple regression, species -specific R^2 was calculated from the square of correlations between the predicted tree ring index (based on the multiple regression in Table 2) and the observed tree ring index both on individual and mean chronology level, see Supplementary data Table S2. Additionally, the standard deviation of TRI was used as an indicator of growth sensitivity, because it captures the overall annual variation in growth that might be attributed to all climatic factors, and it is therefore an indicator of the overall climate sensitivity of a tree species. All models were implemented with the package “nlme” (Pinheiro *et al.*, 2017) in the R statistical environment (R Core Team, 2019).

To quantify the stem growth potential of species, we calculated for each tree the slope between the estimated stem radius calculated from added annual ring widths and tree age for the first twenty years, i.e., stem diameter growth (in mm/yr). We restricted this analysis to the first 20 years because in this period the canopy of the stand was probably relatively

open, resulting in a relatively linear relationship during this period, which got lost over longer periods (Fig. S2.4a, b). Similar analyses using basal area increment are shown too (Fig. S2.4c, d). The slopes were calculated by running a linear mixed effect model, using cumulative annual ring width as the response variable, the corresponding age of that ring and species as fixed factors, and the slope between corresponding age and individual as random coefficients (Saunders & Wagner, 2008). This random slope linear mixed model allows tree ring variables associated with the individual trees to predict changes in coefficients that generate smoothed estimates of annual radial growth over time (McLane *et al.*, 2011). *Pseudotsuga menziesii* was not included in the model because we did not take the samples to the pith; thus, we cannot determine the first twenty years during their growth period. Instead, the cumulative ring width data was used when the first 20 years were available. The linear regression used cumulative ring widths as dependent factor, year as fixed factor and individual as random factors. Hence, the slope of the regression was used to estimate the growth potential for *P. menziesii*. Given that biomass may reflect real growth and stem area growth (BAI) may indicate size growth and timber volume production, the averaged stem area growth (in cm^2/yr, Table 2.1) and stem mass growth (in kg/yr/m) were also provided as alternative proxies of growth potential. Stem mass growth was calculated by multiplying stem area growth (m^2/yr) and wood density (kg/m^3), and reflect the biomass increment per meter stem length (Sterck *et al.*, 2012).

To estimate to what extent growth sensitivity and growth potential are phylogenetically controlled, we calculated Blomberg's *K* (Blomberg *et al.*, 2003) using the "phytools" package (Revell, 2012) in R (R Core Team, 2019). Blomberg's *K* assumes a Brownian motion of evolution, where temperature leads to random mutations and changes in the genome. K value compares the observed phylogenetic signal in a trait to traits under Brownian motion trait evolution. *K* is calculated as the quotient of observed and expected ratios of mean square errors (MSE) (Equation 1). The observed ratio is the MSE_0 of the tip data from the phylogenetically correct mean, divided by the MSE of the data calculated using the variance-covariance matrix derived from the tree. The expected ratio is the expected variation under Brownian motion relative to the number of taxa in the phylogeny (Blomberg *et al.*, 2003; Adams, 2014).

$$K = \text{observed}\frac{MSE_0}{MSE}/\text{expected}\frac{MSE_0}{MSE} \quad \text{Equation 1,}$$

K values may range from 0 (the null expectation) to infinity. *K* values around 1 indicate that there is a significant phylogenetic signal as expected under the Brownian motion model; K values lower than one indicate that the trait is less phylogenetically controlled than expected; K values closer to 0 indicate that trait is not phylogenetically controlled (i.e., that the trait has evolved independently of phylogeny), and *K*>1 indicates the trait is strongly phylogenetically conserved (CaraDonna & Inouye, 2015). The statistical significance of *K* values was tested

followed the method of Kembel *et al.* (2010)

2.3 Results

2.3.1 General climate-growth relationships

For all 19 conifer species studied, annual stem growth variation was expressed by the tree-ring width index (TRI) and correlated with multiple climatic factors (Fig. 2.1). TRI of 37% of the conifer species was significantly negatively affected by the number of spring frost days in March and April (Fig. 2.1a, Table 2.2). At the same time, the growth of 32% of the species was significantly positively correlated with warmer conditions during the winter months December, January and February (Fig. 2.1b, Table 2.2). *Cryptomeria japonica*, *Tsuga heterophylla* and the *Taxus baccata* were most sensitive in their stem growth response to cold winters (Table 2.2). During summer, the correlation between growth and temperature became generally negative (Fig. 2.1b). Yet, species show different trends in sensitivity to cold winters and to dry summers. Growth was positively correlated with variables reflecting positive water balance (i.e., high SPEI values and precipitation, low summer temperature and PET) (Fig. 2.1c, d, e), which indicates that water availability during summer was limiting stem growth in >50% of the conifer species, with the strongest negative impact for the *Picea* species, *Pinus nigra* and *Taxus baccata* (Fig. 2.1e). In all species annual stem growth significantly increased with the summer SPEI (and this was significant for 89%), i.e., with water availability in June, July and August, and with summer SPEI of the preceding year (21% of the species, Table 2.2). The large absolute values of the standardized regression coefficients indicate that species growth is generally highly sensitive to climatic variation. Yet, it also became apparent that the three *Abies* species seem to be less responsive to especially spring frost and water availability during summer compared to the rest of the conifer species.

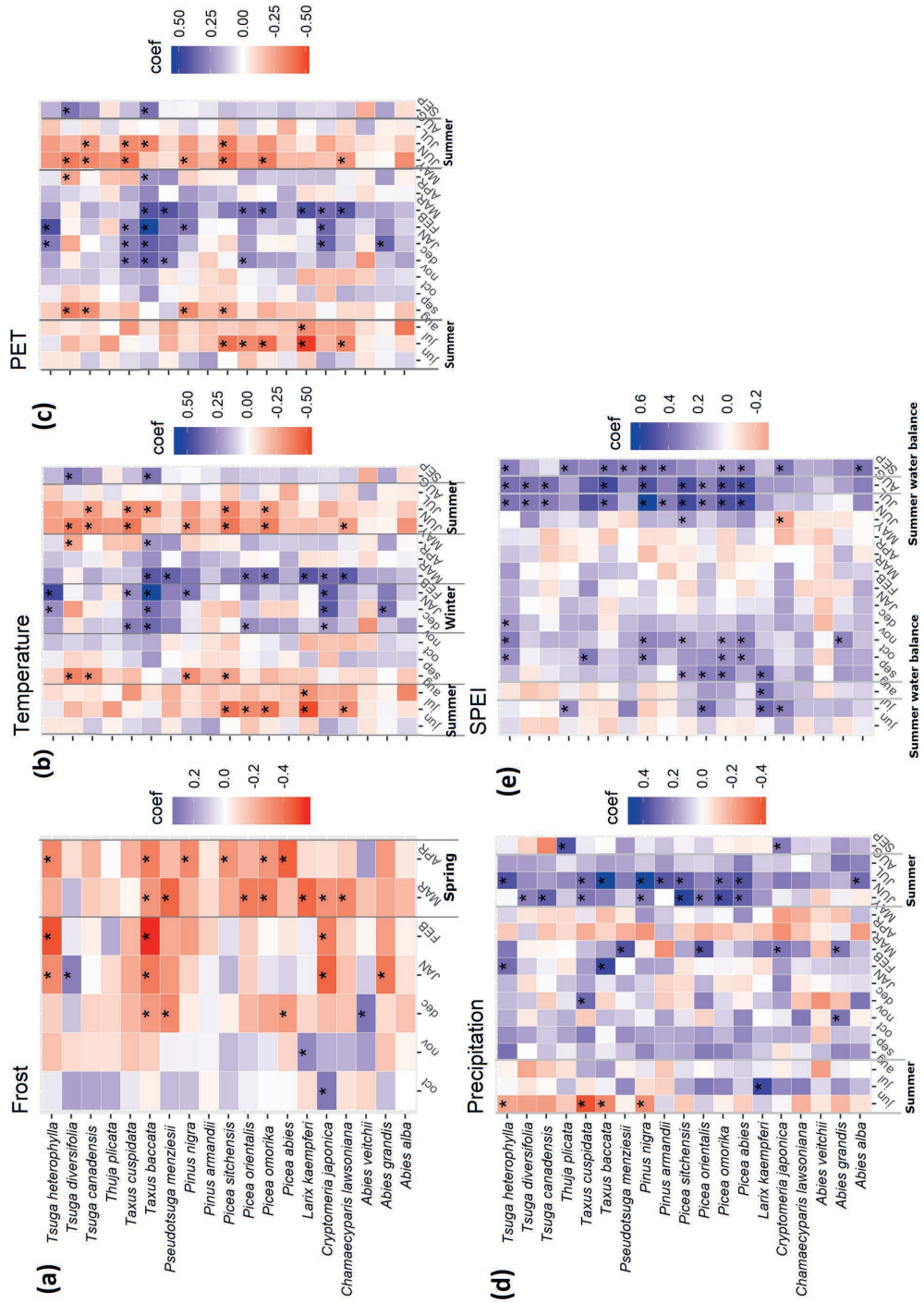
(a)
Frost
(b)
Temperature
(c)
PET
(d)
Precipitation
(e)
SPEI
coef
Spring
Winter
Summer
Summer water balance
Tsuga heterophylla
Tsuga diversifolia
Tsuga canadensis
Thuja plicata
Taxus cuspidata
Taxus baccata
Pseudotsuga menziesii
Pinus nigra
Pinus armandii
Picea sitchensis
Picea orientalis
Picea omorika
Picea abies
Larix kaempferi
Cryptomeria japonica
Chamaecyparis lawsoniana
Abies veitchii
Abies grandis
Abies alba

Fig. 2.1 Bivariate bootstrapped correlation coefficients between tree-ring width index (TRI) and climate variables were calculated for 19 coniferous species (in rows) and monthly climate data (in columns) for a) the number of frost days, b) mean temperature, c) potential evapotranspiration (PET), d) precipitation, e) standardized precipitation evapotranspiration index (SPEI). Correlations are made between TRI and monthly climatic conditions from previous year June (jun) to current year September (SEP). For 17 species correlations were made across a 44 years period from 1974-2017 (N= 44 per species), whereas correlations for *P. armandii* and *A. veitchii* were based on a 37-year period 1981-2017 (N=37 per species). The Standardized Precipitation-Evapotranspiration Index (SPEI) is calculated over a 3 months period (i.e. SPEI AUG reflects water availability from Jun to Aug). Lower-and upper-case letters represent monthly climate data from last year and current year for tree-ring formation, respectively. Blue/purple cells indicate positive correlations, red/orange cells indicate negative correlations, and asterisks indicate significant (P<0.05) correlations.

.

Table 2.2 Results of a species-specific multiple regression analysis of stem growth (i.e., tree-ring index) of 19 coniferous tree species on five selected environmental variables; number of spring frost days, summer SPEI from June to August (i.e., the Standardized Precipitation Evapotranspiration Index) in the current years, summer SPEI in the previous year, and winter temperature. Regressions were based on common period from 1974 to 2017. Standardized regression coefficients are shown. Coefficients in bold refer to statistically significant relationships (P<0.05). Linear mixed effect models were used to explain stem growth, using interaction terms between species and environmental variables as fixed factors, and individual as random variable. R^2m is the marginal and R^2c is the conditional R^2. Mixed models have the same R^2m and R^2c because random effects nearly explained zero in the model. For species-specific R^2, see Table S2.2.

Species	Spring Frost	Current Summer SPEI	Previous Summer SPEI	Winter Temperature
Abies alba	-0.012	**0.040**	0.012	0.006
Abies grandis	-0.017	0.020	0.012	**0.042**
Abies veitchii	-0.004	0.024	-0.019	0.007
Chamaecyparis lawsoniana	**-0.039**	**0.028**	0.023	0.023
Cryptomeria japonica	0.014	**0.050**	**0.033**	**0.125**
Larix kaempferi	**-0.121**	**0.052**	**0.102**	**-0.043**
Pinus armandii	-0.020	**0.044**	0.004	-0.021
Pinus nigra	-0.021	**0.053**	-0.017	0.016
Picea abies	**-0.055**	**0.077**	0.003	**-0.038**
Picea omorika	**-0.081**	**0.064**	**0.026**	**-0.042**
Picea orientalis	**-0.057**	**0.050**	**0.044**	0.018
Picea sitchensis	**-0.050**	**0.061**	0.008	**-0.040**
Pseudotsuga menziesii	**-0.054**	**0.032**	0.017	**0.032**
Taxus baccata	-0.003	**0.077**	-0.017	**0.103**
Taxus cuspidata	0.028	**0.047**	-0.020	**0.053**
Thuja plicata	-0.023	**0.046**	0.002	-0.005
Tsuga canadensis	-0.027	**0.038**	-0.018	-0.008
Tsuga diversifolia	0.011	**0.066**	**-0.029**	-0.028
Tsuga heterophylla	-0.017	**0.049**	-0.020	**0.057**
R^2m/R^2c	0.129/0.129			

2.3.2 Relationship between stem growth potential and growth sensitivity to climate

Among three proxies for growth potential (i.e., stem diameter growth, stem mass growth and stem area growth), stem diameter growth rate varied >3-fold across species, with *Abies grandis* being the fastest-growing species (0.61 cm diameter growth per year) and species from the genus *Taxus* the slowest growing species (*Taxus baccata*: 0.20 cm per year, *Taxus cuspidata* 0.19 cm per year, Fig. 2.2); similar trends were found for stem mass growth and stem area growth, and both of them varied >10-fold across species, ranging from *Taxus cuspidata* (0.23 kg/yr/m, 3.91 cm^2/yr, Supplementary data Fig. S2.5b-c) to *Abies grandis* (2.94

kg/yr/m, 55.90 cm^2/yr, Supplementary data Fig. S5b-c). Unexpectedly, there were no positive relationships between growth potential and growth sensitivity to spring frost (Table 2.3). Instead, only one proxy of growth potential, i.e., stem diameter growth, was negatively correlated with stem growth sensitivity to current summer SPEI, although this was only marginally significant (Table 2.3, r=-0.40, n=19, *P*=0.08; Fig. 3). The correlation was mainly driven by *Abies grandis* (high growth and low sensitivity to summer SPEI) and the opposite combination was shown by *Taxus baccata* (i.e., low growth and high sensitivity).

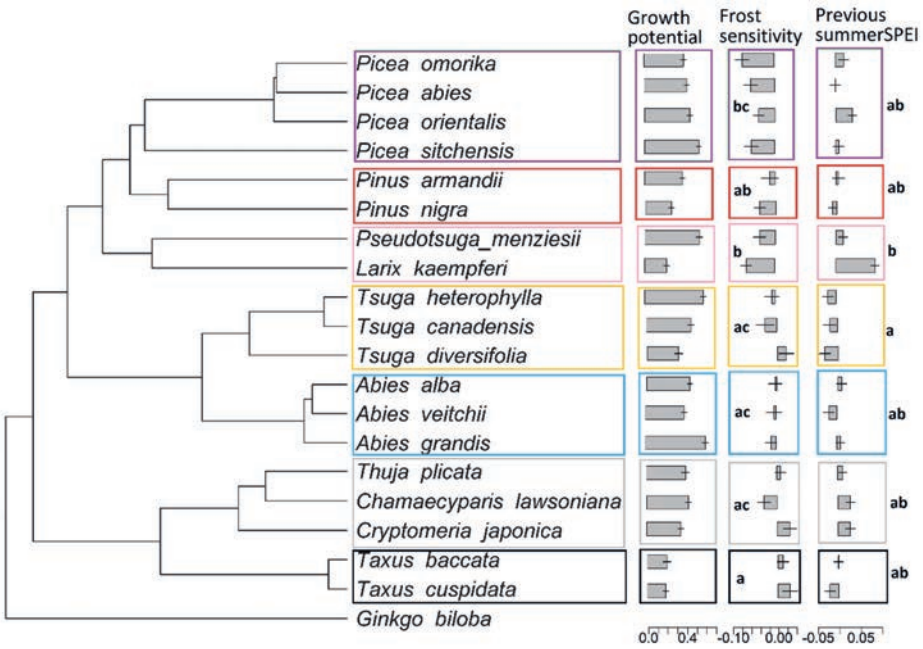

Fig. 2.2 A visualization of the significant phylogenetic signals with stem growth sensitivity to climate and growth potential (See Table 2.4): growth potential refers to the stem growth rate (cm/yr) during the first twenty years for 19 species; frost sensitivity refers to the stem growth response to number of frost days in March and April; and Previous summer SPEI refers to the stem growth sensitivity to summer SPEI in the previous year. The effects are shown as bar plots corresponding to the tips of the phylogeny. *Ginkgo biloba* is selected as outlier and reference. Molecular phylogeny is from Zanne *et al.* (2014). Different colours indicate different genera. Significant differences are also tested between genera and significant differences are shown indicated by using different letters. The horizontal line is the error bar.

Table 2.3 Pearson correlations between stem growth sensitivity and growth potential of conifer species (N=19 species). Growth potential refers to stem diameter growth (cm/yr), stem area growth (cm^2/yr), stem mass growth (kg/yr/m) and stem standardized (Std.) area growth (cm^2/cm/yr). The growth sensitivity to spring frost days, summer SPEI (i.e., the Standardized Precipitation Evapotranspiration Index) in the current years, summer SPEI in the previous year, and winter temperature was quantified using the multiple regression coefficients of Table 2.2. Standard deviation (sd) for tree ring index (TRI) from time series was also used as an indicator of growth sensitivity. Pearson correlation coefficient (r) and *P*-value (*P*)are shown.

Growth sensitivity	Stem growth potential							
	Diameter growth		Area growth		Mass growth		Std. area growth	
	r	*P*	r	*P*	r	P	r	*P*
spring frost	-0.16	0.52	-0.23	0.35	-0.24	0.33	0.05	0.84
current SPEI	-0.40	0.08	-0.37	0.12	-0.29	0.23	-0.01	0.98
previous SPEI	-0.03	0.91	0.16	0.51	0.13	0.60	0.07	0.78
winter temperature	-0.12	0.63	-0.01	0.97	-0.03	0.90	0.11	0.65
sd (TRI)	-0.22	0.36	0.10	0.68	0.04	0.86	0.07	0.78

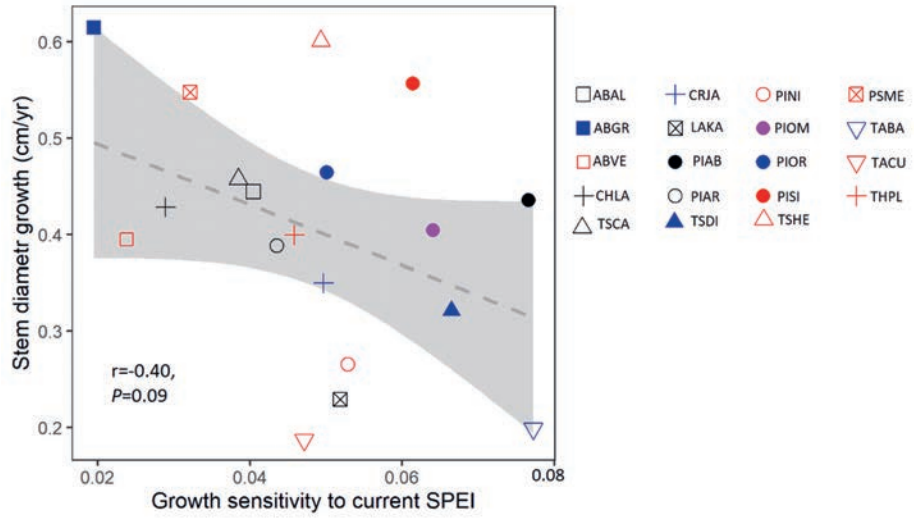

Fig. 2.3 Relationships between stem diameter growth (cm/yr) and growth sensitivity to summer SPEI of current year in the currents. Regression lines and 95% confidence intervals (grey), Pearson correlation coefficient (*r*) and *P*-value are shown. For species abbreviations, see Table 2.1.

2.3.3 The phylogenetic signal on stem growth sensitivity to climate and growth potential

Few significant phylogenetic signals were observed for stem growth sensitivity to climate factors. Only stem growth sensitivity to spring frost (K=0.87, P<0.01) and previous summer SPEI (K=0.78, P<0.01) showed significant phylogenetic signals (Table 2.4). This is also supported by ANOVA's that show that some main phylogenetic groups differed in their stem growth sensitivity to spring frost (ANOVA, $F_{6,12}$=6.11, P=0.004: the Taxaceae, Cupressaceae (*Chamaecyparis, Thuja,* and *Cryptomeria*) and *Abies* were less sensitive to spring frost compared to *Pseudotsuga* and *Larix* (Tukey post-hoc test, P<0.05) (Fig. 2.2). The phylogenetic groups also differed in their sensitivity to previous summer SPEI (ANOVA, $F_{6,12}$=3.63, P=0.03); *Pseudotsuga* and *Larix* were more sensitive in stem growth responses to previous summer SPEI compared to *Tsuga* species (Table 2.2, Fig. 2.2). Stem diameter growth was significantly phylogenetically conserved (K=0.55, P=0.04) (Table 2.4), although the main genera/phylogenetic groups did not significantly differ in their stem diameter growth (ANOVA, $F_{6,12}$=2.08, P=0.13), whereas stem area growth and stem mass growth did not show any phylogenetic signal (Table 2.4). Overall, these phylogenetic trends were relatively weak, indicating that stem growth sensitivity to climatic factors and growth potential are relatively labile.

Table 2.4 Phylogenetic signal of growth sensitivity to spring frost, summer drought, winter temperature and growth potential for 19 conifer species. Growth potential refers to stem diameter growth (cm/yr), stem area growth (cm^2/yr), standardized stem area growth (cm^2/cm/yr), and stem mass growth (kg/yr/m). Significant values (P<0.05) are shown in bold, and indicate that growth sensitivity is phylogenetically conserved.

Phylogenetic trait	Blomberg's	
	K value	*P* value
Growth sensitivity to spring frost	**0.87**	0.003
Growth sensitivity to previous SPEI	**0.78**	0.008
Growth sensitivity to current SPEI	0.34	0.39
Growth sensitivity to winter temperature	0.44	0.17
Stem diameter growth during whole period	0.27	0.67
Stem diameter growth for the first twenty years	**0.55**	0.04
Stem area growth	0.28	0.59
Standardized stem area growth	0.20	0.90
Stem mass growth	0.25	0.70

2.4 Discussion

We analyzed how 19 conifer species that were planted in a common garden experiment and growing under a mild maritime climate differed in their growth responses to winter

temperature, spring frost and summer drought over 44 years. Almost all species showed a significant reduction in their stem growth in response to summer droughts, but the magnitude of this response varied 4-fold across species (Table 2.2). About one-third of the species showed the expected reduced stem growth with more frost days during spring (37%), or increased stem growth with a higher mean winter temperature (32%). We found no positive relation between stem growth potential and growth sensitivity to climate across species (Table 2.3). Here, we will discuss how selected climate factors and phylogeny affect the annual variation in stem growth of conifer species, and the possible implications of climate change for the future productivity and resilience of conifer species and forests.

2.4.1 Summer droughts

It was expected that even under mild maritime conditions, with an on average evenly distributed rainfall regime, summer droughts would reduce stem growth of nearly all conifer species. Most of the studied conifer species (89%) indeed showed reduced stem growth in response to summer droughts during the growing season and, to a lesser extent (32%), during the previous growing season (Table 2.2). Summer droughts were expected to reduce stem growth because trees avoid excessive water by closing their leaf stomata, resulting in reduced gas exchange, photosynthetic carbon gain and ultimately also stem growth (Sala *et al.*, 2010). For similar climate conditions, such growth rate reductions were also observed for broadleaf species (Weemstra *et al.*, 2013). The effect on stem growth may also result from low stem water potentials that come with dry conditions, hamper cell division and cell expansion, and limit stem growth (Cuny & Rathgeber, 2016). Alternatively, trees may shift their allocation of carbohydrates from stem growth towards the formation of new roots for increasing water uptake (Markesteijn & Poorter, 2009; Oberhuber *et al.*, 2017; Huang *et al.*, 2018), or towards the storage of non-structural carbohydrates (NSC) to facilitate future growth when environmental conditions are more benign (Piper *et al.*, 2017).

The growth sensitivity to summer droughts expressed by the regression coefficients - varied 4-fold across species (Table 2.2). *Picea abies* and *Tsuga diversifolia* were amongst the most drought sensitive species. These species may possess shallow roots that only absorb water from the topsoil (Schmid & Kazda, 2001; Bolte & Villanueva, 2006; Takahashi & Obata, 2014), and face therefore high risks to encounter dry conditions during rainless periods. Another drought sensitive species was *Larix kaempferi* (Table 2.2). *L. kaempferi* is a winter deciduous conifer and has the largest tracheid size (i.e., 16.0±0.4 µm), thinnest wall thickness (2.1±0.2 µm), largest specific leaf area (120.3±6.0 $cm^2\ g^{-1}$) and smallest leaf density (0.2±0.03 $g\ cm^{-3}$) among the 19 conifer species in our study (Song et al. unpublished data). These acquisitive traits contribute to fast carbon gain and photosynthesis but come at the expense

of high water loss and hence, a reduced cavitation resistance to drought (Chave *et al.*, 2009). The two least drought sensitive species were *Abies grandis* and *Abies veitchii* (Table 2.2). Their weak response to summer drought could be related to their timing of cambial activity with high growth rates early in the growing season (Cuny *et al.*, 2012), because the effects of drought were largest when droughts occurred during the stem growing season peaks (D'Orangeville *et al.*, 2018). The cambial activity of these two species deserves therefore further study. Additionally, the deep root system of *Abies grandis* probably may allow the species to acquire water from deeper soil layers during dry periods and be less drought sensitive (Xu *et al.*, 1997). The fact that species showed a 4-fold difference in stem growth sensitivity to summer drought means that species selection is key to create future forests that are more drought resilience under future climate change.

2.4.2 Winter temperature and late spring frost

The 19 conifer species differed in their stem growth responses to winter temperature. For six out of the 19 study species (32%), we observed that warmer winter conditions significantly favoured stem growth in the following growing season. The relation was particularly strong for *Cryptomeria japonica* and *Taxus baccata* (Table 2.2). These species probably increase metabolic rates at higher winter temperatures and thus extend the growing season length, with either increasing photosynthesis facilitating plant growth or benefitting from stored carbohydrates fuelling stem diameter growth during favourable winter temperatures (Huang *et al.*, 2010; D'Orangeville *et al.*, 2016; Puchi *et al.*, 2019). However, four of the 19 species (21%), i.e., *Larix* and three *Picea* species, showed the opposite response as they reduced stem growth with higher winter temperatures (Table 2.2). These four species were also negatively affected by spring frosts (Table 2.2). Possibly, for these species early growth initiation during higher winter temperatures creates more risk of being injured by spring frosts (Vitasse *et al.*, 2019), which then ultimately leads to the observed negative effects of higher winter temperatures for these four species. Additionally, the shallow-rooted *Picea* species (Blackwell *et al.*, 1990; Schmid & Kazda, 2001; Park *et al.*, 2012) may experience water shortage during transpiring when the topsoil is frozen. These divergent effects of winter conditions are remarkable. However, the mechanisms behind the observed patterns remain speculative and require further in-depth study (e.g., Eysteinsson *et al.* (2009)). Nevertheless, our results indicate that high winter temperature affects conifer stem growth, but in contrasting ways for different species.

Seven out of the 19 species (37%) reduced growth with an increasing number of spring frost days (Fig. 2.1a, Table 2. 2), although the majority of species did not show this expected response. Especially *Picea omorika* and the deciduous *Larix kaempferi* were sensitive to spring

frost. Reduced stem growth with spring frost was also found for trees in other temperate lowland coniferous forests (DeSoto *et al.*, 2014; Shestakova *et al.*, 2016). Normally the effects of spring frost on growth are quantified by the degree-days > 5°C until last frost < -2°C, since damaging frost events are more harmful after prolonged warm periods (Vitasse *et al.*, 2019). The mild maritime climate in our study area makes it difficult to use the same method with Vitasse *et al.* (2019) to quantify such kind of frost days , whereas the frost days (minimum temperature <0 °C) in this study still physiologically affects stem growth.

We did not find any tissue damage at the beginning of the tree rings, which indicates that cell formation either did not start yet or was well underway. Yet, we found tissue damages in the xylem of some branch samples used for another study we conducted on the same trees, which can indicate that branches were affected by frost events prior to the period when wood formation stared in the lower stem parts. Conifer species can still maintain their cambial activity in February and March with low *minimum* temperature (< 0°C), see Begum *et al.* (2010). Moreover, it was recorded that the temperature of cambial activity (i.e. production of new cells) for conifer species varied between 10–14 °C for *maximum* air temperature (Rossi *et al.*, 2008). In our study site, the conifer species had already experienced high maximum temperature between 10-14 °C in January or February. It is very likely that species has already started the cambial activity and they are going to be affected by the frost days in March and April. Hence, the spring frost may reduce the cambial activity and growth. In addition, spring forst may damage buds and delaying the start of the growing season for leaf-out (Zohner *et al.*, 2020), or probably causing freezing-induced cavitation of newly formed tracheids and thus impairing water transport (Pittermann & Sperry, 2003), or leading to stomatal closure or desiccation and tissue loss in the leaves (Davis *et al.*, 1999; Mayr *et al.*, 2006) resulting in a decline in photosynthetic activity and carbon gain (Augspurger, 2011; Vitra *et al.*, 2017). Although such mechanisms are poorly studied, this suggests that species differences in timing of stem growth and leaf or cambial phenology may be important for explaining species differences in sensitivity to spring frost.

2.4.3 Are species with a high growth potential also more sensitive to climatic variation?

We hypothesized that species with a high growth potential would also be more sensitive to climatic variation. It was assumed that traits associated with high inherent growth rates, such as large cells with thin cell walls that facilitate high metabolic activity, would lead to a higher sensitivity to extreme climate events such as spring frost or summer drought. However, we only observed a weak pattern that contrasted with the expected positive relationship, since stem diameter growth and growth sensitivity to summer drought were negatively – and not positively – associated (r=-0.40, P=0.08) (Fig. 2.3, Table 2.3). Particularly *Abies grandis*

combined a large growth potential with high tolerance to climate extremes, as shown by the low impact of spring frost and summer drought on stem growth of this species (Fig. 2.1). Among all investigated species, *Abies grandis* had the second-largest tracheid diameter (14.0±0.8 µm) (Song et al. unpublished data), which allows the species to have a high hydraulic conductivity, high transpiration rates and photosynthetic rates, and thus a large wood production (Chave *et al.*, 2009). Possible detrimental effects of climate extremes could be counterbalanced by the high stomata conductance even during drought (Puritch, 1973) or the potentially deep roots that can assure water uptake from deeper soil layers under dry conditions (Foiles, 1959; Xu *et al.*, 1997). Also, the relatively mild maritime climate in our study site, creates favorable growing conditions during large parts of the growing season and may have resulted in a weaker relationship between growth potential and climate sensitivity for our study species. Overall, our study implies that for a given site, forest managers have the option to select and plant conifer species that combine a high growth rate with a high tolerance to summer droughts. This is an important prerequisite for designing climate-smart forests for the future (Nabuurs *et al.*, 2018) that combine a high productivity with a large carbon storage potential and strong drought resilience.

2.4.4 Is growth potential of conifers phylogenetically conserved?

Since conifers radiated in recent evolutionary times into different habitats (Zanne *et al.*, 2014), we hypothesized that the growth potential and climate sensitivity of the growth of conifer species are phylogenetically weakly conserved. Although weak, we nevertheless found some indications for phylogenetical control of stem growth (Table 2.4, Fig. 2.2) and that, for example, *Abies* and *Picea* species grow faster than *Taxus* species. In our common garden experiment established under maritime climate conditions, *Abies grandis* was the fastest-growing species, with an average radial stem growth rate of 0.61 cm per year, while the two most slow-growing species were *Taxus baccata* (0.20 cm/yr) and *Taxus cuspidata* (0.19 cm/yr) (Fig. 2.2). *Abies grandis* can grow fast because it has fast-growth traits, such as relatively wide tracheids, high specific leaf area and high photosynthetic rates compared to other species (Song et al. unpublished results). *Taxus* has very dense and heavy wood with narrow tracheids and dense wood, which tend to reduce growth rates (Thomas & Polwart, 2003). Overall, species differences in productivity are only partially phylogenetically controlled.

2.4.5 Is growth sensitivity to climate of conifers phylogenetically conserved?

Of the five seasonal potentially growth-limiting climate conditions, only the growth sensitivity to spring frost and previous summer water availability (summer SPEI) were found to be phylogenetically controlled (Table 2.4). *Larix kaempferi* and several *Picea* species particularly

decreased stem growth in response to spring frost (Fig. 2.2) and each species might be sensitive for a different reason. First, *Larix kaempferi*, a winter deciduous species, normally starts to open buds in early May and it takes three weeks to fully extend leaves (Hirano *et al.*, 2003; Nakagawa, 2020). The late spring frosts between March and April in our study area may damage larch buds, consequently, limit leaf expansion and reduce growth. The probably earlier timing of leaf flush for larch owing to global warming may thus maintain such spring frost risks for this species. Second, *Picea omorika* showed the second strongest negative growth response to spring frosts (Fig. 2.2, Table 2.2), while it has been considered tolerant (Dallimore, 1937). Possibly, the contrast between its natural distribution restricted to the banks of the river Drina in South-Eastern Europe and the water-drained sandy soils affect the phenology of the species and cause high late spring frost risks (Dallimore, 1937; Schmidt, 1999). Third, for *Picea abies*, the low frost resistance may be related to a reduced solute concentration of the cell sap (i.e., much less negative osmotic potential at full saturation), reducing the osmotic potential and increasing freezing and damaging ice crystal formations in stem cells (Santarius, 1973; Neuner & Beikircher, 2010). Fourth, for *Taxus* species, it is known that a high content of leaf mucilages can cause strong water-binding and prevent frost damage (Distelbarth & Kull, 1985). Overall, our results imply that early production of leaves in combination with high sensitivity to winter frost may cause stronger stem growth reductions for *Larix*, *Picea*, *Pseudotsuga menziesii* compared to, for example, *Taxus* and *Abies.*

Remarkably, growth sensitivity to previous summer SPEI seems to be phylogenetically controlled, whereas growth sensitivity to current summer SPEI is not phylogenetically controlled (Table 2.4). *Larix* and *Pseudotsuga* belong to the same phylogenetic clade, and both species significantly increased their stem growth in response to previous summer SPEI, possibly as a result of the strategy to increase carbohydrate storage for the next year or the formation of more leaf buds for the following year. In contrast, *Tsuga* species (Fig. 2.3) – and particularly *Tsuga diversifolia* (Table 2.2) – reduced their stem growth in response to previous summer rain, for which we do not have a clear explanation.

2.4.6 Implications for forest management under climate change

Climate change scenarios predict a warmer, drier and more variable climate for Europe (e.g. (Ballester *et al.*, 2010). Warmer spring conditions can induce an earlier start of the growing season, which advances stem and leaf phenology, with increased risks of damage by late spring frosts (Vitasse *et al.*, 2018). Given that all 19 conifer species in our common garden experiment reduced stem growth with reduced water availability during summer and 37% of species reduced stem growth with more spring frost, a warmer future climate likely reduces the productivity of conifer species and forests. This not only applies to the maritime climate

of our northwest European study site, but also to many other regions in the Northern hemisphere (Hogg *et al.*, 2002; Montwé *et al.*, 2018). Our study nevertheless implies that forest managers can design relatively climate-smart forests by favoring those species that combine a high growth rate with a positive response to winter warming (e.g., *Tsuga heterophylla*), or low sensitivity to spring frost (e.g., *Abies grandis*) or summer drought (e.g., *Abies grandis*) for temperate maritime climate conditions. While such species choices likely depend on local-specific site conditions, comparative information on stem growth responses to climate can help create productive and resilient forests for a warmer and drier future.

ACKNOWLEDGEMENTS

We are very grateful to Jop de Klein and Els van Ginkel from Schovenhorst estate for supporting this study; Allan Buras, Chenxuan Li, Ellen Wilderink, Matteo Dell'Oro, Xiaohan Yin, Zulin Mei, and Zexin Fan for assistance with fieldwork and lab work, Jose Medina Vega and Masha T. van der Sande for help with statistics. We thank Paul Copini for his suggestions on the impacts of frost on stem growth and are grateful to two anonymous reviewers for their helpful comments.

FUNDING

The study was supported by the Oudemans Foundation, and Yanjun Song was supported by the China Scholarship Council (CSC, No.201706140106).

Supplementary information

Table S2.1 Summary statistics related to cross-dating are provided for 19 conifer species.

Species	Period considered	Mean ring width (sd) (mm)	Rbar	EPS	MS
Abies alba	1958-2018	4.73 (2.16)	0.239	0.787	0.280
Abies grandis	1940-2017	4.36 (2.47)	0.242	0.821	0.275
Abies veitchii	1979-2018	3.00 (1.72)	0.405	0.881	0.390
Chamaecyparis lawsoniana	1911-2017	3.21 (1.58)	0.336	0.807	0.360
Cryptomeria japonica	1969-2018	3.20 (1.82)	0.443	0.901	0.406
Larix kaempferi	1945-2018	2.93 (1.48)	0.607	0.953	0.450
Picea abies	1969-2018	3.99 (1.58)	0.426	0.907	0.277
Pinus armandii	1981-2018	2.97 (1.30)	0.322	0.874	0.255
Pinus nigra	1945-2018	2.44 (1.18)	0.302	0.867	0.264
Picea omorika	1953-2018	2.75 (1.28)	0.316	0.813	0.301
Picea orientalis	1944 -2017	3.03 (1.58)	0.46	0.915	0.302
Picea sitchensis	1972 -2018	4.65 (1.65)	0.279	0.848	0.222
Pseudotsuga menziesii	1916-2017	3.68 (1.69)	0.402	0.867	0.311
Taxus baccata	1957-2018	2.15 (0.85)	0.48	0.900	0.284
Taxus cuspidate	1974 2018	1.62 (0.71)	0.341	0.834	0.252
Thuja plicata	1942-2017	4.02 (236)	0.329	0.861	0.414
Tsuga canadensis	1972-2018	3.39 (1.59)	0.315	0.751	0.199
Tsuga diversifolia	1972-2018	2.70 (1.24)	0.435	0.884	0.278
Tsuga heterophylla	1971-2017	4.87 (2.20)	0.282	0.850	0.284

Rbar indicates interseries correlation, EPS indicates expressed population signals, MS indicates sensitivity.

Table S2.2 Species-specific R^2 was calculated from the square of correlations between the predicted tree ring index (based on the multiple regression in Table 2.2) and the observed tree ring index. R^2ind indicates species-specific R^2 based on the individual level and R^2sp indicates species-specific R^2 based on mean chronology (i.e., species) level.

Species	R^2ind	R^2sp
Abies alba	0.044	0.121
Abies grandis	0.067	0.185
Abies veitchii	0.010	0.019
Chamaecyparis lawsoniana	0.080	0.173
Cryptomeria japonica	0.196	0.368
Larix kaempferi	0.226	0.304
Pinus armandii	0.054	0.089
Pinus nigra	0.141	0.280
Picea abies	0.199	0.360
Picea omorika	0.195	0.460
Picea orientalis	0.172	0.268
Picea sitchensis	0.197	0.372
Pseudotsuga menziesii	0.134	0.262
Taxus baccata	0.277	0.524
Taxus cuspidate	0.112	0.197
Thuja plicata	0.022	0.050
Tsuga canadensis	0.087	0.185
Tsuga diversifolia	0.107	0.207
Tsuga heterophylla	0.167	0.336

Fig. S2.1 Climate change of the De Bilt weather station, the Netherlands: (a), monthly mean precipitation (bars) and temperature (line) over the common period 1974–2017; (b), annual mean temperature over the period from 1901 to 2018; (c) annual aggregate frost days over the period from 1901 to 2018. Regression lines and 95% confidence intervals (grey), coefficients of determination (R^2) and *P*-value are shown.

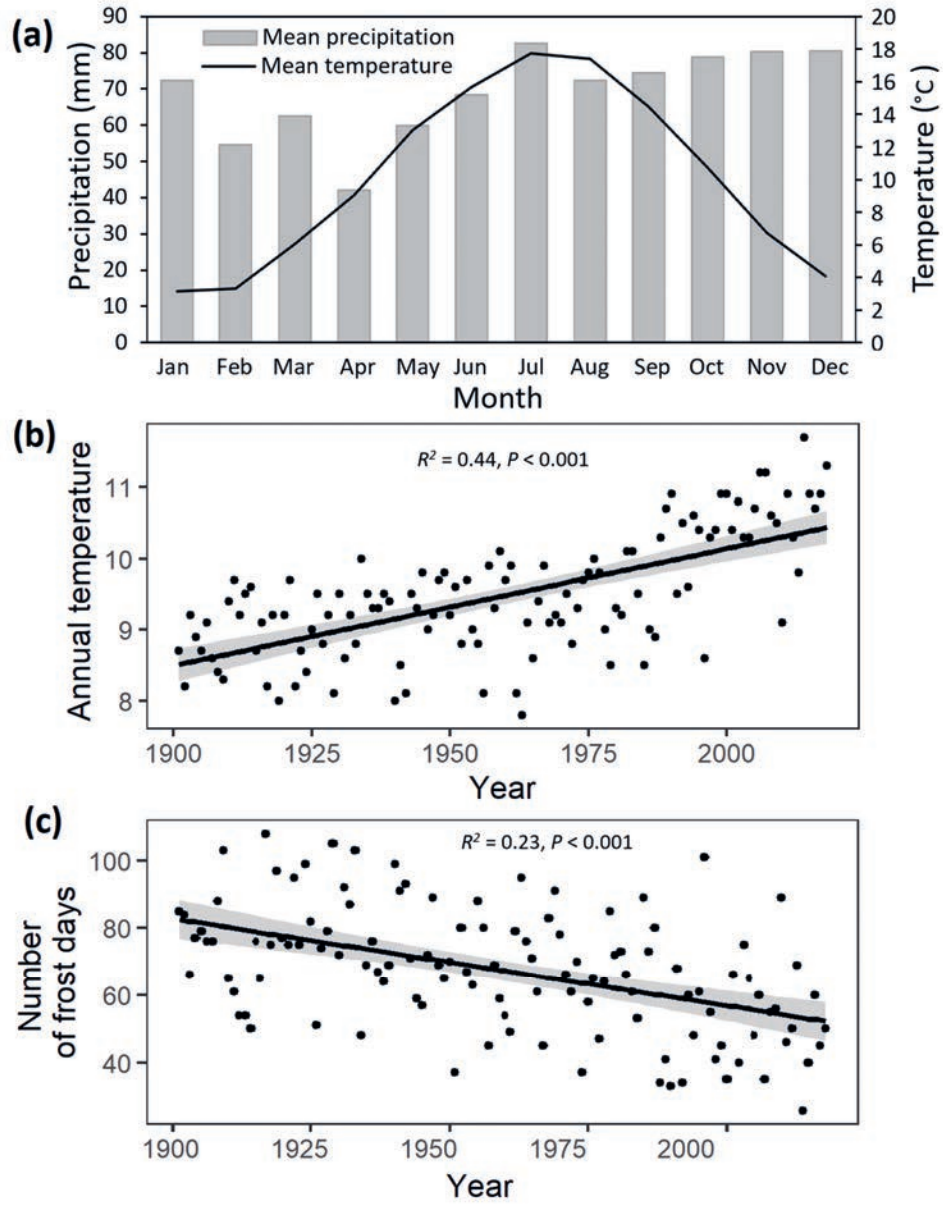

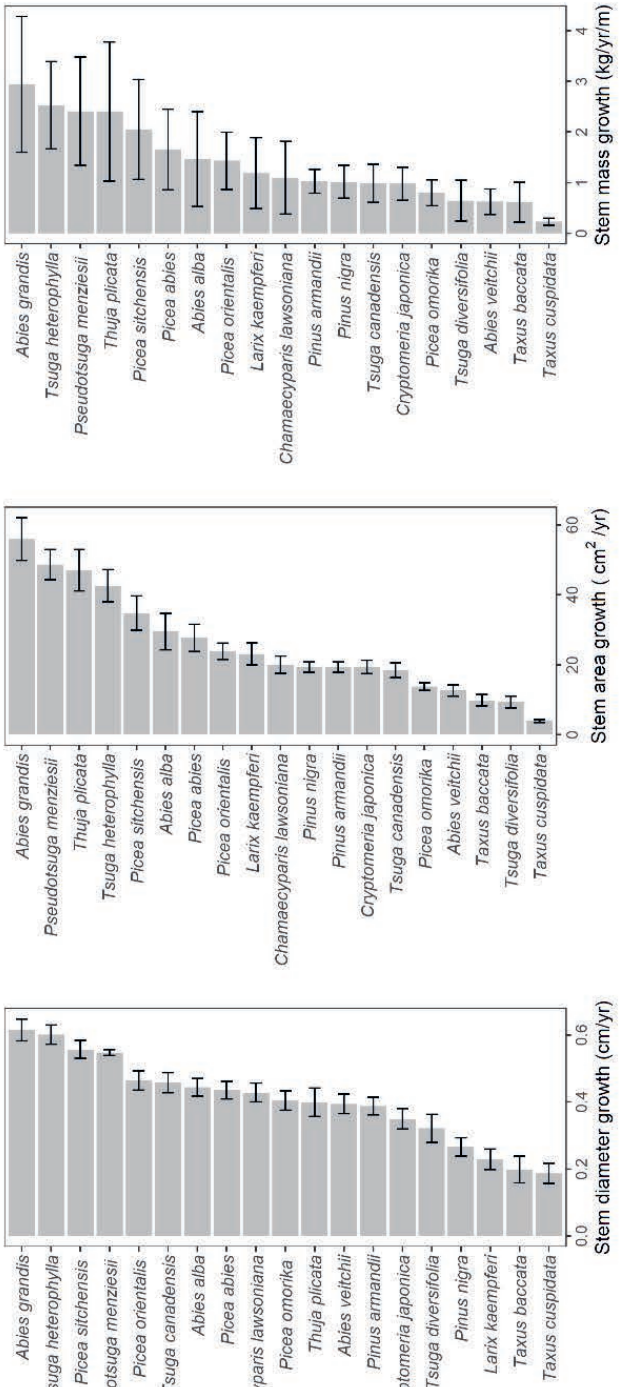

Fig. S2.2 Alternative proxies of stem growth potential for 19 conifer species for a) stem diameter growth (in cm) based on first twenty years, b) stem area growth (in cm^2/cm) over the period between 1911-2018 (*C. lawsoniana*) and 1981-2018 (*P. armandii*), c) stem mass growth (in kg yr^{-1} m^{-1}) calculated from stem area growth and wood density. Error bars (± standard error of the mean value) are shown.

Fig. S2.3 Relationships between cumulative growth and ages for a) cumulative ring width and the whole period, b) cumulative ring width and the first twenty years, c) cumulative basal area and the whole period, d) cumulative basal area and the first twenty years.

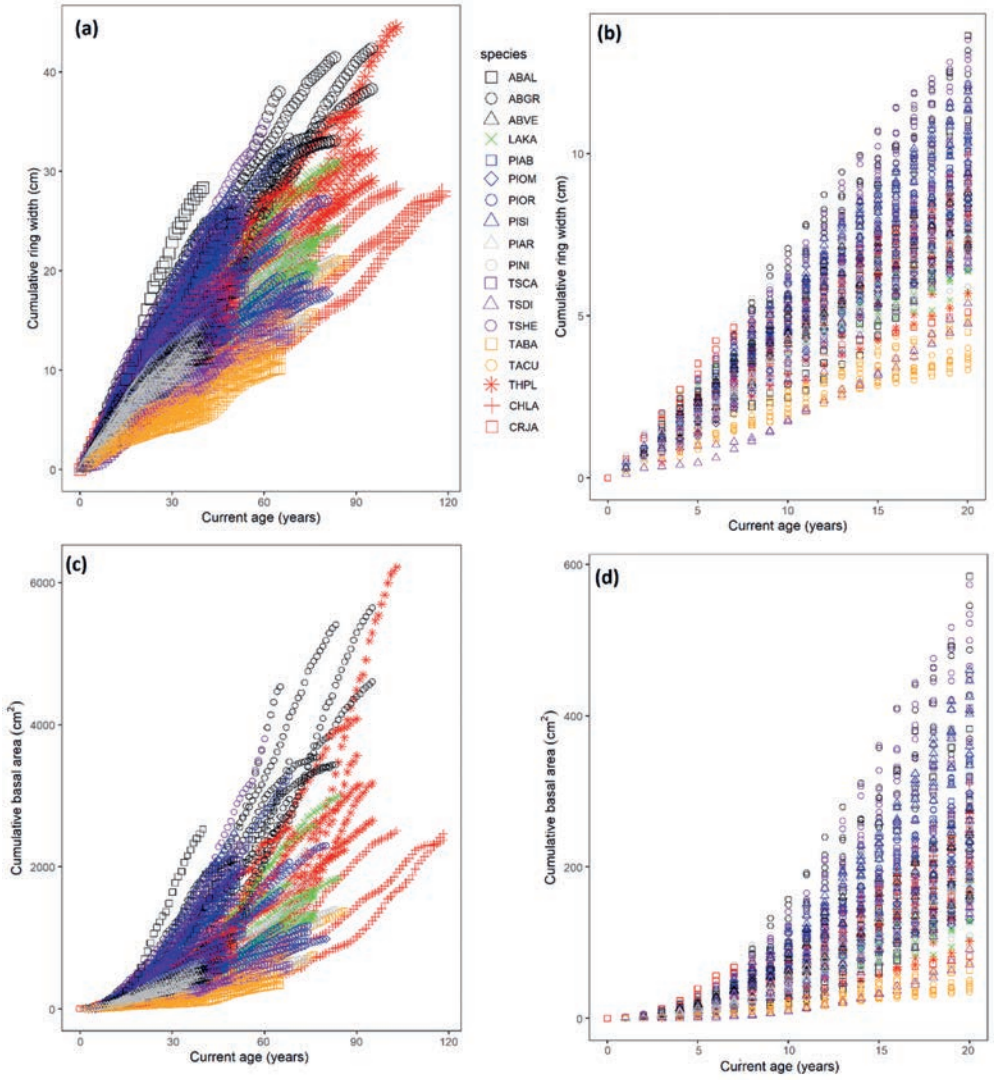

Fig. S2.4 Relationships between stem diameter growth for the first twenty years when climate factors were included and excluded from the model.

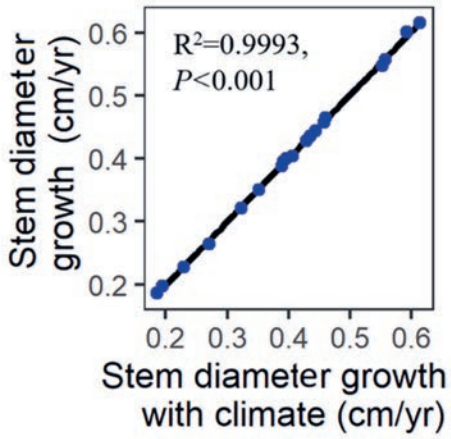

Fig. S2.5 The plots for residuals in the mixed model for growth potential for a) a Q-Q (quantile-quantile) plot, b) a residual plot, c) a frequency diagram for the residuals.

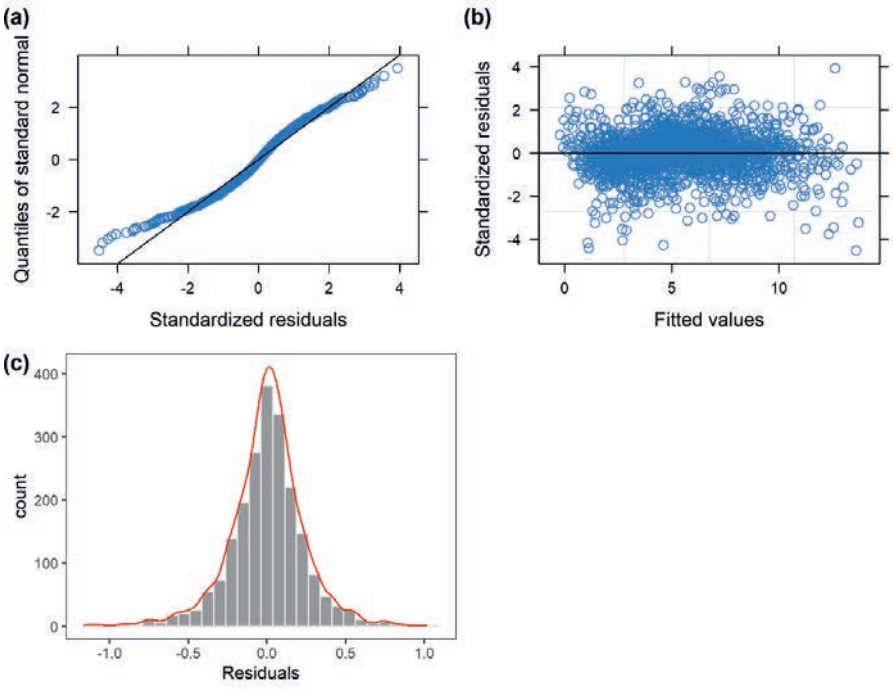

Fig. S2.6 The plots for residuals in the mixed model for growth sensitivity for a) a Q-Q (quantile-quantile) plot, b) a residual plot, c) a frequency diagram for the residuals.

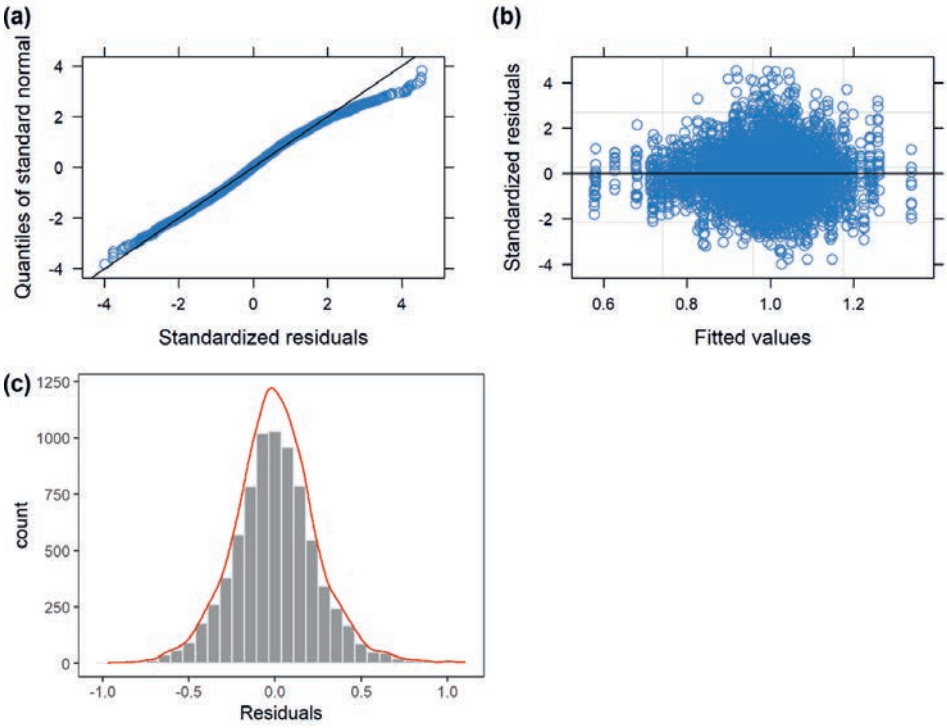

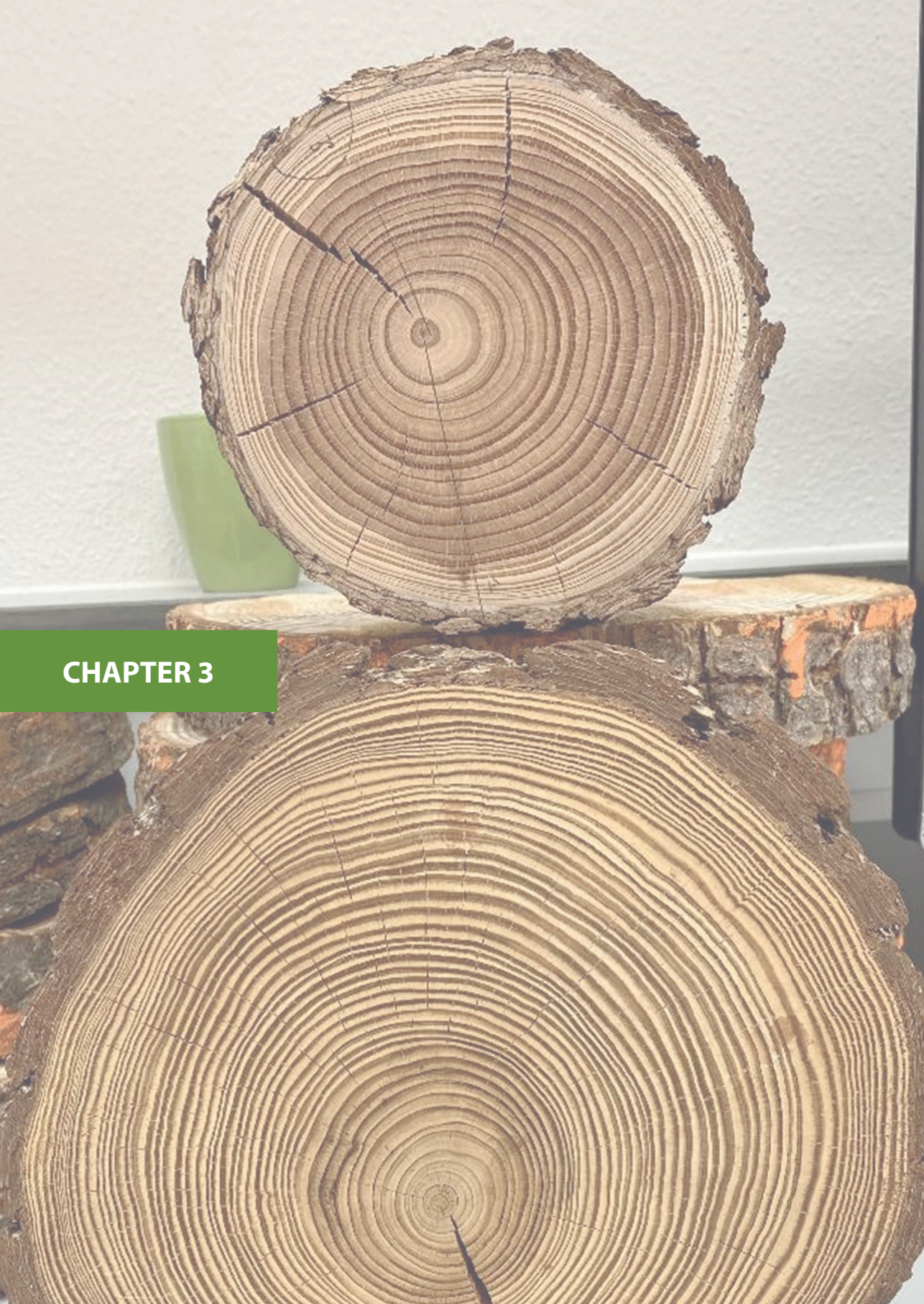

CHAPTER 3

3

Drought resilience of conifer species decreases with early, prolonged and intense droughts and cannot be explained by hydraulic traits

Yanjun Song, Frank Sterck, Ute Sass-Klaassen, Chenxuan Li, Lourens Poorter

Abstract

- Increased drought events reduce growth and survival of conifer species, thus potentially reducing the terrestrial carbon stock. Predicting drought resilience of conifer species is difficult because drought consists of multiple dimensions.
- Drought resilience of 20 conifer species to 11 dry years was compared in a common garden experiment. We assessed 1) relationships among resistance, recovery and resilience, 2) impacts of drought dimensions on resistance, and 3) the underlying mechanisms in terms of growth potential and hydraulic traits.
- Droughts led to 22% reduction in stem growth for 90% of species, but most species (80%) were resilient due to high recovery. Drought resistance decreased with early (significant for 65% of species), prolonged (60%) and intense droughts (55%). Unexpectedly, resilience could not be explained by hydraulic traits and growth potential, possibly because the species grew on poor sandy soils and were acclimated to drought with large hydraulic safety margins.
- Our study shows that in a mild maritime climate almost all conifer species are resilient to drought, and that putative hydraulic traits may be less important for drought resilience. It also highlights the importance of addressing multiple dimensions of drought, i.e. timing, duration and severity to predict species responses to climate change.

Keywords:
conifer species, drought duration, drought severity, drought timing, hydraulic traits, recovery, resilience, resistance

3.1 Introduction

3.1.1 Effects of drought on forests

Climate change threatens forest ecosystems worldwide as an increased frequency and intensity of summer droughts (IPCC, 2013) reduces tree growth and survival (Buras *et al.*, 2020; DeSoto *et al.*, 2020). For example, the extreme dry summer of 2003 greatly reduced the gross primary productivity of European forests, turning those forests from a carbon sink into a carbon source (Ciais *et al.*, 2005b). The summer drought of 2018 resulted in more than 100 million m^3 of wood from dead trees in Europe alone, indicating not only a large loss of living biomass and carbon sequestration potential but also of future timber supply (Nabuurs *et al.*, 2018).

Conifers, which dominate large areas in temperate and boreal forest biomes, have drought adaptations such as needle-type leaves that reduce evapotranspiration and narrow conduits with typical margo-torus pits within most conifers that resist cavitation. Conifers show nevertheless strong reductions in growth and survival to droughts (Lévesque *et al.*, 2013; Truettner *et al.*, 2018), possibly because of hydraulic failure and carbon starvation (Adams *et al.*, 2017). To model and predict forest responses to drought, broad-scale comparative studies are needed to quantify the drought resilience of conifer species and underlying mechanisms. Here we screen a large and phylogenetically diverse group of 20 conifer species for their growth resilience to drought. We do so by 1) comparing trees growing under similar conditions in a 50-year-old common garden experiment, 2) analyzing drought resilience in terms of its underlying components (drought resistance and drought recovery) (cf. (Vitali *et al.*, 2017)) and 3) relating their resilience to three key hydraulic traits that are thought to govern species responses to drought.

3.1.2 Drought resilience is driven by resistance and recovery

Dendrochronology provides an ideal tool to track growth responses to drought over multiple decades (Camarero *et al.*, 2018). Drought resilience is defined as the ability of a tree to recover stem growth after a drought event (Lloret *et al.*, 2011), which consists of two components; drought resistance and drought recovery. Drought resistance implies the capacity to maintain growth during drought, and drought recovery indicates the ability to regrow after drought (Depardieu *et al.*, 2020). Hence, species can adopt two contrasting strategies to deal with drought; either showing a high resistance with only limited need for recovery, or showing a low resistance followed by a strong recovery afterwards (Gazol *et al.*, 2017). Conifers are known for their strong reductions in growth during drought years (e.g. DeSoto *et al*. 2020) but also for their quick recovery after such years (Vitasse *et al.*, 2019; Gazol *et al.*, 2020). Recent studies have shown species differences in this respect. For example, *Abies alba* and

Pseudotsuga menziesii mainly rely on high resistance (Vitali *et al.*, 2017) whereas *Picea glauca* and *Pinus* species mainly rely on high recovery (Gazol *et al.*, 2017; Depardieu *et al.*, 2020). The physiological mechanisms underlying such species differences are however poorly tested because most studies focus on few species only, or did not measure species-specific plant traits (Bréda & Badeau, 2008; Martin-Benito *et al.*, 2017) such as hydraulic traits, that could underly differences in drought resilience.

3.1.3 Limitations in studying drought resilience

Many dendrochronological studies focus on synchronous stem growth reductions during specific dry 'pointer' years (Vitasse *et al.*, 2019). These studies focus on few years with reduced stem growth, but cannot compare the effects of drought dimensions on resilience, such as the frequency, timing, duration and severity of droughts. Negative effects on growth are expected when droughts are frequent, occur early in the growing season, are longer, or become severe (Güney *et al.*, 2017; D'Orangeville *et al.*, 2018; Gao *et al.*, 2018). However, assessments of these multiple dimensions of droughts on resilience simultaneously are largely missing. Better quantification of these drought components will allow for a better prediction of tree growth and forest carbon storage under climate change (D'Orangeville *et al.*, 2018). Here we will use a water balance approach (Gao *et al.*, 2018) to assess how the timing, duration and severity of drought affect stem growth responses of 20 conifer species.

3.1.4 Hydraulic traits and drought resilience

To facilitate tree species selection for a drier future, and to improve forest models and climate change predictions, a better understanding of the physiological mechanisms that underly drought resilience is needed (Pan *et al.*, 2011; Nabuurs *et al.*, 2017; Choat *et al.*, 2018). Plant responses to drought are mediated by a suite of anatomical, morphological, and physiological hydraulic traits related to water uptake, transport, storage, use, and loss (Choat *et al.*, 2018). Recent meta-analyses indicate that tree mortality during drought is often preceded by hydraulic failure due to drought-induced cavitation and, in the case of conifers, also by carbon depletion (Adams *et al.*, 2017). Hydraulic failure is often captured when species have more negative water potential than P_{50}; the xylem potential of which 50% of hydraulic conductivity is lost (Adams *et al.*, 2017). Yet, cavitation resistance could not predict the growth response to drought of the 13 most abundant conifer and broadleaved species from Eastern North America (D'Orangeville *et al.*, 2018). Similarly, species that have a wide hydraulic safety margin (i.e., the difference between minimum leaf water potential and P_{50} in the twigs supporting the leaves) better survive droughts (Anderegg, WR *et al.*, 2018; Li *et al.*, 2020). In contrast, the

ability of plant to recover after drought might be associated with a high hydraulic conductivity (Ks), as this is associated with high stomatal conductance, assimilation, and growth (Santiago *et al.*, 2004).

Apart from hydraulic traits, plant size can modify tree responses to drought. Large trees are more sensitive to drought (Bennett *et al.*, 2015), although they have deeper roots to obtain water from deeper soil layers, and larger carbohydrate reserves that allow them to persist during drought and recover after drought. Perhaps large trees experience more drought stress because their crowns are more exposed to high irradiance and vapor pressure deficits leading to stomatal closure impairing carbon gain and potentially leading to carbon depletion, whereas the longer hydraulic pathlengths make them more sensitive to cavitation to drought (Ryan *et al.*, 2006).

It remains controversial whether and how hydraulic traits can affect the growth resilience of trees to drought. One of the possible reasons is that these studies have focused on broad-scale geographic patterns and species-level traits, and the observed growth responses may be potentially confounded by acclimation responses to local conditions. Here we aim to advance on previous studies, by using a common garden experiment where tree species grow under similar environmental conditions (for soil and climate), and respond to the same annual variation in drought during 11 extremely dry years. This allows us to better test the effects of hydraulic traits on stem growth resilience than earlier studies, because confounding effects of environment and acclimation are avoided. We addressed the following questions and hypotheses:

1) How do drought resistance and drought recovery drive the growth resilience of conifer species? We expect that most species will be resilient to dry years, but in different ways. Some species will be more drought-resistant (showing minor stem growth reductions in response to drought), whereas other species may show strong growth reductions but also large recovery in the years following a dry year.

2) How is drought resistance affected by the timing, duration, and severity of a drought event? Trees are expected to show stronger stem growth reductions (lower resistance) with early prolonged, and severe droughts: early droughts likely hit during the period of maximum growth activity (Güney *et al.*, 2017); prolonged droughts may lead to stomatal closure and carbon starvation whereas intense drought may lead to hydraulic failure (McDowell *et al.*, 2008; Adams *et al.*, 2017). In addition, all these effects may be stronger for larger trees because the longer hydraulic path results in earlier stomatal closure and increases the risk of hydraulic failure.

3) Why do conifer species differ in their resilience to droughts? We predict that fast-growing species show stronger growth reductions in drought years (lower resistance) but also stronger recovery after drought years than slow-growing species. We expect that high cavitation resistance and hydraulic safety margins favor drought resistance (Delzon & Cochard, 2014), whereas high hydraulic conductivity will favor fast growth and drought recovery.

3.2 Materials and Methods

3.2.1 Species selection and tree-ring data

To assess the resilience of conifer species to drought events, we took advantage of a common garden experiment at the Schovenhorst Estate (52.25 N, 5.63 E), Putten, the Netherlands. The site has a mild maritime climate with a mean annual temperature of 10.1°C and mean annual rainfall of 830 mm y^{-1} and is situated on loamy and sandy soils (Cornelissen *et al.*, 2012).

In the common garden experiment monospecific stands were established in the 1960's to screen conifer species for their productivity. No management interventions such as thinning have been carried out in the stands. We selected 20 conifer species that are common in the Northern hemisphere (from North America, Eurasia, East Asia) and are commonly planted in Europe. The 20 species covers a wide diversity of phylogenetic groups (three families, and seven genera).

For each species 10 dominant individuals were selected. To reduce the confounding effects of ontogeny and environment, we tried to select trees of similar age, which occurred under similarly exposed environmental conditions in the canopy of the stand (Table 3.1). Because species differed in their growth rate and adult stature, the mean stem diameter at breast height varied from 14.8-76.9 cm across species.

From each tree, two perpendicular increment cores were taken at 1.3 m stem height using Haglof Pressler increment borers. Tree-ring width (TRW) was measured with 1/100 mm precision and time series were cross-dated to assign a calendar year to each ring using CooRecorder, CDendro and WinTSAP (v. 9.0, Cybis Electronik and Data AB, Sweden, Rinntech, Heidelberg, Germany). Cross-dating was done by first matching the ring-width patterns of individual trees, and then different trees of the same species. A total of 400 cores have been analysed for 20 conifer species, including the period 1974–2017 that was covered by most species. Two of these species, i.e., *Pinus armandii* and *Abies veitchii* were analysed from 1981 to 2017 (Table S3.1) because individuals were established after 1974. To assess the quality of chronologies, additional tree-ring statistics were calculated, such as expressed population signal (EPS) and inter-series correlation (Rbar) (Table S3.1).

Table 3.1 Overview of 20 conifer species, their distribution area, species abbreviation, the growth period considered, the average stem diameter at breast height (DBH) of the sampled trees (*N*=10 per species) in 2017/2018/2020, and the standard deviation (in parentheses). Distribution areas are derived from Farjon and Filer (2013).

Species	Distribution areas	Species abbreviations	Period considered	DBH (cm)
Abies alba	Europe	Ab.al	1958-2018	46.9 (10.3)
Abies grandis	North America	Ab.gr	1940-2017	76.9 (8.7)
Abies veitchii	Northern Honshu, Japan	Ab.ve	1979-2018	27.1 (3.1)
Chamaecyparis lawsoniana	North America (USA)	Ch.la	1911-2017	48.2 (9.6)
Cryptomeria japonica	Eastern Asia	Cr.ja	1969-2018	35.6 (6.2)
Larix kaempferi	Eastern Asia	La.ka	1945-2018	49.4 (6.8)
Pinus armandii	Eastern Asia	Pi.ar	1981-2018	24.0 (3.2)
Pinus nigra	South-Eastern Europe	Pi.ni	1945-2018	44.6 (6.5)
Pinus strobus	North America	Pi.st	1971-2020	51.0 (7.04)
Picea abies	Europe	Pi.ab	1969-2018	43.4 (5.2)
Picea omorika	Europe	Pi.om	1953-2018	30.9 (30.9)
Picea orientalis	Mainland Asia	Pi.or	1944-2017	47.7 (8.1)
Picea sitchensis	North America	Pi.si	1972-2018	44.5 (8.8)
Pseudotsuga menziesii	North America	Ps.me	1916-2017	76.3 (10.1)
Taxus baccata	Europe	Ta.ba	1957-2018	31.2 (9.9)
Taxus cuspidata	Mainland Asia	Ta.cu	1974-2018	14.8 (4.0)
Thuja plicata	North America	Th.pl	1942-2017	74.3 (12.7)
Tsuga canadensis	North America	Ts.ca	1951-2020	31.6 (4.8)
Tsuga diversifolia	Japan	Ts.di	1972-2018	25.3 (3.6)
Tsuga heterophylla	North America	Ts.he	1971-2017	53.2 (6.4)

3.2.2 The selection of SPEI and identification of drought years

We used the standardized precipitation evapotranspiration index (SPEI) to objectively identify drought years over the 1974-2017 period. SPEI reflected the water balance and was calculated for each month as the precipitation (in mm/mo) minus the potential evapotranspiration (PET, in mm/mo), and then summed over consecutive months for every year and standardized with probability function, see Vicente-Serrano *et al.* (2010). A positive value indicates a hydric surplus (i.e., a wet period), whereas a negative value indicates a hydric deficit (i.e., drought). Evapotranspiration was calculated from monthly temperature and latitude using Thornthwaite methods with R 'SPEI' package (Beguería *et al.*, 2017). Monthly temperature and precipitation were rederived from a local climate station (https://www.knmi.nl/nederland-nu/klimatologie/maandgegevens). Drought was identified with the value of SPEI reaching -1 and ending with positive values (Abbasi *et al.*, 2019). We identified drought years as years with SPEI≤-1 (Bose *et al.*, 2020).

To select the most related SPEI to tree growth responses and considering that mainly summer drought impaired tree growth (Song *et al.*, 2021), we tested different SPEI periods and timings and found the 4 months from June to September most influential on growth (Table S3.2). Over the period from 1974 to 2017, we identified 11 drought years where SPEI_Sep4 < -1 (Bose *et al.*, 2020); 1975, 1976, 1982, 1983, 1986, 1989, 1990, 1995, 1996, 2003 and 2013 (Fig. 3.1).

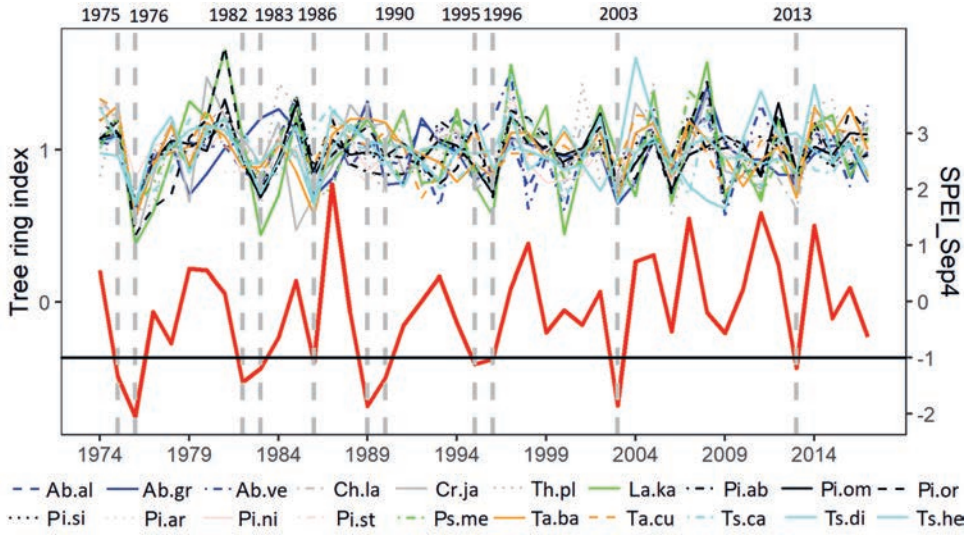

Fig. 3.1 Identification of drought years in the period from 1974 to 2017, based on the standardized precipitation evapotranspiration index (SPEI, red line). SPEI was calculated for each year for the 4 months period from June to September. The black horizontal line indicates the threshold to identify a drought year (SPEI <-1), and vertical dashed lines indicate the 11 drought years (shown at the top). The annual tree ring index of the 20 different tree species (each line is a different species) is shown at the top. Tree ring index was obtained from Song *et al.* (2021). For species abbreviations, see Table 3.1.

3.2.3 Drought indices

To assess how drought affects the growth-related resilience components, we used a water-balance method to quantify the timing of drought (i.e., the timing of drought onset and drought peak), drought duration and severity of drought (i.e., drought intensity, water deficit, annual cumulative water balance) for each of the 11 selected drought years (Fig. 3.2). The daily water balance was calculated as the difference between daily precipitation and daily evapotranspiration (https://www.knmi.nl/nederland-nu/klimatologie/daggegevens). To quantify the water availability for each drought year, we calculated the cumulative water balance (CWB, ml) by starting on the 1st of January and summing up daily water balances. The

drought onset was defined as the day of the year (DOY) when CWB became negative for the first time that year. The drought peak was defined as the calendar day when CWB was most negative during that year. Drought duration was defined as the number of days from drought onset until the day when CWB became positive again. Drought intensity (in ml) was quantified as the most negative value reached by CWB, and drought deficit (in ml) as the sum of daily CWB during the drought period. Using this intra-annual analysis, it turned out that two years that were identified as drought year based on the annual basis (SPEI4 September), i.e., 1983 and 1995, did not experience a negative cumulative water deficit (Fig. 3.2). The reason was too much rainfall accumulated in winter and spring, and hence accumulated relatively high and positive water balance in summer. These two years were hence excluded from further analysis on drought onset and drought duration. This resulted in 9 drought years used to assess how the timing, duration and severity of drought affect drought resistance, recovery and resilience (Fig. 3.2).

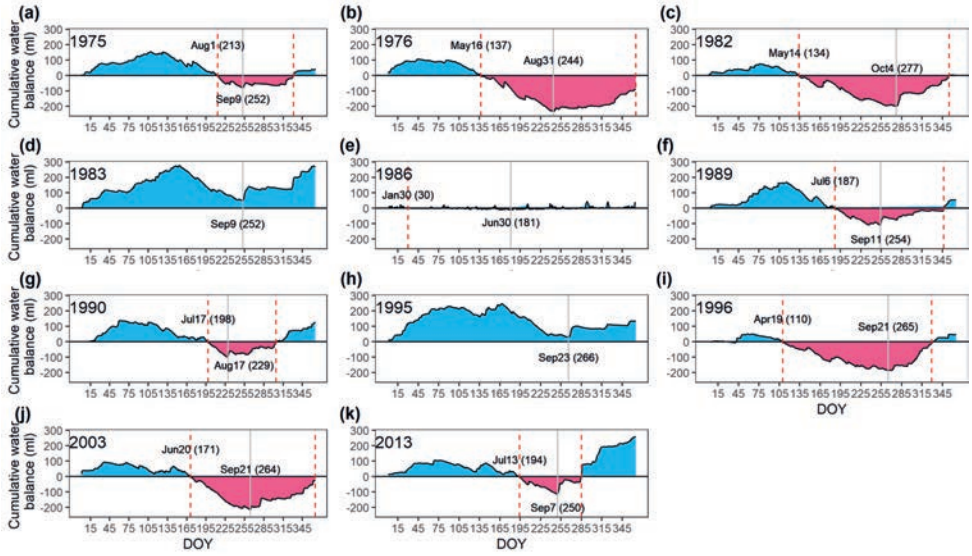

Fig. 3.2 Annual development of the cumulative water balance (CWB) for 11 drought years (a-k). DOY indicates the day of the year. The daily water balance is cumulatively summed starting from January 1st, resulting in wet periods with a hydric surplus (CWB >0, blue areas) and dry periods with a hydric deficit (CWB<0, red areas). The timing of drought is indicated as the drought onset (when the CWB becomes negative, first vertical dashed red line) and drought peak (moment of the most negative CWB, vertical grey line). Drought duration is indicated by the period between the two red lines. The corresponding calendar day is indicated (with Julian day in parentheses). The severity of drought is indicated as the drought intensity (most negative CWB corresponding to the grey line), water deficit (the

sum of negative CWBs in the period for the red area) and annual cumulative water balance (CWM at day 365).

3.2.4 The definition of drought resilience components

To assess stem growth responses to drought, we quantified drought resilience components (i.e., resistance, recovery and resilience), which were derived from radial growth reactions (Lloret *et al.*, 2011). Resistance quantifies the capacity to continue growth during drought, recovery indicates the ability to regrow after drought, and resilience suggests the capacity of regaining the pre-drought growth level and hence to buffer the impact of drought. The resilience indices were calculated as follows (Vitali *et al.*, 2017):

$$\text{Resistance} = \frac{\text{TRW}_t}{\overline{\text{TRW}_{t-2}}} \quad (1)$$

$$\text{Recovery} = \frac{\overline{\text{TRW}_{t+2}}}{\text{TRW}_t} \quad (2)$$

$$\text{Resilience} = \frac{\overline{\text{TRW}_{t+2}}}{\overline{\text{TRW}_{t-2}}} \quad (3)$$

where TRW_t is the tree ring width at the drought year t, $\overline{TRW_{t-2}}$ is the average ring width of two years before the drought year t and $\overline{TRW_{t+2}}$ is the average ring width of two years after the drought year t. TRW_t reflects the growth in the drought year t. The resilience indices were calculated using four different time intervals (1-4 years) before and after the drought year, as short-intervals better reflect growth around the drought year, whereas longer time intervals may provide a better estimate of long-term growth performance. Because different time intervals gave similar results (Fig. S3.1) and because in non-arid environments, like ours, legacy effects on tree growth generally last 1-2 years following drought events (Anderegg *et al.*, 2015; Schwalm *et al.*, 2017), we used two years to calculate the resilience components.

3.2.5 Hydraulic trait measurements

To assess whether drought resilience could be explained by the hydraulic traits of the species, we measured for each species minimum water potential (Ψ_{min}, in MPa), and cavitation resistance (i.e., the xylem potential regarding 50% loss of hydraulic conductivity; P_{50}, in MPa), which should be closely related to drought resistance, and hydraulic conductivity (Ks, in kg m^{-1} s^{-1} MPa^{-1}) which should be closely related to drought recovery. The three hydraulic traits were measured for 4-5 individuals per species in 2018 (Song *et al.* submitted), a very dry year in Europe (Buras *et al.*, 2020).

To alleviate the effects of ontogeny and environment on individuals, branch samples were taken from fully exposed positions. The height of sampled trees varied from 10-40 m and the mean stem diameter at breast height varied between 14.8-76.9 cm across species. We collected one 38-45 cm long branch from four individuals per species at around 6 m (5-7m)

above the forest floor. The minimum water potential for twigs was measured in July 2018 at noon between 12:30 and 13:30 for four twig samples per species using a pressure chamber (Model 600, PMS Instruments, Albany, OR, USA).

We used the same method to select branches for measuring cavitation resistance and hydraulic conductivity in October 2018. To reduce transpiration and cavitation, only main branches were retained by removing leaves and side branches and wrapped in wet papers in black plastic bags for transport to the lab in France. Cavitation resistance and hydraulic conductivity were measured at the GENOBOIS platform (a high-throughput phenotyping platform for physiological traits, CaviPlace lab; University of Bordeaux; Pessac; France http://sylvain-delzon.com/caviplace/) using the standard 'Cavitron' method. This technique uses a centrifugal force to establish negative pressure in the xylem to provoke drought-induced cavitation (Cochard *et al.*, 2005), see Delzon *et al.* (2010). For further details see Song *et al*. (submitted). Finally, the hydraulic safety margin (HSM, in MPa) was calculated as the difference between minimum water potential (Ψ_{min}, in MPa) and cavitation resistance (P_{50}, in MPa). Large, positive values of HSM indicate a high capacity to resist drought, whereas negative values or marginally positive values of HSM indicate that species face a high risk of hydraulic failure (Benito Garzón *et al.*, 2018). Mean species values were used for all further analyses.

3.2.6 Statistics

To assess the relationships among drought resilience components, linear mixed models were performed using one of the resilience indices as a dependent factor, one of the other indices as a fixed factor, and individuals as random factors. To evaluate whether drought had a significant effect on tree growth, we calculated average resistance, recovery, and resilience and checked whether their 95% confidence intervals excluded 1. We first did this for each of the 11 drought years (pooling for each year all trees and species), and then separately for each of the 20 species (pooling for each species all trees and years). To verify whether there was a trade-off between resilience and growth potential, 11 linear regressions based on 11 drought years were used considering the mean species growth potential (cm/year) as independent variables and one index of 3R (i.e., resistance, recovery and resilience) as the dependent variable. Mean species growth potential was obtained from Song *et al.* (2021)and quantified as the annual stem diameter, stem area and stem mass growth during the first twenty years.

To evaluate whether tree size, the timing, duration and severity of drought affected 3R, a series of linear mixed models were used, with resistance as the dependent variable, DBH (diameter at breast height) and one of the six drought indices (timing of onset, timing of peak, duration, intensity, deficit and annual cumulative water balance) as fixed factors, and

individuals as random factors (Table S3.3). To compare coefficients, the drought indices were standardized before analysis by subtracting the mean from the original values and dividing it by the standard deviation. To evaluate which climatic factors were more critical, multiple regressions were performed. To avoid collinearities in the model, drought indices were firstly selected with a Variance Inflation Factor (VIF) < 5 (Gould *et al.*, 2016). Secondly, DBH, the timing of drought (or duration) and water deficit were selected. Thirdly, linear mixed models were performed again considering the interactions between these three selected factors and species as fixed factors and individuals as a random factor (Table 3.2). Finally, species-specific models were conducted as well to assess more precise relationships (Table S3.4; Table S3.5).

To evaluate whether hydraulic traits affect drought resistance, recovery and resilience, linear mixed modes were used on mean species level with the three hydraulic traits (Ψ_{min}, P_{50} and HSM) as fixed factors and 11 drought years as a random factor. Statistical analyses were carried out using the R "nlme" package (Pinheiro *et al.*, 2017). The assumption of normality and homogeneity for residuals of linear mixed models was checked with a Q-Q plot and a frequency histogram. All statistics were performed using R version 4.0.2 (R Core Team, 2020).

3.3 Results

3.3.1 Relationships among drought resistance, recovery and resilience

When all trees of the 20 species were considered we found a trade-off between resistance and recovery, with a regression slope of -0.67 (P<0.001, Fig. 3.3a). Resilience increased more strongly with drought resistance (slope = 0.66) than with drought recovery (slope = 0.43, P<0.001; Fig. 3.3b, 3c), indicating that drought resistance is a stronger driver of drought resilience.

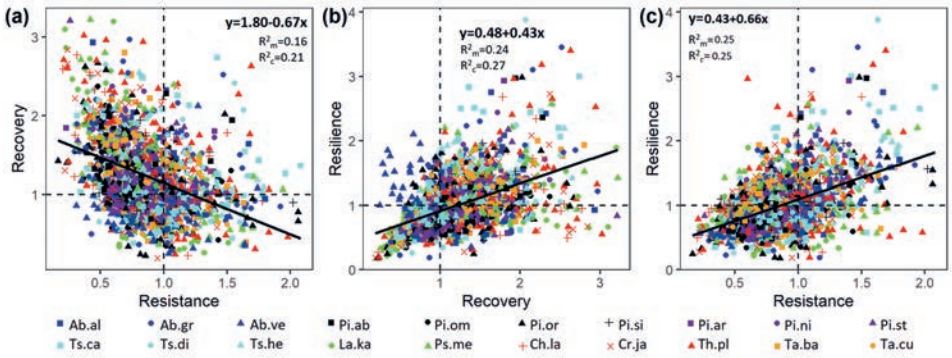

Fig. 3.3 Relationships between drought resistance and recovery (a), drought resilience and recovery (b) and drought resilience and resistance (c) of individual conifer trees (n=1922 individuals). Data are shown for 20 conifer species (as indicated by different colours and symbols) and 11 drought years. Regression lines are based on linear mixed models with species nested with individuals as random factors. All regression are significant (P<0.05). R^2m is the marginal R^2 (i.e., variance explained by fixed factor) and R^2c is the conditional R^2 (i.e., variance explained by the entire model). Dashed lines indicate a value of 1. For species abbreviations, see Table 3.1.

3.3.2 Variation in drought resilience across drought years

Resistance. The average drought resistance across 11 years was 0.87 (Fig. 3.4a). For four out of the 11 drought years (1975, 1989, 1990, and 1995) the drought resistance was not significantly different from 1 indicating that on average the tree collective did not show a growth depression. For the other seven years, stem growth was on average reduced by 22% (Fig. 3.4a), as indicated by an average drought resistance of 0.78. The average frequency of perceived droughts that affected tree growth was approximately once every 6.3 years (i.e., 7 droughts in 44 years). Hence, with a drought event in 16% of the years (once in every 6.3 years) and a growth reduction of 22% during drought, this would mean that with the current drought regime, conifer trees lose on the long-term 3.5% of their overall productivity due to drought events.

Recovery. Only for one year (1975) recovery after drought was significantly less than 1 but this was because the following year (1976) was a drought year as well (Fig. 3.4b). After the droughts in 1982 and 1989, also followed by another drought year, recovery was similar to 1, indicating that trees did not recover but grew equally slow as during the drought year. After the seven drought years, which led to significant growth reductions (resistance <1), however, the drought recovery was significantly larger than 1, indicating that trees recovered from drought.

Resilience. For 73% of the years, drought resilience was equal or larger than one, indicating full recovery-, or even over-compensation after drought (Fig. 3.4c). Drought resilience was significantly lower than 1 for three drought years (1975, 1976 and 1982). Whereas the resilience in 1975 and 1982 was also affected by drought in the following years, the low resilience to the drought event in 1976 indicates that this drought had a long-lasting effect on the growth performance of the study species.

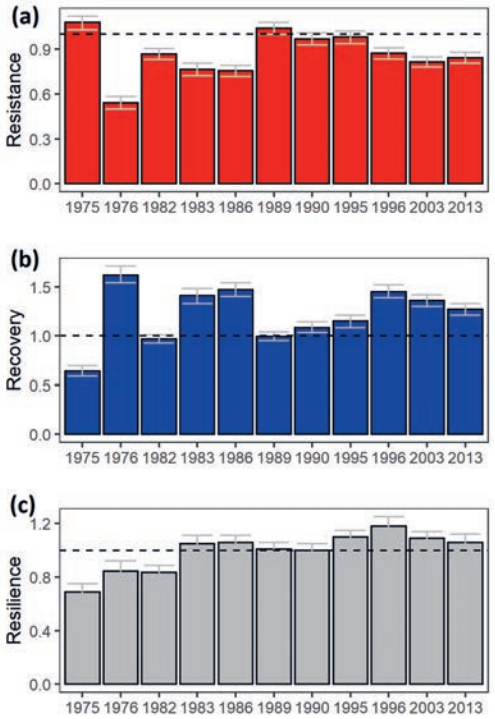

Fig. 3.4 Mean drought resistance (red; a), recovery (blue, b) and resilience (grey; c) of 20 conifer species represented by 1922 individuals in total for 11 drought years. Error bars represent the 95% of confidence intervals and the dashed line indicates a value of 1 (i.e., no drought effect).

3.3.3 Variation in drought resilience across species

Of the 20 species, the growth of only two species, i.e., *Thuja plicata* and *Tsuga canadensis,* was not significantly reduced by drought, as indicated by a resistance similar to 1 (Fig. 3.5a). The remaining 90% of the species showed a significant negative impact of drought on growth, with a drought resistance ranging from 0.80 to 0.92. Species with the lowest drought resistance were *Larix kaempferi* (resistance = 0.82), *Picea omorika* (0.80) and *Picea abies* (0.80) (Fig. 3.5a).

All species, with the exception of *Abies veitchii,* which had a relatively high resistance, had a growth recovery after drought significantly larger than 1, indicating that they recovered and grew significantly faster in the year after the drought (Fig. 3.5b).

Four species, i.e., *Larix kaempferii*, *Picea omorika*, *Picea abies* and *Picea orientalis,* showed resilience values significantly lower than 1, indicating that droughts had long-lasting negative impacts on stem growth. Most of the species (80%) however had a drought resilience equal to or significantly larger than 1, indicating that they grew at the same rate or even faster than before the drought year (Fig. 3.5c). The species with resilience>1 included *Thuja plicata*, *Pseudotsuga menziesii*, *Tsuga canadensis* and *Abies grandis*.

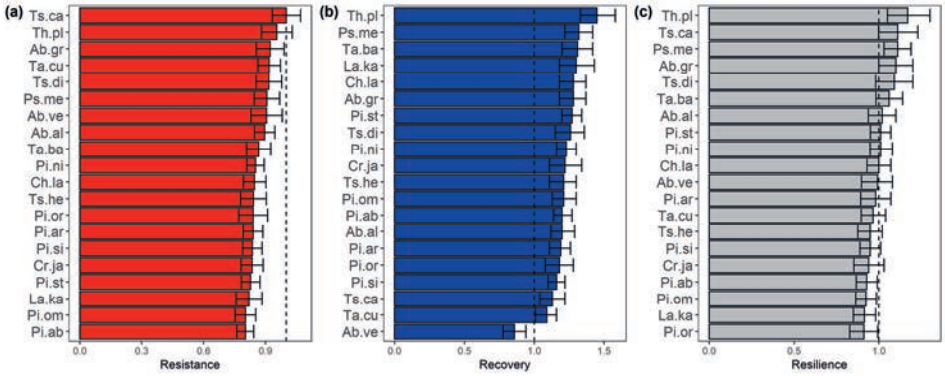

Fig. 3.5 Mean drought resistance (red; a), recovery (blue; b) and resilience (grey; c) for 20 conifer species based on 11 selected drought years (n=63-110 individuals per species). Error bars represent 95% confident interval and the dashed line indicates the value of 1. For species abbreviations, see Table 3.1. For each panel, species are ranked from high to low values.

3.3.4 Effects of drought indices on resistance

To evaluate the effects of the timing, duration and severity of drought and correcting for possible tree size effects on resistance, linear mixed models were used. Generally, resistance decreased with 1) stem diameter; 2) early droughts, both in terms of drought onset and drought peak, 3) drought length; and 4) increased drought severity (in terms of low annual cumulative water balance and more negative water deficit and drought intensity, Table S3.3). There were significant interactions between species and drought indices, and species and tree size, indicating that species respond differently to the intensity and timing of drought (Table 3.2). Species-specific models indicated that, drought resistance decreased for 25% of the species with tree size (Fig. 3.6a), for 65% of the species when droughts occurred earlier in the year (Fig. 3.6b; see 1996 in Fig. 3.2i), and for 55% of the species when droughts were severe in terms of strong negative water deficit (Fig. 3.6c; see 1976 and 2003 in Fig. 3.2). Similarly, resistance also decreased for 60% of the species when droughts lasted longer (Fig. 3.6d; see 1976, 1982 and 1996 in Fig. 3.2; Table S3.5). Overall, drought resistance was more strongly

affected by the timing, duration and severity of drought than stem diameter. Drought severity and duration had especially negative effects on the drought resistance of *Picea orientalis* and *Larix kaempferi* (Fig. 3.6c, 3.7d; Table S3.4, S3.5).

Table 3.2 Multiple regressions of resistance on DBH (diameter at breast height), the timing of drought onset and water deficit (*N* = 1482). A linear mixed model was performed to assess the impacts of drought and DBH on resistance, using species, DBH, the timing of drought onset, water deficit and the interactions between species and these factors as fixed factors and individual as a random factor. The bold coefficients indicate *P*<0.05. The mixed model has the same conditional R_m^2 and marginal R_c^2 because random effects nearly explain zero in the model.

Species	Species abbreviations	DBH	Drought onset	Water deficit
Abies alba	Ab.al	-0.005	**0.114**	**-0.149**
Abies grandis	Ab.gr	0.010	0.106	**-0.050**
Abies veitchii	Ab.ve	**-0.470**	0.127	**0.193**
Chamaecyparis lawsoniana	Ch.la	-0.077	0.093	**-0.036**
Cryptomeria japonica	Cr.ja	-0.049	0.101	-0.198
Larix kaempferi	La.ka	-0.078	0.122	**-0.255**
Pinus armandii	Pi.ar	-0.117	0.127	**0.066**
Pinus nigra	Pi.ni	-0.123	0.108	-0.103
Pinus strobus	Pi.st	0.018	0.113	**-0.004**
Picea abies	Pi.ab	-0.088	0.046	-0.111
Picea omorika	Pi.om	-0.117	0.089	-0.087
Picea orientalis	Pi.or	-0.076	0.072	-0.230·
Picea sitchensis	Pi.si	0.020	0.029·	**-0.005**
Pseudotsuga menziesii	Ps.me	-0.035	0.164	-0.083
Taxus baccata	Ta.ba	**-0.169**	0.066	-0.124
Taxus cuspidata	Ta.cu	-0.161	0.027	**-0.021**
Thuja plicata	Th.pl	0.007	0.156	-0.064·
Tsuga canadensis	Ts.ca	0.140	**-0.102**	-0.160
Tsuga diversifolia	Ts.di	-0.139	0.092	**0.136**
Tsuga heterophylla	Ts.he	-0.026	0.112	-0.108
N/df/R_m^2/R_c^2				1482/82/0.26/0.26

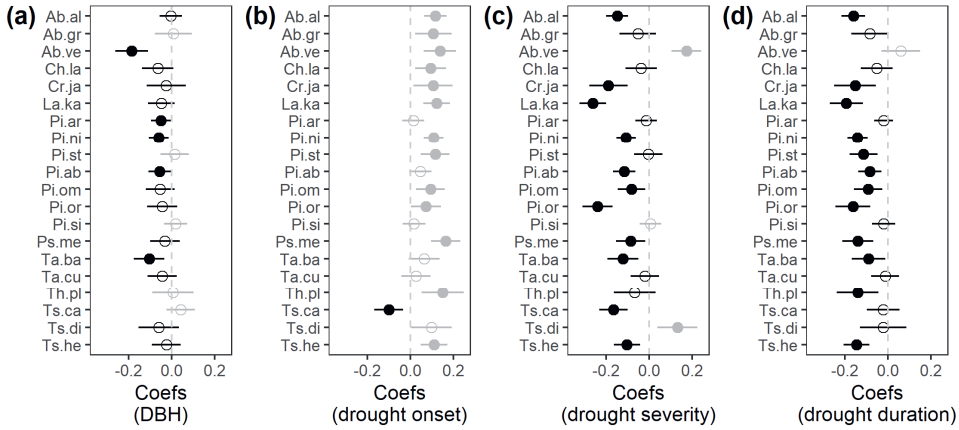

Fig. 3.6 Species-specific effects of (a) DBH (the stem diameter at breast height), (b) drought onset, (c) drought severity (i.e., water deficit) and d) drought duration on growth resistance to drought for 20 conifer species. Multiple regressions include DBH, drought onset and drought severity. Linear mixed effect models were used to explain drought resistance, using DBH, drought onset and drought severity as fixed factors, and individual as a random factor. The timing of drought onset has high collinearity with drought duration. To avoid collinearity problems, the impacts of drought duration on resistance was therefore assessed in a separate model. Regression coefficients and 95% confidence intervals are shown. Black color means negative coefficient and grey color means positive coefficient. Closed circles indicate significant coefficients whereas open circles refer to non-significant coefficients. The species are ordered alphabetically from the top to the bottom. Detailed statistic information sees Table S4 and S5. For species abbreviations, see Table 3.1.

3.3.5 The effects of hydraulics on resistance, recovery and resilience

Surprisingly, no relationships were found between the growth potential of the species, and their drought resistance, recovery or resilience (Fig. S3.2). Drought resistance, recovery and resilience were neither significantly related to the cavitation resistance, minimum water potential, hydraulic safety margin, or hydraulic conductivity of the species, for any of the 11 evaluated drought years (Fig. S3.3).

3.4 Discussion

We assessed the growth resilience of 20 conifer species to 11 drought years. We found that most species had reduced stem growth (resistance<1) during drought but recovered well (recovery>1) in the two years following drought, and they were therefore drought resilient. Stem growth reductions were strongest in response to prolonged and severe droughts that

started early in the growing season. Surprisingly, hydraulic traits and growth potential could not explain drought responses. We will discuss how different droughts dimensions affect the drought resistance of tree species and their implications for predicting productivity under climate change.

3.4.1 Most conifer species are highly resilient due to a high recovery capacity

We asked how resistance and recovery drove drought resilience. The trade-off between resistance and recovery implies two contrasting growth strategies to cope with drought (Fig. 3.3a) (Gazol *et al.*, 2017). Most species showed reduced growth for these 11 drought years (averaged resistance=0.87), but because of a high recovery (1.23) they can be considered drought resilient (1.01, Fig. 3.5). This supports the idea that droughts have an instantaneous effect on the water- and carbon balance of trees in the drought year. Carbon gain can be stopped because of stomatal closure (Bréda *et al.*, 2006) and, in addition, stem growth may cease due to reduced cambial activity (Steppe *et al.*, 2015; Fernández-de-Uña *et al.*, 2017). Alternatively, during drought trees may allocate their carbon to roots or carbohydrate storage rather than to stem growth (Lévesque *et al.*, 2013; Gessler *et al.*, 2020). We found that resilience was more strongly driven by resistance (66%) than by recovery (44%) (Fig. 3.3), indicating that resistance is especially important for the resilience of trees and forests.

Across the 20 studied conifers we do not find an indication that drought years have strong legacy effects on stem growth. This is in line with observations on carbon fluxes in European forests showing that coniferous stands largely maintained their productivity after the extreme summer drought in 2018 (Fu *et al.*, 2020). Conifers may continue to function during drought because of their extreme drought-tolerant traits, such as a needle-like evergreen leaf habit (Egger *et al.*, 1996), stomates below waxy layers (Burkhardt *et al.*, 1995), and narrow conduits (Sperry *et al.*, 2006). It should be stressed that in this study we only assessed drought resilience of living and healthy trees. By contrast, DeSoto *et al.* (2020) conducted a comparative study on drought resilience of 14 conifer species based on historic growth responses of living and dead or dying trees. They observed that individuals that showed a lower drought resilience had an increased likelihood to die in the future.

3.4.2 Species vary in drought resistance and recovery

We asked how resilient conifer species were to drought events, and we found that drought impacts varied across species. Only 10% of the species was drought-resistant; 70% of the species that showed stem growth reductions during drought recovered in the two years following a drought year and were resilient, but 20% of the species did not fully recover and were therefore not drought resilient (Fig. 3.5).

The most resilient species (with resilience significantly >1) were *Thuja plicata*, *Tsuga canadensis*, *Pseudotsuga menziesii* and *Abies grandis* (Fig. 3.5c). In contrast, four species were not drought resilient (resilience <1); *Larix kaempferi*, *Picea abies*, *Picea omorika*, and *Picea orientalis.* The major reason could be related to root depth. Deep roots as observed for some of these species(e.g., *T. plicata, P. menziesii, A. grandis*), allowing water uptake from deeper soil layers (Antos *et al.*, 2016). Such trees can thus maintain stomal conductance and photosynthesis (Puritch, 1973), and keep stems hydrated and growing during drought (Vitali *et al.*, 2017). The shallow root systems for three *Picea* species (Ballian *et al.*, 2016; Martin-Benito *et al.*, 2018) probably explain their low resilience. Moreover, *Picea* species are dying at our research site, in the Netherlands (Reichgelt & Sinke, 2020) and across Europe (Lopatka, 2019; Dell'Oro *et al.*, 2020). Another reason may be related to growth strategy. *Larix kaempferi* has large specific leaf area and wide tracheids (Song *et al.* unpublished results), facilitating fast growth but which comes at the expense of reduced drought tolerance (Chave *et al.*, 2009).

3.4.3 Not all dry years lead to growth reduction and drought impacts on productivity are small

Climatologically dry years do not always have a drought impact; of the 11 years that were a-priori identified as climatologically dry years, only 64% was indeed perceived by the trees as a drought year (Fig. 3.4). The strongest growth reductions were found for the year 1976, a well-known drought year across Europe (Cavin *et al.*, 2013), which at the study sites can be characterized as early, prolonged and intensive drought. Years that are, on average, climatologically dry do thus not always impair tree growth because this depends on the timing, intensity and duration of drought.

Although drought indeed impaired biomass production during these seven dry years (resistance=0.78), drought had a very limited effect on productivity with a loss of 3.25 % over 44 years. The low loss of productivity is possible because of the relatively mild, maritime climate at the research site in the Netherlands. Additionally, trees may have been acclimated to drought, as they grow on deep sandy soils with a low water retention capacity, and far above (>19 m) the water table (TNO-NITG, 2020). The fact that dry years are quite rare and that conifer trees are very drought resilient indicates that drought impacts should not only be assessed by using single, extremely dry, pointer years. To put drought impacts into perspective, an assessment should be made throughout the full life cycle of a tree or a stand.

3.4.4 Drought impacts depend on the timing, intensity, and duration of drought

Because most species show high drought recovery (Fig. 3.5), recovery and resistance are negatively related (Fig. 3.3a), we focus our discussion on how drought affects resistance, since

reduced growth are mainly driven by resistance (Carnicer *et al.*, 2011). We found support for our hypothesis that resistance decreases when droughts are early (average effect size of significant species = 0.10), prolonged (-0.14) and severe (-0.10), as well as with tree size (-0.09). This implies that conifers will become more susceptible to future increases in the severity, frequency and duration of droughts as predicted by climate change scenarios (cf. Gao *et al.* (2018)). Other studies also found that resistance was negatively affected by drought severity (Zang *et al.*, 2014; Gazol *et al.*, 2017). Compared with other studies, our study is one of the first tests showing that three drought dimensions should be considered to understand the effects of dry periods on stem growth, which helps better predict coniferous forest resilience to drought. Below we discuss these effects for each drought dimension.

Drought onset. Drought resistance decreased with early timing of drought onset for 65% species (Fig. 3.6b). Early drought negatively impacts tree growth as it may lead to leaf desiccation and hydraulic failure (Brodribb *et al.*, 2014). It moreover hits many species just before or at the moment of maximum cambial activity (D'Orangeville *et al.*, 2018). Northern hemisphere conifers show maximal growth in the period from June to July (Deslauriers *et al.*, 2003; McCarroll *et al.*, 2003; Rossi *et al.*, 2006), whereas at our temperate forest site, cell production peaks earlier in the growing season, in May (Rathgeber *et al.*, 2011; Hartmann *et al.*, 2017). The fact that most drought events started around or before July (Fig. 3.2), explaining the negative impacts of early drought on the resistance for most study species, e.g., *Picea* and *Abies* species. However, the timing for cambium activity may differ among species. For example, resistance for *Tsuga canadensis* decreased with late timing of drought, since the peak growing season may start late in August (Kessell, 1979). Future studies should obtain species-specific information on cambium phenology, to better understand how drought onset affects resistance across species (Fernández-de-Uña *et al.*, 2017; Schwarz *et al.*, 2020).

Drought duration. Prolonged drought episodes reduced the drought resistance for 60% of our study species (Fig. 3.6d). This generalizes an earlier finding that prolonged drought reduced the growth of *Pinus sylvestris* (Bose *et al.*, 2020) to a broad set of species. To avoid hydraulic failure during drought (Hammond *et al.*, 2019), plants may close stomata (Choat *et al.*, 2018), reducing photosynthesis (Mitchell *et al.*, 2013). Additionally, such prolonged droughts in combination with heatwaves can cause photodamage and leaf desiccation, leading to reduced canopy leaf area. Over long periods, such reduced photosynthetic carbon gain requires the tree to use most of its stored carbohydrates. This is especially problematic for conifers because they have fewer parenchyma cells and carbon storage capacity compared to broadleaved trees (Martínez-Vilalta *et al.*, 2016), which may induce die-back and ultimately to plant death (Adams *et al.*, 2017).

Drought severity. For 55% of the species resistance decreased with drought severity (i.e., a strong water deficit, Fig. 3.6b). This is consistent with findings in a previous study on 11 conifer and broadleaved species in southwestern Europe, where drought severity has a negative decisive effect on drought resistance (Gazol *et al.*, 2018). Severe droughts can cause hydraulic failure and reduce water transport to the leaves, leading to wilting and eventually desiccation, which in turn leads to reduced resistance (McDowell *et al.*, 2008; Choat *et al.*, 2018).

Tree size. Drought resistance decreased with tree size (DBH), although this was significant for only 25% of the species (Fig. 3.6a). Within a species larger trees may be more sensitive to drought, because longer hydraulic pathlengths result in lower leaf water potentials (Ryan *et al.*, 2006; Bennett *et al.*, 2015) and because their larger crowns are more exposed to atmospheric drought stress. Larger veteran trees are the ecological keystone for biodiversity, carbon sequestration, hydrological cycle and vegetation restoration (Wullschleger *et al.*, 2001; Lindenmayer *et al.*, 2012; Bennett *et al.*, 2015). Our result indicates the high vulnerability of larger trees to drought, probably impacting the ecosystem biodiversity, carbon storage, vegetation restoration and water cycling.

3.4.5 Hydraulic traits cannot explain resilience differences across conifer species

We hypothesized that resistance could be explained by hydraulic traits, where cavitation resistance (P_{50}), minimum water potential (Ψ_{min}) and hydraulic safety margin (HSM) indicate the species ability to avoid drought cavitation (Choat *et al.*, 2018). Surprisingly, these hydraulic traits cannot explain drought resistance (Fig. S3.3). In our study site, the species maintained their minimum leaf water potentials (ranging from -1.4 to -2.4 MPa) far above the water potential for cavitation (-3.0 to -6.9 MPa). This indicates that all species use tight stomatal control as a strategy to avoid water loss, thus reducing the risk of hydraulic failure (Fernández-de-Uña *et al.*, 2017). Such high hydraulic safety margins may also be an acclimation response to the deep and dry sandy soils at our study site. By contrast, studies from more extreme arid environments, such as the dry Juniper forest, suggesting that cavitation resistance can explain drought growth and survival responses (West *et al.*, 2008; Plaut *et al.*, 2012).

We conclude that, surprisingly, hydraulic traits are not decisive factors in explaining growth response to drought during the four decades. Alternatively, species differences in drought resistance may be explained by differences in rooting depth (Chaves *et al.*, 2003), stomatal control, carbohydrate storage (Choat *et al.*, 2018), or phenology (Fernández-de-Uña *et al.*, 2017).

3.4.6 The lack of relationships between growth potential and drought resilience components

We expected that fast-growing species would have low resistance but high recovery, since hydraulic traits such as large conduits and pits benefit fast growth via high water transport and hence high photosynthesis, however at the cost of drought resistance (Chave *et al.*, 2009). Nevertheless, we neither found a trade-off between growth potential and drought resistance, nor a positive relationship between growth potential and drought recovery (Fig. S3.2). The fact that growth potential is decoupled with drought resilience components, allows selecting species with both high growth rate and high resistance and resilience, such as *Thuja plicata*, *Abies grandis,* and *Pseudotsuga menziesii*.

3.4.7 Implication for climate-smart forestry

We found that under these relatively mild maritime conditions droughts caused only a minor productivity loss of 3.5%. Yet, global warming and the compounding effects of multiple extreme events could further reduce species productivity and increase mortality (Mitchell *et al.*, 2013), which is now already observed. Forests that are resilient to climate change are urgently needed to alleviate the impacts of drought on production and to mitigate climate change effects via carbon sequestration (Körner, 2017). We identified four species that are currently resilient to drought (i.e., *Abies grandis*, *Tsuga canadensis*, *Thuja plicata* and *Pseudotsuga menziesii*) and these could be selected for planting in maritime climate zones, whereas species with low drought resistance and resilience (such as *Larix* and *Picea* species) should be avoided.

3.4.8 Conclusions

We used an innovative water-balance method to compare the effects of drought dimensions on stem growth resistance across 20 conifers. Although conifer species were highly drought resilient due to high recovery, duration, severity and timing of drought onset all reduced drought resistance. Drought resistance was most strongly affected by drought duration, followed by drought severity and timing of drought onset. While conifer species significantly differed in drought resilience components, their differences could not be explained by hydraulic traits, possibly because of the relatively mild maritime climatic conditions and species acclimation to sandy soils. This indicates that drought adaptations are context-dependent. Instead, other traits such as rooting depth, carbohydrate storage, leaf and cambial phenology may explain drought resilience differences across species and need further study. Our study highlights the potential to use resilience differences across species for species selection to assure forest resilience and productivity in the face of climate change.

Acknowledgments

This study was supported by the KNAW Fonds Ecology under Grant number KNAWWF/87/19033, Oudemans Foundation, LEB fonds (2018-051C Song) and the China Scholarship Council (CSC, No.201706140106). We acknowledge the support from Jop de Klein and Els van Ginkel from Schovenhorst estate. We are very grateful to Angelina Horsting, Ellen Wilderink, Linar.Akhmetzyanov, Leo Goudzwaard, Matteo Dell'Oro, Qi Liu for assistance with fieldwork and lab work.

Author Contributions

Y.S., F.S., and L.P. designed the study, Y.S. and C.L. collected data. Y.S., F.S., U.S. and L.P analysed and interpreted the data. Y.S. wrote the first draft of the manuscript that was intensively edited by all authors.

Data Availability Statement

The data is available upon reasonable request from the authors.

Supplementary information

Table S3.1 Statistics related to cross-dating are provided for 20 conifer species. The numbers in paratheses indicate standard deviation.

Species	Period considered	Ring width mean (sd) (mm)	Rbar	EPS	MS
Abies alba	1958-2018	4.73 (2.16)	0.239	0.787	0.280
Abies grandis	1940-2017	4.36 (2.47)	0.242	0.821	0.275
Abies veitchii	1979-2018	3.00 (1.72)	0.405	0.881	0.390
Chamaecyparis lawsoniana	1911-2017	3.21 (1.58)	0.336	0.807	0.360
Cryptomeria japonica	1969-2018	3.20 (1.82)	0.443	0.901	0.406
Larix kaempferi	1945-2018	2.93 (1.48)	0.607	0.953	0.450
Picea abies	1969-2018	3.99 (1.58)	0.426	0.907	0.277
Pinus armandii	1981-2018	2.97 (1.30)	0.322	0.874	0.255
Pinus nigra	1945-2018	2.44 (1.18)	0.302	0.867	0.264
Pinus strobus	1971-2020	4.80 (1.85)	0.621	0.800	0.269
Picea omorika	1953-2018	2.75 (1.28)	0.316	0.813	0.301
Picea orientalis	1944 -2017	3.03 (1.58)	0.46	0.915	0.302
Picea sitchensis	1972 -2018	4.65 (1.65)	0.279	0.848	0.222
Pseudotsuga menziesii	1916-2017	3.68 (1.69)	0.402	0.867	0.311
Taxus baccata	1957-2018	2.15 (0.85)	0.480	0.900	0.284
Taxus cuspidate	1974 2018	1.62 (0.71)	0.341	0.834	0.252
Thuja plicata	1942-2017	4.02 (236)	0.329	0.861	0.414
Tsuga canadensis	1951-2020	1.76 (1.25)	0.56	0.806	0.307
Tsuga diversifolia	1972-2018	2.70 (1.24)	0.435	0.884	0.278
Tsuga heterophylla	1971-2017	4.87 (2.20)	0.282	0.850	0.284

Rbar indicates interseries autocorrelation, EPS indicates expressed population signals, and MS indicates sensitivity.

Table S3.2 The most significant Pearson correlations between SPEI (Standardized Precipitation and Evapotranspiration Index) from July to September, calculated for different time scales, and the tree ring index (TRI) for 20 species. SPEI is calculated based on summer period from July to October. For each month SPEI is calculated based on different time scales ranging from 1- to 12-month length and the specific time scale with highest correlation value is identified for that month. Since species show varying sensitivity to SPEI, the SPEI at the specific time scale with highest proportions of significant correlations is used to quantify the 11 drought years. Non-significant correlations are not shown. For example, a SPEI of September 4 represents SPEI being calculated based on 4-month scale from June to September of the current year. The four-month period ending in September is identified as the period with the highest proportions of significant correlations (9 species) among 20 conifer species.

Species	Period considered	July		August		September		October	
		Time Scale	Correlation	Time Scale	Correlation	Time Scale	Correlation	Time Scale	Correlation
Abies alba	1974-2017	11	0.36	12	0.41	6	0.40	4	0.36
Abies grandis	1974-2017					2	0.30		
Abies veitchii	1981-2017								
Chamaecyparis lawsoniana	1974-2017								
Cryptomeria japonica	1974-2017	10	0.32	11	0.32	12	0.36	12	0.36
Larix kaempferi	1974-2017	5	0.32	6	0.30				
Picea abies	1974-2017	5	0.58	5	0.64	4	0.61	7	0.49
Pinus armandii	1981-2017	3	0.45	4	0.44	4	0.45	4	0.39
Pinus nigra	1974-2017	3	0.59	4	0.54	4	0.57	6	0.49
Pinus strobus	1974-2017	3	0.64	4	0.59	4	0.59	6	0.51
Picea omorika	1974-2017	2	0.53	4	0.56	4	0.47	7	0.45
Picea orientalis	1974-2017	5	0.47	12	0.44	7	0.39	8	0.44
Picea sitchensis	1974-2017	2	0.56	4	0.54	4	0.50	5	0.47
Pseudotsuga menziesii	1974-2017	5	0.32	12	0.32	7	0.36	4	0.34
Taxus baccata	1974-2017	2	0.53	3	0.47	4	0.41	4	0.39
Taxus cuspidate	1974-2017	8	0.53	4	0.50	4	0.47	4	0.38
Thuja plicata	1974-2017					6	0.40	4	0.38
Tsuga canadensis	1974-2017	4	0.31						
Tsuga diversifolia	1974-2017	3	0.38	5	0.42	4	0.44		
Tsuga heterophylla	1974-2017	11	0.53	12	0.56	12	0.46	12	0.40
Selected scale with largest propotion of significant correlations		3 or 5(4/20)		4 (6/20)		4 (9/20)		4 (6/20)	

Table S3.3 Results of DBH (the stem diameter at the breast height), the timing, duration, and severity of drought explaining resistance (N = 1482). The bold coefficients indicate P<0.05. Linear mixed model was performed to assess the impacts of DBH and drought on resistance. The single regressions (1-7, in blue) used species and each index for drought separately as a single fixed factor and individual as a random factor. Three multiple regression are shown (8-10, in grey) which combine different indices for drought without risks of collinearity. For that reason, drought onset, drought peak and drought severity (deficit) replaced one another in model 8, 9 and 10, respectively. In those multiple regression models, several drought indices were included as fixed factors and individual as a random factor. The effects of 20 species on these 10 mixed models is not shown. Mixed models have the same conditional R^2m and marginal R^2c because random effects nearly explain zero variance in the model. ΔAIC indicates difference in AICc (corrected Akaike Information Criterion) between this model and the best model, and is used to compare models with each other. All coefficients estimated by the models are shown, also the non-significant ones, but the significant ones (*P*<0.05) are indicated in bold.

Models		**DBH**	**The timing of drought**		**Drought duration**	**Drought severity**			**df**	**R^2m/R^2c**
			onset	peak		Intensity	CWB	Deficit		
Single regressions	1	-0.01							23	0.02
	2		**0.09**						23	0.09
	3			**0.04**					23	0.04
	4				**-0.10**				23	0.10
	5					**0.07**			23	0.06
	6						**0.07**		23	0.07
	7							**-0.10**	23	0.10
Multiple regressions	8	**-0.04**	**0.09**					**-0.09**	25	0.16
	9	**-0.07**		**0.17**				**-0.20**	25	0.24
	1	**-0.04**			**-0.07**			**-0.05**	25	0.13
ΔAIC (9/10/8/4/7/11/2/6/5/3/1)			0.0/55.1/68.8/78.2/85.2/89.7/99.3/135.5/147.8/181.7/201.3							

Table S3.4 Effects of DBH (the diameter at the breast height), the timing of drought onset and drought severity (i.e., water deficit) on the stem growth resistance based on 20 mixed models, one model for each of the 20 species (N = 27-88 per species). Linear mixed models were performed per species to assess the impacts of drought and DBH on resistance, using the timing of drought onset and water deficit as fixed factors, and individual as random factor. The **bold** coefficients indicate *P*<0.05. Mixed models have the same conditional R_m^2 and marginal R_c^2 for some cases because random effects nearly explain zero variance in the model.

Species	Species abbreviations	DBH	Drought onset	Water deficit	N	R_m^2/R_c^2
Abies alba	Ab.al	-0.004	**0.12**	**-0.15**	81	0.41/0.41
Abies grandis	Ab.gr	0.01	**0.11**	-0.05	87	0.09/0.09
Abies veitchii	Ab.ve	**-0.19**	**0.14**	**0.17**	57	0.45/0.45
Chamaecyparis lawsoniana	Ch.la	-0.06	**0.09**	-0.04	88	0.10/0.10
Cryptomeria japonica	Cr.ja	-0.03	**0.11**	**-0.19**	64	0.27/0.27
Larix kaempferi	La.ka	-0.05	**0.12**	**-0.26**	88	0.51/0.51
Pinus armandii	Pi.ar	**-0.05**	0.01	-0.01	52	0.08/0.32
Pinus nigra	Pi.ni	**-0.06**	**0.11**	**-0.11**	90	0.35/0.36
Pinus strobus	Pi.st	0.01	**0.12**	-0.004	82	0.14/0.14
Picea abies	Pi.ab	**-0.06**	0.05	**-0.12**	88	0.22/0.22
Picea omorika	Pi.om	-0.05	**0.09**	**-0.08**	66	0.18/0.18
Picea orientalis	Pi.or	-0.04	**0.07**	**-0.24**	81	0.39/0.39
Picea sitchensis	Pi.si	0.02	0.02	0.01	73	0.02/0.02
Pseudotsuga menziesii	Ps.me	-0.03	**0.16**	**-0.09**	87	0.26/0.26
Taxus baccata	Ta.ba	**-0.10**	0.06	**-0.12**	71	0.24/0.24
Taxus cuspidate	Ta.cu	-0.04	0.03	-0.02	58	0.04/0.04
Thuja plicata	Th.pl	0.01	**0.15**	-0.07	83	0.13/0.13
Tsuga canadensis	Ts.ca	0.04	**-0.10**	**-0.17**	86	0.27/0.27
Tsuga diversifolia	Ts.di	-0.06	0.10	**0.13**	27	0.34/0.34
Tsuga heterophylla	Ts.he	-0.02	**0.11**	**-0.10**	73	0.22/0.24

Table S3.5 Species-specific effects of drought duration on stem growth resistance using 20 mixed models, one model for each of 20 species (n=27-88 per species). A linear mixed model was performed for each species to assess the impacts of drought duration on resistance, using duration as fixed factor, and individual as random factor. The **bold** coefficients indicate P<0.05. Mixed models have the same conditional R_m^2 and marginal R_c^2 for some cases because random effects nearly explained zero variance in the model.

Species	Species abbreviations	Drought duration	N	R_m^2/R_c^2
Abies alba	Ab.al	**-0.16**	81	0.29/0.29
Abies grandis	Ab.gr	-0.09	87	0.04/0.04
Abies veitchii	Ab.ve	0.06	57	0.03/0.03
Chamaecyparis lawsoniana	Ch.la	-0.05	88	0.02/0.02
Cryptomeria japonica	Cr.ja	**-0.15**	64	0.13/0.13
Larix kaempferi	La.ka	**-0.19**	88	0.22/0.22
Pinus armandii	Pi.ar	-0.02	52	0.01/0.24
Pinus nigra	Pi.ni	**-0.14**	90	0.27/0.30
Pinus strobus	Pi.st	**-0.11**	82	0.13/0.13
Picea abies	Pi.ab	**-0.08**	88	0.10/0.10
Picea omorika	Pi.om	**-0.09**	66	0.10/0.10
Picea orientalis	Pi.or	**-0.16**	81	0.16/0.16
Picea sitchensis	Pi.si	-0.02	73	0.01/0.01
Pseudotsuga menziesii	Ps.me	**-0.14**	87	0.14/0.14
Taxus baccata	Ta.ba	**-0.09**	71	0.07/0.07
Taxus cuspidate	Ta.cu	-0.01	58	0.002/0.003
Thuja plicata	Th.pl	**-0.14**	83	0.09/0.09
Tsuga canadensis	Ts.ca	-0.02	86	0.004/0.004
Tsuga diversifolia	Ts.di	-0.02	27	0.01/0.07
Tsuga heterophylla	Ts.he	**-0.15**	73	0.21/0.33

Table S3.6 Results of DBH (stem diameter at the breast height), the timing of drought onset, and drought severity (i.e., water deficit) on the stem growth recovery and resilience based on 20 mixed models, one model for each of the 20 species (n = 27-88 per species). Linear mixed models were performed per species to assess the impacts of drought and DBH on recovery or resilience, using the timing of drought onset and water deficit as fixed factors, and individual as a random factor. Bold coefficients are significant (P<0.05). In some cases mixed models have the same conditional R_m^2 and marginal R_c^2 , because random effects nearly explained zero in the model. For species abbreviations see Table 3.1.

Species	Species abbreviations	DBH	Drought onset	Water deficit	N	R_m^2/R_c^2
Recovery	Ab.al	-0.03	**-0.07**	**0.11**	68	0.19/0.19
	Ab.gr	0.03	**-0.12**	**0.10**	74	0.16/0.16
	Ab.ve	0.03	**-0.13**	0.05	45	0.12/0.15
	Ch.la	0.07	**-0.12**	-0.01	75	0.07/0.07
	Cr.ja	**0.27**	**-0.27**	**0.12**	53	0.49/0.53
	La.ka	**0.18**	**-0.22**	**0.19**	75	0.29/0.30
	Pi.ar	0.003	**-0.10**	-0.02	37	0.15/0.15
	Pi.ni	**0.06**	**-0.16**	0.03	77	0.32/0.36
	Pi.st	**0.07**	**-0.11**	0.01	69	0.15/0.21
	Pi.ab	**0.10**	**-0.08**	**0.10**	75	0.24/0.24
	Pi.om	0.07	**-0.11**	0.08	54	0.16/0.16
	Pi.or	**0.20**	**-0.24**	**0.19**	69	0.48/0.53
	Pi.si	**0.07**	**-0.07**	**0.11**	59	0.25/0.25
	Ps.me	**0.29**	**-0.18**	**0.12**	74	0.40/0.63
	Ta.ba	**0.37**	**-0.31**	**0.07**	59	0.58/0.81
	Ta.cu	**0.13**	**-0.12**	**0.09**	45	0.34/0.34
	Th.pl	**0.16**	**-0.19**	0.09	70	0.23/0.23
	Ts.ca	0.07	**-0.16**	0.07	73	0.20/0.21
	Ts.di	-0.01	-0.14	0.01	20	0.12/0.12
	Ts.he	**0.14**	**-0.16**	0.06	60	0.30/0.30
Resilience	Ab.al	-0.004	0.03	-0.05	68	0.03/0.03
	Ab.gr	0.01	-0.03	0.06	74	0.02/0.02
	Ab.ve	-0.08	**0.12**	0.09	45	0.14/0.14
	Ch.la	-0.05	-0.01	-0.02	75	0.02/0.02
	Cr.ja	**0.23**	**-0.15**	-0.08	53	0.34/0.38
	La.ka	**0.19**	**-0.10**	-0.07	75	0.20/0.30
	Pi.ar	-0.03	**-0.09**	-0.04	37	0.17/0.20
	Pi.ni	0.01	-0.06	**-0.07**	77	0.07/0.13
	Pi.st	**0.07**	0.01	0.01	69	0.06/0.06
	Pi.ab	0.04	-0.03	-0001	75	0.04/0.05
	Pi.om	0.02	-0.04	0.003	54	0.01/0.01
	Pi.or	**0.16**	**-0.17**	-0.05	69	0.20/0.26
	Pi.si	**0.09**	-0.05	**0.11**	59	0.17/0.17
	Ps.me	**0.19**	-0.003	0.02	74	0.19/0.42
	Ta.ba	**0.28**	**-0.24**	-0.06	59	0.43/0.76
	Ta.cu	**0.09**	**-0.09**	0.07	45	0.16/0.16
	Th.pl	**0.17**	-0.01	0.05	70	0.11/0.11
	Ts.ca	**0.11**	**-0.26**	**-0.10**	73	0.28/0.28
	Ts.di	-0.07	-0.04	0.14	20	0.11/0.11
	Ts.he	**0.13**	-0.06	-0.04	60	0.17/0.22

Fig. S3.1 The correlations among three resilience indices between 2 years and 4 years calculations in (a), resistance; (b), recovery and (c), resilience of individual trees for 20 conifer species across 11 drought years (n = 1846). The red line indicates the 1:1 line. All regression lines (in blue) are significant, and regression equations are shown. For species abbreviations, see Table 3.1

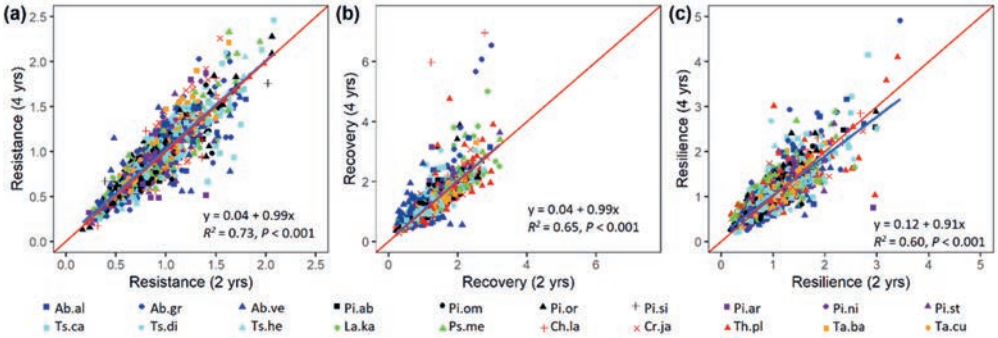

Fig. S3.2 The across species variation in stem growth potential cannot explain the variation in resilience indices, i.e., (a) resistance, (b) recovery and (c) resilience for 20 conifer species. Resistance, recovery and resilience are calculated as the mean values per species based on 11 drought years. For species abbreviations see Table 3.1. Dashed lines indicate non-significant trends.

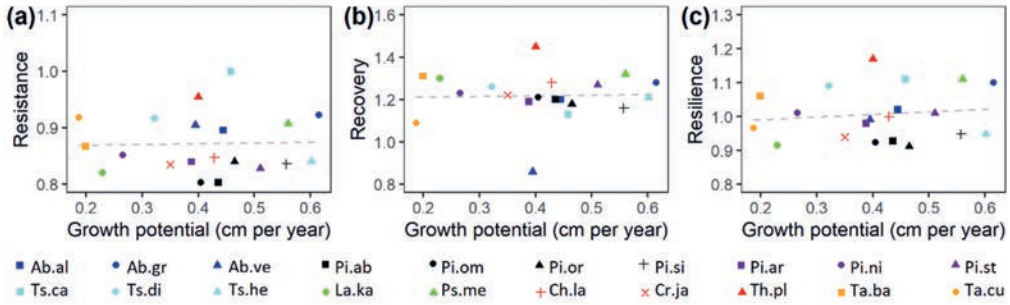

Fig. S3.3 Hydraulic traits did not explain the drought responses of 20 conifer tree species: (a-d) drought resistance, (e-h) drought recovery and (i-l) drought resilience are shown versus absolute cavitation resistance ($|P_{50}|$, left column), absolute minimum water potential for twigs ($|\Psi_{min}|$, second column), hydraulic safety margins ($HSM=\Psi_{min}-P_{50}$, third column), and xylem specific hydraulic conductivity (Ks, right column). Resistance, recovery and resilience are calculated as the mean values per species based on their responses to 11 drought years. Dashed lines indicate non-significant ($P>0.05$) regression lines. Species abbreviations see Table 3.1.

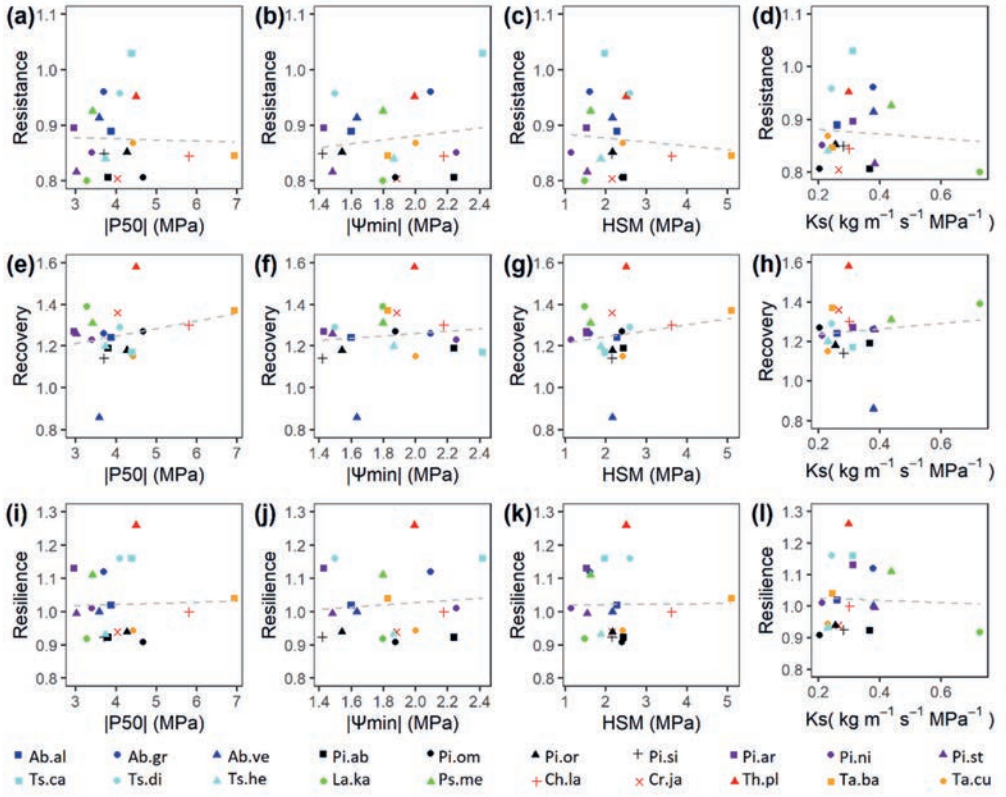

CHAPTER 4

4

Pits and tracheids explain the hydraulic safety- but not the hydraulic efficiency of 28 conifer species

Yanjun Song, Lourens Poorter, Angelina Horsting, Sylvain Delzon, Frank Sterck

A modified version was published in *Journal of Experimental Botany* (2021). https://doi.org/10.1093/jxb/erab449

Abstract

Conifers face increased drought mortality risks because of drought-induced cavitation in their vascular system. Variation in cavitation resistance may result from species differences in pit structure and function, as pits control the air seeding between water transporting conduits. This study quantifies variation in cavitation resistance and hydraulic conductivity for 28 conifer species grown in a 50-year-old common garden experiment and assesses the underlying mechanisms. Conifer species with a small pit aperture, high pit aperture resistance and large valve effect were more resistant to cavitation, as they all may reduce air seeding. Surprisingly, hydraulic conductivity was only negatively correlated with tracheid cell wall thickness. Cavitation resistance and its underlying pit traits were stronger phylogenetically controlled than hydraulic conductivity and tracheid traits. Conifers differed in hydraulic safety and hydraulic efficiency, but there was no trade-off between safety and efficiency because they are driven by different xylem anatomical traits that are under different phylogenetic control.

Key words: cavitation resistance, conifer species, hydraulic efficiency, phylogeny, pit sealing, pit size

4.1 Introduction

Drought triggers tree mortality across the globe, because it can lead to impairment of water transport and eventually hydraulic failure, desiccation and tree death (Urli *et al.*, 2013; Choat *et al.*, 2018). The risk for hydraulic failure depends on the hydraulic architecture of a tree, which consists of a series of water transporting conduits in the xylem and tiny pits that connect these neighbouring conduits. Gymnosperm trees (i.e., conifers) are considered on average more drought resistant than Angiosperm trees due to specific anatomical features. Conifers possess many narrow and short conduits called tracheids that allow for slow but safe water transport, and for resistance against drought- and freezing-induced cavitation (Davis *et al.*, 1999). These tracheids are interconnected through pits, which usually possess a torus that acts as a safety valve and seals the pit and can thus avoid drought-induced cavitation (Pittermann *et al.*, 2005). These unique anatomical properties of conifers may contribute to their success and dominance in harsh habitats, either in cold boreal and mixed temperate forests, or in dry Mediterranean forests (Augusto *et al.*, 2014). Despite these unique anatomical features, conifer species still vary substantially in their vulnerability to drought (Larter *et al.*, 2017).

4.1.1 The function of pits for hydraulic strategies

Cavitation spreads through air-seeding from one conduit to adjacent conduit, leading to an embolism in the xylem, i.e., a thrombosis that blocks the water flow in the xylem conduits (Cochard, 2006). The seeding of air bubbles into the conduits is thought to occur through the inter-conduit pits (Zimmermann, 1983). Normally, these pits in the xylem of conifer species consist of an aperture through which water can flow from one tracheid to the other and an impermeable torus that can seal the pit under tension (Bauch *et al.*, 1972; Hacke *et al.*, 2004). The torus is surrounded by a flexible margo that allows the torus to move and seal the pit. The margo also acts as a membrane, through which water can flow when the pit is not sealed (Hacke *et al.*, 2004; Sperry *et al.*, 2006). This pit structure plays an important role in the hydraulic efficiency, which is often quantified by Ks (xylem specific hydraulic conductivity), and cavitation resistance, which is often quantified by P_{50} (the water potential at which 50% of the conductivity is lost) (Delzon *et al.*, 2010) (Fig. 4.1). A larger pit aperture reduces the resistance to water flow and thus increases hydraulic efficiency, but may indirectly reduce torus overlap (Hacke & Jansen, 2009; Jansen & McAdam, 2019), facilitating torus slippage or movement and therefore mass flow of gas that causes cavitation (Fig. 4.1). Cavitation resistance may increase with torus overlap, when there is a large overlap between torus and pit aperture, and with a flexible margo, as high flexibility may better seal a pore (Fig. 4.1). Considerable uncertainty remains about the role of margo flexibility, as some studies found

that margo flexibility does not determine cavitation resistance (Hacke *et al.*, 2004; Bouche *et al.*, 2014; Bouche *et al.*, 2015). In combination, the torus overlap and margo flexibility result in a valve effect (i.e., effective sealing) of the pit (Fig. 4.1), which has been found to be the best predictor of cavitation resistance across 40 conifer tree species (Sperry *et al.*, 2006; Delzon *et al.*, 2010).

4.1.2 The function of tracheids for hydraulic strategies

Cavitation resistance and hydraulic efficiency are also related to tracheid traits. Conifer xylem mainly consists of tracheids and small areas of parenchyma. As there is only limited space to pack the tracheids, there is a trade-off between tracheid density and tracheid diameter. Theoretical specific hydraulic conductivity increases linearly with tracheid density, as each additional tracheid contributes equally to water transport, but increases with the tracheid diameter to the power four, as in wide conduits there is relatively less friction between water and the cell wall (Tyree & Ewers, 1991; Sterck *et al.*, 2008). In addition, tracheid wall thickness can also indirectly affect hydraulic conductivity, because thick cell walls reduce the water flow via a reduced lumen diameter (Sperry *et al.*, 2006), and increase the water flow path through pits and thus the pit hydraulic resistance (Hacke *et al.*, 2004; Bouche *et al.*, 2014). Greater ratio of wall thickness to tracheid diameter reinforces the mechanical resistance against tracheid implosion because of increased tension during drought (Jansen *et al.*, 2009). As plants with high cavitation resistance have to withstand lower negative pressures in their vascular system, wood safety traits are positively associated with cavitation resistance (Bouche *et al.*, 2014; Fig. 1). It should be noted that tracheid implosion has rarely been observed in nature, probably because the conduits are mechanically overbuilt. Despite the mechanistic basis of these links between the tracheid traits and hydraulic performance, a five decades old common garden experiment enables us to fully assess the underlying mechanisms in hydraulic performance across a broad range of conifer species within the same environment.

4.1.3 Trade-off between hydraulic efficiency and safety

Conifer species with small pits and tracheids may thus have a high resistance to drought-induced cavitation, which is also known as hydraulic 'safety', but this comes at the cost of water transport capacity, which is also known as hydraulic 'efficiency' (Liu *et al.*, 2019). Yet, several studies observed only a weak or even no trade-off between hydraulic safety and hydraulic efficiency (Pittermann *et al.*, 2006a; Larter *et al.*, 2017), possibly because some of the postulated mechanisms are causing stronger constraints on these processes than others. The current consensus seems that cavitation resistance is mainly determined by pit sealing

(Delzon *et al.*, 2010; Bouche *et al.*, 2014), whereas hydraulic efficiency is thought to be mainly determined by tracheid size and density (Sterck *et al.*, 2008).

In this study, we compare the hydraulic conductivity and cavitation resistance of 28 dominant conifer species from the Northern hemisphere that cover a broad range in phylogenetic and ecology diversity. They come from different habitats including cold habitats where conifers are supposed to have narrow tracheids to avoid freezing-induced cavitation (Leslie *et al.*, 2012; Zanne *et al.*, 2014), and xeric habitats with high resistance to cavitation. While earlier studies evaluated cavitation resistance of conifer species by comparing species sampled from different areas (Hacke & Jansen, 2009; Delzon *et al.*, 2010; Bouche *et al.*, 2014; Losso *et al.*, 2018), our common garden approach allows us to focus on inherent species differences not confounded by acclimation to different environmental conditions. In addition, we will use phylogenetic analysis to show phylogenetic effects on trait variation. We address the following three questions and corresponding hypotheses (Fig. 4.1):

1). How is xylem resistance to cavitation determined by tracheid and pit traits? We expect that cavitation resistance increases when the likelihood of air-seeding is reduced, either because of smaller pit dimensions (due to smaller tracheid dimensions, see Hacke *et al.,* 2004) or more efficient pit sealing properties (i.e., large torus overlap, margo flexibility, and valve effect). We expect species with high cavitation resistance to have mechanically enforced tracheids (high thickness to span ratio) and tissues (high wood density) to protect tracheid against collapse under extreme tension.

2). How is hydraulic conductivity determined by tracheid and pit traits? We expect hydraulic conductivity to increase with tracheid width and pit aperture, because they reduce the friction between water and the cell wall and facilitate therefore water flow.

3). To what extent are the hydraulic traits of conifer species phylogenetically controlled? We expect that cavitation resistance and the related pit traits, hydraulic conductivity and the related tracheid traits, exhibit strong phylogenetic signals because radiation in conifer species only followed after adaptation to drought or water availability (Larter *et al.*, 2017).

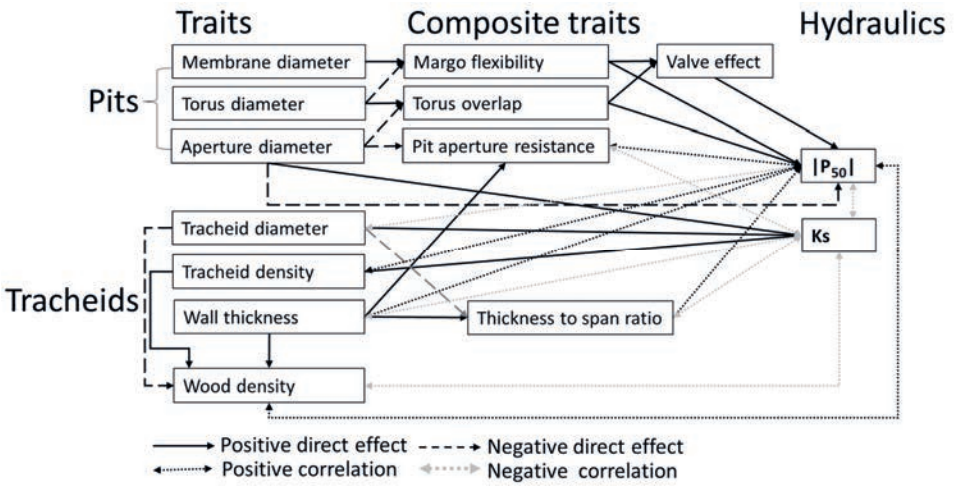

Fig. 4.1. Conceptual models showing how the function of different traits affect cavitation resistance ($|P_{50}|$) and hydraulic conductivity (Ks). The traits are grouped according to pits and tracheids; composite traits, i.e., pit sealing; hydraulics i.e., hydraulic conductivity (Ks) and cavitation resistance ($|P_{50}|$).

4.2 Materials and Methods

4.2.1 Study site and species selection

We conducted our study in the Schovenhorst Estate (52.25 N, 5.63 E) in Putten, the Netherlands. Within this region the mean annual temperature is 10.1°C, the maximum annual temperature is 13.5°C, the minimum annual temperature is 6.0°C, the mean annual rainfall is 830 mm, and the elevation is approximately 15 m below sea level (TNO-NITG, 2020). Soils are derived from postglacial loamy sand deposits, forming well-drained and acidic (pH ~4) podzolic soils of low fertility (Cornelissen *et al.,* 2012; van der Wal *et al.,* 2016).

The research was carried out in a common garden experiment, where > 30 conifer species from the Northern hemisphere have been introduced and planted in 1966 in monospecific stands (Willinge Gratama-Oudemans, 1992). Such a common garden experiment allows to compare the performance of different species under similar climatic and soil conditions, thus correcting for potentially confounding phenotypic responses to environmental variation. We selected 28 conifer species with sufficient replicate trees available for this study (Table S4.1).

These species were selected if at least five healthy individuals reached the forest canopy, and were thus fully exposed and able to achieve full growth potential. Species had an average stem diameter at breast height of 35.8 cm (range 5.0-86.3 cm). We sampled one 38-45 cm long branch for each of the five individuals per species. These branches were fully exposed to

reduce phenotypic variation and collected at approximately 6 m (5-7m) above the forest floor. After cutting, the main stem segment of the branch was stripped from leaves and side branches, and wrapped in wet paper and sealed in a plastic bag to avoid transpiration and cavitation. Samples were sent to the GENOBOIS platform (a high-throughput phenotyping platform for physiological traits, CaviPlace lab; University of Bordeaux; Pessac; France http://sylvain-delzon.com/caviplace/) and stored in a fridge at 3-5 °C prior to measurements.

We measured the vulnerability curve for these five branches, and for three out of those five branches, pit and tracheid properties were measured. Another group of branches was collected in June 2019 to measure wood density based on five individuals per species.

4.2.2 Vulnerability curves

Five branches per species were collected on adult trees to characterize xylem resistance to cavitation using the standard 'Cavitron' method, where a centrifugal force was used to establish negative pressure in the xylem to provoke drought-induced cavitation (Cochard *et al.*, 2005). Centrifugal force was created using a 27-cm-wide custom-built honeycomb aluminium rotor (DGmeca, Gradignan, France) mounted on a temperature-controlled high-speed centrifuge (Sorvall RC5C Plus Refrigerated Centrifuge, USA). All measurements were done at the PHENOBOIS platform at INRAE-University of Bordeaux. Prior to measurements, all samples were re-cut underwater to a length of 27 cm and the bark was removed using a razor blade. A solution of 10 mM KCl and 1 mM $CaCl_2$ in ultrapure deionized water was used as the reference ionic solution. The rotor was first spun at low xylem pressure (−0.8 MPa) and the rotation speed of the centrifuge was then gradually increased by −0.3 or −0.8 MPa, depending on the species, to expose samples to lower xylem pressures. After exposing the sample at the required speed for 2 min, hydraulic conductance (k in m^2 MPa^{-1} s^{-1}) was measured three times per speed step. The xylem specific hydraulic conductivity (Ks in kg m^{-1} MPa^{-1} s^{-1}, i.e., hydraulic efficiency) was estimated when xylem pressure (P in MPa) was close to zero, which was calculated by dividing the maximum hydraulic conductance (k_{max} in m^2 MPa^{-1} s^{-1}) by sample length and sapwood area (Larter *et al.*, 2017). Vulnerability curves show the percentage loss of hydraulic conductance in response to increased negative xylem pressure (Fig. 4.2). The percentage loss of hydraulic conductance (PLC) at each pressure was subsequently calculated as:

$$PLC=100(1-k/k_{max}) \quad (1)$$

Then a sigmoid function was performed to fit the curves as follows (Fig. 2):

$$PLC=100/[1+\exp(S/25*(P-P_{50}))] \quad (2)$$

where S (% MPa^{-1}) is the slope at the inflection point in the vulnerability curve, and P_{50} (MPa) is the xylem pressure when 50% of hydraulic conductance is lost (Delzon *et al.*, 2010). All values were averaged at the species level (Fig. S4.1). The absolute value of P_{50} ($|P_{50}|$) is then used for further analysis and is referred to as cavitation resistance.

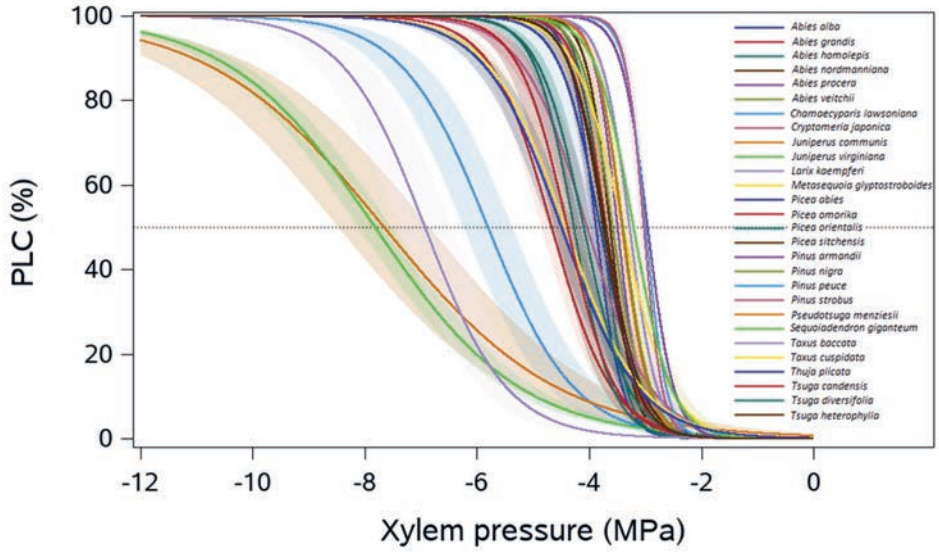

Fig. 4.2. The vulnerability curves for 28 conifer species in this study. PLC indicates the percentage loss of hydraulic conductivity. Different colour indicates different species.

4.2.3 Xylem anatomy measurements

After the vulnerability curves measurements, two 2-3 cm segments for three individual branches per species were reserved for measuring pit and tracheid anatomical traits (Table 4.1). Traits related to pit size and pit sealing were measured in the earlywood using scanning electron microscopy at the PHENOBOIS platform (SEM, PhenomG2 pro; FEI, The Netherlands). For this purpose, ten pit membranes were measured per selected segment. Those segment samples were first dried for 24 hours in an oven at 65 °C and then cut by a razor blade in a radial direction. Samples were subsequently coated with a thin golden layer using a sputter coater (108 Auto; Cressington, UK) for 40 s at 20 mA (Bouche *et al.*, 2014). The following pit size measurements were estimated in earlywood using ImageJ v. 1.52a.: pit aperture diameter (DPA), torus diameter (DT), and pit membrane diameter (DPM) (Fig. 4.3). We focused on pit characteristics of earlywood because earlywood has the strongest effect on the cavitation resistance of plants (Domec & Gartner, 2002). To assess the sealing function of the torus for cavitation resistance, three anatomical traits were calculated according to Delzon *et al.* (2010):

margo flexibility (MF), torus overlap (TO), and valve effect (VE). MF was estimated as a proxy for flexibility based on the length of the margo stretch, although it does not account for the mechanical properties of the margo. Margo flexibility (MF), torus overlap (TO), and valve effect (VE) were calculated as follows (Delzon *et al.*, 2010):

$$TO=(DT-DPA)/DT \quad (3)$$

$$MF=(DPM-DT)/DPM \quad (4)$$

$$VE=TO\times MF \quad (5)$$

To evaluate how hydraulic resistance affects hydraulic conductivity and cavitation resistance, pit aperture resistance (R_{PA}) was calculated following Pittermann *et al.* (2010) and Bouche *et al.* (2014):

$$R_{PA} = [128\ T_{pa}\ t/(\pi\ DPA)^4+24t/DPA^3\ ] \quad (6)$$

where t is the viscosity of the water (0.001 Pa s at 20°C) and T_{pa} is the thickness of a single pit border calculated from wall thickness (T_{pa}=81%x2Tw; Domec *et al.*, 2008).

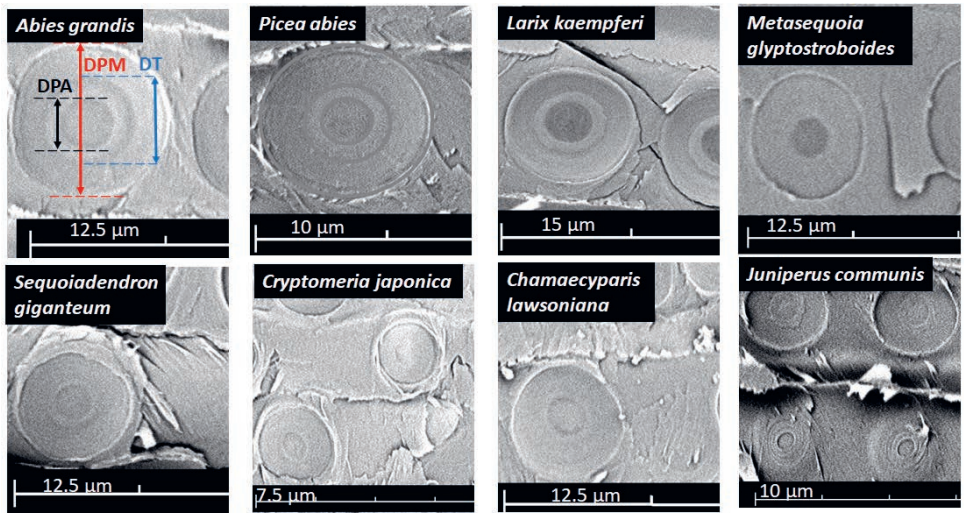

Fig. 4.3. The scanning electron microscopy (SEM) images of pit structure belonging to eight conifers species that represent big variations of pit size in our study. Different pit traits are indicated with different colors. DPM, pit membrane diameter (red color); DT, torus diameter (blue color); DPA, pit aperture diameter (black color).

To explore how tracheid traits affect hydraulic conductivity and cavitation resistance, tracheid diameter, tracheid density and cell wall thickness were subsequently measured on a complete radial segment on cross-sections of three branches per species. For the cross-

sections we used the same three branches that were used for the measurement of the vulnerability curve. These cross-sections were cut with a thickness between 15 and 30 µm. The sections were stained with Astra blue and safranin for 3-5 minutes to assure a better differentiation of the tissues (lignified tissues acquire a red colour and non-lignified tissues acquire a blue colour), they were sequentially washed 1 to 3 times with distilled water, ethanol 50%, 75%, 96% and 100%. Finally, Roti®-Mount was used to fix the samples and make images of transverse sections at 10x or 20x magnification with a Leica DM 2500 camera microscope and LAS V 3.8 software. To get a complete image of the radial section, we used photo stitching software PTGui v.9.2.0 to stitch those pictures (Fig. S4.2). Pictures of the tracheid diameter (in µm), tracheid density (i.e., tracheid number per area in mm^{-2}) and cell wall thickness (in µm) were measured using ImageJ v.1.52a. Tracheid diameter (D), tracheid density (TD) and cell wall thickness (Tw) were averaged on a minimum of 200 tracheids per sample. Thickness to span ratio (TSR) was calculated as the square of the ratio of double wall thickness to lumen diameter (Hacke *et al.*, 2001). To reduce the measurement errors caused by the irregular shapes of tracheids, we measured the area of tracheid, and from this we mathematically derived the tracheid diameter, assuming a circular shape. For five tracheid traits (tracheid diameter, tracheid density, wall thickness, and thickness to span ratio) we calculated average tracheid characteristics in three ways; 1) for the complete radial section, which should best reflect whole-branch functioning, 2) for the earlywood, as this may contribute most to hydraulic conductivity and conductivity loss during cavitation, 3) for the latewood. Hydraulic diameter (D_h) was calculated based on the whole radial section, as it best reflects hydraulic conductivity of the whole branch, and as it weighs already for differences in tracheid diameter between earlywood and latewood by using the Hagen-Poiseuille equation. A PCA analysis shows that, across species, tracheid characteristics of earlywood, latewood, and the whole radial section were strongly aligned (Fig. S4.3). Additional statistical analysis based on earlywood tracheid values and for latewood tracheid values (Fig. S4.3, 4.4; Table S4.3) gave very similar results as for the average tracheid values, indicating that the results are robust. For further analysis, we used therefore the average tracheid characteristics across the whole radial section as this should best reflect whole-branch functioning. The thickness to span ratio (TSR) and hydraulic diameter (Dh) were calculated as (Sterck *et al.*, 2008; Poorter *et al.*, 2010):

$$TSR = (2xTw/D)^2 \quad (7)$$

$$D_h = \sqrt[4]{\frac{1}{n}\sum_{i=1}^{n} Di^4} \quad (8)$$

where *Di* is the *i*th conduit of *n* measured tracheids.

Table 4.1 Overview of traits, the abbreviations and units as used and measured for trees of 28 conifer species in the Netherlands.

Classification	Trait name	Abbreviation	Units
Pit	Pit membrane diameter	DPM	µm
	Torus diameter	DT	µm
	Pit aperture diameter	DPA	µm
	Torus overlap	TO	-
	Margo flexibility	MF	-
	Valve effect	VE	-
	Pit aperture resistance	R_{PA}	MPa s m^{-3}
Tracheid	Hydraulic diameter	Dh	µm
	Tracheid density	TD	mm^{-2}
	Tracheid diameter (earlywood)	D_E	µm
	Tracheid diameter (latewood)	D_L	µm
	Tracheid density (earlywood)	TD_E	mm^{-2}
	Tracheid density (latewood)	TD_L	mm^{-2}
	Wall thickness	Tw	µm
	Wall thickness (earlywood)	Tw_E	µm
	Wall thickness (latewood)	Tw_L	µm
	Thickness to span ratio	TSR	um um^{-1}
	Thickness to span ratio (earlywood)	TSR_E	um um^{-1}
	Thickness to span ratio (latewood)	TSR_L	um um^{-1}
	Wood density	WD	g cm^{-3}
Hydraulics	Cavitation resistance	$\|P_{50}\|$	MPa
	Xylem specific hydraulic conductivity	Ks	Kg m^{-1} s^{-1} MPa^{-1}

4.2.4 Wood density

A section with 10 cm length was selected to measure wood density (WD, in g cm^{-3}). Wood fresh volume was measured using the water displacement method (Poorter *et al.*, 2010). Wood samples without bark were dried in an oven at 70°C to get constant dry weight after 48 h, and wood density was calculated as the dry mass to volume ratio per sample.

4.2.5 Data analysis

To explore the significant differences of P_{50} and Ks among 28 conifer species, data was cleaned by removing outliers and transformed to meet the normality and homogeneity assumptions of ANOVA, then post-hoc Turkey (HSD) test was performed.

To evaluate how traits are associated with each other, a Principal Components Analysis (PCA) was firstly carried out, using the 22 traits of 28 species (Table 4.1). We then used regression analyses and Pearson correlations to explore the pairwise relationships between tracheid, pit and hydraulic traits. To evaluate whether the present-day cross-species correlation is the result of repeated independent adaptations during evolution, we also

calculated correlations based on phylogenetically independent contrasts (PIC), using the R package "ape" (Paradis *et al.*, 2004; Poorter *et al.*, 2010).

To assess how pit and tracheid traits affect cavitation resistance and hydraulic conductivity, a multiple regression was performed using the dredge function in the R package "MuMIn" (Barton & Barton, 2015). A dredge function allows to evaluate the importance of all possible driving variables underlying variation in P_{50} and Ks, avoiding the statistical bias of dropping or entering variables in a backward or forward regression approach. To avoid problems with multicollinearity, only traits were selected with a Variance Inflation Factor (VIF) < 5 (Comont *et al.*, 2012; Gould *et al.*, 2016). We focused on traits that could be mechanistically linked to Ks and P_{50}. The potential regression model for Ks included DPA , MF, and VE, and the potential regression model for P_{50} included Dh, TD, and R_{PA}. The best model was the model with the lowest Akaike information criterion (AICc). Delta AICc for *i*th model was calculated as the difference AICc for the *i*th model and the best model. A set of models with delta AICc < 2 was selected (Araujo *et al.*, 2019).

To explore the cause-and-effect pathways of pit traits on cavitation resistance and tracheid traits on hydraulic conductivity, we performed structural equation models (SEMs). The structure of SEMs was based on our conceptual models (Fig. 4.1). To compare the effect sizes, all data were standardized prior to analysis by subtracting the mean from the trait values and dividing it by the standard deviation. The model was accepted when the *P*-value of χ^2 statistic was > 0.05 (Poorter *et al.*, 2017). SEMs were built in the R package "lavaan" (Rosseel, 2012).

To evaluate to what extend hydraulic features are phylogenetically controlled, Blomberg's *K* (Blomberg *et al.*, 2003) values were calculated with the R "phytools" package (Revell, 2012). *K* values close to 0 indicate that traits show no phylogenetic signal (i.e., close relatives differ more in their trait values than distant relatives because of the independent evolution of traits). *K* values close to 1 indicate a significant phylogenetic signal in the evolution of traits under Brownian motion, a random motion model; and *K* > 1 indicates the trait is strongly phylogenetically conserved (Kamilar & Cooper, 2013). Differences between large phylogenetic groups based on subfamily (i.e., Pinoideae, Piceoideae, Laricoideae, Abietoideae, Sequoioideae, Cupressoideae, Taxodioideae, and Taxaceae) were evaluated using one-way ANOVA with Tukey's (HSD) post hoc tests. As there was no subfamily within Taxaceae, Taxaceae was used here for the analysis. All data were implemented in the R statistical environment (R Core Team, 2020).

4.3 Results

4.3.1 Interspecific variation for P_{50} and Ks

The cavitation resistance (P_{50}) varied significantly across species (ANOVA, $F_{27,110}$=34.2, *P*<0.001), and ranged from -2.96 MPa for *Pinus armandii* to -7.82 MPa for *Juniperus virginiana* (Fig. 4.2, Fig. 4.8, Fig. S4.1a). P_{50} also varied strongly amongst families (ANOVA, $F_{2,135}$=22.4, *P*<0.001) and amongst species within the Pinaceae (ANOVA, $F_{18,74}$=19.1, *P*<0.001), Cupressaceae (ANOVA, $F_{6,28}$=39.5, *P*<0.001) and Taxaceae ($F_{1,8}$ =31.22, *P*<0.001). The hydraulic conductivity (Ks) also varied significantly across species (ANOVA, $F_{27,112}$=4.15, *P*<0.001), and ranged from 0.15 kg^{-1} m s^{-1} MPa^{-1} for *Picea omorika* to 0.68 kg^{-1} m s^{-1} MPa^{-1} for *Larix kaempferi* (Fig. 4.8, Fig. S4.1b). Ks also differed significantly amongst species within the Pinaceae (ANOVA, $F_{18,72}$=4.87, *P*<0.001) and Cupressaceae (ANOVA, $F_{6,32}$=3.0, *P*=0.02). However, there were no differences for Ks amongst families (ANOVA, $F_{2,137}$=2.5, *P*=0.09) and amongst species within Taxaceae ($F_{1,8}$=0.2, *P*=0.68).

4.3.2 Trait associations

The first two PCA axes explained 68.3% of variation and we found two spectra of traits (Fig. 4.4). The first axis reflects a trade-off between hydraulic safety and hydraulic efficiency, with high cavitation resistance, pit aperture resistance and margo flexibility for mainly Cupressaceae and Taxaceae species on the right side of the axis, and high hydraulic conductivity and wide pit dimensions for multiple Pinaceae species on the left side. The second axis reflects a trade-off between tracheid number (at the bottom) and tracheid size (at the top), dense (bottom) versus porous wood (high Dh, top), and strong pit sealing (high TO and VE). Therefore, three spectra can be defined along the second axis, i.e., a size-number spectrum for tracheids, ranging from large numbers of tracheids at the bottom to wide tracheids at the top, a toughness spectrum ranging from hardwood with dense wood (WD) and strong cell wall reinforcement (TSR) at the bottom to softwood at the top and a pit sealing spectrum ranging from strong sealing at the bottom to weak sealing at the top. These hydraulic spectra reflect an old split between cavitation-resistant Cupressaceae and Taxaceae with high margo flexibility (MF) to the right, and conductive Pinaceae with wide pits and potentially fast growth to the left. Within these two groups, species vary along a gradient from tough and expensive tissues (high WD) to soft, porous, and cheap tissues (high Dh).

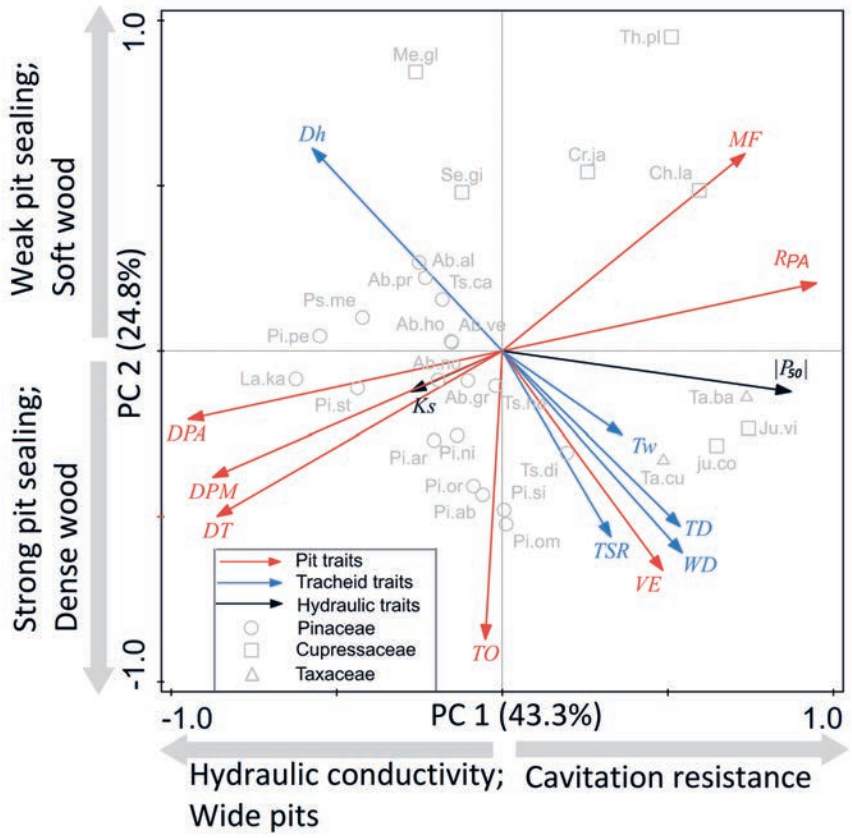

Fig. 4.4. Principal components analysis (PCA) of multivariate trait associations across 28 conifer species. The first two PCA axes and the loadings of 14 traits are shown. Different trait groups are indicated with different colored arrows (pit traits=red, tracheid traits=blue, hydraulic traits=black). Different families (Cupresssaceae, Pinaceae, Taxaceae) are indicated by different symbols. For trait abbreviations (in Italic black), see Table 4.1, for species abbreviations (in black) see Table S4.1.

4.3.3 Effects of pit and tracheid characteristics on cavitation-resistance

First, we used pairwise and multiple regression to statistically explore what traits (best) predict P_{50} and Ks. The pairwise regressions between $|P_{50}|$ and pit and tracheid traits showed that pit size (i.e., pit aperture diameter, membrane diameter and torus diameter) and tracheid size (i.e., hydraulic diameter) were negatively related to cavitation resistance, whereas tracheid density, margo flexibility and mechanical resistance (R_{PA}, pit aperture resistance; WD, wood density) were positively related to cavitation resistance (Fig. 4.5). The multiple regression indicated that cavitation resistance increased significantly with valve effect (VE) and

decreased with pit aperture size (DPA) (Table 4.2).

Second, we tested our conceptual path model (Fig. 4.1) how traits are organized in a hierarchical way, and affect each other through a chain of cause-effect relationships. As expected, valve effect and pit aperture resistance directly and positively affected $|P_{50}|$ (Fig. 4.6a). Margo flexibility and torus overlap had significantly indirect and positive effects on $|P_{50}|$ through their positive effects on the valve effect (Fig. 4.6a, Table S4.2). Similar results were obtained when we used tracheid trait values of earlywood (Fig. S4.4a) or latewood (Fig. S4.4b).

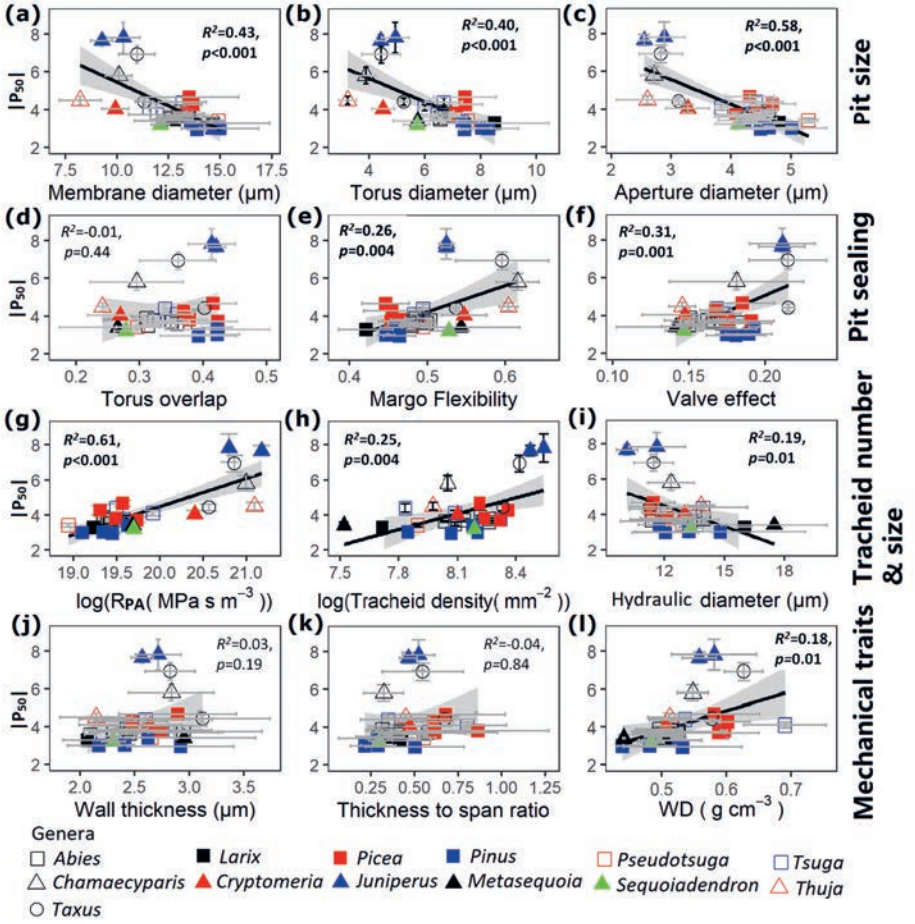

Fig. 4.5. Bi-variate relationships between cavitation resistance (P_{50}) and underlying properties for 28 conifer tree species. The traits are grouped in rows according to their function; pit size, pit sealing, tracheid traits, and mechanical traits. For trait abbreviations, see Table 4.1. Bi-variate error bars (± standard error of the mean value), regression lines and 95% confidence intervals (grey), coefficients of determination (R^2) and *p*-value are shown.

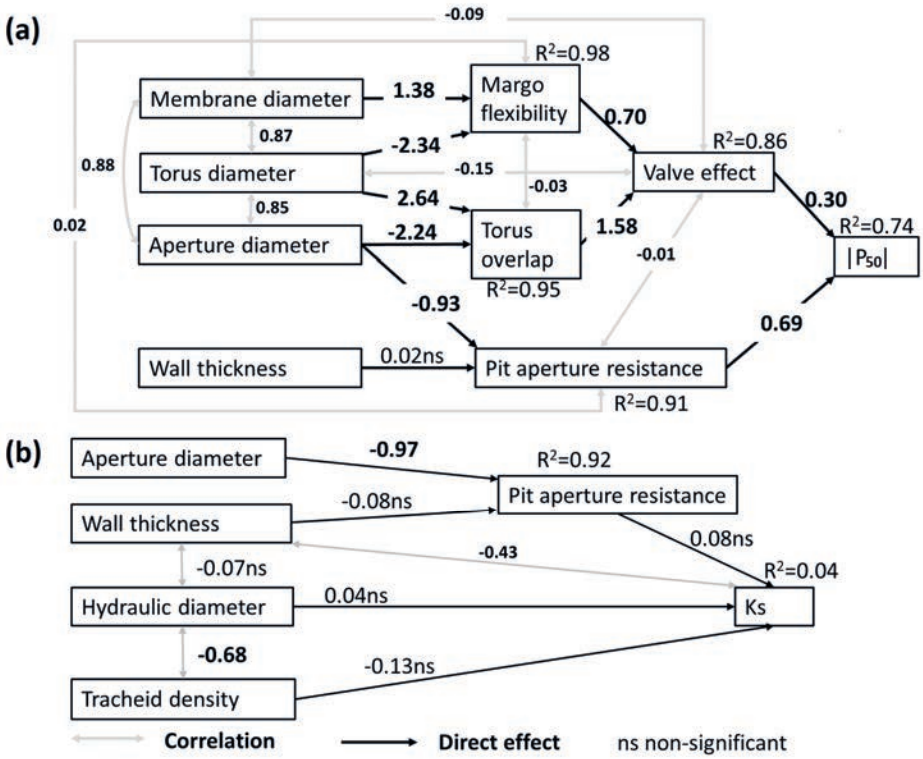

Fig. 4.6. Structural equation models for the effects of pit and tracheid traits on hydraulics for 28 conifer species: (a) cavitation resistance ($|P_{50}|$) (χ^2=27.17, df=18, *P*=0.08), (b) hydraulic conductivity (Ks) (χ^2=13.71, df=7, *P*=0.06). Significant standardized coefficients are shown in bold, and ns means non-significance. The standardized coefficients, significant effects and total effects of traits on $|P_{50}|$ or Ks can be found in Supporting Information Table S 4.2.

4.3.4 Effects of pit and tracheid characteristics on hydraulic conductivity

The pairwise regression between Ks, pit and tracheid traits showed that Ks was only significantly and negatively related to wall thickness (Fig. 4.7). Multiple regression of Ks on tracheid density, Dh and pit aperture resistance showed that none of these traits could significantly explain Ks (Table 4.2). The structural equation model further proved that only conduit wall thickness was negatively correlated with Ks (Fig. 4.6b), which was the same when we constrained the analyses based on tracheid traits of earlywood (Fig. S4.4c). Surprisingly, there was no trade-off between hydraulic conductivity and cavitation resistance (Fig. 4.7i).

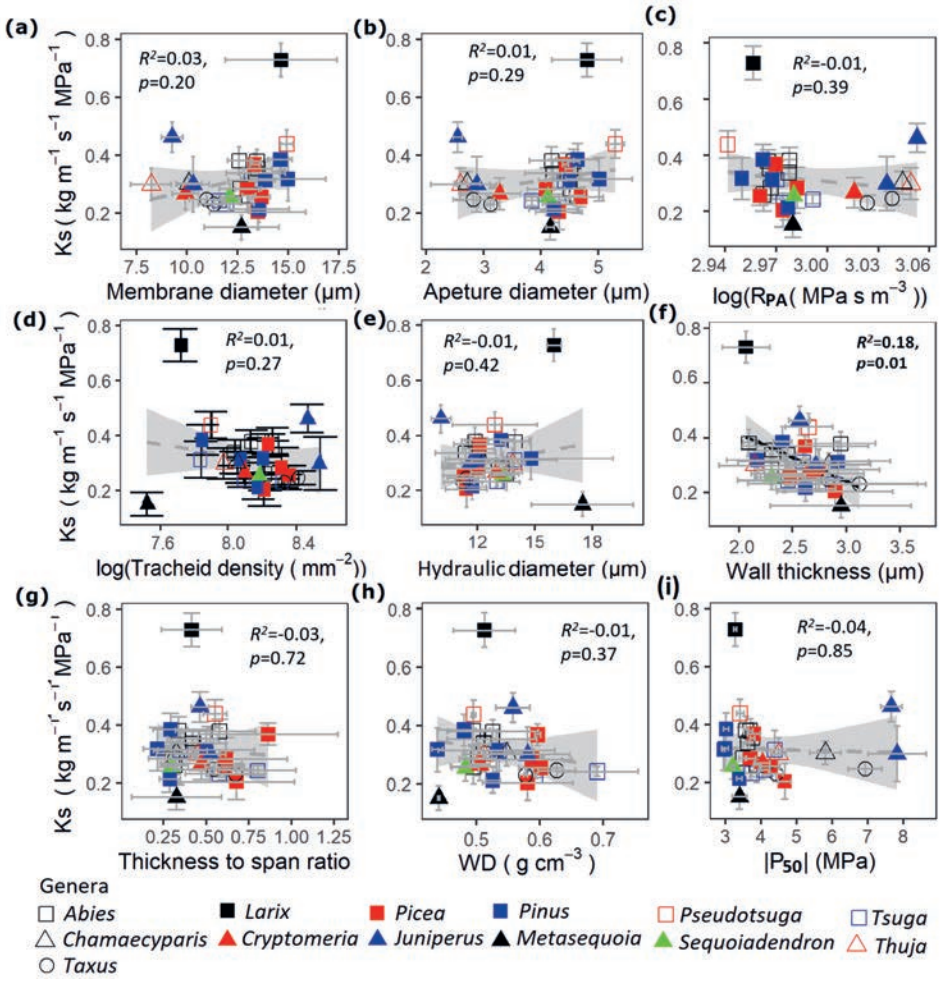

Fig. 4.7. Bi-variate relationships between maximum specific hydraulic conductivity (Ks) and underlying properties (a-h) for 28 conifer tree species. The trade-off between Ks and cavitation resistance ($|P_{50}|$) is shown (i). The traits are grouped in rows according to their function; pit traits (a-c), tracheid traits (d-e), and mechanical traits (f-h). For trait abbreviations, see Table 4.1. Bi-variate error bars (± standard error of the mean value), regression lines and 95% confidence intervals (grey), coefficients of determination (R^2) and *p*-value are shown.

Table 4.2 The results of a multi-model comparison showing how cavitation resistance ($|P_{50}|$) and hydraulic conductivity (Ks) depend on pit and tracheid traits. Only the best models (delta AIC<2) were included, and averaged (in the case of Ks). Bold fonts indicate significant coefficients.

model	DPA	VE	Dh	TD	df	logLik	AICc	Weight	R^2_{adj}	*P*
$\|P_{50}\|$=DPA+MF+VE										
1	**-0.64**	**0.31**			4	-23.59	56.90	0.62	0.65	<0.001
Ks=Dh+TD+R_{PA}										
1				-0.20	3	-38.63	84.30	0.21		
2			0.16		3	-38.87	84.70	0.16		
Avg			0.03	-0.05						
Imp			0.21	0.27						
P			0.77	0.69						

Notes: Values indicate regression coefficients of the selected variables in the model. Per model, degrees of freedom (df), the log likelihood (logLik), corrected Akaike information criterion (AICc), and the AICc weight are given. Models are selected based on ΔAIC<2. The average model was calculated based on the selected models. The average coefficients (Avg), relative importance (Imp), and significances (*P*) are shown. Relative importance of the predictor variables is calculated as the sum of the Akaike weights over the best selected models. Dh, hydraulic diameter; TD, tracheid density; DPA, pit aperture diameter; MF, margo flexibility; VE, valve effect; R_{PA}, pit aperture resistance.

4.3.5 Phylogenetic correlations and phylogenetic signals

We used Blomberg's *K* metrics to evaluate whether P_{50}, Ks and related pit and tracheid traits of conifer species are phylogenetically conserved. The hydraulic traits P_{50}, Ks, and most traits related to pit size and pit sealing showed significant phylogenetic signals (Table 4.4). To explore how phylogenetic groups differed from each other, the 28 species were classified into eight groups based on subfamily (Table 4.4; Fig. 4.8). Cupressoideae differed significantly from Laricoideae, Pinoideae and Sequoioideae, but not from the Taxaceae. Compared with Abietoideae, Piceoideae and Laricoideae, Cupressoideae were more drought-tolerant and cavitation-resistant (high $|P_{50}|$) because of a smaller pit size (DPM, DT, DPA) and had higher pit aperture resistance and margo flexibility (Table 4.4).

Out of the 91 possible pairwise trait correlations, 27 correlations were significant, both

across species and using phylogenetic correlations (Table 4.3). Eleven significant cross-species correlations became non-significant when using phylogenetic correlations. These correlations mainly referred to the relation between P_{50} and tracheid traits (i.e., Dh and TD) and Ks vs. Tw. Two correlations that were not significant across species became significant using a phylogenetic correlation; WD was negatively related to pit aperture diameter (DPA) and resistance (R_{PA}) (Table 4.3).

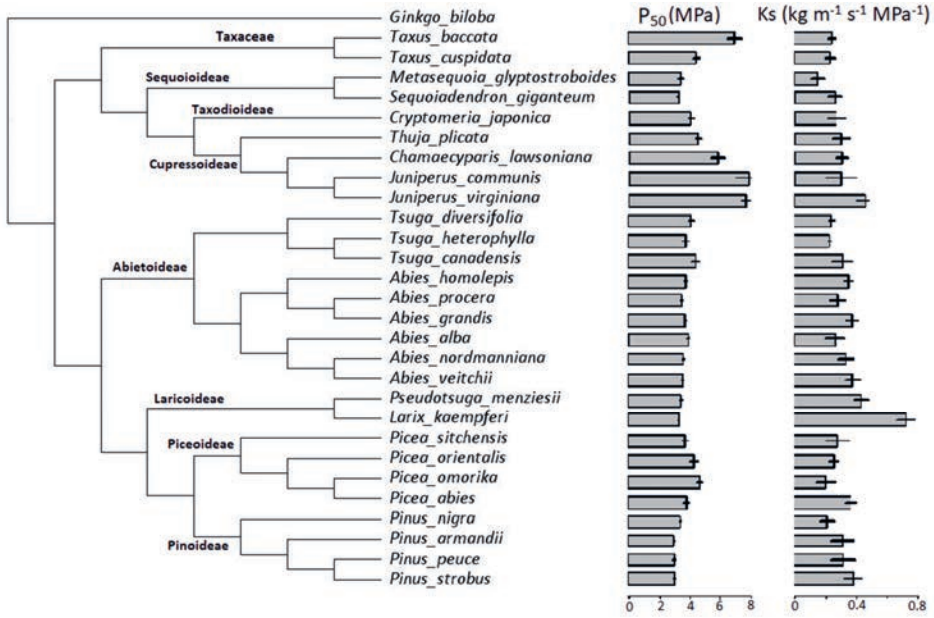

Fig. 4.8. Phylogenetic tree of the 28 conifer species with cavitation resistance (|P_{50}|) and hydraulic conductivity (Ks) in this study, based on the molecular phylogeny from Zanne *et al.* (2014). *Ginkgo biloba* is selected as outlier and reference. Error bars (± standard error of the mean value) are shown.

Table 4.3 Correlations between traits related to hydraulics (white columns), tracheid traits (grey columns), pit traits (blue columns) and wood mechanical traits (green column) for 28 conifer species. Pairwise Pearson correlations (below the diagonal) and phylogenetically independent contrast correlations (above the diagonal) are shown. Bold values represent significant correlations at $P<0.05$. For trait abbreviations see Table 4.1.

Trait	Hydraulics		Tracheid traits				Pit traits							WD
	P_{50}	Ks	Dh	TD	Tw	TSR	DPM	DT	DPA	TO	MF	VE	R_{PA}	
P_{50}		0.11	-0.20	0.22	-0.02	-0.05	-0.13	-0.34	**-0.52**	0.19	**0.44**	**0.49**	**0.53**	**0.47**
Ks	-0.05		-0.18	-0.03	-0.28	0.06	0.00	-0.07	-0.11	0.09	0.13	0.18	0.11	0.02
Dh	**-0.51**	0.03		**-0.52**	0.10	-0.24	0.32	0.20	**0.46**	-0.37	0.003	**-0.42**	**-0.46**	**-0.53**
TD	**0.53**	-0.09	**-0.75**		-0.08	0.27	-0.30	-0.04	-0.17	0.23	-0.30	0.08	0.17	**0.53**
Tw	0.29	**-0.48**	-0.22	0.14		**0.59**	0.28	0.30	0.11	0.36	-0.16	0.31	-0.09	0.20
TSR	0.20	-0.11	-0.33	0.34	**0.47**		-0.13	0.06	-0.14	0.36	-0.24	0.26	0.15	**0.61**
DPM	**-0.69**	0.17	0.27	-0.29	-0.09	-0.14		**0.83**	**0.78**	0.35	-0.19	0.29	**-0.77**	-0.32
DT	**-0.67**	0.22	0.19	-0.19	-0.14	-0.03	**0.96**		**0.85**	**0.55**	**-0.70**	0.19	**-0.84**	-0.27
DPA	**-0.80**	0.14	**0.38**	-0.35	-0.21	-0.08	**0.93**	**0.93**		0.03	**-0.50**	-0.28	**-0.99**	**-0.51**
TO	0.10	0.27	**-0.43**	0.36	0.11	0.13	**0.38**	**0.50**	0.14		**-0.51**	**0.83**	-0.02	0.33
MF	**0.56**	-0.26	-0.09	0.04	0.20	-0.12	**-0.78**	**-0.92**	**-0.79**	**-0.60**		0.06	**0.50**	0.07
VE	**0.52**	0.13	**-0.61**	**0.49**	0.29	0.08	-0.09	-0.04	**-0.39**	**0.81**	-0.02		0.28	**0.44**
R_{PA}	**0.80**	-0.14	**-0.38**	0.35	0.22	0.08	**-0.93**	**-0.93**	**-1.00**	-0.14	**0.79**	**0.40**		**0.51**
WD	**0.52**	-0.13	**-0.66**	**0.53**	0.37	**0.72**	-0.27	-0.18	-0.33	0.35	0.02	**0.47**	0.33	

Table 4.4 Differences in hydraulics and underlying traits among 8 phylogenetic groups (Piceoideae, Pinoideae, Laricoideae, Abietoideae, Cupressoideae, Taxodioideae, Sequoioideae and Taxaceae, see Fig. 4.8). Phylogenetic test for traits and One-way ANOVA with Tukey's (HSD) post hoc test. Groups that are significantly different (P<0.05) are indicated with different letters. Bold values represent significant values.

Traits		Phylogenetic test		One-way ANOVA		Mean value							
		Blomberg's *K*-value	*P-value*	$F_{7, 20}$	P	Piceoideae	Pinoideae	Laricoideae	Abietoideae	Cupressoideae	Taxodioideae	Sequoioideae	Taxaceae
Pit size	Membrane diameter (DPM) (µm)	**1.28**	**0.001**	25.48	**<0.001**	13.37 ^{DE}	14.25 ^{E}	14.78 ^{E}	12.81 ^{CD}	9.48 ^{A}	9.93 ^{AB}	12.39 ^{BCD}	11.15 ^{ABC}
	Torus diameter (DT) (µm)	**1.82**	**0.001**	34.91	**<0.001**	7.28 ^{DE}	7.78 ^{E}	8.03 ^{E}	6.60 ^{CD}	4.11 ^{A}	4.49 ^{AB}	5.73 ^{BC}	4.84 ^{AB}
	Aperture diameter (DPA) (µm)	**1.62**	**0.001**	19.39	**<0.001**	4.38 ^{CD}	4.59 ^{A}	5.05 ^{E}	4.35 ^{CD}	2.69 ^{A}	3.28 ^{ABC}	4.14 ^{BCD}	2.98 ^{AB}
Pit sealing	Torus overlap (TO)	**0.60**	**0.002**	3.15	**0.02**	0.40 ^{AB}	0.41 ^{B}	0.36 ^{AB}	0.34 ^{AB}	0.34 ^{AB}	0.27 ^{A}	0.27 ^{A}	0.38 ^{AB}
	Margo flexibility (MF)	**0.89**	**0.001**	11.62	**<0.001**	0.45 ^{A}	0.45 ^{A}	0.46 ^{A}	0.48 ^{A}	0.57 ^{B}	0.55 ^{AB}	0.54 ^{AB}	0.57 ^{B}
	Valve effect (VE)	**0.56**	**0.001**	4.78	**0.003**	0.18 ^{AB}	0.18 ^{AB}	0.16 ^{A}	0.16 ^{A}	0.19 ^{AB}	0.15 ^{A}	0.14 ^{A}	0.22 ^{B}
Tracheid size	Hydraulic diameter (Dh) (µm)	0.42	0.07	2.37	0.06	11.73 ^{A}	12.95 ^{A}	14.46 ^{A}	12.72 ^{A}	11.97 ^{A}	12.99 ^{A}	15.40 ^{A}	11.36 ^{A}
	Tracheid density (TD) (mm^{-2})	0.34	0.13	2.36	0.06	$3.96x10^{3}$ ^{A}	$3.24x10^{3}$ ^{A}	$2.47x10^{3}$ ^{A}	$3.46x10^{3}$ ^{A}	$3.98x10^{3}$ ^{A}	$3.29x10^{3}$ ^{A}	$2.72x10^{3}$ ^{A}	$4.35x10^{3}$ ^{A}
Mechanics	Wall thickness (Tw) (µm)	0.27	0.38	0.89	0.53	2.68 ^{A}	2.53 ^{A}	2.36 ^{A}	2.50 ^{A}	2.57 ^{A}	2.64 ^{A}	2.63 ^{A}	2.97 ^{A}
	Thickness to span ratio (TSR)	**0.43**	**0.02**	**3.26**	**0.02**	0.69 ^{B}	0.32 ^{A}	0.48 ^{AB}	0.46 ^{AB}	0.44 ^{AB}	0.47 ^{AB}	0.31 ^{AB}	0.61 ^{AB}
	Wood density (WD) ($g\,cm^{-3}$)	**0.62**	**0.002**	3.23	**0.02**	0.59 ^{B}	0.49 ^{AB}	0.50 ^{AB}	0.54 ^{AB}	0.55 ^{AB}	0.51 ^{AB}	0.46 ^{AB}	0.60 ^{B}
	Pit aperture resistance (R_{PA}) ($MPa\,s\,m^{-3}$)	**1.04**	**0.001**	18.57	**<0.001**	$3.06x10^{8}$ ^{BC}	$2.66x10^{8}$ ^{AB}	$1.97x10^{8}$ ^{A}	$3.12x10^{8}$ ^{BC}	$1.35\ x10^{9}$ ^{E}	$7.27\ x10^{8}$ ^{CDE}	$3.57\ x10^{8}$ ^{BCD}	$1.00\ x10^{9}$ ^{DE}
Hydraulics	Cavitation resistance ($\lvert P_{50} \rvert$) (MPa)	**0.53**	**0.03**	13.69	**<0.001**	4.11 ^{BC}	3.09 ^{A}	3.35 ^{AB}	3.81 ^{AB}	6.44 ^{D}	4.04 ^{ABC}	3.30 ^{AB}	5.67 ^{CD}
	Maximum specific hydraulic conductivity (Ks) ($kg\,m^{-1}\,s^{-1}\,MPa^{-1}$)	**0.49**	**0.04**	3.67	**0.01**	0.28 ^{A}	0.31 ^{A}	0.58 ^{B}	0.31 ^{A}	0.34 ^{AB}	0.27 ^{A}	0.20 ^{A}	0.24 ^{A}

4.4 Discussion

We show how 28 conifer species differed in P_{50} and Ks, and how those differences were explained by the underlying anatomical pit and tracheid traits. We found that the valve effect and pit aperture resistance determined the xylem cavitation resistance. Hydraulic conductivity was, surprisingly, not explained by pit and tracheid size, but was only negatively related to wall thickness. Cavitation resistance and its underlying anatomical traits were under stronger phylogenetic control than hydraulic efficiency. Below we will discuss how pit and tracheid traits affect cavitation resistance and hydraulic conductivity, and how pit traits, tracheid traits and hydraulics are phylogenetically controlled.

4.4.1 Cavitation resistance: the function of pits and tracheids

We hypothesized that cavitation resistance would increase with high pit aperture resistance resultant from a small pit aperture and thick cell wall, and with strong pit sealing properties and particularly with a strong valve effect as driven by large torus overlap and high margo flexibility. We indeed found support for this hypothesis. As expected, small pit dimensions (as characterized by small pit aperture diameter, membrane diameter and torus diameter) were indeed associated with a high cavitation resistance (Fig. 4.5a-c, i). The structural equation model implies that the effects of small pits, in combination with thick cell walls, particularly increase the pit aperture resistance, which increases the cavitation resistance (Fig. 4.6a, Fig. S4.4a). This is in line with the idea that a small pit size increases cavitation resistance due to a relatively increased torus overlap, because the torus size remains fairly constant whereas a reduction in pit aperture leads to a stronger increase in torus overlap (Bouche *et al.*, 2014; Jansen & McAdam, 2019), but adds a significant role for the cell wall thickness of earlywood (Fig. S4.4a). The structural equation model also showed that the valve effect positively affected cavitation resistance (Fig. 4.6a), which is thought to be the best integrator of pit sealing properties (Delzon *et al.*, 2010). Both torus overlap and margo flexibility had a significant indirect effect via the valve effect on cavitation resistance (Fig. 4.6a, Table S4.2). These results are at least partially supported by the bi-variate relationships with cavitation resistance (Fig. 4.5): the valve effect showed the strongest relation (Fig. 4.5f), followed by margo flexibility (Fig. 4.5e), but remarkably torus overlap did not have any bivariate trend with $|P_{50}|$ (Fig. 4.5d) despite a strong contribution to variation in the valve effect (Fig. 4.6). These results are in line with the aspiration hypothesis, which suggests that air-seeding occurs when the torus cannot perfectly seal the aperture against the pit border (the inner wall of pit membrane) (Pittermann *et al.*, 2010). The positive trend between margo flexibility and cavitation resistance (Fig. 4.5e) is also in line with Hacke *et al.* (2004), implying that a flexible margo enables the torus to seal the aperture perfectly against the pit border (Delzon *et al.*,

2010). Our results nevertheless most strongly support the aspiration hypothesis in the sense that a stronger valve effect is the most direct way of sealing the pit aperture with a direct positive effect on cavitation resistance (Fig. 4.5f, Fig. 4.6).

The torus capillary-seeding hypothesis is an alternative hypothesis for linking pit traits to cavitation resistance, and suggests that air seeding occurs at the pores of the torus (Jansen *et al.*, 2009; Bouche *et al.*, 2014). In a study of 13 conifer species, it was observed that cavitation resistance was indeed determined by the size of torus pores, as air-seeding occurs firstly at the largest pore (Jansen *et al.*, 2012). Because we did not measure the pores in the punctured tori, we cannot test for this mechanism. Finally, we found that cavitation resistance increased with tracheid density (Fig. 4.5h), which is consistent with other studies (Jacobsen *et al*., 2016, see Table S1; Larter *et al*., 2017, see Fig. 4b). Perhaps, a larger amount of smaller tracheids provides extra safety because there are more functional tracheids left to take over the role of embolized tracheids.

4.4.2 Why is hydraulic conductivity not explained by pit and tracheid traits?

Hydraulic conductivity (Ks) is often found to increase with pit and tracheid size (Pittermann *et al.*, 2006a; Sperry *et al.*, 2006; Woodruff *et al.*, 2008; Hacke & Jansen, 2009), as water transport through wide structures reduces friction between water and plant cells, and facilitates water flow (Roskilly *et al.*, 2019). In contrast to these predictions, neither pit aperture diameter nor hydraulic diameter was related to hydraulic conductivity in our study (Fig. 4.6b, 4.7b, 4.7e) (cf. Larter *et al.,* 2017). We found that hydraulic conductivity was only significantly and negatively related to tracheid cell wall thickness (Fig. 4.6b, 4.7f). Thick cell walls may affect hydraulic conductivity in two ways; it may increase the hydraulic pathlength within the pits, and therefore pit aperture resistance, or it may reduce the lumen area available for fluid flow (Hacke *et al.*, 2004). Yet, none of these two mechanisms are likely to have played a role in our study. First, cell wall thickness contributed little to pit aperture resistance (which is mostly determined by pit aperture diameter), and pit aperture resistance did not have a significant effect on Ks (Fig. 4.6b, Fig. 4.7c, Fig. S4.4c). Second, although there is indeed a negative correlation between wall thickness and hydraulic diameter (r=-0.22, Table 4.3), this is not significant. In addition, in our multiple regression analysis (Table 4.2) and structural equation model (Fig 4.6b) we checked for independent effects of cell wall thickness and Dh on Ks, and found that Dh had never a significant effect. Hence, cell wall thickness is associated with Ks, but for unknown reasons.

It should be noted that the observed range of hydraulic conductivity is rather small (ranging from 0.15-0.46 kg m^{-1} s^{-1} MPa^{-1} across species, excluding the outlier *Larix* (Fig. 4.7) which may explain our inability to detect significant relationships between Ks and putative

tracheid traits. Alternatively, it could be that hydraulic conductivity is determined by other hydraulic bottlenecks, such as the sizes of pores in the margo (Schulte *et al.*, 2015), the overlapping tracheid tips due to bent tracheids, or tracheid length since that determines the flow path or affects the end-wall conductivity which nearly contributes to 64% of total resistivity in tracheids (Pittermann *et al.*, 2006a; Sperry *et al.*, 2006), but those properties were not considered here.

4.4.3 Traits association and trade-offs

It was expected that there would be a trade-off between hydraulic efficiency and hydraulic safety, because large tracheids and pits potentially increase the hydraulic conductivity but come at the cost of reduced cavitation resistance to air seeding. We found, however, no relationship between hydraulic conductivity and cavitation resistance (Fig. 4.7i) as previously reported by several studies (Gleason *et al.*, 2016). We used a PCA to identify major hydraulic spectra and trade-offs (Fig. 4.4). The first PCA axis represents the major axis of hydraulic trait variation, showing a trade-off between hydraulic safety (i.e., high cavitation resistance and pit resistance) and pit dimensions (i.e., pit size). Species with high cavitation resistance need small pits to enhance resistance to air seeding (Sano, 2016), which we also observed in the bivariate trait associations (Fig. 4.5a-c, Table 4.3). The second PCA axis shows three spectra, i.e., a size-number spectrum for tracheids, a toughness spectrum and a pit sealing spectrum (Fig. 4.4). These three spectra indicate that species with strong pit sealing capacity need to invest resources in tough structures such as dense wood, thick cell wall reinforcement and dense tracheids to prevent cavitation, which comes at the cost of water transport through tracheids. Structural equation models proved that hydraulic conductivity was only related to tracheid wall thickness (Fig. 4.6b, Fig. 4.4c), whereas cavitation resistance was determined by pit size and pit sealing properties through valve effect (Fig. 4.6a). The major variation in cavitation resistance and hydraulic efficiency is driven by different suits of traits, which explains why hydraulic efficiency and hydraulic safety were disconnected. In such sense, our study is in line with other recent studies (Willson *et al.*, 2008; Larter *et al.*, 2017), which fails to show a trade-off between these potentially competing hydraulic functions, and does provide a possible explanation for this.

4.4.4 Phylogenetic signal and trait evolution

P_{50} varied significantly across species, with *Pinus* species being the most drought intolerant and *Juniperus* species being the most drought tolerant (Fig. 4.8). *Blomberg's K* values showed that cavitation resistance and its underlying pit traits (pit size and pit sealing) were phylogenetically conserved, indicating that they are the result of old phylogenetic splits. The

ancestral traits are largely maintained because insufficient time has passed since the evolutionary divergence (Ackerly, 2003) (Table 4.4). Most of the significant correlations phylogenetic trait correlations (PIC) were among P_{50} and pit traits, indicating that increased cavitation resistance has evolved in combination with decreased pit aperture size, and increased pit aperture resistance and valve effect (Table 4.3). Traits that reflect mechanical reinforcement (i.e., Tw, TSR and R_{PA}) and, hence, material construction costs (Poorter *et al.*, 2018) also showed a significant phylogenetic signal (cf. Chave *et al.*, 2006).

Pit size traits were more conserved than pit sealing traits (MF, TO, VE), probably because pit size is closely related to- and the result of- cell size, which may be more difficult to change in response to different environmental conditions during evolution (David-Schwartz *et al.*, 2016). Pit sealing traits may be easier to modify, as they result from two underlying pit size traits (Fig. 4.1); a small increase in one pit size trait combined with a small decrease in another may therefore lead to larger changes and more flexibility in pit sealing traits.

The strong phylogenetic control of pit size traits explains therefore the relatively strong phylogenetic control of cavitation resistance and drought adaptation. Cupressoideae and Taxaceae were the most cavitation resistant (i.e., high $|P_{50}|$) phylogenetic groups because of their small pit sizes, strong pit sealing property (MF) and high pit aperture resistance (R_{PA}). Instead, the fast-growing and light-demanding Pinoideae (Webb & Scanga, 2001) and Laricoideae (Dobrovolný *et al.*, 2013) had larger pit dimensions (DPM, DT and DPA) and weaker pit sealing (MF) than the slow-growing Cupressoideae. We conclude that closely joined evolution of high cavitation resistance with small pit size, a higher valve effect and pit aperture resistance has enabled conifer species to be very resistant to drought (Pittermann *et al.*, 2010).

By contrast, hydraulic conductivity and its underlying tracheid traits (tracheid size, number and cell wall thickness) were under much weaker phylogenetic control, suggesting that hydraulic conductivity traits may have allowed species to radiate into different habitats (Panek, 1996). Weakly phylogenetic signals in hydraulic conductivity have also been found in other studies on broadleaf species (Liang *et al.*, 2019) and conifer species (Corcuera *et al.*, 2011), probably because phenotypic plasticity plays a vital role in the variation of hydraulic traits which rely a lot on water availability (Liang *et al.*, 2019). Although conifers have a stable pit size that reflect ancestral traits, they have an advanced water utilization strategy by having a highly plastic hydraulic architecture. It enables individuals in wet habitats to have high hydraulic conductivity, grow fast and attain high productivity, and individuals in dry habitats to have low hydraulic conductivity and grow slowly. Thus, the capacity for a plastic response in tracheid traits and hydraulic conductivity allows species to track changes in the environment and persist under climate change (Corcuera *et al.*, 2011).

4.4.5 Conclusions

We compared the hydraulics of 28 conifer species grown under standardized conditions in a common garden experiment. Pit sealing properties, tracheid size and numbers indeed affect the cavitation resistance of conifer species. Anatomical stem traits (pit size, margo flexibility, torus overlap and valve effect) of conifers are phylogenetically conserved and strongly control species differences in cavitation resistance and, hence, drought resistance. Unexpectedly, hydraulic conductivity was weakly phylogenetically controlled, and negatively related to tracheid wall thickness, rather than being related to hydraulic diameter or pit aperture size. Future studies could explore the role of tracheid length and margo pores in hydraulic conductivity. In sum, conifer species differ largely in cavitation resistance and the underlying traits, and in hydraulic conductivity, and they may therefore differ strongly in their climatic distribution and drought responses to climate change.

Acknowledgements

We acknowledge Jop de Klein and Els van Ginkel from Schovenhorst estate for supporting this study, and Leo Goudzwaard for help with fieldwork. We are grateful to Anne-Isabelle Gravel, Gaëlle Capdeville and Regis Burlett for the training of hydraulic measurements, Qi Liu for organizing anatomical pictures of tracheids, Sophie Zwartsenberg and Marsha van der Sande for helpful suggestions on the phylogenetic part. We thank two anonymous reviewers for their helpful comments. This work was supported by the KNAW Fonds Ecology (KNAWWF/87/19033), LEB fonds (2018-051C Song) from Wageningen University, and the China Scholarship Council (CSC, No.201706140106).

Author Contributions

F.S., L.P., and Y.S. designed the study, S.D supervised the measurement and analyses of cavitation resistance and pit structure; Y.S. and A.H. collected data. Y.S. analysed the data with the supervision of L.P. and F.S.. S.D., L.P., F.S. and Y.S. discussed and explained the results. Y.S. wrote the first draft of the manuscript that was intensively edited by all authors.

Data availability statement

The data is available upon reasonable request from the authors.

Conflicts of interest

The authors have no conflict of interest to declare.

Supplementary information

Table S4.1 Overview of species, abbreviations, family, subfamily and genera of 28 conifer species in the Netherlands.

Species	Abbreviation	Family	Subfamily	Genera
Abies alba	Ab.al	Pinaceae	Abietoideae	*Abies*
Abies grandis	Ab.gr	Pinaceae	Abietoideae	*Abies*
Abies homolepis	Ab.ho	Pinaceae	Abietoideae	*Abies*
Abies nordmanniana	Ab.no	Pinaceae	Abietoideae	*Abies*
Abies procera	Ab.pr	Pinaceae	Abietoideae	*Abies*
Abies veitchii	Ab.ve	Pinaceae	Abietoideae	*Abies*
Chamaecyparis lawsoniana	Ch.la	Cupressaceae	Cupressoideae	*Chamaecyparis*
Cryptomeria japonica	Cr.ja	Cupressaceae	Taxodioideae	*Cryptomeria*
Larix kaempferi	La.ka	Pinaceae	Laricoideae	*Larix*
Metasequoia glyptostroboides	Me.gl	Cupressaceae	Sequoioideae	*Metasequoia*
Juniperus communis	Ju.co	Cupressaceae	Cupressoideae	*Juniperus*
Juniperus virginiana	Ju.vi	Cupressaceae	Cupressoideae	*Juniperus*
Picea abies	Pi.ab	Pinaceae	Piceoideae	*Picea*
Picea orientalis	Pi.or	Pinaceae	Piceoideae	*Picea*
Picea omorika	Pi.om	Pinaceae	Piceoideae	*Picea*
Picea sitchensis	Pi.si	Pinaceae	Piceoideae	*Picea*
Pinus armandii	Pi.ar	Pinaceae	Pinoideae	*Pinus*
Pinus nigra	Pi.ni	Pinaceae	Pinoideae	*Pinus*
Pinus peuce	Pi.pe	Pinaceae	Pinoideae	*Pinus*
Pinus strobus	Pi.st	Pinaceae	Pinoideae	*Pinus*
Pseudotsuga menziesii	Ps.me	Pinaceae	Laricoideae	*Pseudotsuga*
Sequoiadendron giganteum	Se.gi	Cupressaceae	Sequoioideae	*Sequoiadendron*
Taxus baccata	Ta.ba	Taxaceae	-	*Taxus*
Taxus cuspidata	Ta.cu	Taxaceae	-	*Taxus*
Thuja plicata	Th.pl	Cupressaceae	Cupressoideae	*Thuja*
Tsuga canadensis	Ts.ca	Pinaceae	Abietoideae	*Tsuga*
Tsuga diversifolia	Ts.di	Pinaceae	Abietoideae	*Tsuga*
Tsuga heterophylla	Ts.he	Pinaceae	Abietoideae	*Tsuga*

Table S4.2 Results of the structural equation models for the effects of pit and tracheid traits on cavitation resistance ($|P_{50}|$) (indicated in grey) and hydraulic conductivity (Ks) (indicated in green) shown in Fig. 6. Per relationship, standardized regressions (beta), standard error (SE), Z-value, P-value, direct effects and indirect effects are given. Bold fonts indicate significant regressions.

Response variable	Predictor variable	beta	SE	Z	*P*
	Direct effects				
$\|P_{50}\|$	Valve effect (VE)	**0.30**	0.10	3.01	0.003
	Pit aperture resistance (R_{PA})	**0.69**	0.11	5.99	<0.001
Valve effect	Torus overlap (TO)	**1.58**	0.07	22.29	<0.001
	Margo flexibility (MF)	**0.70**	0.09	7.72	<0.001
Torus overlap	Aperture diameter	**-2.34**	0.07	-33.20	<0.001
	Torus diameter	**2.64**	0.08	31.75	<0.001
Margo flexibility	Membrane diameter	**1.38**	0.05	28.95	<0.001
	Torus diameter	**-2.24**	0.05	-42.14	<0.001
Pit aperture resistance	Aperture diameter	**-0.93**	0.05	-17.45	<0.001
	Wall thickness	0.02	0.02	0.71	0.48
	Indirect effects				
$\|P_{50}\|$	Torus overlap (via VE)	**0.48**	0.16	2.98	0.003
$\|P_{50}\|$	Margo flexibility (via VE)	**0.21**	0.08	2.81	0.005
$\|P_{50}\|$	Aperture diameter(via TO and R_{PA})	**-1.75**	0.34	-5.12	<0.001
$\|P_{50}\|$	Wall thickness (via R_{PA})	0.01	0.02	0.70	0.48
	Direct effects				
Ks	Hydraulic diameter	0.04	0.27	0.13	0.89
	Tracheid density	-0.13	0.25	-0.53	0.59
	Pit aperture resistance (R_{PA})	0.08	0.16	0.47	0.64
Pit aperture resistance	Aperture diameter	**-0.97**	0.06	-17.47	<0.001
	Wall thickness	-0.08	0.06	-1.44	0.15
	Indirect effects				
Ks	Aperture diameter (via R_{PA})	-0.07	0.16	-0.47	0.64
Ks	Wall thickness (via R_{PA})	-0.01	0.01	-0.44	0.66

Table S4.3 Results of a multi-model comparison showing how hydraulic conductivity (Ks) depends on the tracheid traits of earlywood (in blue) and latewood (in green). Only the best(delta AIC<2) and averaged models were included. Bold fonts indicate significant coefficients. Adjust R^2 (R^2_{adj}) and *P*-value are shown.

model	Dh	TD	R_{PA}	df	logLik	AICc	Weight	R^2_{adj}	*P*
Earlywood: Ks= D+TD+R_{PA}									
1				2	-39.22	82.90	0.42	0	1
2	0.20			3	-38.64	84.30	0.21	<0.01	0.30
Avg	0.07								
Imp	0.34								
P	0.65								
Latewood: Ks= D+TD+R_{PA}									
1				2	-39.22	82.90	0.48		

Notes: Values indicate regression coefficients of the selected variables in the model. Per model, degrees of freedom (df), the log likelihood (logLik), corrected Akaike information criterion (AICc), and the AICc weight are given. Models are selected based on ΔAIC<2. The average model was calculated based on the selected models. The average coefficients (Avg), relative importance (Imp), and significances (*P*) are shown. Relative importance of the predictor variables is calculated as the sum of the Akaike weights over the best selected models. D, tracheid diameter; TD, tracheid density; R_{PA}, pit aperture resistance.

Fig. S4.1 Boxplot of P_{50} (the xylem pressure when 50% of hydraulic conductance is lost) and Ks (maximum specific hydraulic conductivity) across 28 conifer species (*N* = 3-7 trees/species). Species with different letters are significantly different (Tukey HSD post hoc test, *P*<0.05). Error bars (± standard error of the mean value) are shown.

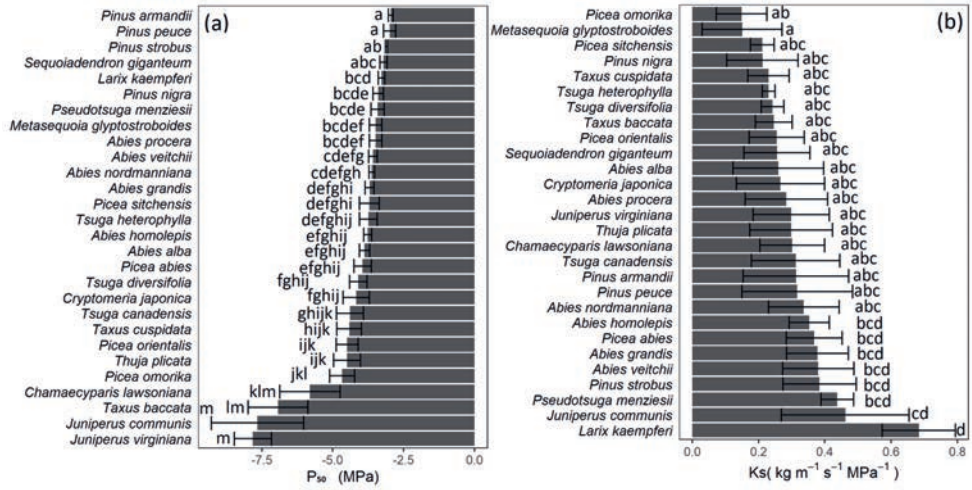

Fig. S4.2 An example of a radial subsection (blue) from the cross-section for the measurements of *Tsuga heterophylla*. The tracheid diameter and wall thickness for earlywood (green) and latewood (black) were measured based on a radial subsection (blue).

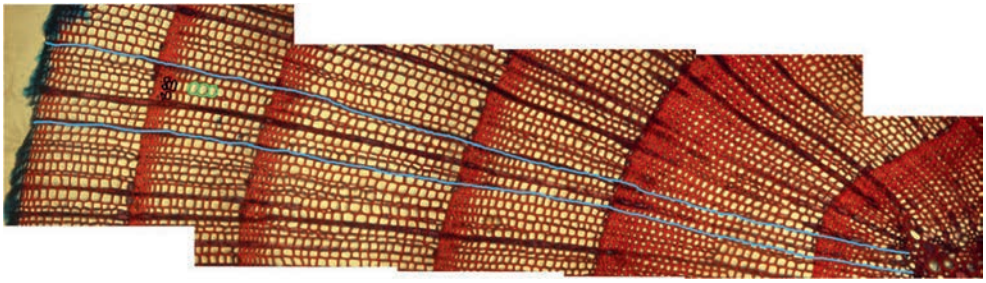

Fig.S4.3 Principal components analysis (PCA) of multivariate trait associations across 28 conifer species. The first two PCA axes and the loadings of 14 traits are shown. Different trait groups are indicated with different colored arrows for pit traits (red), earlywood traits (blue), latewood traits (green), average wood traits of early and latewood (purple), and hydraulic traits (black). Different families (Cupressaceae, Pinaceae, Taxaceae) are indicated by different symbols. For trait abbreviations (in Italics), see Table 4.1, for species abbreviations (in grey) see Table S4.1.

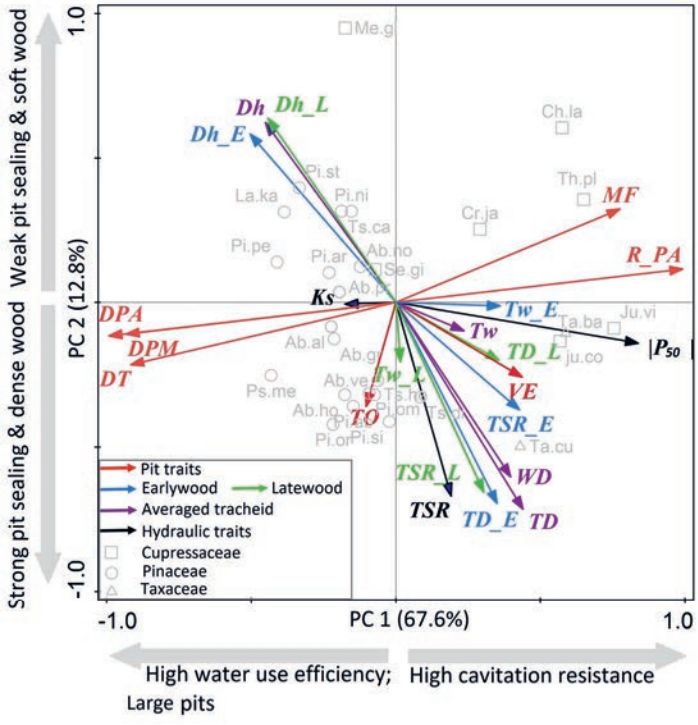

Fig. S4.4 Structural equation models for the effects of pit traits and tracheid traits of earlywood (a, c) and latewood (b, d) on the cavitation resistance ($|P_{50}|$) and hydraulic conductivity (Ks) for 28 conifer species: (a) earlywood and $|P_{50}|$ (χ^2=23.38, df=17, *P*=0.053), (b) latewood and ($|P_{50}|$) (χ^2=20.34, df=18, *P*=0.31), (c) earlywood and Ks (χ^2=19.18, df=7, *P*=0.01), (d) latewood and Ks (χ^2=15.76, df=7, *P*=0.03). The pit characteristics were all for earlywood, except pit aperture resistance could vary between early and latewood for P_{50}; and tracheid diameter, density, and wall thickness for Ks. Significant coefficients are shown in bold, and ns means non-significance. The models for Ks cannot be accepted as in both cases *P*<0.05.

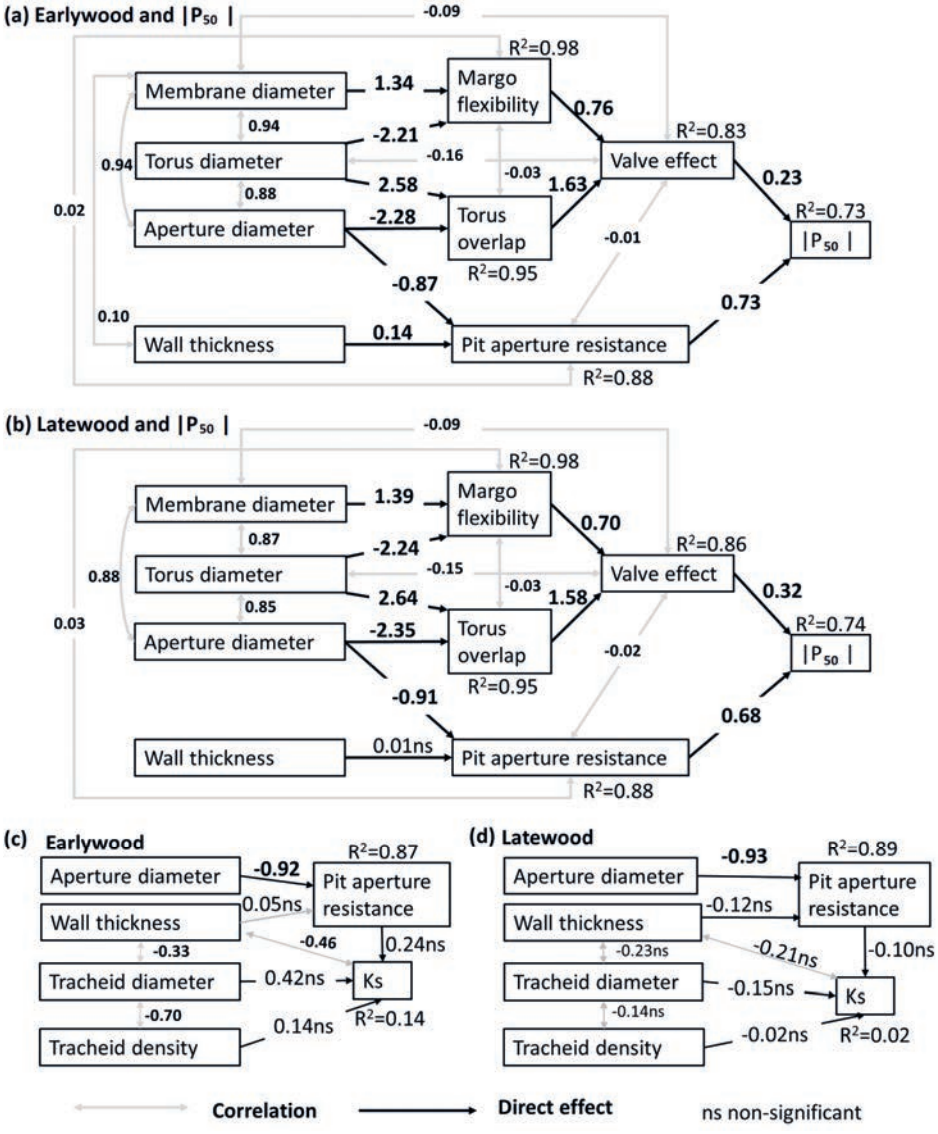

CHAPTER 5

5

Drought resilience of conifer species is driven by leaf lifespan and not by hydraulic traits

Yanjun Song, Frank Sterck, Xiaqu Zhou, Qi Liu, Bart Kruijt, Lourens Poorter

Abstract

- Global warming and increased droughts impair tree growth worldwide. This study analyses the hydraulic and carbon traits of conifer species, and how they shape species strategies in terms of their growth rate and drought resilience.
- We measured 43 functional traits for 28 conifer species growing in a 50 y old common garden experiment in the Netherland. We assessed 1) how multiple leaf and stem drought- and carbon-related traits are associated across conifer species, and 2) how these traits affect stem growth and drought resilience.
- We found two trait spectra, reflecting a trade-off between hydraulic- and biomechanical safety versus hydraulic efficiency, and a trade-off between tough, long-lived tissues versus high carbon assimilation rate. Network analysis showed that pit aperture size occupied a central position in the trait network.
- Stem growth rate only increased with hydraulic efficiency (i.e., pit aperture diameter) and drought resilience decreased with leaf lifespan, indicating that species with long-lived leaves suffer from legacy effects due to tough tissues and slow turnover rate, and drought-damaged leaves with long lifespan cannot recover quickly from drought.

Key words: conifer species, drought resilience, functional trait, leaf lifespan, pit size, stem growth, trait spectra

5.1 Introduction

5.1.1 Climate change and conifer species

One of the most important challenges in ecology is to predict the impacts of climate change on plants, and its cascading effects on plant species distributions, community structure, ecosystem functioning, and ecosystem services (Bellard *et al.*, 2012; Jump *et al.*, 2017). Here we focus on conifer species as they are important components of many temperate and boreal forests because they provide timber, carbon storage, food and shelter (Pan *et al.*, 2011; Hämäläinen *et al.*, 2018; Davies *et al.*, 2020). Global warming and the increased, frequent and intense droughts are endangering the growth and survival of tree species worldwide (IPCC, 2013; Lévesque *et al.*, 2013; Choat *et al.*, 2018; Brodribb *et al.*, 2020), including conifer species (DeSoto *et al.*, 2020). This study analyses the hydraulic and carbon traits of conifer species, and how they shape species strategies in terms of their growth rate and drought resilience.

5.1.2 Functional traits and the plant economics spectrum

Functional traits are defined as morphological, physiological, or phenological characteristics that impact species performance in growth, survival and reproduction (Violle *et al.*, 2007). The ecological strategies of plant species are often analyzed in terms of their resource economy, where plant traits determine the uptake, transport, use and loss of essential resources such as water, nutrients and carbon (Choat *et al.*, 2018). Worldwide a plant economics spectrum has been identified ranging from species with conservative resource use, slow growth, and high survival to species with acquisitive resource use, fast growth but slow survival (Reich, 2014; Díaz *et al.*, 2016). The characteristics of different plant organs (i.e., leaves, stems and roots) are expected to be associated since they jointly determine resource use (Reich, 2014). The global acquisitive-conservative spectrum is also known as the leaf economics spectrum (LES), as it has initially been developed and tested for leaves (Wright *et al.*, 2004). Yet, it is more controversial and debated for stems (Yang *et al.*, 2021) and even more so for roots (Weemstra *et al.*, 2016; Bergmann *et al.*, 2020) because stem and root strategies might be driven by multiple environmental drivers (Weemstra *et al.*, 2016; Rosas *et al.*, 2019).

Conifers tend to occupy the conservative end of this global spectrum (Diaz et al. 2016) because of their specific features, such as tough, needle-like evergreen leaves, and their narrow conduits, which reduce their water transport capacity but makes them more tolerant to drought and cold. Most large-scale comparative studies find the LES because they focus on a broad range of angiosperms species or compare angiosperms and gymnosperms. However, a comparative study on gymnosperm species failed to find the LES (Anderegg, LD *et al.*, 2018), which is - apart from the large variation in leaf life span probably due to the relatively narrow range of trait values within this group (cf. Song *et al*., 2021). In addition, it remains unclear to

what extent leaf and stem traits are coordinated, and whether conifer species show a plant economics spectrum that integrates leaf and stem traits (Rosas *et al.*, 2019). Here we address this knowledge gap by quantifying stem and leaf traits of 28 conifer tree species growing in a common garden experiment. We assess the existence of economic spectra across leaves and stem, with a special emphasis on hydraulic traits, and explore the implications for stem growth and drought resilience.

5.1.3 Traits and tree strategies

Tree growth and survival depend on a complex network of interrelated morphological and physiological traits (Sterck *et al.*, 2014; Roskilly *et al.*, 2019). Traits that increase carbon gain, water transport and soft tissue structure also increase growth (Reich, 2014). Traits related to hydraulic failure and carbon starvation have advanced our physiological understanding of drought-induced mortality (Allen *et al.*, 2015; Adams *et al.*, 2017; Choat *et al.*, 2018). Specifically, acquisitive leaf trait values such as a high specific leaf area, stomatal conductance and nutrient concentrations, but low leaf dry matter content and short leaf lifespans, may contribute to a higher growth rate (Sterck *et al.*, 2006; Kitajima & Poorter, 2010) but may come at the cost of higher mortality risks with a low resistance to drought (Chapter 3). Inversely, conservative leaves facilitate high physical strength and resistance to drought stress, but come at the cost of a slow growth rate (Onoda *et al.*, 2017; Cui *et al.*, 2020).

In comparison, acquisitive stem trait values with a high hydraulic conductivity consist of large pits and tracheids, favoring high growth rates in conifer species, but this may come at the expense of reduced drought tolerance (Pittermann *et al.*, 2006a; Chave *et al.*, 2009). There are however very few studies that explore growth responses of larger numbers of conifers using a broad range of functional traits (Walters & Gerlach, 2013; Anderegg, LD *et al.*, 2018), and even less that link those the resultant spectra to differences in stem growth or drought resilience across conifer species (Martínez‐Vilalta *et al.*, 2010). Some of the species' generalizations may therefore be premature for conifers.

In this study, we quantified 43 leaf and stem traits of 28 conifer species growing in a common garden experiment and used dendrochronology to quantify stem growth and drought resilience. Resilience consists of two components, the reduction in stem growth during dry years (resistance) and the level of increase in stem growth (recovery) after dry years. We addressed two questions:

1) How are functional traits associated with each other? We expect that traits that contribute to similar functions are more closely correlated than traits linked to other functions. From this,

we predict that traits can be classified into different clusters, reflecting for example structural construction costs, drought tolerance, water transport and carbon assimilation. Moreover, we expect that such groups imply divergent species growth strategies for water, carbon and nutrients economics to adopt multiple strategies to climate change (Chave *et al.*, 2009; Li *et al.*, 2015; Rosas Torrent, 2019). As a result, a strategy spectrum runs from conservative slow-growing species with dense tissues and high hydraulic safety to acquisitive fast-growing species with soft tissues and high hydraulic efficiency and carbon assimilation.

2) How do functional traits predict the growth and drought resilience of conifer species? We hypothesize that traits related to hydraulic efficiency and carbon assimilation predict conifer species' growth since these traits allow species to have high photosynthesis (Chave *et al.*, 2009). We expect that different traits act as strong drivers of the two components of drought resilience; drought resistance and drought recovery. Drought resistance will increase with higher values for multiple hydraulic safety traits (Delzon & Cochard, 2014). Drought recovery will increase with fast-growth features linked with high carbon assimilation rates and soft tissues.

5. 2 Materials and Methods

5. 2.1 Study site and Species selection

This study was conducted in a 50-year-old common garden experiment at the Schovenhorst Estate (52.25 N, 5.63 E), near Putten, the Netherlands. The study site is characterized by a temperate maritime climate. The mean annual temperature is 10.1°C and the mean annual rainfall is 830 mm. The area is underlain with dry, loamy, sandy and nutrient-poor soils with a low water retention capacity (Cornelissen *et al.,* 2012) and a long-distance (19 m) to the soil water table (TNO-NITG, 2020). In the 1960's a common garden experiment was established, where >30 conifer species from the Northern hemisphere were planted in monospecific stands. To assess the relationships among functional traits and how these traits affect species performance in terms of growth and drought resilience, we selected 28 conifer species from different climatic origins (Table S5.1). To measure functional traits, we selected three to six individuals per species with exposed crowns, at the top of the stand. The trees had an average stem diameter at breast height of 35.8 cm, which varied from 5.0-86.3 cm across species. One branch per individual was selected for the following measurements.

5.2.2 Sample collection and functional traits measurements

5.2.2.1 Sample collection

Between 2018 and 2019, we collected 43 traits for 28 conifer species (Table 5.1). These traits were related to leaf size and display (3 traits), carbon assimilation and nutrient investments (7 traits), tissue toughness (6 traits), wood anatomy (13 traits), hydraulics and cavitation resistance (8 traits), and pressure-volume traits (6 traits). To reduce phenotypic variation among individuals and species, we harvested branches (*c.* 65 cm long) in the most illuminated position with an average height of 6 m (5-7m). Due to time limitations, traits related to wood anatomy and pressure-volume traits were measured based on three individuals per species. For the remaining traits, five or six individuals per species were measured. All trait values were averaged at the species level.

To measure wood density (WD, g cm^{-3}), bark density (BD, g cm^{-3}) and wood dry matter content (WDMC, g g^{-1}), we selected the samples from the last 10 cm segment of the main branch stem, which was about 55-65 cm from the apex. Branch parts were weighted, both the volume with and without bark was measured with the water displacement method, and subsequently oven-dried for 72 h at 105 °C until a constant mass was obtained.

To measure specific leaf area (SLA, cm^2 g^{-1}) and leaf dry matter content (LDMC, g g^{-1}), we randomly selected 100 mature and healthy needles from the main branches. We weighted fresh mass for these needles, scanned these needles for total leaf area using ImageJ v. 1.52a, and then dried for dry weight at 75 °C for 72 h.

To measure leaf mass fraction (LMF, g g^{-1}) at branch level and leaf number per unit branch length (LN_{BL}, # mm^{-1}), we harvested the current-year branch samples (*c*. 1-10 cm length). Branch pieces and leaf pieces were separately dried at 75 °C for 72 h for dry mass.

To measure leaf density (LD, g cm^{-3}), a separate bunch of healthy and mature needles was collected. Leaf fresh volume was determined with the water displacement method and then we dried samples for leaf dry weight at 75 °C for 72 h.

Table 5.1 Overview of 43 functional traits for 28 conifer species in this study: trait name; abbreviation; unit; median, 5th percentile, 95th percentile and coefficient of variation (CV) based on trait values (n=3-6 individuals*28 species).

Traits function	Trait name	Abbreviation	Unit	Median	Percentiles		CV
					5th	95th	
Leaf size and display (3)	Specific leaf area	SLA	$cm^2\ g^{-1}$	59.20	36.10	116.72	0.45
	Leaf mass fraction	LMF	$g\ g^{-1}$	0.84	0.54	0.93	0.15
	Leaf number per branch length	LN_{BL}	$\#\ mm^{-1}$	1.44	0.48	3.94	0.73
Carbon and nutrient investments (7)	Photosynthetic rate (area)	A_{area}	$\mu mol\ CO_2\ m^{-2}\ s^{-1}$	8.03	4.31	14.97	0.39
	Photosynthetic rate (mass)	A_{mass}	$nmol\ CO_2\ g^{-1}$	47.37	24.12	90.44	0.46
	Stomatal conductance	g_s	$mol\ H_20\ m^{-2}\ s^{-1}$	0.06	0.03	0.14	0.52
	Intrinsic water-use efficiency	iWUE	$mmol\ CO_2\ (molH_2O)^{-1}$	132.40	69.34	181.16	0.26
	Leaf nitrogen concentration	N	%	1.45	0.98	2.37	0.27
	Leaf phosphorus concentration	P	%	0.13	0.06	0.24	0.43
	Leaf potassium concentration	K	%	0.44	0.24	0.83	0.38
Tissue toughness (6)	Leaf density	LD	$g\ cm^{-3}$	0.41	0.23	0.49	0.20
	Leaf dry matter content	LDMC	$g\ g^{-1}$	0.48	0.37	0.53	0.16
	Wood dry matter content	WDMC	$g\ g^{-1}$	0.51	0.42	0.58	0.11
	Bark density	BD	$g\ cm^{-3}$	0.42	0.34	0.51	0.14
	Wood density	WD	$g\ cm^{-3}$	0.53	0.44	0.66	0.12
	Leaf lifespan	LL	yr	5.00	1.00	9.00	0.52
Wood anatomy (13)	Hydraulic diameter	Dh	µm	12.49	10.35	17.76	0.18
	Tracheid density	TD	$\#\ mm^{-2}$	$3.57x10^3$	$2.34x10^3$	$4.69x10^3$	0.21
	Wall thickness (earlywood)	Tw_E	µm	2.34	1.82	3.16	0.18
	Wall thickness (latewood)	Tw_L	µm	2.92	2.37	3.75	0.52
	Thickness to span ratio (earlywood)	TSR_E	$\mu m\ \mu m^{-1}$??	0.17	0.08	0.51	0.79
	Thickness to span ratio (latewood)	TSR_L	$\mu m\ \mu m^{-1}$??	0.78	0.15	1.98	0.84
	Pit aperture diameter	DPA	µm	4.29	3.12	5.16	0.16
	Pit aperture resistance	R_{PA}	$MPa\ s\ m^{-3}$	$3.28x10^8$	$2.10x10^8$	$1.00x10^9$	0.71
	Pit membrane diameter	DPM	µm	12.83	9.86	15.31	0.14
	Torus diameter	DT	µm	0.35	0.28	0.44	0.14
	Margo flexibility	MF	-	0.48	0.44	0.58	0.09
	Torus overlap	TO	-	0.35	0.28	0.44	0.14
	Valve effect	VE	-	0.17	0.14	0.20	0.11
Hydraulics and cavitation resistance (8)	Predawn water potential	$\|\Psi_{pre}\|$	MPa	1.13	0.73	1.91	0.30
	Minimum water potential	$\|\Psi_{mid}\|$	MPa	1.83	1.45	2.25	0.15
	Xylem specific hydraulic conductivity	Ks	$Kg\ m^{-1}\ s^{-1}\ MPa^{-1}$	0.29	0.08	0.67	0.59
	Pit specific hydraulic conductivity	Kpit	$kg\ m^{-1}\ s^{-1}\ MPa^{-1}$	0.34	0.24	0.81	0.45
	Xylem pressure when 12% of hydraulic conductivity is lost	$\|P_{12}\|$	MPa	3.05	2.31	5.09	0.26
	Xylem pressure when 50% of hydraulic conductivity is lost	$\|P_{50}\|$	MPa	3.72	2.92	7.34	0.32
	Xylem pressure when 88% of hydraulic conductivity is lost	$\|P_{88}\|$	MPa	4.33	3.37	9.83	0.38
	Hydraulic safety margin	HSM	MPa	2.16	1.27	5.33	0.51
Pressure-volume traits (6)	Turgor loss point	$\|\Psi_{TLP}\|$	MPa	1.57	0.90	1.93	0.24
	Osmotic potential at full turgor	$\|\pi_0\|$	MPa	1.02	0.62	1.51	0.29
	Bulk modulus of elasticity of cell walls	ε	MPa	10.99	4.07	20.94	0.51
	Hydraulic capacitance at full turgor	CFT	$mol\ m^{-2}\ MPa^{-1}$	0.06	0.04	0.14	0.53
	Saturated Water Content	SWC	$g\ g^{-1}$	1.76	1.19	2.60	0.26
	Relative water content at turgor loss point	RWC_{tlp}	%	90.72	75.14	95.90	0.16

5.2.2.2 Traits measurements

Leaf size and display. Specific leaf area (SLA), leaf mass fraction (LMF) and leaf number per unit branch length (LN_{BL}) imply the capacity of light capture, since SLA represents biomass efficiency for leaf display, LMF represents biomass allocation to leaves, and LN_{BL} indicates the efficiency of branches packing their leaves (Poorter *et al.*, 2018). SLA was calculated as leaf area per unit dry mass. LMF was calculated as leaf dry mass divided by branch dry mass. LN_{BL} was calculated as the number of needles divided by branch length.

Carbon and nutrient investments. To estimate the carbon assimilation rate, the maximum photosynthetic rate per unit leaf area (A_{area}, μmol CO_2 m^{-2} s^{-1}) and stomatal conductance (g_s, mol H_20 m^{-2} s^{-1}) were measured using a portable photosynthetic system (Li-6400, Li-Cor). To obtain the maximum photosynthetic rate, the relatively light intensity was set at 1500 μmol m^{-2} s^{-1} and CO_2 concentration at 400 ppm. Maximum photosynthetic rate and associated variables were measured when the photosynthetic rate saturated and became stable. Given that the physiological efficiency of plants is better expressed on a mass basis, and that the leaf economics spectrum is more pronounced when being expressed on a mass basis (Osnas *et al.*, 2013), we used the maximum photosynthetic rate per unit leaf mass (A_{mass}, nmol CO_2 g^{-1}) as our indicator of the carbon assimilation capacity (He *et al.*, 2019). A_{mass} was obtained by multiplying A_{area} with SLA. Intrinsic water use efficiency (iWUE, mmol CO_2 $(molH_2O)^{-1}$) was calculated as A_{area}/g_s (Yao *et al.*, 2021). Leaf nutrient concentrations were measured by re-drying needles at 75°C for three days, and then ground them into fine powders (<250 μm.). Samples were then sent to the Chemical Laboratory of Wageningen University for the measurements of leaf nitrogen concentration (N, %), leaf phosphorus concentration (P, %) and leaf potassium concentration (K, %). Leaf N, P and K concentrations were measured using a flow-injection auto-analyzer.

Tissue toughness. Leaf density (LD), Leaf lifespan (LL), bark density (BD), wood density (BD), leaf dry matter content (LDMC) and wood dry matter content (WDMC) all contribute to toughness construction and structural enforcement (Wright *et al.*, 2005; Poorter *et al.*, 2018). LD, BD and WD were calculated as the corresponding dry mass divided fresh volume. LDMC and WDMC were calculated as the corresponding dry mass divided by fresh mass. LL was defined by the oldest leaf along the main branch, cutting down the branch at the position where the oldest leaf appeared and counting the annual rings. Deciduous species were all counted as one year for their LL.

Wood anatomy. Wood anatomical traits indicate species capacity for hydraulic transport (i.e., conduits and pits) and cavitation resistance (i.e., pit size and sealing) (Delzon *et al.*, 2010;

Poorter *et al.*, 2010). On transverse section, conduit diameter (D, µm), tracheid density (TD, mm^{-2}), wall thickness for earlywood (Tw_E, µm), wall thickness for latewood (Tw_L, µm), thickness to span ratio for earlywood (TSR_E, µm $µm^{-1}$), and thickness to span ratio for latewood (TSR_E, µm $µm^{-1}$) were measured. Tracheid density (TD, # mm^{-2}) was determined as the number of tracheids per cross-sectional area. Hydraulic diameter (Dh, µm) was quantified as the hydraulically weighted conduit diameter (Sterck *et al.*, 2008; Poorter *et al.*, 2010), and thickness to span ration (TSR, µm $µm^{-1}$) was calculated as the square of double-wall thickness over lumen diameter (Hacke *et al.*, 2001):.

$$Dh = \sqrt[4]{\frac{1}{n}\sum_{i=1}^{n} Di^4} \quad (1)$$

$$\mathrm{TSR} = \left(\frac{2\mathrm{xTw}}{\mathrm{D}}\right)^2 \quad (2)$$

where *Di* is the tracheid diameter of the *i*th of n measured tracheids, Tw is the wall thickness, and D is the adjacent tracheid lumen diameter.

On the tangential section, the diameter of pit aperture (DPA, µm), pit membrane (DPM, µm) and torus (DT, µm) were measured. Subsequently, traits related to pit aperture resistance (i.e., R_{PA}, MPa s m^{-3}) and pit sealing (i.e., margo flexibility, torus overlap and valve effect) were calculated following Delzon *et al.* (2010). Margo flexibility (MF) is calculated by comparing the torus and the pit membrane diameter [MF = (DPM–DT)/DPM], and indicates the capacity of movement of the torus inside the pit; torus overlap (TO) is calculated by comparing the torus against the pit aperture [TO=(DT–DPA)/DT], thus reflecting the sealing capacity of the torus for the aperture. The two contribute to a valve effect (VE = TO x M, indicating the capacity to seal the pit aperture when cavitation occurs. A strong valve effect consists of a large TO and VE, contributing to a high cavitation resistance. For the detailed measurements, see Chapter 3.

Hydraulics and cavitation resistance. The xylem specific hydraulic conductivity (Ks in kg m^{-1} MPa^{-1} s^{-1}), xylem potential specific hydraulic conductivity (Kp in kg m MPa^{-1} s^{-1}) and pit specific hydraulic conductivity (Kpit in kg m^{-1} MPa^{-1} s^{-1}) all indicate species water transport efficiency (Domec *et al.*, 2006; Poorter *et al.*, 2010). The whole-wood specific conductivity (Ks) was quantified as the maximum xylem specific hydraulic conductivity when we measured cavitation resistance (Song *et al.*, submitted). As Ks indicates the overall conductivities of lumen (Kp) and pits (Kpit), Kp (the xylem potential specific hydraulic conductivity) and Kpit (parallel conductivity of pits on a tissue level) were calculated as follows (Domec *et al.*, 2006; Sterck *et al.*, 2008):

$$\mathrm{Kp} = \left(\frac{\pi\rho}{128\eta}\right) \times \mathrm{TD} \times \mathrm{Dh}^4 \quad (3)$$

$$\mathrm{Kpit} = \left(\frac{1}{\mathrm{Ks}} - \frac{1}{\mathrm{Kp}}\right)^{-1} \quad (4)$$

where Kp (kg m MPa^{-1} s^{-1}) is the xylem potential specific hydraulic conductivity, ρ is the water density at 20 °C (998.2 kg m^{-3}), η is the viscosity of water at 20 °C (1.002×10^{-3} Pa s),TD is tracheid density, and Dh is the hydraulically weighted tracheid diameter (equation 1).

We used xylem pressures when 12%, 50% or 88% of hydraulic conductivity were lost (P_{12}, P_{50} and P_{88}) to indicate species cavitation resistance to cavitation. Predawn water potential (Ψ_{pre}, MPa) and minimum water potential (Ψ_{mid}, MPa) for the twigs were obtained from Song et al. (2021, submitted). Hydraulic safety margin (HSM, MPa) was calculated as the difference between P_{50} and Ψ_{mid} (Delzon & Cochard, 2014). P_{12}, P_{50}, P_{88}, Ψ_{mid} and HSM are good predictors for species hydraulic safety and drought resistance (Bhaskar & Ackerly, 2006; Anderegg *et al.*, 2016). For the detailed measurements, see Chapter 4.

Pressure-volume traits. Leaf water potential at turgor loss point (i.e., the water potential at which leaves lose turgor; Ψ_{TLP}, in MPa) is the good predictor for drought tolerance; a more negative turgor loss point implies species have lower leaf wilting risks and would be more drought tolerance (Bartlett *et al.*, 2012; Maréchaux *et al.*, 2015). We measured therefore pressure-volume curves to quantify the traits related to the turgor loss point. Considering that conifers have very tiny pointed needles (e.g., *Picea* species) or scale leaves (e.g., *Thuja plicata*), it is difficult to measure leaf water potential. Instead, we measured the water potential of the twigs. To assure that twigs were fully hydrated before measurements, branches were rehydrated overnight. Three or four individuals per species were measured using the bench-drying method to construct pressure-volume curves. Species can have more negative Ψ_{TLP} through accumulating solutes (more negative π_0) or increasing cell wall flexibility (decreasing Ɛ), where π_0 is the osmotic potential at full turgor (π_0, MPa) indicating the solutes concentration in cells at full turgor, and Ɛ is the bulk modulus of elasticity of the cell wall (MPa) indicating cell wall stiffness (Bartlett *et al.*, 2012). The saturated water content (SWC, g g^{-1}) is defined as the ratio of water mass at 0 MPa to dry mass in a fully saturated sample, relative water content at turgor loss point (RWC_{tlp}, %) is defined as the ratio of water mass when plants lose their turgor to saturated water mass, and the hydraulic capacitance at full turgor (CFT, mol m^{-2} MPa^{-1}) is estimated as the slope of the P–V curve between full turgor and Ψ_{TLP}, see López *et al.* (2021). They were all determined from pressure-volume curves as described by Sack *et al.* (2011). SWC, RWC_{tlp} and CFT indicate the water storage capacity of species (Campany *et al.*, 2021). It should be noted that pressure-volume curves and these parameters are normally measured on leaves, but because conifer needles are so small we measured

pressure-volume curves on twigs, and therefore in our case SWC, RWC_{tlp} and CFT are twig-level properties, rather than leaf-level properties.

5.2.3 Growth potential and drought resilience components

To indicate growth strategy, growth potential and growth resilience to drought and its underlying components (i.e., drought resistance, recovery and resilience) were quantified from tree-ring data (Song *et al.*, 2021). Drought resistance indicates species ability to retain growth during drought, drought recovery and resilience indicate species capacity to regrow after drought (Vitali *et al.*, 2017). To represent different dimensions of growth in terms of diameter and biomass, stem growth rate (cm yr^{-1}) for the first twenty years, stem area growth rate (cm yr^{-1}), and stem mass growth rate (cm yr^{-1}) were used to indicate growth potential. For detailed methods see Chapter 2 and 3.

5.2.4 Data analysis

To assess whether all these 43 traits can be classified into different functional groups, we used cluster analysis, and to evaluate how traits were associated, we used a Principal Component Analysis (PCA). Prior to analysis, data were log_{10}-transformed to improve normality and homoscedasticity. We used the absolute values of Pearson correlation to do the cluster analysis. Pearson correlation and cluster analysis were carried out with the R packages “Hmisc” and "pheatmap", respectively. Secondly, PCA was performed in Canoco 5 based on identified groups from cluster analysis.

The cluster analysis resulted in eight clusters of closely associated traits. To assess which traits are ‘central traits’ or ‘key traits’, that for mechanistic or ecological reasons are closely associated with other traits, a network analysis was done. With 28 species, the maximum number of traits that can be included in network analysis is eight traits. We selected therefore from eight of the eight identified clusters one representative and relevant ecological trait. Subsequently, the network analysis was done with eight trait names as nodes, and partial correlation coefficients between every two nodes after controlling all other variables in the dataset as edges (Epskamp *et al.*, 2018). To assess the importance of nodes in the network, centrality was computed by summing the absolute values of partial correlations to get the higher values quantified as important traits (Epskamp *et al.*, 2018; Epskamp & Fried, 2018). Network analysis was performed with R package “bootnet” (Epskamp *et al.*, 2015).

To assess how functional traits affect growth potential and drought resilience, we first used bivariate Pearson’s correlations and then used model selection with dredge function in “MuMIn” package (Barton & Barton, 2015) based on the selected groups from cluster analysis. To compare the effect size of different traits all traits were standardized by subtracting the

mean and dividing by the standard deviation. Finally, to assess the cause-effect relationships between traits and growth or drought resilience (Shipley, 2000). Shipley's d-step analysis was used in the R package "piecewiseSEM" (Lefcheck *et al.*, 2016). All data analyses were performed using R version 4.0.2 (R Core Team, 2020).

5.3 Results

5.3.1 Classifications of traits

To classify 43 traits, hierarchical clustering was used and identified eight functional trait groups (Fig. 5.1). The first cluster (in light blue) consisted of three traits related to **drought tolerance** since it contains predawn and minimum branch water potential (Ψ_{pre} and Ψ_{mid}), and it was also associated with leaf phosphorus (P). The second cluster (in purple) consisted of four traits related to **branch toughness,** including wood density (WD), wood dry matter content (WDMC) and bark density (BD). The third cluster (in blue) consisted of traits related to **water transport**, including stem-specific conductivity (Ks), pit conductivity (Kpit), cell wall thickness and thickness to span ratio of the earlywood (Tw_E and TSR_E). The fourth cluster (in red) consisted of traits related to **water use efficiency** (iWUE, g_s, Dh and TD) **and cavitation resistance** (P_{12}, P_{88}, P_{50}, HSM). The fifth cluster (in pink) contained three traits related to **leaf toughness**, i.e., leaf dry matter content (LDMC), leaf density (LD) and leaf lifespan (LL). The sixth cluster (in green) was composed of traits related to **carbon assimilation** (SLA, N, and A_{mass}) **and water status** of the symplast ($|\Psi_{TLP}|$ and $|\pi_0|$). The seventh cluster (in grey) reflected **branch-level traits** mainly associated with structure such as leaf mass fraction (LMF), latewood structure such as cell wall thickness and thickness to span ratio (Tw_L and TSR_L). The eighth cluster (in black) was the largest and involved 12 **pit traits**, i.e., related to pit size such as the diameter of pit aperture, pit membrane, and torus (DPM, DPA and DT), and pit sealing such as torus overlap, margo flexibility, and valve effect (TO, MF, VE).

We then further explored the relationships among these traits and the eight groups using PCA (principal components analysis). The first two PCA axes explained 63% of the variation and showed two trait spectra (Fig. 5.2). The first axis reflected a trade-off between hydraulic- and biomechanical safety (red, blue and light blue) at the left and the hydraulic efficiency (black and blue) at the right. It also indicated a conservative strategy with high cavitation resistance (red), cell wall thickness (Tw_E, blue) and thickness-to-span ratio of earlywood (TSR_E; blue) on the left side of the axis; and an acquisitive strategy with high water use efficiency (iWUE; red) and wide pits (DPA, DPM and DT; black) on the right side. These hydraulic spectra reflected an old split between cavitation resistant Cupressaceae and Taxaceae with high margo flexibility (MF) to the left, and conductive Pinaceae with wide pits and potentially fast growth to the right.

The second axis reflected a trade-off between leaf tissues toughness and lifespan at the lower end of the axis versus carbon assimilation at the higher end of the axis, where tissues toughness (pink) was associated with high leaf density (LD), leaf lifespan (LL) and leaf dry matter content (LDMC) at the bottom; and carbon assimilation (green) associated with high specific leaf area (SLA), photosynthetic rate (A_{mass}), and hydraulic diameter (Dh) at the top (Fig. 5.1, 5.2).

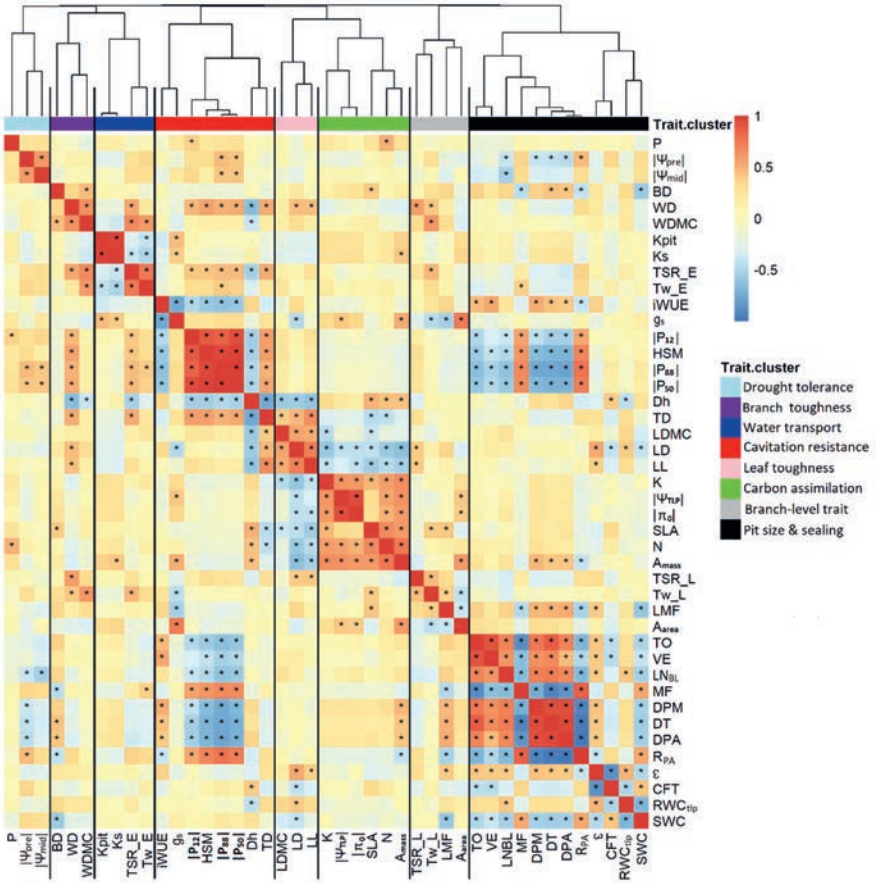

Fig. 5.1. Covariance of plant functional traits (n = 28 species) analysed by cluster analysis (hierarchical clustering) combined with a heatmap of covariation among the 43 traits. Trait correlations are indicated using colours, warm (red) shades indicate positive correlations and cool (blue) shades indicate negative correlations. The distance tree of traits derived from hierarchical clustering is illustrated on the top. Eight resulting clusters are: **group1. drought tolerance** comprising P, $|\Psi_{pre}|$ and $|\Psi_{mid}|$; **group 2. branch toughness** comprising BD, WD and WDMC; **group 3. water transport** comprising Kpit, Ks, TSR_E and Tw_E; **group 4. cavitation resistance** comprising iWUE, g_s, $|P_{12}|$, $|P_{50}|$, $|P_{88}|$, HSM, Dh and TD; **group 5. leaf toughness** comprising LDMC, LeafD and LL; **group 6. carbon assimilation and water status** comprising SLA, N, K, A_{mass}, K, $|\Psi_{TLP}|$ and $|\pi_0|$; **group 7. branch-level trait associated with structure** comprising TSR_L, Tw_L, LMF and A_{area}; and **group 8. pit size and pit sealing** comprising DPA, DPM, DT, MF, TO, VE, RPA,LNBL, Ɛ, CFT, RWC_{tlp} and SWC. *, P<0.05. For trait abbreviations see Table 5.1.

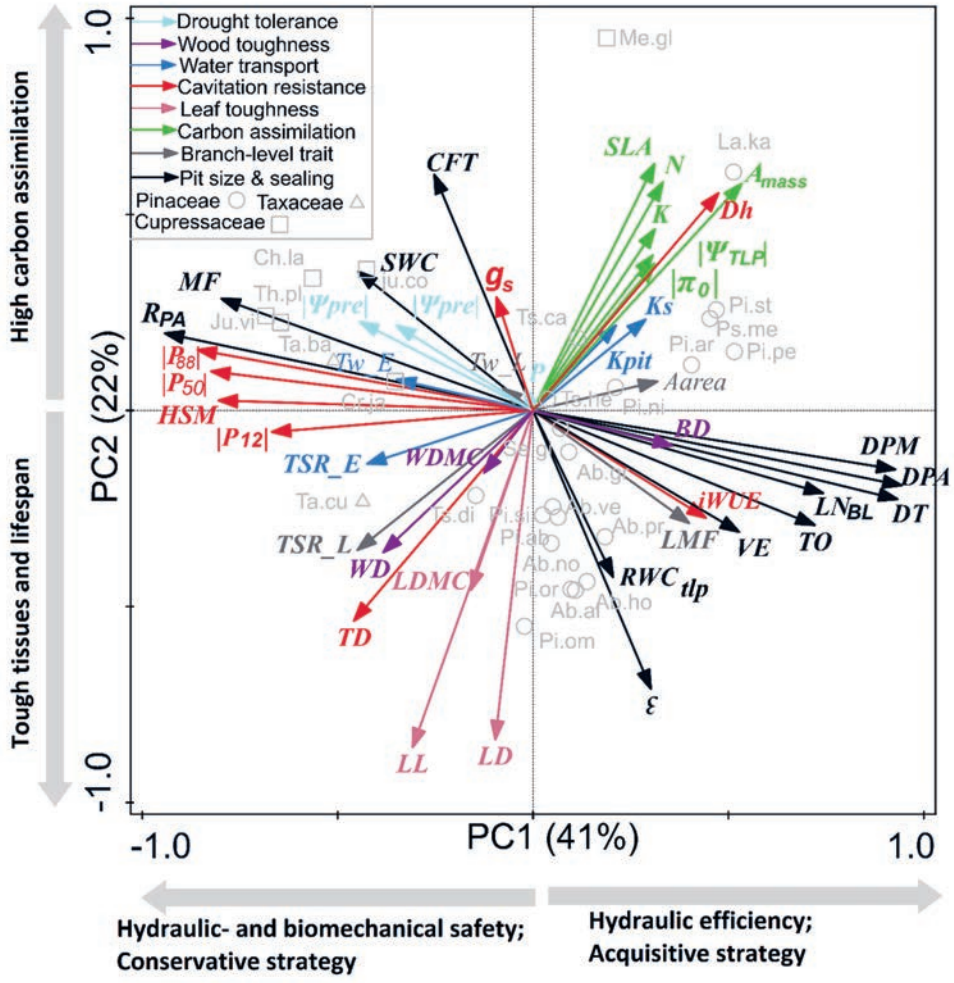

Fig. 5.2 Principal components analysis (PCA) for the first two PCA axes of 43 traits across 28 conifer species were shown. Eight trait groups were classified based on cluster analysis in Fig. 5.1 and indicated with arrows in different colors. Different families (Cupresssaceae, Pinaceae, Taxaceae) are indicated by different symbols. For trait abbreviations see Table 5.1; for species abbreviations (in light grey) see Table S5.1.

5.3.2 Network analysis

To evaluate what traits are central to plant functioning, a network analysis was carried out. We selected one key trait from each of the identified eight groups in cluster analysis. The most central trait was the diameter of pit aperture (DPA) that was positively related to carbon assimilation (A_{mass}, photosynthetic rate) and negatively related to drought tolerance ($|\Psi_{pre}|$, absolute value of predawn branch water potential), followed by four traits with a similar centrality; hydraulic safety margin (HSM), wood density (WD), leaf lifespan (LL) and photosynthetic rate (A_{mass}) (Fig. 5.3).

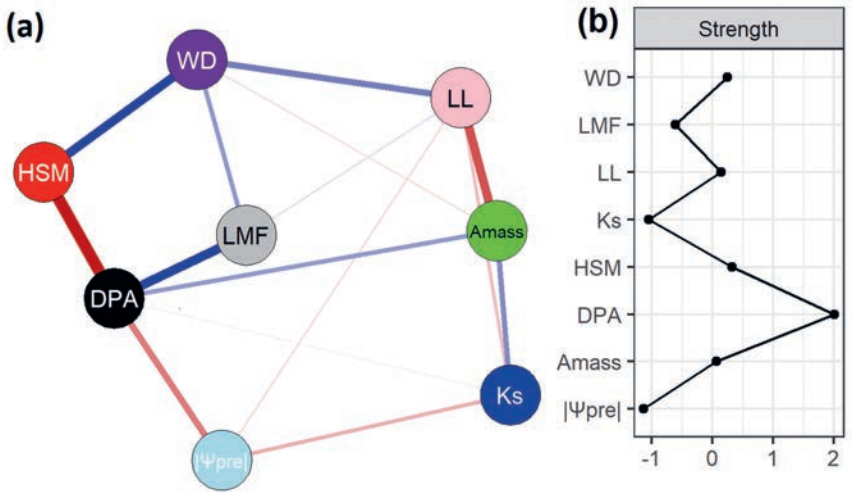

Fig. 5.3 Network analysis among eight main functional traits from eight different clusters in (a), and the strength of centrality indices in (b). Node colors vary among the different groups, see Fig. 5.1. Each trait is a node and connections represent partial correlation coefficients between two variables after conditioning on all other variables. The links in blue indicate positive coefficients and the links in red indicate negative coefficients in the model. The value of partial correlation is proportional to the thickness of the links. Strength was calculated from accumulated values of absolute partial coefficients between a focal node and all other connected nodes in the network. Strength was standardized by subtracting the mean from the specific values and dividing it by the standard deviation. Large strength values indicate high central traits. For trait abbreviations see Table 5.1.

5.3.3 Effects of traits on growth and drought resilience

To assess how functional traits affected species growth and drought resilience with its underlying components (resistance and recovery), multiple methods were used, such as bivariate Pearson's correlations, multiple regression and path analysis.

Of all 43 traits, stem diameter growth only increased with pit aperture diameter (Fig. 5.4a), which was also confirmed by the path analysis (Fig. 5.5a). Meanwhile, stem diameter growth was also negatively affected by cavitation resistance ($|P_{88}|$) due to small pit aperture size (Fig. 5b-c). Compared to stem diameter growth, stem area growth (BAI) and mass growth increased with hydraulic tracheid diameter (Fig. 5.4b-c). Unexpectedly, growth rate was not significantly related to any of the two PCA axes that reflect multivariate trait strategies (Figure S5.1). In sum, the stem growth of conifer species was determined by pit aperture size and hydraulic tracheid diameter.

Bivariate correlations showed that drought recovery decreased with an increase in leaf mass fraction (LMF), leaf dry matter content (LDMC), and leaf lifespan (LL) (Fig. 5.4d-f, 5e; Table 5.2). Drought recovery also increased with the second PCA axis, reflecting a trade-off between carbon assimilation and leaf toughness and – to a lesser extent – branch toughness (R^2=0.19, P=0.03; Fig 5.4g). Multiple regression indicated that drought resilience was negatively affected by leaf lifespan (LL) (Fig. 5.5d) and, surprisingly, also negatively affected with high photosynthetic rate (A_{mass}) (Table 5.2). The negative impact of A_{mass} on drought resilience disappeared in the path model (Fig. 5.5d), which suggests that the relationship between A_{mass} and drought resilience is weak or indirect. Surprisingly, none of the traits could explain drought resistance. In sum, species with a slow turnover rate (i.e., long leaf lifespan) have reduced drought recovery and resilience.

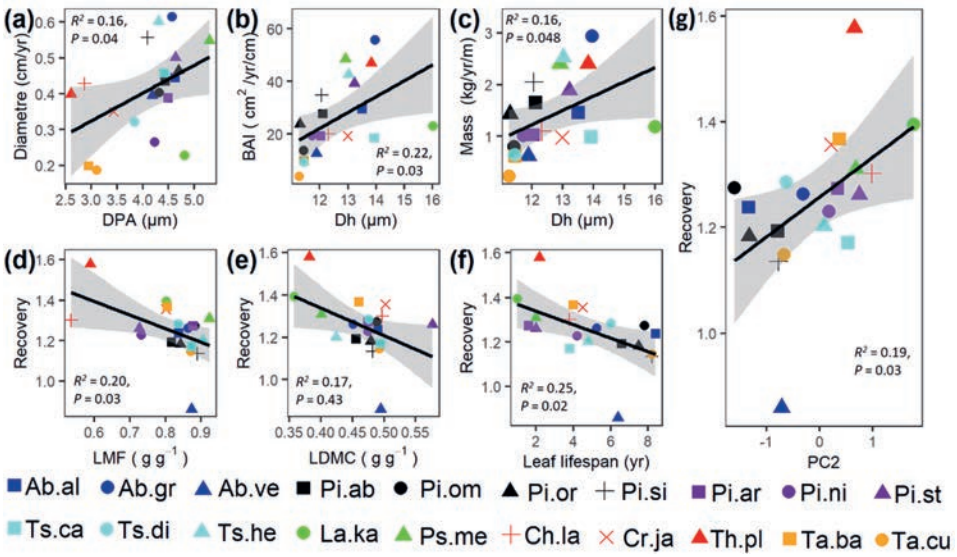

Fig. 5.4 Bi-variate significant relationships between growth rate and traits for **a**). stem diameter growth and pit aperture diameter(DPA), **b**). stem area growth and hydraulic diameter (Dh), **c**). stem mass growth and hydraulic diameter; and relationships between recovery and traits or PC2 scores for d-g: **d**. leaf mass fraction (LMF), **e**. leaf dry matter content (LDMC), **f**. leaf lifespan, **g**. PC2 scores from the result of PCA analysis. R^2 and *P* values are shown. The same color indicates the same genera. For species abbreviations, see Table S5.1.

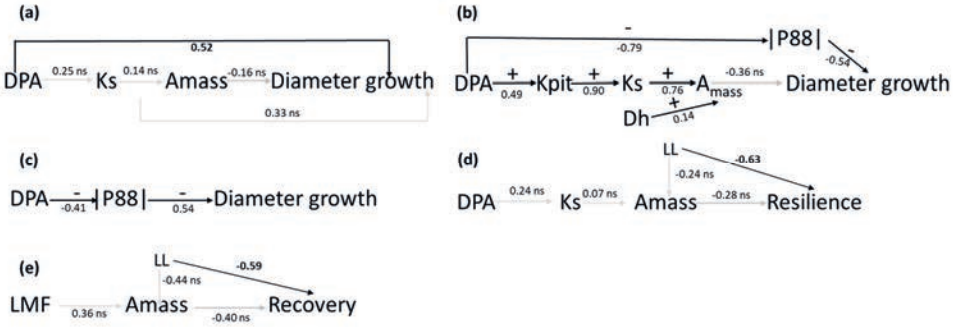

Fig. 5.5 Alternative accepted multivariate models linking functional traits and growth resilience for a-c) stem diameter growth; d) drought resilience; and e) drought recovery. Significant coefficients are shown in bold, and ns means non-significance.

Table 5.2 The results of averaged models based on best models (delta AIC<2) showing how these functional traits from eight different cluster groups affect conifer species stem growth (in light blue) and drought resilience (in light grey). Significant coefficients are shown in bold.

model	$\lvert\Psi_{pre}\rvert$	WD	Ks	HSM	LL	A_{mass}	LMF	DPA
Stem diameter growth								
Avg						**-0.48**		**0.62**
Imp						0.73		1.00
P						0.04		0.01
Stem area growth								
Avg		-0.35	0.32	-0.37	-0.26			0.30
Imp		0.34	0.10	0.18	0.15			0.18
P		0.16	0.18	0.13	0.28			0.22
Stem mass growth								
Avg	-0.22	-0.27	0.26	-0.37	-0.22			0.32
Imp	0.09	0.11	0.11	0.23	0.09			0.16
P	0.38	0.27	0.29	0.12	0.38			0.19
Resistance								
Avg						-0.22		
Imp						1.00		
P						0.35		
Recovery								
Avg	0.27			0.30	**-0.52**		-0.40	-0.34
Imp	0.11			0.14	0.89		0.31	0.24
P	0.20			0.16	0.02		0.08	0.09
Resilience								
Avg					**-0.72**	-0.57		
Imp					1.00	1.00		
P					0.004	0.02		

Notes: The model indexes, degrees of freedom (df), the log likelihood (logLik), corrected Akaike information criterion (AICc), and the AICc weight are given in Table S5.2. The average coefficients (Avg), relative importance (Imp), and significances (*P*) are shown. Relative importance of the predictor variables is calculated as the sum of the Akaike weights over the best selected models. $\lvert\Psi_{pre}\rvert$, predawn water potential; WD, wood density; Ks, xylem specific hydraulic conductivity; HSM, hydraulic safety margin; LL, leaf lifespan; A_{mass}, photosynthetic rate (mass) ;LMF, leaf mass fraction; DPA, pit aperture diameter.

5.4 Discussion

We assessed associations and clusters amongst 43 functional traits and showed how traits affected stem growth and drought resilience of conifer species. Two trait spectra were found. The first reflects a hydraulics spectrum driven by traits related to pit size, pit sealing and cavitation resistance, and can be interpreted as a trade-off between hydraulic safety and hydraulic efficiency. The second spectrum reflects a leaf economics spectrum, driven by traits

related to leaf toughness and carbon assimilation, and reflects a trade-off between leaf persistence and high leaf carbon assimilation. The stem growth rate increased with traits of the first spectrum (i.e., diameter of tracheids and pits), whereas drought recovery and resilience increased with traits related to the second spectrum (leaf toughness and lifespan). Below we discuss how traits are associated and how they underlie growth and drought resilience.

5.4.1 Traits associations and function for growth strategy

5.4.1.1 Trait clusters and associations

We expected that traits are clustered according to their main functions. We found eight clusters related to structural traits and physiological traits at different organizational scales. Structural trait clusters at different organizational scales ranged from sub-cellular level (pit traits) to branch (branch toughness, and other branch level traits) and leaf level (leaf toughness). Physiological trait clusters were related to hydraulics (drought tolerance, water use efficiency and cavitation resistance, water transport) and leaf physiology (carbon assimilation and water status). This suggests that that the strongest integration is within each organizational level (e.g., pit, leaf, branch) and less across these organizational levels, probably because of developmental reasons or optimization of specific physiological processes at each organizational level. The presence of these different types of clusters indicates that there is less tight integration across organs and functions. This means suboptimal solutions at the whole-plant level and that different clusters may be important under different environmental conditions.

Despite the weaker integration across clusters and their functions, we found that leaf economics spectrum and stem hydraulic traits were at least partly coupled (Fig 5.1, 5.2). Species with an acquisitive strategy for leaves, such as high leaf nutrient concentrations (N, K), SLA, stomatal conductance (g_s), photosynthetic rate (A_{mass}) had a larger hydraulic diameter (Dh) in the branches, and a more negative twig turgor loss point ($|\Psi_{TLP}|$) and branch osmotic potential at full turgor ($|\pi_0|$). Since wider tracheids increase hydraulic conductivity and water supply (Sterck *et al.*, 2008), this may allow for a higher stomatal conductance, transpiration rate and, coupled to that, photosynthetic rate (Brodribb & Feild, 2000; Chave *et al.*, 2009) and growth for both conifers (Sterck *et al.*, 2012) and broadleaf trees (Poorter *et al.*, 2010). The key traits for carbon, nutrient and water economics are thus partly coordinated across leaf and stem. This indicates that an integrated whole-plant economics spectrum (Reich 2014) also exists across conifer tree species (Rosas Torrent, 2019).

In contrast to our expectation, an acquisitive leaf strategy was associated with a large absolute (i.e., 'safe') leaf turgor loss point (Ψ_{TLP}). Such large turgor loss point values are

commonly interpreted as an indicator of drought tolerance worldwide (Bartlett *et al.*, 2012). Given that the needles were dense and tiny, we used twigs for pressure-volume curves to infer leaf turgor loss point, reflecting the turgor loss point of twigs rather than needles. It may lead to different findings for twigs compared with leaves, probably twigs with their parenchyma and bark have a larger hydraulic capacitance (CFT, SWC; see Fig. 5.2). the reason for our contradicting result remains puzzling and requires further attention in future studies.

5.4.1.2 Trait spectra and plant strategies

The PCA shows that the trait clusters are loosely organized into different multivariate plant strategy axes (Fig. 5.2). The first axis is strongly associated with trait clusters related to pit size and hydraulic safety measures, indicating that wider pits that facilitate hydraulic conductivity come at the expense of increased risk of drought-induced cavitation and reduced hydraulic safety (Roskilly *et al.*, 2019). Overall, the first axis reflects a hydraulics spectrum, running from a conservative strategy with high hydraulic- and biomechanical safety (i.e., high cavitation resistance, more negative water potential, large hydraulic safety margin and dense wood with high wood dry matter content) to a more acquisitive strategy with a higher hydraulic efficiency (i.e., a high conductivity and wide hydraulic diameter). The trade-off between hydraulic- and biomechanical safety and efficiency has been frequently found in Mediterranean forest (Quero *et al.*, 2011; Ramírez-Valiente *et al.*, 2020), tropical and temperate forest (Hacke *et al.*, 2006; van der Sande *et al.*, 2019; López *et al.*, 2021), whereas the trade-off across conifer species in the temperate area are rarely reported or the trade-off is lacked within species (López *et al.*, 2013; Rosas *et al.*, 2019). Hence, our study supports the evidence that such a safety-efficiency spectrum is not only found across angiosperm and gymnosperm species, where gymnosperms occupy the safe end of angiosperm and gymnosperm (Yang *et al*., 2021), but also within gymnosperm species. We conclude that the hydraulics spectrum exists in different forest ecosystems, influencing the water use strategy to a changing climate environment.

The second axis reflected a trade-off between the leaf toughness cluster (high leaf dry matter content, leaf density, leaf lifespan, bulk modulus of elasticity of cell walls) with lower water storage capacity at branch level (low saturated water content and hydraulic capacitance at full turgor) versus the carbon assimilation cluster (high specific leaf area, nitrogen, potassium, photosynthetic rate). This indicates that tough tissues and increased leaf lifespan come at the expense of a reduced photosynthetic capacity (Fig. 5.1, 5.2). This is consistent with the literature showing that thick, dense leaves increase the resistance and pathlength for CO_2 diffusion (Niinemets, 2001), nitrogen investment in cell wall defence cannot be invested in the photosynthetic enzyme Rubisco (Onoda *et al.*, 2017), and the observation that small

and thick cells are metabolically less active (Brown *et al.*, 2004). In the long-run, both leaf strategies may have a similar lifetime carbon gain, as short-lived leaves have a high capacity, and long-lived leaves have a long photosynthetic revenue stream over the lifetime of a leaf (Westoby, 1998; Edwards *et al.*, 2014). High leaf toughness was also associated with lower water storage capacity at the branch level. Such lower water storage capacity implies high water potential fluctuations, which may cause stomatal closure, and thus reduce carbon gain (Sack & Tyree, 2005). In sum, the second axis thus mainly reflects a leaf economics spectrum, running from a conservative strategy with high leaf toughness and long leaf lifespan to an acquisitive strategy with leaf trait values that increase carbon gain (Fig. 5.2).

5.4.1.3 Functional trait network

We further assessed the relationships among eight different clusters using trait networks. Pit aperture diameter (DPA) is the most central trait in the trait network (Fig. 5.3). Pit aperture size is associated with increased carbon assimilation (as indicated by the positive correlation with A_{mass}) but comes at the cost of reduced hydraulic safety, as indicated by the negative correlation with hydraulic safety margin (HSM) and absolute predawn water potential ($|\Psi_{pre}|$). Pit aperture can present a hydraulic bottleneck during drought stress, because wide pits not only facilitate hydraulic transport but they may also result in relatively small torus overlap and, hence, higher cavitation risks (Jansen & McAdam, 2019).

The second-most central trait in the network analysis is HSM. HSM is positively linked with wood density, indicating that tough tissues, that can avoid tracheid implosion, are also safer (Hacke *et al.*, 2001). High HSM indicates that plants follow a hydraulically safe strategy by reducing the risk of drought-induced cavitation and hydraulic failure. The importance of HSM is also highlighted by a global meta-analysis (Choat *et al.*, 2012), where tree species from biomes that differ strongly in aridity operate at very similar hydraulic safety margins just above zero, presumably to balance the need for safety to survive in a certain environment, with the need to increase carbon gain to effectively compete with other species. Although HSM is calculated as the difference between P_{50} and Ψ_{mid}, HSM was, surprisingly, not related to predawn water potential (Ψ_{pre}), despite the fact that Ψ_{pre} is closely correlated with Ψ_{mid}, ($r=0.62$, $P<0.001$, $n=28$ species), Ψ_{mid} was neither correlated with HSM, because all species have a rather similar Ψ_{pre} (range -2.31 Mpa–0.60 MPa) and Ψ_{mid} (range -2.42 Mpa-1.42 MPa), Predawn water potential depends strongly on rooting depth and soil conditions (Brum *et al.*, 2017). All species may have a similar Ψ_{pre} during the dry summer, because they all grow on deep sandy soils out of reach of the water table (>15 m) (Song *et al.*, 2021).

The network analysis further highlights some level of coordination between leaf traits and stem traits across conifer species. There are clear associations between leaf

photosynthetic capacity (A_{mass}) and the hydraulic water supply to the leaf (DPA and Ks), probably because the latter facilitates gas exchange. The positive association between wood density (WD) and leaf lifespan (LL) indicates that plants with a conservative strategy of resource use (e.g., shade-tolerant or drought-tolerant) have both long-lived leaves and dense wood (Fig. 5.3). The coupled relationship between leaf and stem is consistent with previous studies that leaf traits and wood traits were more related for both species in different temperate forests (Kawai & Okada, 2019) and species co-existing in temperate forests (Maherali *et al.*, 2006).

5.4.2 Mechanisms underlying growth and drought resilience

5.4.2.1 Pit aperture and tracheid determine stem growth

We expected that the stem growth of conifer species would increase with stem traits that increase water transport capacity, with leaf traits that increase photosynthetic carbon gain, and with cheap tissue construction costs. Although hydraulic conductivity did not affect species growth, the underlying water transport traits such as pit aperture and tracheid size did increase the stem growth of conifer species (Fig. 5.4a-c, 5.5a; Table 5.2). Pit aperture forms an important hydraulic bottleneck in plants, since a larger pit aperture contributes to higher hydraulic efficiency but lower hydraulic safety (Jansen & McAdam, 2019). Both larger DPA and Dh reflect larger tracheid dimensions and lower construction costs. This indicates that realized growth of conifer species on these deep sandy soils is driven by the trade-off between water transport capacity and drought resistance, rather than by traits directly related to carbon gain. The important role of DPA is also consistent with the central role it plays amongst traits from the eight different clusters (Fig. 5.3). To our knowledge, this is the first study that highlights the importance of pit aperture for stem diameter growth.

5.4.2.2 Leaf lifespan reduces drought resilience

Stem growth resilience responses to drought consist of drought resistance and drought recovery. We expected that drought resistance is explained by hydraulic stem and leaf traits, whereas drought recovery and resilience are explained by traits that increase carbon gain and growth. Surprisingly, none of the putative drought tolerance traits of stems (e.g., small pits, strong pit sealing, and large cavitation resistance) and leaves (e.g., negative turgor loss point and high hydraulic safety margin) could explain drought resistance. These findings reinforce our previous finding that drought resistance was not related to hydraulic traits (Chapter 3). Hydraulic traits such as P_{50} may increase drought tolerance in extremely arid systems (Plaut *et al.*, 2012), but maybe less important under the relatively mild maritime climatic conditions

of our study site where drought avoidance, for example through deep roots may become important (Choat *et al.*, 2018).

Leaf toughness and leaf lifespan were the best predictors of drought recovery and resilience. We observed that tree species with a longer leaf life span (and tougher leaves) recovered more poorly after drought and were less drought resilient. This observation is in line with predictions from a theoretical model, showing that slower organ turnover rates can cause stronger legacy effects on growth (Zweifel & Sterck, 2018; Zweifel *et al.*, 2020). Droughts can damage leaves, leading to bleaching, photodamage, and membrane rupture that impair leaf functioning (Thomas & Gay, 1987; Hansen & Dörffling, 2003; Brodribb *et al.*, 2016). Species with a short leaf life span can rapidly replace damaged leaves with well-functioning leaves, but species with long leaf life spans cannot (Zweifel & Sterck, 2018; Mackay *et al.*, 2020; Zweifel *et al.*, 2020). To our knowledge, this is the first study that shows that species with a conservative leaf economic strategy (long leaf lifespan) have such a lower drought recovery and resilience. This adds an important ecological dimension to leaf longevity, which is known as a key trait for multiple functions for plant strategies, such as increasing stress tolerance and conserving nutrient, carbon and nutrient cycling (Edwards *et al.*, 2014; Yu & He, 2017). We did, however, not observe the often observed trade-off between leaf lifespan and growth rate for other tree species and forests (Wright & Cannon, 2001; Cavender‐Bares, 2019), suggesting that some leaf lifespan driven trade-offs are context-dependent. Whether the observed legacy effects of leaf life span on drought resilience is something particular for conifers, or also occurs across broadleaf species or other forests, remains to be tested.

5.4.3 Conclusions

This study shows that leaf and stem traits are coordinated in terms of carbon assimilation and hydraulic efficiency. Two main strategy spectra were identified, i.e., hydraulics spectrum and leaf economics spectrum. The hydraulics spectrum runs from a conservative strategy with high hydraulic- and biomechanical safety to an acquisitive strategy with high hydraulic efficiency (i.e., water transport capacity). The leaf economics spectrum runs from a conservative strategy with tough tissues and long lifespan to an acquisitive strategy with high carbon assimilation. Pit aperture size is the central trait linking hydraulics spectrum and leaf economics spectrum. As pits from the “hydraulic bottleneck,” a large pit size is associated with increased stem diameter growth. A long leaf lifespan reduces drought recovery and resilience because of a reduced ability to replace drought-damaged tissues and track new climatic conditions with new, acclimated leaves. These insights may be used to improve our models and predictions of how trees may respond to an uncertain and drier future.

Acknowledgments

This study was funded by the KNAW Fonds Ecology under Grant number KNAWWF/87/19033, Oudemans Foundation, LEB fonds (2018-051C Song) and the China Scholarship Council (CSC, No.201706140106). We are very grateful to Jop de Klein and Els van Ginkel on administration. We acknowledge Angelina Horsting, Chenxuan Li, Dainius Masiliūnas, Ellen Wilderink, Jose A. Medina-Vega, Leo Goudzwaard, Manuel Rodriguez Carracedo, Matteo Dell'Oro, Na Wang, Sylvain Delzon, Weixuan Peng, Xiaohan Yin, Yanjie Xu, Zexin Fan and Zulin Mei for assistance with fieldwork and lab work.

Supplementary information

Table S5.1 Overview of 28 conifer species, abbreviations and distribution area.

Species	Abbreviation	Distribution area
Abies alba	Ab.al	Europe
Abies grandis	Ab.gr	North America
Abies homolepis	Ab.no	Japan
Abies nordmanniana	Ab.no	Main land Asia and Japan
Abies procera	Ab.pr	North America
Abies veitchii	Ab.ve	Northern Honshu, Japan
Chamaecyparis lawsoniana	Ch.la	North America
Cryptomeria japonica	Cr.ja	Eastern Asia
Larix kaempferi	La.ka	Eastern Asia
Metasequoia glyptostroboides	Me.gl	Main land Asia
Juniperus communis	Ju.co	Europe
Juniperus virginiana	Ju.vi	Europe
Picea abies	Pi.ab	Europe
Picea orientalis	Pi.or	Main land Asia
Picea omorika	Pi.om	Europe
Picea sitchensis	Pi.si	North America
Pinus armandii	Pi.ar	Eastern Asia
Pinus nigra	Pi.ni	South-Eastern Europe
Pinus peuce	Pi.pe	Europe
Pinus strobus	Pi.st	North America
Pseudotsuga menziesii	Ps.me	North America
Sequoiadendron giganteum	Se.gi	North America
Taxus baccata	Ta.ba	Europe
Taxus cuspidata	Ta.cu	Mainland Asia
Thuja plicata	Th.pl	North America
Tsuga canadensis	Ts.ca	North America
Tsuga diversifolia	Ts.di	Japan
Tsuga heterophylla	Ts.he	North America

Table S5.2 The results of a multi-model comparison showing how these functional traits from nine different cluster groups affect conifer species growth (in lightblue), drought recovery and drought resilience (in light grey). The best models (delta AIC<2) and averaged models were included. Bold fonts indicate significant coefficients.

model	|Ψpre|	WD	Ks	HSM	LL	Amass	LMF	DPA	df	logLik	AICc	Weight	R^2
Stem diameter growth													
1						**-0.48**		**0.69**	4.00	-22.98	56.6	0.41	0.31
2								**0.45**	3.00	-25.55	58.6	0.15	0.16
Avg						**-0.48**		**0.62**					
Imp						0.73		1.00					
P						0.04		0.01					
Stem area growth													
1				-0.40					3	-26.10	59.7	0.19	0.12
2		-0.39							3	-26.18	59.9	0.18	0.11
3								0.33	3	-26.71	60.9	0.10	0.06
4			0.32						3	-26.77	61.0	0.10	0.05
5		-0.27		-0.28					4	-25.40	61.5	0.08	0.13
6					-0.29				3	-27.00	61.5	0.08	0.03
7				-0.37	-0.23				4	-25.44	61.5	0.08	0.12
8		-0.33						0.25	4	-25.48	61.6	0.07	0.12
Avg		-0.35	0.32	-0.37	-0.26			0.30					
Imp		0.34	0.10	0.18	0.15			0.18					
P		0.16	0.18	0.13	0.28			0.22					
Stem mass growth													
1				-0.37					3	-26.40	60.3	0.23	0.09
2								0.32	3	-26.80	61.1	0.16	0.05
3		-0.27							3	-27.13	61.8	0.11	0.02
4			0.26						3	-27.17	61.8	0.11	0.02
5	-0.22								3	-27.39	62.3	0.09	<0.001
6					-0.22				3	-27.39	62.3	0.09	<0.001

Avg	-0.22	-0.27	0.26	-0.37	-0.22			0.32				
Imp	0.09	0.11	0.11	0.23	0.09			0.16				
P	0.38	0.27	0.29	0.12	0.38			0.19				
Resistance												
1						-0.22			3	-27.36	62.2	0.17	<0.001
Recovery												
1						-0.22			3	-27.36	62.2	0.17	<0.001
1					**-0.55**			-0.34	4	-22.72	56.1	0.24	0.33
2					-0.41		-0.35		4	-22.87	56.4	0.20	0.32
3					**-0.53**				3	-24.51	56.5	0.19	0.25
4				0.30	**-0.58**				4	-23.23	57.1	0.14	0.3
5	0.27				**-0.53**				4	-23.45	57.6	0.11	0.28
6							**-0.50**		3	-25.05	57.6	0.11	0.2
Avg	0.27			0.30	**-0.52**		-0.40	-0.34					
Imp	0.11			0.14	0.89		0.31	0.24					
P	0.20			0.16	0.02		0.08	0.09					
Resilience												
1					**-0.72**	**-0.57**			4	-22.39	55.5	0.52	0.35

Notes: Values indicate regression coefficients of the selected variables in the model. Per model, degrees of freedom (df), the log likelihood (logLik), corrected Akaike information criterion (AICc), and the AICc weight are given. The average coefficients (Avg), relative importance (Imp), and significances (*P*) are shown. Relative importance of the predictor variables is calculated as the sum of the Akaike weights over the best selected models. LMF, leaf mass fraction; DPA, pit aperture diameter; iWUE, intrinsic water-use efficiency; RWC, Relative water content at full turgor; Ψpre, predawn water potential; Ks, xylem specific hydraulic conductivity; WD, wood density; Amass, Photosynthetic rate (mass); HSM, hydraulic safety margin; Dh, tracheid diameter; LL, maximum leaf lifespan.

Fig. S5.1 Bi-variate relationships between the first two PCA scores and growth rate for a-f: a. stem diameter growth, b. steam area growth (i.e. basal area increment, BAI) and c. stem mass growth rate (Mass); and relationships between the first two PCA scores and drought resilience components for g-k. The dashed lines indicate non-significant regressions. For species abbreviations, see Table S5.1.

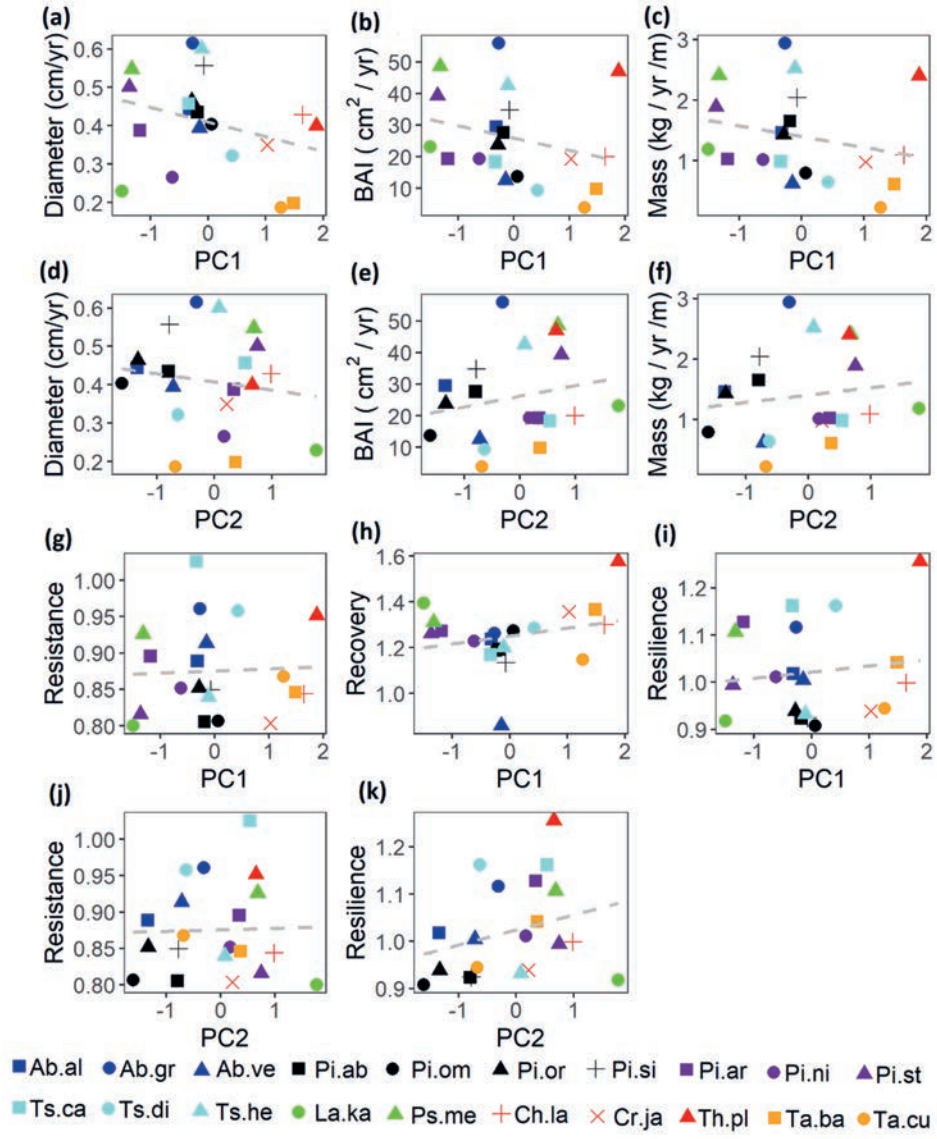

CHAPTER 6

6

General discussion

Conifer species (co-) dominate in many temperate and boreal forests and are important for timber production. Climate change threatens forest ecosystems worldwide as an increased frequency and intensity of summer droughts (IPCC, 2013) reduces the growth and survival of conifer trees (Lévesque *et al.*, 2013; DeSoto *et al.*, 2020). This dissertation aims to assess how and why conifer species differ in their growth responses to drought and other climate variables. I therefore studied stem growth of 28 conifer species growing for more than 50 years in a common garden experiment in the Netherlands. Using tree ring analysis, this experiment allowed me to show species differences in stem growth to temporal climate variation over a period of 40-50 years. I analyzed growth in terms of growth sensitivity to climate variation and in terms of drought resilience, which included drought resistance (reduction in stem growth during a dry year) and drought recovery (a measure of achieving pre-drought growth rate). I also measured 43 plant traits –related to the hydraulic- and carbon- relationships in trees – for all species to identify possible mechanisms driving species differences in growth. I thus aim at a better understanding of stem growth differences to climate from underlying plant traits and related mechanisms, and to reduce the uncertainty in predicting growth of conifers under climate-change scenarios. I addressed the following four questions in this thesis:

1) How do conifer species respond to climatic variation?
2) How do drought and hydraulic traits affect the drought resilience of conifer species?
3) How do pit and tracheid traits determine the cavitation resistance and hydraulic conductivity?
4) How are functional traits associated and how do they determine the growth and drought resilience of conifer species?

In this chapter, I synthesize and discuss the results, indicate the implications of climate change for forest functioning, and provide recommendations for climate-smart forestry and future research.

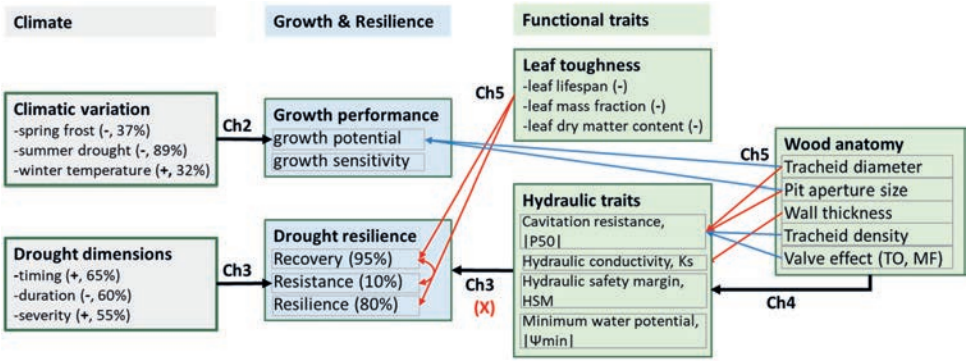

Fig. 6.1 A conceptual diagram summarizing the results of this thesis. It indicates the connections between the questions addressed in the different chapters: how climate affects stem growth (ch2) and drought resilience (ch3) and the underlying hydraulic mechanisms (ch3 & ch4), and how functional traits affect the growth and drought resilience of conifer species (ch5). The direction of effect is shown for significantly positive effects (+, or blue solid arrows) and significant negative effects (- or red solid arrows). The percentage of species significantly affected by climatic variation is included in brackets. In Chapter 3, none of the four hydraulic traits could predict stem growth and drought resilience (as indicated by a red cross).

6.1 The effects of climatic variation on stem growth and drought resilience

In Chapter 2, I analyzed how various climate variables affected the stem growth of conifers. I predicted that stem diameter growth decreased with more spring frost days, summer drought and cold winter because spring frost would delay the growing season; summer drought would reduce growth due to stomatal closure and hence low photosynthesis (McDowell *et al.*, 2008); and a warm winter might benefit growth via high photosynthesis of the evergreen needles or reduce growth through increased or strong water deficit (Larsen *et al.*, 2007; DeSoto *et al.*, 2014). I found the growth of conifers was most negatively affected by summer drought (significantly for 89% of species), followed by spring frost (37%) and winter cold (32%) (Fig. 6.1, Ch2). It implies that conifer species will lose productivity in a warmer and drier future climate during the growing season. Although the warmer winters and fewer spring frosts increase the stem growth, the severe summer drought mostly decreased stem growth of conifer species, which adds to the risk of increased tree mortality with recent warming and droughts (Allen *et al.*, 2010). I further hypothesized that there would be a positive relationship between growth potential and growth sensitivity since fast-growing species have wide tracheids which may come at the cost of high vulnerability to freezing- and drought-induced cavitation (Mayr *et al.*, 2006; Chave *et al.*, 2009). Surprisingly, there was no positive relation between stem growth

potential and growth sensitivity to climate across species, indicating that they vary independently.

6.2 How do multiple dimensions of drought affect stem growth resilience?

In Chapter 3, I quantified drought resilience and its two underlying components (i.e., drought recovery and resilience). I described multiple aspects of drought (timing, severity and length) over 44 years and assessed how these so-called drought dimensions affect the stem growth resilience of 20 species to the 11 dry years observed over the 44 year period. I expected that species would be resilient in different ways, either high resistance during drought or high recovery after drought, since there is a trade-off between resistance and recovery (Gazol *et al.*, 2017). I found that only 10% of the species is drought resistant, 20% of the species is not resistant and cannot recover after drought, and 70% of species is not resistant but recover well, and thus is drought resilient (Chapter 3, Fig. 3.5). Hence, 80% of the species is drought resilient.

Over the 44 years, there were 11 identified climatically dry years, but growth was not affected by all these drought years. Climatologically dry years did thus not always impair tree growth, because such negative effects on tree growth largely depended on the timing, severity and duration of drought. Overall, the seven droughts (i.e., perceived as drought by species) over the 44 years thus resulted in a modest long-term drought-related reduction in productivity (3.5%). I argued that this low productivity loss is possible because of the relatively mild, maritime climatic conditions in the Netherlands. Yet, even here the productivity loss may ultimately be much higher if trees run at risks of high mortality.

Afterwards, I quantified the climatic water balance for each drought year to identify the timing, severity and duration of drought, which affect the hydric status of plants. I predicted that negative effects on stem growth would occur when droughts appear early, last long and/or are severe, because all these aspects can lead to increased risks on hydraulic failure, leaf desiccation, carbon starvation, or a combination of these (Martínez-Vilalta *et al.*, 2016; Choat *et al.*, 2018). Drought resistance indeed decreased when droughts occurred early (significant for 65% of species), lasted longer (60%) or were more intense (55%) (Chapter 3, Fig. 3.7; Fig 6.1, Ch3). Compared with other studies, this study is one of the first that shows that all these three components should be considered to understand the effects of dry periods on stem growth, which is the key to better predict coniferous forest resilience to drought.

I subsequently evaluated whether hydraulic traits can explain species differences in stem growth resilience. I hypothesized that high cavitation resistance and high hydraulic safety margins favour drought resistance. I also hypothesized that high hydraulic conductivity increases growth and drought recovery, since high conductivity increases stomatal

conductance and hence photosynthetic rate. Surprisingly, none of the hydraulic traits could predict drought resilience (Chapter 3, Fig. S3.3; Fig. 6.1, Ch3). Apparently, other traits or mechanisms are responsible for the observed drought resilience differences across species. For example, drought avoidance traits such as deep roots, leaf shedding or early leaf and cambial phenology before summer drought (Gruber *et al.*, 2010) allow species to avoid negative effects of drought on stem growth (Fig. 6.3). However, these traits are not quantified in my study and need further study.

6.3 What determines cavitation resistance and hydraulic conductivity?

The variation in growth and drought resistance might be determined by tracheids and pits since they could affect hydraulic safety and efficiency. In Chapter 4, I evaluated whether there is a trade-off in stem conductivity and cavitation resistance across a set of 28 conifer species, and measured the underlying anatomical and physiological traits that were supposed to drive this trade-off. As expected, I found that cavitation resistance increased with pit aperture resistance (that consists of small pit size and thick cell walls), and a strong valve effect of the pit membrane (through a high torus overlap and margo flexibility) (Fig. 4.7, Fig. 6.1). This is in line with the idea that a small pit size reduces the spread of air bubbles from one conduit to another, and that the valve effect is a good integrator of pit sealing properties (Delzon *et al.*, 2010). It also highlights an important role for cell wall thickness in cavitation resistance.

Hydraulic conductivity was expected to increase with tracheid and pit size, since they reduce the friction between water and the cell wall and facilitate therefore water flow (Pittermann *et al.*, 2006a). Surprisingly, none of the tracheid and pit traits could predict hydraulic conductivity, and hydraulic conductivity was only found to decrease with the cell wall thickness (Chapter 4, Fig. 4.7; Fig. 6.1). This implies that a longer hydraulic path length within the pit can be a major cause of friction of water flow. Alternatively, it could be that cell wall thickness is just an indirect proxy for hydraulic conductivity, and that it is correlated with other unmeasured traits. Hydraulic conductivity can also be determined by other hydraulic bottlenecks that I did not measure, such as the sizes of pores in the margo (Schulte *et al.*, 2015), or tracheid length since that determines the flow path or affects the end-wall conductivity which nearly contributes to 64% of total resistivity in tracheids (Pittermann *et al.*, 2006b; Sperry *et al.*, 2006). I recommend therefore that future studies should assess the role of tracheid length and margo pores in the pit structure, to better explain variation in hydraulic conductivity across conifer species.

6.4 How are traits associated and how do they determine the growth and drought resilience?

Traits associations

Plant responses to drought are ultimately governed by the characteristics of the species (traits) and their plant strategies (i.e., the trait combinations that allow species to respond in a certain way to environmental conditions), see Fig. 6.3. Worldwide, a global spectrum of plant strategies is distinguished, that runs from species with 'conservative' trait values (such as, low specific leaf area, long leaf lifespan, low nutrient concentrations and photosynthetic rate, and dense wood) that conserve carbon and nutrients and increase plant persistence to species with 'acquisitive' trait values (i.e., the opposite trait values) that increase resource acquisition and growth (Wright *et al.*, 2004; Chave *et al.*, 2009; Díaz *et al.*, 2016). In Chapter 5, I integrate leaf and stem traits and assess whether they can predict species whole-plant performance. I find two spectra of plant strategies for conifer species. The first axis reflects a hydraulics spectrum, running from a conservative strategy with high hydraulic- and biomechanical safety to an acquisitive strategy with high hydraulic efficiency (i.e., transport capacity) (Chapter 5, Fig. 5.2). The second axis reflects a leaf economics spectrum, running from a conservative strategy with tough tissues and long longevity to an acquisitive strategy with high carbon assimilation (Chapter 5, Fig. 5.2).

The global acquisitive-conservative spectrum is also known as the leaf economics spectrum, as it has initially been developed and tested for leaves (Wright *et al.,* 2004), but the question is whether it also adequately describes variation in stem traits (Yang *et al*., 2021) and – though not considered in my study - root traits (Weemstra *et al.*, 2016; Bergmann *et al.*, 2020). For conifers, I found that the leaf economics spectrum and stem hydraulic traits are partially integrated. Species with acquisitive leaf strategies (i.e., high nutrient concentrations, SLA, stomatal conductance and photosynthetic rate) also had efficient xylem for water transport (i.e., a large hydraulic diameter). This efficient water transport, surprisingly, combined with a hydraulically 'safe' negative branch turgor loss point (high $|\Psi_{TLP}|$), which may allow for stomatal conductance and carbon gain under dry conditions (Bartlett *et al.*, 2012). It indicates a plant economics spectrum running from an acquisitive strategy with leaves and stem being 'fast' in carbon assimilation hydraulic transport to a conservative strategy with leaves and stem being 'slow' in leaf structure investment and hydraulic transport. Counterintuitively, these 'fast' strategies were combined with a more negative (i.e., 'safe') Ψ_{TLP} perhaps possibly because I used twigs for pressure-volume curves, to infer leaf turgor loss point. In contrast, Rosas Torrent *et al.* (2019) found a positive coordination between conservative leaf economic strategies (i.e., low SLA or low leaf nitrogen concentration) and high xylem hydraulic safety (high $|P_{50}|$) within two conifer species. The fact that I found only a partial coordination between acquisitive leaf economic strategies and stem hydraulic efficiency facilitates may allow for a greater variety of strategies (Li *et al.*, 2015). Such multiple alternative strategies allow species to adapt to a climate environment, facilitating species

coexistence and biodiversity (Sterck *et al.*, 2011), and hence ecosystem stability (Majeková *et al.*, 2014).

Functional traits underlie the stem growth and drought resilience

I further assessed how these 43 functional traits affect the stem growth and drought resilience of conifer species. I found that pit aperture size had a positive effect on stem diameter growth and leaf toughness and longevity had a negative effect on the drought recovery or resilience of conifer species (Chapter 5, Fig. 5.4; Fig. 6.1).

Pit aperture diameter (DPA) is also the central trait in the plant trait network (Chapter 5, Fig. 5.3), since it is associated with carbon assimilation but this comes at the cost of reduced hydraulic safety (Fig. 5.3a). Accordingly, pit aperture is expected to be the hydraulic bottleneck, because a wide pit aperture facilitates hydraulic transport but results in a relatively small torus overlap and, hence, a high risk for hydraulic failure due to low capacity to seal the pore (Jansen & McAdam, 2019). To my knowledge, this is the first study that shows the important role of pit aperture for stem diameter growth via its effect on cavitation resistance ($|P_{88}|$), but not on hydraulic conductivity (Fig 5.5). This indicates that realized growth differences between conifer species on these deep sandy soils are driven by a trade-off between water transport capacity and drought resistance, rather than by traits directly related to carbon gain.

We had expected that hydraulic stem and leaf traits could explain drought resilience, but surprisingly we found structural leaf traits to be the best predictors of drought resilience (Chapter 5, Fig. 5.4; Fig. 6.1). Drought recovery and resilience decreased with structural leaf enforcement (leaf dry matter content, LDMC) and, hence, also with leaf longevity. Species with a longer leaf lifespan and tough leaf tissue can buffer short-term environmental disturbances, e.g. drought events, but can create negative legacy effects for recovery after drought due to slow turnover rate, which is consistent the predictions from modelling studies (Zweifel & Sterck, 2018) and the first empirical tests for such modelling (Zweifel *et al.*, 2020). This is the first study showing that species with a conservative leaf economics strategy (long leaf lifespan) have low drought recovery and resilience. Our results thus confirm the hypothesized legacy effects of slow leaf turnover on stem growth recovery and resilience.

6.5 The phylogeny of functional traits and growth strategy

In Chapters 2 and 4 I also assessed whether stem growth and hydraulic traits of different species growing under the same environmental conditions were phylogenetically controlled. A strong phylogenetic signal implies that ancestral traits still govern, and that species from the same phylogenetic group show similar traits and ecological strategies, and similar responses

to environmental conditions (Cornwell *et al.*, 2014). I found that P_{50}, and its underlying determinants such as pit size and pit sealing were phylogenetically conserved. Pit size traits are more conserved than pit sealing traits, probably because pit size is closely related to cell size, which may be more difficult to change in response to varying environments during evolution (David-Schwartz *et al.*, 2016). It therefore explains the relatively strong phylogenetic control of cavitation resistance and drought adaptation, and why species differ in their drought tolerance. Of all phylogenetic groups considered, the Cupressoideae and Taxaceae were most drought resistant, the Pinoideae, Laricoideae, Abietoideae and Sequoioideae were the least drought resistant, with the Taxodioideae and Piceoideae in between. In contrast, hydraulic conductivity and its underlying tracheid traits (tracheid size and density) showed a weak phylogenetic signal. Both phylogenetic inertia and environmental selection determine trait values (Felsenstein, 1985; Fajardo & Piper, 2011). The weak phylogenetic signal of traits related to hydraulic conductivity indicates that these traits are evolutionarily labile (Corcuera *et al.*, 2011).

6.6 Implications for future research

The frequency and intensity of droughts are globally increasing (IPCC, 2013) and it is, therefore, timely and urgent to study how species respond to drought and explain those responses from underlying physiological processes (McDowell *et al.*, 2008; Allen *et al.*, 2010; Adams *et al.*, 2017; Choat *et al.*, 2018). This thesis reveals that the timing, duration, and intensity of drought are important for the growth of conifer species, and the underlying mechanisms help a better understanding of tree growth and survival. Specifically, this study provides new perspectives for future study in the following aspects (Fig. 6.3):

- **Beyond hydraulics.** Hydraulic traits are thought to govern tree responses to drought (Brodribb & Cochard, 2009; Anderegg, WR *et al.*, 2018). This study shows that under mild maritime climatic conditions, hydraulic traits are generally poor predictors for growth resilience to drought (Fig. 6.1, Ch3). Instead, leaf lifespan was the best predictor: a longer leaf life span was associated with a lower drought resilience. This indicates that we should go beyond hydraulics, and measure other traits and processes to understand conifer growth responses to drought. Moreover, it will be important to account for the roles of the different dimensions of drought (timing, duration, and severity). I speculate that the negative effects of the early onset of drought on the growth of species are exacerbated by early cambial activity or strong synchrony in leaf or cambial phenology (D'Orangeville *et al.*, 2018). The negative effects of drought duration on growth are possibly related to carbon starvation due to reduced non-structural carbohydrate reserves since conifers have fewer parenchyma cells and carbon storage capacity compared to broadleaved trees (McDowell *et al.*, 2008; Martínez-Vilalta *et al.*, 2016; Adams *et al.*, 2017). The negative effects of severe drought on growth are probably

related to the shallow root, since deeper roots would help species to maintain water uptake from deeper soils and thus – at least partially - avoid drought events (Voltas *et al.*, 2015). Hence, I recommend that future studies should especially focus on the role of plant phenology, non-structural carbohydrate reserves, biomass allocation to roots, and belowground root traits to unravel their importance for conifer growth responses to drought.

- **Context dependence.** Most of our theoretical generalizations come from studies across broad scales or extreme arid environments, such as the pinyon-juniper woodlands in the southern US (West *et al.*, 2007). Based on these studies there has been a strong emphasis on the role of cavitation resistance and carbon starvation in explaining drought tolerance (McDowell *et al.*, 2008). However, at my mild and maritime climatic site P_{50} and HSM could not explain drought resilience. Despite a wide range in P_{50} (ranging from -6.9 to -3.0 MPa) and hydraulic safety margins (1.1-5.1 MPa) across my study species, these species were rather similar in their minimum leaf water potentials (-2.4 to -1.4 MPa). This suggests that the mechanisms underlying drought resilience may be different in our study, see my explanation in last paragraph.
- **Leaf lifespan and pit aperture size.** When we look at how traits are integrated and affect the growth and resilience of conifer species, leaf lifespan negatively affects stem recovery and resilience after drought and large pit aperture size increases the tree growth through releasing the hydraulic bottleneck for transport efficiency coming at the costs of safety (Chapter 5). Hence, to adequately model and predict species responses to climate change and its consequences for the carbon cycle, leaf lifespan and pit-constrained hydraulics should be included in process-based individual tree models (such as a whole-tree model, Weemstra *et al.*, 2020) and dynamic global vegetation models (such as a trait-based DGVM, Sakschewski *et al*., 2015). My study therefore provides guidelines for growth- and survival-related physiological and modelling studies, thus improving our predictions of forest productivity, ecosystem functioning, and their consequences for the carbon cycle.
- **Beyond tissue traits.** To determine the mechanisms underlying plant responses to drought I measured a complete set of 43 leaf and branch traits and I went to great lengths to measure 'hard' hydraulic traits. Yet, they were surprisingly poor predictors for whole-plant stem growth and drought resilience. Hence, these tissue and organ-level traits cannot predict the growth when we scale up to the whole-plant level. Other studies also found that traits have strong effects on the growth and survival of small seedlings (e.g., Poorter & Bongers, 2006) but are weakly related to the growth and survival of large trees (e.g., Poorter *et al*., 2008, Wright *et al*., 2010, van der Sande *et al*., 2015, Weemstra *et al*., 2013). Large trees are more robust, and their performance is probably more determined by the number of growing buds and the quantity of leaves and branches, than by "the quality" of leaves or sapwood (Sterck & Schieving, 2007). Similarly, large trees have more non-structural carbohydrate reserves that

may buffer them better against environmental hazards. Hence, for large trees quantity may simply overrule tissue quality. I advocate tree models related to growth and survival should integrate structure, development and whole plant functional traits , such as root mass fraction, rooting depth, leaf area to root area ratio, whole-plant carbon balance, non-structural carbohydrates, or crown vitality (Schippers *et al.*, 2015a; Schippers *et al.*, 2015b; Weemstra *et al.*, 2020).

- **Conifers vs angiosperms.** Compared to angiosperms, conifers are normally unique because of their small tracheids, unique torus-margo pits and needle-shaped leaves, which results in strong convergence in traits (e.g., cavitation resistance and pit traits) compared to angiosperms. The hydraulic traits may be more important for broadleaf species to resist drought, as the variation in anatomical traits (e.g., vessels, parenchyma and fibers) is larger and more divergent for broadleaf species than for gymnosperms (Yang *et al.,* 2021). Besides, conifers vary more in leaf lifespan than broad leaf trees in temperate forests, and my study shows that this variation in leaf lifespan may largely determine the drought resilience of conifers. It would be interesting to assess whether leaf lifespan could play a universal role in predicting drought resilience for angiosperms in all types of forests since the deciduous species have a very short leaf lifespan.

6.7 Implications for climate-smart-forestry

Climate smart forestry has been defined as forest management aiming at sustaining or increasing forest production, resilience and carbon stocks with ongoing climate change. Most conifer species are sensitive to summer drought, but there is no significant relationship between growth sensitivity and growth potential. This means that to design climate smart forestry, species can be selected that combine a low climate sensitivity with a high growth potential, such as *Abies grands* and *Thuja plicata*.

Although the growth of conifer species decreases with early, prolonged and severe droughts, most conifer species are highly resilient due to a high recovery after drought. Thus, productivity only declines modestly by 3% over 44 years due to droughts. Growth is of course only one indicator of plant performance in response to drought, whereas survival is even more important. Long-term reductions in growth can eventually lead to a reduction in survival because of an overall reduction in vitality, reduced carbohydrate reserves, and increased sensitivity to insect pests and pathogens (Cailleret *et al.*, 2017). I screened the species for their long-term mortality and found that species that were less growth-resilient to drought (i.e., they had a resilience less than 1) had a high tree mortality rate after the three successive drought years (2018-2020) (Fig. 6. 2), indicating that productivity loss over the life time of the stand is much higher. I therefore advocate planting highly resilient species (e.g. *Abies grandis*,

Thuja plicata, *Tsuga canadensis* and *Pseudotsuga menziesii*) to cope with drought events, and to avoid planting species with low drought resilience, such as *Picea* species.

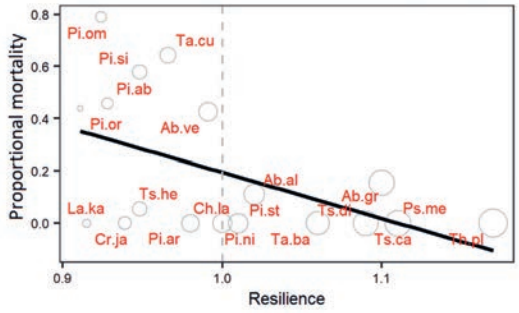

Fig. 6.2 Relationship between long-term tree mortality (as a proportion of all trees in the stand) and the growth resilience to drought of 20 conifer species. For species abbreviations, see Table 1.1. Resilience is defined as the average growth 2 years after a drought year, divided by the average growth 2 years before the drought year. A resilience index<1 indicates that species cannot recover their growth after drought events and a resilience index >1 indicates species are very flexible and can recover their growth to a level higher than before the drought event. Resilience values are obtained from chapter 3. For proportional mortality, I scored the fractions of dead individuals in the species population in a 5 decades old common garden experiment in May 2021, after three dry summers (2018-2020).

6.8 Towards a new conceptual framework for drought responses

Based on my research results, I propose a new conceptual framework that integrates a variety of traits and mechanisms that jointly determine the resilience of trees to drought. Such a more elaborative framework is required to understand tree response to drought in different environmental contexts, including very dry system and much milder systems. Conifer species can mainly adopt three ecological strategies to cope with drought events (Fig. 6.3); **i**) avoiding drought, **ii**) tolerating drought, or **iii**) quick recovering with high flexibility after drought.

First, tree species can adopt a **drought avoidance strategy** by **a**) allocating biomass to belowground roots to uptake up water from deep soils (Ding *et al.*, 2021), **b**) shedding leaves to conserve water and energy (Markesteijn *et al.*, 2011), **c**) showing isohydric behavior or **d**) having earlier leaf and cambial activity before the dry summer (Gruber *et al.*, 2010).

Secondly, tree species can adopt a **drought tolerance strategy** by having high hydraulic safety margins to buffer the drought impacts, or by having enough carbohydrate reserves to repair damaged tissues (for example in mild maritime climates).

Thirdly species can also adopt to dry conditions with **strong flexibility regarding turnover rate and vitality to recover growth** after drought, since long-lasting droughts lead to reserved carbon depletion and tree species need to use stored carbohydrate reserves to maintain plant functioning. The strong legacy effects of leaf tissues (tough leaf tissues with long leaf lifespan) slow down the recovery rates due to the slow turnover rate and tough structural construction (Zweifel & Sterck, 2018).

These multifarious strategies enable tree species to adapt to varying climatic niches, and help us to improve our predictions on species distribution, productivity, mortality and forest carbon sequestration under future climate change scenarios. It therefore allows for a better integration in tree and forest models.

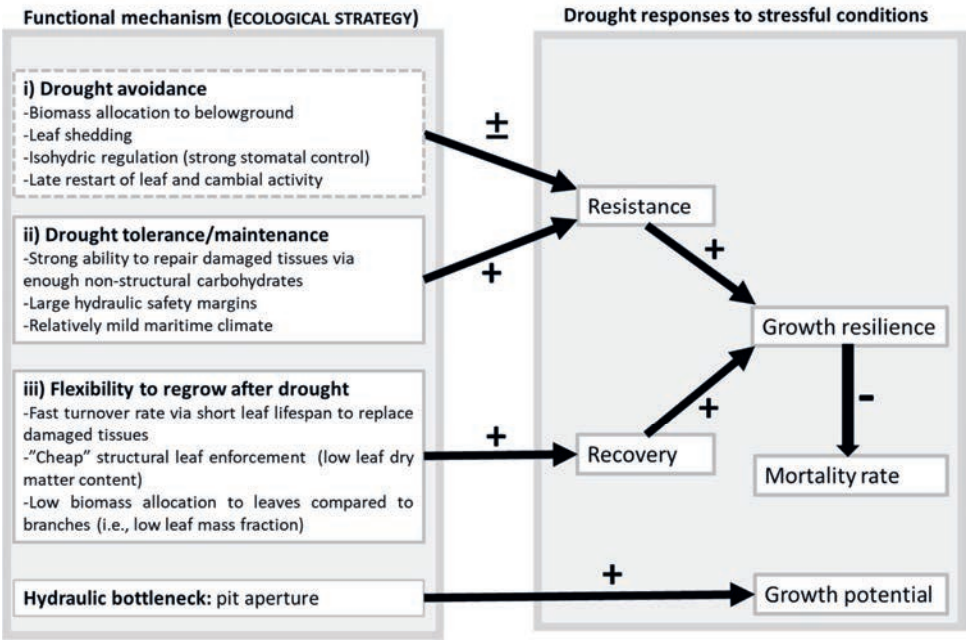

Fig. 6.3 Conceptual diagram showing three ecological strategies to cope with drought events of conifer species. Boxes with dashed lines indicate suggestions for future studies and boxes with solid lines are supported by results from this PhD thesis. **+**, positive effects; **-**, negative effects; **±** positive or negative effects.

6.9 Conclusions

This dissertation assessed how conifer species differ in growth and drought resilience and to what extent this could be explained by 43 underlying functional traits. Stem growth reductions were strongest in response to prolonged and severe droughts that started early in the growing season. Surprisingly, hydraulic traits and growth potential could not explain the drought responses of conifer species. Although hydraulic traits cannot explain the stem growth resistance to drought, studying the mechanisms of cavitation resistance still helps to elucidate species differences in hydraulic safety and efficiency at an anatomical level. Instead, my study shows an important role for leaf lifespan and pit aperture in explaining plant growth and plant resilience to drought. This dissertation has shown that conifer species show three alternative strategies to deal with a future drier climate. These different plant strategies can enhance species coexistence (Sterck *et al.*, 2011; Adler *et al.*, 2013), biodiversity (Shipley *et al.*, 2006; Kraft *et al.*, 2008) and biomass production (Cadotte, 2017), and hence enhancing forest ecosystem stability (Majeková *et al.*, 2014).

Highlights of this thesis

- Most conifers are highly resilient due to high recovery, but have low resistance particularly in years with early, prolonged and intense droughts.
- Drought resilience cannot be explained by hydraulic traits.
- Small pit size and strong pit sealing capacity through a large valve effect, margo flexibility, and torus overlap facilitate cavitation resistance. Yet, none of the pit and tracheid traits can predict hydraulic conductivity except wall thickness.
- Pit aperture size is positively associated with stem diameter growth. It highlights the dominant role of pit aperture in explaining species differences in growth performance.
- Structural leaf traits and leaf lifespan are the best predictors of drought resilience, where leaf lifespan negatively relates to drought resilience.
- Future studies on biomass allocation, root depth, plant phenology and non-structural carbohydrate reserves are needed to better understand drought resilience.
- This study provides guidelines for conifer species selection to assure a climate-smart forest with high resilience, productivity and carbon storage in forests in the face of climate change.

References

Abbasi A, Khalili K, Behmanesh J, Shirzad A. 2019. Drought monitoring and prediction using SPEI index and gene expression programming model in the west of Urmia Lake. *Theoretical and Applied Climatology* **138**(1): 553-567.

Ackerly DD. 2003. Community assembly, niche conservatism, and adaptive evolution in changing environments. *International Journal of Plant Sciences* **164**(S3): S165-S184.

Adams DC. 2014. A generalized K statistic for estimating phylogenetic signal from shape and other high-dimensional multivariate data. *Systematic biology* **63**(5): 685-697.

Adams HD, Zeppel MJ, Anderegg WR, Hartmann H, Landhäusser SM, Tissue DT, Huxman TE, Hudson PJ, Franz TE, Allen CD. 2017. A multi-species synthesis of physiological mechanisms in drought-induced tree mortality. *Nature Ecology & Evolution* **1**(9): 1285-1291.

Adler PB, Fajardo A, Kleinhesselink AR, Kraft NJ. 2013. Trait-based tests of coexistence mechanisms. *Ecology Letters* **16**(10): 1294-1306.

Allen CD, Breshears DD, McDowell NG. 2015. On underestimation of global vulnerability to tree mortality and forest die-off from hotter drought in the Anthropocene. *Ecosphere* **6**(8): 1-55.

Allen CD, Macalady AK, Chenchouni H, Bachelet D, McDowell N, Vennetier M, Kitzberger T, Rigling A, Breshears DD, Hogg ET. 2010. A global overview of drought and heat-induced tree mortality reveals emerging climate change risks for forests. *Forest Ecology and Management* **259**(4): 660-684.

Anderegg LD, Berner LT, Badgley G, Sethi ML, Law BE, HilleRisLambers J. 2018. Within-species patterns challenge our understanding of the leaf economics spectrum. *Ecology Letters* **21**(5): 734-744.

Anderegg WR, Klein T, Bartlett M, Sack L, Pellegrini AF, Choat B, Jansen S. 2016. Meta-analysis reveals that hydraulic traits explain cross-species patterns of drought-induced tree mortality across the globe. *Proceedings of the National Academy of Sciences* **113**(18): 5024-5029.

Anderegg WR, Konings AG, Trugman AT, Yu K, Bowling DR, Gabbitas R, Karp DS, Pacala S, Sperry JS, Sulman BN. 2018. Hydraulic diversity of forests regulates ecosystem resilience during drought. *Nature* **561**(7724): 538-541.

Anderegg WR, Schwalm C, Biondi F, Camarero JJ, Koch G, Litvak M, Ogle K, Shaw JD, Shevliakova E, Williams A. 2015. Pervasive drought legacies in forest ecosystems and their implications for carbon cycle models. *Science* **349**(6247): 528-532.

Antos JA, Filipescu CN, Negrave RW. 2016. Ecology of western redcedar (Thuja plicata): Implications for management of a high-value multiple-use resource. *Forest Ecology and Management* **375**: 211-222.

Araujo FDC, Tng DYP, Apgaua DMG, Morel JD, Pereira DGS, Santos PF, Santos RMd. 2019. Flooding regime drives tree community structure in Neotropical dry forests. *Journal of Vegetation Science* **30**(6): 1195-1205.

Augspurger CK. 2011. Frost damage and its cascading negative effects on Aesculusglabra. *Plant Ecology* **212**(7): 1193-1203.

Augusto L, Davies TJ, Delzon S, De Schrijver A. 2014. The enigma of the rise of angiosperms: can we untie the knot? *Ecology Letters* **17**(10): 1326-1338.

Babst F, Poulter B, Trouet V, Tan K, Neuwirth B, Wilson R, Carrer M, Grabner M, Tegel W, Levanic T. 2013. Site-and species-specific responses of forest growth to climate across the E uropean continent. *Global ecology and biogeography* **22**(6): 706-717.

Ballester J, Rodó X, Giorgi F. 2010. Future changes in Central Europe heat waves expected to mostly follow summer mean warming. *Climate dynamics* **35**(7-8): 1191-1205.

Ballian D, Ravazzi C, Caudullo G. 2016. Picea omorika in Europe: distribution, habitat, usage and threats. *European Atlas of Forest Tree Species. Publications Office of the European Union, Luxembourg*: 117-117.

Baraloto C, Timothy Paine C, Poorter L, Beauchene J, Bonal D, Domenach AM, Hérault B, Patiño S, Roggy JC, Chave J. 2010. Decoupled leaf and stem economics in rain forest trees. *Ecology Letters* **13**(11): 1338-1347.

Bartlett MK, Scoffoni C, Sack L. 2012. The determinants of leaf turgor loss point and prediction of drought tolerance of species and biomes: a global meta-analysis. *Ecology Letters* **15**(5): 393-405.

Barton K, Barton MK. 2015. Package 'mumin'. *Version* **1**: 18.

Bauch J, Liese W, Schultze R. 1972. The morphological variability of the bordered pit membranes in gymnosperms. *Wood Science and Technology* **6**(3): 165-184.

Beguería S, Vicente-Serrano S. 2013. Calculation of the standardised precipitation-evapotranspiration index. *SPEI R package version* **1**.

Beguería S, Vicente-Serrano SM, Beguería MS 2017. Package 'SPEI'.

Begum S, Nakaba S, Oribe Y, Kubo T, Funada R. 2010. Cambial sensitivity to rising temperatures by natural condition and artificial heating from late winter to early spring in the evergreen conifer *Cryptomeria japonica*. *Trees* **24**(1): 43-52.

Bellard C, Bertelsmeier C, Leadley P, Thuiller W, Courchamp F. 2012. Impacts of climate change on the future of biodiversity. *Ecology Letters* **15**(4): 365-377.

Benito Garzón M, González Muñoz N, Wigneron JP, Moisy C, Fernández-Manjarrés J, Delzon S. 2018. The legacy of water deficit on populations having experienced negative hydraulic safety margin. *Global ecology and biogeography* **27**(3): 346-356.

Bennett AC, McDowell NG, Allen CD, Anderson-Teixeira KJ. 2015. Larger trees suffer most during drought in forests worldwide. *Nature Plants* **1**(10): 1-5.

Bergmann J, Weigelt A, van Der Plas F, Laughlin DC, Kuyper TW, Guerrero-Ramirez N, Valverde-Barrantes OJ, Bruelheide H, Freschet GT, Iversen CM. 2020. The fungal collaboration gradient dominates the root economics space in plants. *Science advances* **6**(27): eaba3756.

Bhaskar R, Ackerly D. 2006. Ecological relevance of minimum seasonal water potentials. *Physiologia Plantarum* **127**(3): 353-359.

Bhuyan U, Zang C, Menzel A. 2017. Different responses of multispecies tree ring growth to various drought indices across Europe. *Dendrochronologia* **44**: 1-8.

Biondi F. 1997. Evolutionary and moving response functions in dendroclimatology. *Dendrochronologia* **15**(139-150).

Biondi F, Waikul K. 2004. DENDROCLIM2002: A C++ program for statistical calibration of climate signals in tree-ring chronologies. *Computers & geosciences* **30**(3): 303-311.

Blackwell P, Rennolls K, Coutts M. 1990. A root anchorage model for shallowly rooted Sitka spruce. *Forestry: An International Journal of Forest Research* **63**(1): 73-91.

Blomberg SP, Garland Jr T, Ives AR. 2003. Testing for phylogenetic signal in comparative data: behavioral traits are more labile. *Evolution* **57**(4): 717-745.

Bolte A, Villanueva I. 2006. Interspecific competition impacts on the morphology and distribution of fine roots in European beech (*Fagus sylvatica* L.) and Norway spruce (*Picea abies* (L.) Karst.). *European Journal of Forest Research* **125**(1): 15-26.

Bose AK, Gessler A, Bolte A, Bottero A, Buras A, Cailleret M, Camarero JJ, Haeni M, Hereş AM, Hevia A. 2020. Growth and resilience responses of Scots pine to extreme droughts across Europe depend on pre-drought growth conditions. *Global Change Biology*.

Bouche PS, Jansen S, Cochard H, Burlett R, Capdeville G, Delzon S. 2015. Embolism resistance of conifer roots can be accurately measured with the flow-centrifuge method.

Bouche PS, Larter M, Domec J-C, Burlett R, Gasson P, Jansen S, Delzon S. 2014. A broad survey of hydraulic and mechanical safety in the xylem of conifers. *Journal of Experimental Botany* **65**(15): 4419-4431.

Bréda N, Badeau V. 2008. Forest tree responses to extreme drought and some biotic events: towards a selection according to hazard tolerance? *Comptes Rendus Geoscience* **340**(9-10): 651-662.

Bréda N, Huc R, Granier A, Dreyer E. 2006. Temperate forest trees and stands under severe drought: a review of ecophysiological responses, adaptation processes and long-term consequences. *Annals of Forest Science* **63**(6): 625-644.

Brodribb T, Feild T. 2000. Stem hydraulic supply is linked to leaf photosynthetic capacity: evidence from New Caledonian and Tasmanian rainforests. *Plant, Cell & Environment* **23**(12): 1381-1388.

Brodribb TJ, Bienaimé D, Marmottant P. 2016. Revealing catastrophic failure of leaf networks under stress. *Proceedings of the National Academy of Sciences* **113**(17): 4865-4869.

Brodribb TJ, Cochard H. 2009. Hydraulic failure defines the recovery and point of death in water-stressed conifers. *Plant physiology* **149**(1): 575-584.

Brodribb TJ, McAdam SA, Jordan GJ, Martins SC. 2014. Conifer species adapt to low-rainfall climates by following one of two divergent pathways. *Proceedings of the National Academy of Sciences* **111**(40): 14489-14493.

Brodribb TJ, Powers J, Cochard H, Choat B. 2020. Hanging by a thread? Forests and drought. *Science* **368**(6488): 261-266.

Brown JH, Gillooly JF, Allen AP, Savage VM, West GB. 2004. Toward a metabolic theory of ecology. *Ecology* **85**(7): 1771-1789.

Brum M, Teodoro GS, Abrahão A, Oliveira RS. 2017. Coordination of rooting depth and leaf hydraulic traits defines drought-related strategies in the campos rupestres, a tropical montane biodiversity hotspot. *Plant and Soil* **420**(1): 467-480.

Bunn AG. 2008. A dendrochronology program library in R (dplR). *Dendrochronologia* **26**(2): 115-124.

Buras A, Rammig A, Zang CS. 2020. Quantifying impacts of the 2018 drought on European ecosystems in comparison to 2003. *Biogeosciences* **17**(6): 1655-1672.

Burkhardt J, Peters K, Crossley A. 1995. The presence of structural surface waxes on coniferousneedles affects the pattern of dry deposition of fine particles. *Journal of Experimental Botany* **46**(7): 823-831.

Cadotte MW. 2017. Functional traits explain ecosystem function through opposing mechanisms. *Ecology Letters* **20**(8): 989-996.

Cailleret M, Jansen S, Robert EM, Desoto L, Aakala T, Antos JA, Beikircher B, Bigler C, Bugmann H, Caccianiga M. 2017. A synthesis of radial growth patterns preceding tree mortality. *Global Change Biology* **23**(4): 1675-1690.

Camarero JJ, Gazol A, Sangüesa-Barreda G, Cantero A, Sánchez-Salguero R, Sánchez-Miranda A, Granda E, Serra-Maluquer X, Ibáñez R. 2018. Forest growth responses to drought at short-and long-term scales in Spain: squeezing the stress memory from tree rings. *Frontiers in Ecology and Evolution* **6**: 9.

Campany CE, Pittermann J, Baer A, Holmlund H, Schuettpelz E, Mehltreter K, Watkins Jr JE. 2021. Leaf water relations in epiphytic ferns are driven by drought avoidance rather than tolerance mechanisms. *Plant, Cell & Environment*.

CaraDonna PJ, Inouye DW. 2015. Phenological responses to climate change do not exhibit phylogenetic signal in a subalpine plant community. *Ecology* **96**(2): 355-361.

Carnicer J, Coll M, Ninyerola M, Pons X, Sanchez G, Penuelas J. 2011. Widespread crown condition decline, food web disruption, and amplified tree mortality with increased climate change-type drought. *Proceedings of the National Academy of Sciences* **108**(4): 1474-1478.

Cavender-Bares J. 2019. Diversification, adaptation, and community assembly of the American oaks (*Quercus*), a model clade for integrating ecology and evolution. *New Phytologist* **221**(2): 669-692.

Cavin L, Mountford EP, Peterken GF, Jump AS. 2013. Extreme drought alters competitive dominance within and between tree species in a mixed forest stand. *Functional Ecology* **27**(6): 1424-1435.
Charney ND, Babst F, Poulter B, Record S, Trouet VM, Frank D, Enquist BJ, Evans ME. 2016. Observed forest sensitivity to climate implies large changes in 21st century North American forest growth. *Ecology Letters* **19**(9): 1119-1128.
Chave J, Coomes D, Jansen S, Lewis SL, Swenson NG, Zanne AE. 2009. Towards a worldwide wood economics spectrum. *Ecology Letters* **12**(4): 351-366.
Chave J, Muller-Landau HC, Baker TR, Easdale TA, Steege Ht, Webb CO. 2006. Regional and phylogenetic variation of wood density across 2456 neotropical tree species. *Ecological applications* **16**(6): 2356-2367.
Chaves MM, Maroco JP, Pereira JS. 2003. Understanding plant responses to drought—from genes to the whole plant. *Functional plant biology* **30**(3): 239-264.
Choat B, Brodie TW, Cobb AR, Zwieniecki MA, Holbrook NM. 2006. Direct measurements of intervessel pit membrane hydraulic resistance in two angiosperm tree species. *American journal of botany* **93**(7): 993-1000.
Choat B, Brodribb TJ, Brodersen CR, Duursma RA, Lopez R, Medlyn BE. 2018. Triggers of tree mortality under drought. *Nature* **558**(7711): 531-539.
Choat B, Jansen S, Brodribb TJ, Cochard H, Delzon S, Bhaskar R, Bucci SJ, Feild TS, Gleason SM, Hacke UG. 2012. Global convergence in the vulnerability of forests to drought. *Nature* **491**(7426): 752-755.
Chudnovskii A. 1949. Zamorozki (Light Frosts). *Leningrad: Gidrometeoizdat*.
Ciais P, Reichstein M, Viovy N, Granier A, Ogée J, Allard V, Aubinet M, Buchmann N, Bernhofer C, Carrara A. 2005a. Europe-wide reduction in primary productivity caused by the heat and drought in 2003. *Nature* **437**(7058): 529.
Ciais P, Reichstein M, Viovy N, Granier A, Ogée J, Allard V, Aubinet M, Buchmann N, Bernhofer C, Carrara A. 2005b. Europe-wide reduction in primary productivity caused by the heat and drought in 2003. *Nature* **437**(7058): 529-533.
Cochard H. 2006. Cavitation in trees. *Comptes Rendus Physique* **7**(9-10): 1018-1026.
Cochard H, Damour G, Bodet C, Tharwat I, Poirier M, Améglio T. 2005. Evaluation of a new centrifuge technique for rapid generation of xylem vulnerability curves. *Physiologia Plantarum* **124**(4): 410-418.
Comont RF, Roy HE, Lewis OT, Harrington R, Shortall CR, Purse BV. 2012. Using biological traits to explain ladybird distribution patterns. *Journal of Biogeography* **39**(10): 1772-1781.
Cook ER, Briffa K, Shiyatov S, Mazepa V. 1990. Tree-ring standardization and growth-trend estimation. *Methods of dendrochronology: applications in the environmental sciences*: 104-123.
Cook ER, Briffa KR, Meko DM, Graybill DA, Funkhouser G. 1995. The'segment length curse'in long tree-ring chronology development for palaeoclimatic studies. *The Holocene* **5**(2): 229-237.
Corcuera L, Cochard H, Gil-Pelegrin E, Notivol E. 2011. Phenotypic plasticity in mesic populations of *Pinus pinaster* improves resistance to xylem embolism (P_{50}) under severe drought. *Trees* **25**(6): 1033-1042.
Cornelissen JHC, Sass-Klaassen U, Poorter L, van Geffen K, van Logtestijn RSP, van Hal J, Goudzwaard L, Sterck FJ, Klaassen RKWM, Freschet GT, et al. 2012. Controls on Coarse Wood Decay in Temperate Tree Species: Birth of the LOGLIFE Experiment. *Ambio* **41**(3): 231-245.
Cornwell WK, Westoby M, Falster DS, FitzJohn RG, O'Meara BC, Pennell MW, McGlinn DJ, Eastman JM, Moles AT, Reich PB. 2014. Functional distinctiveness of major plant lineages. *Journal of Ecology* **102**(2): 345-356.
Cui E, Weng E, Yan E, Xia J. 2020. Robust leaf trait relationships across species under global environmental changes. *Nature communications* **11**(1): 1-9.
Cuny HE, Rathgeber CB. 2016. Xylogenesis: coniferous trees of temperate forests are listening to the climate tale during the growing season but only remember the last words! *Plant physiology* **171**(1): 306-317.
Cuny HE, Rathgeber CB, Lebourgeois F, Fortin M, Fournier M. 2012. Life strategies in intra-annual dynamics of wood formation: example of three conifer species in a temperate forest in north-east France. *Tree Physiology* **32**(5): 612-625.
D'Orangeville L, Maxwell J, Kneeshaw D, Pederson N, Duchesne L, Logan T, Houle D, Arseneault D, Beier CM, Bishop DA. 2018. Drought timing and local climate determine the sensitivity of eastern temperate forests to drought. *Global Change Biology* **24**(6): 2339-2351.
D'Orangeville L, Duchesne L, Houle D, Kneeshaw D, Côté B, Pederson N. 2016. Northeastern North America as a potential refugium for boreal forests in a warming climate. *Science* **352**(6292): 1452-1455.
Dallimore W. 1937. The more recently introduced conifers and their value for planting in the British Isles. *Forestry: An International Journal of Forest Research* **11**(1): 1-5.
David-Schwartz R, Paudel I, Mizrachi M, Delzon S, Cochard H, Lukyanov V, Badel E, Capdeville G, Shklar G, Cohen S. 2016. Indirect evidence for genetic differentiation in vulnerability to embolism in *Pinus halepensis*. *Frontiers in plant science* **7**: 768.
Davies S, Bathgate S, Petr M, Gale A, Patenaude G, Perks M. 2020. Drought risk to timber production–A risk versus return comparison of commercial conifer species in Scotland. *Forest Policy and Economics* **117**: 102189.
Davis SD, Sperry JS, Hacke UG. 1999. The relationship between xylem conduit diameter and cavitation caused by freezing. *American journal of botany* **86**(10): 1367-1372.
de Lange C, de Klein J. 1998. Naar duurzame bosbeelden op Schovenhorst.
Dell'Oro M, Mataruga M, Sass-Klaassen U, Fonti P. 2020. Climate change threatens on endangered relict Serbian spruce. *Dendrochronologia* **59**: 125651.
Delzon S, Cochard H. 2014. Recent advances in tree hydraulics highlight the ecological significance of the hydraulic safety margin. *New Phytologist* **203**(2): 355-358.

Delzon S, Douthe C, Sala A, Cochard H. 2010. Mechanism of water-stress induced cavitation in conifers: bordered pit structure and function support the hypothesis of seal capillary-seeding. *Plant, Cell & Environment* **33**(12): 2101-2111.
Depardieu C, Girardin MP, Nadeau S, Lenz P, Bousquet J, Isabel N. 2020. Adaptive genetic variation to drought in a widely distributed conifer suggests a potential for increasing forest resilience in a drying climate. *New Phytologist* **227**(2): 427-439.
Deslauriers A, Morin H, Begin Y. 2003. Cellular phenology of annual ring formation of Abies balsamea in the Quebec boreal forest (Canada). *Canadian Journal of Forest Research* **33**(2): 190-200.
DeSoto L, Cailleret M, Sterck F, Jansen S, Kramer K, Robert EM, Aakala T, Amoroso MM, Bigler C, Camarero JJ. 2020. Low growth resilience to drought is related to future mortality risk in trees. *Nature communications* **11**(1): 1-9.
DeSoto L, Varino F, Andrade JP, Gouveia CM, Campelo F, Trigo RM, Nabais C. 2014. Different growth sensitivity to climate of the conifer Juniperus thurifera on both sides of the Mediterranean Sea. *International journal of biometeorology* **58**(10): 2095-2109.
Díaz S, Kattge J, Cornelissen JH, Wright IJ, Lavorel S, Dray S, Reu B, Kleyer M, Wirth C, Prentice IC. 2016. The global spectrum of plant form and function. *Nature* **529**(7585): 167-171.
Dietrich L, Delzon S, Hoch G, Kahmen A. 2019. No role for xylem embolism or carbohydrate shortage in temperate trees during the severe 2015 drought. *Journal of Ecology* **107**(1): 334-349.
Ding Y, Nie Y, Chen H, Wang K, Querejeta JI. 2021. Water uptake depth is coordinated with leaf water potential, water-use efficiency and drought vulnerability in karst vegetation. *New Phytologist* **229**(3): 1339-1353.
Distelbarth H, Kull U. 1985. PHYSIOLOGICAL INVESTIGATIONS OF LEAF MUCILAGES II. THE MUCILAGE OF TAXUS BACCATA L. AND OF THUJA OCCIDENTALE L. *Israel Journal of Plant Sciences* **34**(2-4): 113-128.
Dobrovolný L, Štěrba T, Kodeš J. 2013. Effect of stand edge on the natural regeneration of spruce, beech and douglas-fir. *Acta Universitatis Agriculturae et Silviculturae Mendelianae Brunensis* **60**(6): 49-56.
Domec J-C, Lachenbruch B, Meinzer FC, Woodruff DR, Warren JM, McCulloh KA. 2008. Maximum height in a conifer is associated with conflicting requirements for xylem design. *Proceedings of the National Academy of Sciences* **105**(33): 12069-12074.
Domec JC, Gartner BL. 2002. How do water transport and water storage differ in coniferous earlywood and latewood? *Journal of Experimental Botany* **53**(379): 2369-2379.
Domec JC, Lachenbruch B, Meinzer FC. 2006. Bordered pit structure and function determine spatial patterns of air-seeding thresholds in xylem of Douglas-fir (*Pseudotsuga menziesii*; Pinaceae) trees. *American journal of botany* **93**(11): 1588-1600.
Dy G, Payette S. 2007. Frost hollows of the boreal forest as extreme environments for black spruce tree growth. *Canadian Journal of Forest Research* **37**(2): 492-504.
Edwards EJ, Chatelet DS, Sack L, Donoghue MJ. 2014. Leaf life span and the leaf economic spectrum in the context of whole plant architecture. *Journal of Ecology* **102**(2): 328-336.
Egger B, Einig W, Sclereth A, Wallenda T, Magel E, Loewe A, Hampp R. 1996. Carbohydrate metabolism in one-and two-year-old spruce needles, and stem carbohydrates from three months before until three months after bud break. *Physiologia Plantarum* **96**(1): 91-100.
Ellis W, Groenendijk D, de Vos R. 2004. 1928: een seizoen op Schovenhorst. *Vlinders* **19**(3): 4-6.
Epskamp S, Borsboom D, Fried EI. 2018. Estimating psychological networks and their accuracy: A tutorial paper. *Behavior Research Methods* **50**(1): 195-212.
Epskamp S, Fried EI. 2018. A tutorial on regularized partial correlation networks. *Psychological methods* **23**(4): 617.
Epskamp S, Fried EI, Epskamp MS. 2015. Package 'bootnet'.
Eysteinsson T, Karlman L, Fries A, Martinsson O, Skulason B. 2009. Variation in spring and autumn frost tolerance among provenances of Russian larches (Larix Mill.). *Scandinavian Journal of Forest Research* **24**(2): 100-110.
Fajardo A, Piper FI. 2011. Intraspecific trait variation and covariation in a widespread tree species (*Nothofagus pumilio*) in southern Chile. *New Phytologist* **189**(1): 259-271.
Falster DS, Duursma RA, FitzJohn RG. 2018. How functional traits influence plant growth and shade tolerance across the life cycle. *Proceedings of the National Academy of Sciences* **115**(29): E6789-E6798.
Farjon A. 2010. *A Handbook of the World's Conifers (2 vols.)*: Brill.
Farjon A, Filer D. 2013. *An atlas of the world's conifers: an analysis of their distribution, biogeography, diversity and conservation status*: Brill.
Felsenstein J. 1985. Phylogenies and the comparative method. *The American Naturalist* **125**(1): 1-15.
Fernández-de-Uña L, Rossi S, Aranda I, Fonti P, González-González BD, Cañellas I, Gea-Izquierdo G. 2017. Xylem and leaf functional adjustments to drought in *Pinus sylvestris* and *Quercus pyrenaica* at their elevational boundary. *Frontiers in plant science* **8**: 1200.
Foiles MW. 1959. *Silvics of grand fir*: Intermountain Forest and Range Experiment Station.
Fritts H. 1976. Tree rings and climate, Acad. *Press: London*.
Fry D, Phillips I. 1977. Photosynthesis of conifers in relation to annual growth cycles and dry matter production: II. Seasonal photosynthetic capacity and mesophyll ultrastructure in *Abies grandis*, *Picea sitchensis*, *Tsuga heterophylla* and *Larix leptolepis* growing in SW England. *Physiologia Plantarum* **40**(4): 300-306.
Fu Z, Ciais P, Bastos A, Stoy PC, Yang H, Green JK, Wang B, Yu K, Huang Y, Knohl A. 2020. Sensitivity of gross primary productivity to climatic drivers during the summer drought of 2018 in Europe. *Philosophical Transactions of the Royal Society B* **375**(1810): 20190747.
Gao S, Liu R, Zhou T, Fang W, Yi C, Lu R, Zhao X, Luo H. 2018. Dynamic responses of tree-ring growth to multiple dimensions of drought. *Global Change Biology* **24**(11): 5380-5390.

Gärtner H, Nievergelt D. 2010. The core-microtome: a new tool for surface preparation on cores and time series analysis of varying cell parameters. *Dendrochronologia* **28**(2): 85-92.

Gauthey A, Peters JM, Carins-Murphy MR, Rodriguez-Dominguez CM, Li X, Delzon S, King A, López R, Medlyn BE, Tissue DT. 2020. Visual and hydraulic techniques produce similar estimates of cavitation resistance in woody species. *New Phytologist* **228**(3): 884-897.

Gazol A, Camarero J, Anderegg W, Vicente-Serrano S. 2017. Impacts of droughts on the growth resilience of Northern Hemisphere forests. *Global ecology and biogeography* **26**(2): 166-176.

Gazol A, Camarero JJ, Colangelo M, de Luis M, del Castillo EM, Serra-Maluquer X. 2019. Summer drought and spring frost, but not their interaction, constrain European beech and Silver fir growth in their southern distribution limits. *Agricultural and Forest Meteorology* **278**: 107695.

Gazol A, Camarero JJ, Sánchez-Salguero R, Vicente-Serrano SM, Serra-Maluquer X, Gutiérrez E, de Luis M, Sangüesa-Barreda G, Novak K, Rozas V. 2020. Drought legacies are short, prevail in dry conifer forests and depend on growth variability. *Journal of Ecology* **108**(6): 2473-2484.

Gazol A, Camarero JJ, Vicente-Serrano SM, Sánchez-Salguero R, Gutiérrez E, de Luis M, Sangüesa-Barreda G, Novak K, Rozas V, Tíscar PA. 2018. Forest resilience to drought varies across biomes. *Global Change Biology* **24**(5): 2143-2158.

Gessler A, Bottero A, Marshall J, Arend M. 2020. The way back: recovery of trees from drought and its implication for acclimation. *New Phytologist* **228**(6): 1704-1709.

Gleason SM, Westoby M, Jansen S, Choat B, Hacke UG, Pratt RB, Bhaskar R, Brodribb TJ, Bucci SJ, Cao KF. 2016. Weak trade-off between xylem safety and xylem-specific hydraulic efficiency across the world's woody plant species. *New Phytologist* **209**(1): 123-136.

Gould IJ, Quinton JN, Weigelt A, De Deyn GB, Bardgett RD. 2016. Plant diversity and root traits benefit physical properties key to soil function in grasslands. *Ecology Letters* **19**(9): 1140-1149.

Gruber A, Strobl S, Veit B, Oberhuber W. 2010. Impact of drought on the temporal dynamics of wood formation in *Pinus sylvestris*. *Tree Physiology* **30**(4): 490-501.

Güney A, Küppers M, Rathgeber C, Şahin M, Zimmermann R. 2017. Intra-annual stem growth dynamics of Lebanon Cedar along climatic gradients. *Trees* **31**(2): 587-606.

Gurskaya M. 2014. Temperature conditions of the formation of frost damages in conifer trees in the high latitudes of Western Siberia. *Biology Bulletin* **41**(2): 187-196.

Hacke UG, Jansen S. 2009. Embolism resistance of three boreal conifer species varies with pit structure. *New Phytologist* **182**(3): 675-686.

Hacke UG, Sperry JS, Pittermann J. 2004. Analysis of circular bordered pit function II. Gymnosperm tracheids with torus-margo pit membranes. *American journal of botany* **91**(3): 386-400.

Hacke UG, Sperry JS, Pockman WT, Davis SD, McCulloh KA. 2001. Trends in wood density and structure are linked to prevention of xylem implosion by negative pressure. *Oecologia* **126**(4): 457-461.

Hacke UG, Sperry JS, Wheeler JK, Castro L. 2006. Scaling of angiosperm xylem structure with safety and efficiency. *Tree Physiology* **26**(6): 689-701.

Hämäläinen S, Fey K, Selonen V. 2018. Habitat and nest use during natal dispersal of the urban red squirrel (*Sciurus vulgaris*). *Landscape and Urban Planning* **169**: 269-275.

Hammond WM, Yu K, Wilson LA, Will RE, Anderegg WR, Adams HD. 2019. Dead or dying? Quantifying the point of no return from hydraulic failure in drought-induced tree mortality. *New Phytologist* **223**(4): 1834-1843.

Hansen H, Dörffling K. 2003. Root-derived trans-zeatin riboside and abscisic acid in drought-stressed and rewatered sunflower plants: interaction in the control of leaf diffusive resistance? *Functional plant biology* **30**(4): 365-375.

Hartmann FP, Rathgeber CB, Fournier M, Moulia B. 2017. Modelling wood formation and structure: power and limits of a morphogenetic gradient in controlling xylem cell proliferation and growth. *Annals of Forest Science* **74**(1): 1-15.

Hartmann H. 2011. Will a 385 million year-struggle for light become a struggle for water and for carbon?–How trees may cope with more frequent climate change-type drought events. *Global Change Biology* **17**(1): 642-655.

Harvey JE, Smiljanić M, Scharnweber T, Buras A, Cedro A, Cruz-García R, Drobyshev I, Janecka K, Jansons Ā, Kaczka R. 2020. Tree growth influenced by warming winter climate and summer moisture availability in northern temperate forests. *Global Change Biology* **26**(4): 2505-2518.

He P, Wright IJ, Zhu S, Onoda Y, Liu H, Li R, Liu X, Hua L, Oyanoghafo OO, Ye Q. 2019. Leaf mechanical strength and photosynthetic capacity vary independently across 57 subtropical forest species with contrasting light requirements. *New Phytologist* **223**(2): 607-618.

Hirano T, Hirata R, Fujinuma Y, Saigusa N, Yamamoto S, Harazono Y, Takada M, Inukai K, Inoue G. 2003. CO2 and water vapor exchange of a larch forest in northern Japan. *Tellus B: Chemical and Physical Meteorology* **55**(2): 244-257.

Hogg E, Brandt JP, Kochtubajda B. 2002. Growth and dieback of aspen forests in northwestern Alberta, Canada, in relation to climate and insects. *Canadian Journal of Forest Research* **32**(5): 823-832.

Huang B. 2000. Role of root morphological and physiological characteristics in drought resistance of plants. *Plant–Environment Interactions. Marcel Dekker Inc., New York*: 39-64.

Huang J, Tardif JC, Bergeron Y, Denneler B, Berninger F, Girardin MP. 2010. Radial growth response of four dominant boreal tree species to climate along a latitudinal gradient in the eastern Canadian boreal forest. *Global Change Biology* **16**(2): 711-731.

Huang M, Wang X, Keenan TF, Piao S. 2018. Drought timing influences the legacy of tree growth recovery. *Global Change Biology* **24**(8): 3546-3559.

Huang W, Fonti P, Larsen JB, Ræbild A, Callesen I, Pedersen NB, Hansen JK. 2017. Projecting tree-growth responses into future climate: a study case from a Danish-wide common garden. *Agricultural and Forest Meteorology* **247**: 240-251.

Inouye DW. 2000. The ecological and evolutionary significance of frost in the context of climate change. *Ecology Letters* **3**(5): 457-463.

IPCC 2013. Climate Change 2013: the physical science basis: Cambridge University Press Cambridge and New York.

Jacobsen AL, Tobin MF, Toschi HS, Percolla MI, Pratt RB. 2016. Structural determinants of increased susceptibility to dehydration-induced cavitation in post-fire resprouting chaparral shrubs. *Plant, Cell & Environment* **39**(11): 2473-2485.

Jansen S, Choat B, Pletsers A. 2009. Morphological variation of intervessel pit membranes and implications to xylem function in angiosperms. *American journal of botany* **96**(2): 409-419.

Jansen S, Lamy JB, Burlett R, Cochard H, Gasson P, Delzon S. 2012. Plasmodesmatal pores in the torus of bordered pit membranes affect cavitation resistance of conifer xylem. *Plant, Cell & Environment* **35**(6): 1109-1120.

Jansen S, McAdam S. 2019. Pits with aspiration explain life expectancy of a conifer species. *Proceedings of the National Academy of Sciences* **116**(30): 14794-14796.

Julio Camarero J, Gazol A, Sangüesa-Barreda G, Cantero A, Sánchez-Salguero R, Sánchez-Miranda A, Granda E, Serra-Maluquer X, Ibáñez R. 2018. Forest Growth Responses to Drought at Short- and Long-Term Scales in Spain: Squeezing the Stress Memory from Tree Rings. *Frontiers in Ecology and Evolution* **6**(9).

Jump AS, Ruiz-Benito P, Greenwood S, Allen CD, Kitzberger T, Fensham R, Martínez-Vilalta J, Lloret F. 2017. Structural overshoot of tree growth with climate variability and the global spectrum of drought-induced forest dieback. *Global Change Biology* **23**(9): 3742-3757.

Kamilar JM, Cooper N. 2013. Phylogenetic signal in primate behaviour, ecology and life history. *Philosophical Transactions of the Royal Society B: Biological Sciences* **368**(1618): 20120341.

Kawai K, Okada N. 2019. Coordination of leaf and stem traits in 25 species of Fagaceae from three biomes of East Asia. *Botany* **97**(7): 391-403.

Kembel SW, Cowan PD, Helmus MR, Cornwell WK, Morlon H, Ackerly DD, Blomberg SP, Webb CO. 2010. Picante: R tools for integrating phylogenies and ecology. *Bioinformatics* **26**(11): 1463-1464.

Kessell SR. 1979. Adaptation and dimorphism in eastern hemlock, *Tsuga canadensis* (L.) Carr. *The American Naturalist* **113**(3): 333-350.

Kitajima K, Poorter L. 2010. Tissue-level leaf toughness, but not lamina thickness, predicts sapling leaf lifespan and shade tolerance of tropical tree species. *New Phytologist* **186**(3): 708-721.

Klesse S, Babst F, Lienert S, Spahni R, Joos F, Bouriaud O, Carrer M, Di Filippo A, Poulter B, Trotsiuk V. 2018. A combined tree ring and vegetation model assessment of European forest growth sensitivity to interannual climate variability. *Global Biogeochemical Cycles* **32**(8): 1226-1240.

Körner C. 2017. A matter of tree longevity. *Science* **355**(6321): 130-131.

Kraft NJ, Valencia R, Ackerly DD. 2008. Functional traits and niche-based tree community assembly in an Amazonian forest. *Science* **322**(5901): 580-582.

Kurz WA, Dymond C, Stinson G, Rampley G, Neilson E, Carroll A, Ebata T, Safranyik L. 2008. Mountain pine beetle and forest carbon feedback to climate change. *Nature* **452**(7190): 987-990.

Larcher W. 2000. Temperature stress and survival ability of Mediterranean sclerophyllous plants. *Plant biosystems* **134**(3): 279-295.

Larsen KS, Ibrom A, Jonasson S, Michelsen A, Beier C. 2007. Significance of cold-season respiration and photosynthesis in a subarctic heath ecosystem in Northern Sweden. *Global Change Biology* **13**(7): 1498-1508.

Larter M, Pfautsch S, Domec JC, Trueba S, Nagalingum N, Delzon S. 2017. Aridity drove the evolution of extreme embolism resistance and the radiation of conifer genus *Callitris*. *New Phytologist* **215**(1): 97-112.

Lefcheck J, Byrnes J, Grace J. 2016. Package 'piecewiseSEM'. *R package version* **1**(1).

Leslie AB, Beaulieu JM, Rai HS, Crane PR, Donoghue MJ, Mathews S. 2012. Hemisphere-scale differences in conifer evolutionary dynamics. *Proceedings of the National Academy of Sciences* **109**(40): 16217-16221.

Lévesque M, Saurer M, Siegwolf R, Eilmann B, Brang P, Bugmann H, Rigling A. 2013. Drought response of five conifer species under contrasting water availability suggests high vulnerability of Norway spruce and European larch. *Global Change Biology* **19**(10): 3184-3199.

Li L, McCormack ML, Ma C, Kong D, Zhang Q, Chen X, Zeng H, Niinemets Ü, Guo D. 2015. Leaf economics and hydraulic traits are decoupled in five species-rich tropical-subtropical forests. *Ecology Letters* **18**(9): 899-906.

Li W-F, Ding Q, Cui K-M, He X-Q. 2013. Cambium reactivation independent of bud unfolding involves de novo IAA biosynthesis in cambium regions in Populus tomentosa Carr. *Acta physiologiae plantarum* **35**(6): 1827-1836.

Li X, Piao S, Wang K, Wang X, Wang T, Ciais P, Chen A, Lian X, Peng S, Peñuelas J. 2020. Temporal trade-off between gymnosperm resistance and resilience increases forest sensitivity to extreme drought. *Nature Ecology & Evolution* **4**(8): 1075-1083.

Liang X, He P, Liu H, Zhu S, Uyehara IK, Hou H, Wu G, Zhang H, You Z, Xiao Y. 2019. Precipitation has dominant influences on the variation of plant hydraulics of the native *Castanopsis fargesii* (Fagaceae) in subtropical China. *Agricultural and Forest Meteorology* **271**: 83-91.

Lindenmayer DB, Laurance WF, Franklin JF. 2012. Global decline in large old trees. *Science* **338**(6112): 1305-1306.

Liu H, Gleason SM, Hao G, Hua L, He P, Goldstein G, Ye Q. 2019. Hydraulic traits are coordinated with maximum plant height at the global scale. *Science advances* **5**(2): eaav1332.

Lloret F, Keeling EG, Sala A. 2011. Components of tree resilience: effects of successive low-growth episodes in old ponderosa pine forests. *Oikos* **120**(12): 1909-1920.

Lloyd-Hughes B. 2014. The impracticality of a universal drought definition. *Theoretical and Applied Climatology* **117**(3): 607-611.

Lopatka J. 2019. Climate change to blame as bark beetles ravage central Europe's forests. *Reuters*.

López R, Cano FJ, Martin-StPaul NK, Cochard H, Choat B. 2021. Coordination of stem and leaf traits define different strategies to regulate water loss and tolerance ranges to aridity. *New Phytologist* **230**(2): 497-509.

López R, López de Heredia U, Collada C, Cano FJ, Emerson BC, Cochard H, Gil L. 2013. Vulnerability to cavitation, hydraulic efficiency, growth and survival in an insular pine (*Pinus canariensis*). *Annals of Botany* **111**(6): 1167-1179.

Losso A, Anfodillo T, Ganthaler A, Kofler W, Markl Y, Nardini A, Oberhuber W, Purin G, Mayr S. 2018. Robustness of xylem properties in conifers: analyses of tracheid and pit dimensions along elevational transects. *Tree Physiology* **38**(2): 212-222.

Mackay DS, Savoy PR, Grossiord C, Tai X, Pleban JR, Wang DR, McDowell NG, Adams HD, Sperry JS. 2020. Conifers depend on established roots during drought: results from a coupled model of carbon allocation and hydraulics. *New Phytologist* **225**(2): 679-692.

Maherali H, Moura CF, Caldeira MC, Willson CJ, Jackson RB. 2006. Functional coordination between leaf gas exchange and vulnerability to xylem cavitation in temperate forest trees. *Plant, Cell & Environment* **29**(4): 571-583.

Majeková M, de Bello F, Doležal J, Lepš J. 2014. Plant functional traits as determinants of population stability. *Ecology* **95**(9): 2369-2374.

Maréchaux I, Bartlett MK, Sack L, Baraloto C, Engel J, Joetzjer E, Chave J. 2015. Drought tolerance as predicted by leaf water potential at turgor loss point varies strongly across species within an Amazonian forest. *Functional Ecology* **29**(10): 1268-1277.

Markesteijn L, Poorter L. 2009. Seedling root morphology and biomass allocation of 62 tropical tree species in relation to drought-and shade-tolerance. *Journal of Ecology* **97**(2): 311-325.

Markesteijn L, Poorter L, Bongers F, Paz H, Sack L. 2011. Hydraulics and life history of tropical dry forest tree species: coordination of species' drought and shade tolerance. *New Phytologist* **191**(2): 480-495.

Martin-Benito D, Anchukaitis KJ, Evans MN, Del Río M, Beeckman H, Cañellas I. 2017. Effects of drought on xylem anatomy and water-use efficiency of two co-occurring pine species. *Forests* **8**(9): 332.

Martin-Benito D, Pederson N, Köse N, Doğan M, Bugmann H, Mosulishvili M, Bigler C. 2018. Pervasive effects of drought on tree growth across a wide climatic gradient in the temperate forests of the Caucasus. *Global ecology and biogeography* **27**(11): 1314-1325.

Martínez-Vilalta J, Mencuccini M, Vayreda J, Retana J. 2010. Interspecific variation in functional traits, not climatic differences among species ranges, determines demographic rates across 44 temperate and Mediterranean tree species. *Journal of Ecology* **98**(6): 1462-1475.

Martínez-Vilalta J, Sala A, Asensio D, Galiano L, Hoch G, Palacio S, Piper FI, Lloret F. 2016. Dynamics of non-structural carbohydrates in terrestrial plants: a global synthesis. *Ecological Monographs* **86**(4): 495-516.

Mayr S, Hacke U, Schmid P, Schwienbacher F, Gruber A. 2006. Frost drought in conifers at the alpine timberline: xylem dysfunction and adaptations. *Ecology* **87**(12): 3175-3185.

McCarroll D, Jalkanen R, Hicks S, Tuovinen M, Gagen M, Pawellek F, Eckstein D, Schmitt U, Autio J, Heikkinen O. 2003. Multiproxy dendroclimatology: a pilot study in northern Finland. *The Holocene* **13**(6): 829-838.

McDowell N, Pockman WT, Allen CD, Breshears DD, Cobb N, Kolb T, Plaut J, Sperry J, West A, Williams DG. 2008. Mechanisms of plant survival and mortality during drought: why do some plants survive while others succumb to drought? *New Phytologist* **178**(4): 719-739.

McLane SC, LeMay VM, Aitken SN. 2011. Modeling lodgepole pine radial growth relative to climate and genetics using universal growth-trend response functions. *Ecological applications* **21**(3): 776-788.

Mitchell PJ, O'Grady AP, Tissue DT, White DA, Ottenschlaeger ML, Pinkard EA. 2013. Drought response strategies define the relative contributions of hydraulic dysfunction and carbohydrate depletion during tree mortality. *New Phytologist* **197**(3): 862-872.

Montwé D, Isaac-Renton M, Hamann A, Spiecker H. 2018. Cold adaptation recorded in tree rings highlights risks associated with climate change and assisted migration. *Nature communications* **9**(1): 1574.

Nabuurs G-J, Delacote P, Ellison D, Hanewinkel M, Hetemäki L, Lindner M. 2017. By 2050 the mitigation effects of EU forests could nearly double through climate smart forestry. *Forests* **8**(12): 484.

Nabuurs G-J, Verkerk PJ, Schelhaas M, González-Olabarria J, Trasobares A, Cienciala E. 2018. *Climate-Smart Forestry: mitigation implact in three European regions*: European Forest Institute.

Nakagawa M. 2020. Effect of Japanese Larch Arable Land Windbreaks on Wind Damage Reduction in the Early Spring Cultivation Season: A Case Study in Kamioribe District, Shihoro Town, Eastern Hokkaido. *Journal of Forest Planning*.

Neuner G, Beikircher B. 2010. Critically reduced frost resistance of Picea abies during sprouting could be linked to cytological changes. *Protoplasma* **243**(1-4): 145-152.

Niinemets Ü. 2001. Global-scale climatic controls of leaf dry mass per area, density, and thickness in trees and shrubs. *Ecology* **82**(2): 453-469.

Oberhuber W, Gruber A, Lethaus G, Winkler A, Wieser G. 2017. Stem girdling indicates prioritized carbon allocation to the root system at the expense of radial stem growth in Norway spruce under drought conditions. *Environmental and experimental botany* **138**: 109-118.

Onoda Y, Wright IJ, Evans JR, Hikosaka K, Kitajima K, Niinemets Ü, Poorter H, Tosens T, Westoby M. 2017. Physiological and structural trade-offs underlying the leaf economics spectrum. *New Phytologist* **214**(4): 1447-1463.

Osnas JL, Lichstein JW, Reich PB, Pacala SW. 2013. Global leaf trait relationships: mass, area, and the leaf economics spectrum. *Science* **340**(6133): 741-744.

Pan Y, Birdsey RA, Fang J, Houghton R, Kauppi PE, Kurz WA, Phillips OL, Shvidenko A, Lewis SL, Canadell JG. 2011. A large and persistent carbon sink in the world's forests. *Science* **333**(6045): 988-993.

Panek JA. 1996. Correlations between stable carbon-isotope abundance and hydraulic conductivity in Douglas-fir across a climate gradient in Oregon, USA. *Tree Physiology* **16**(9): 747-755.

Paradis E, Claude J, Strimmer K. 2004. APE: Analyses of Phylogenetics and Evolution in R language. *Bioinformatics* **20**(2): 289-290.

Park C-W, Ko S, Yoon TK, Han S, Yi K, Jo W, Jin L, Lee SJ, Noh NJ, Chung H. 2012. Differences in soil aggregate, microbial biomass carbon concentration, and soil carbon between *Pinus rigida* and *Larix kaempferi* plantations in Yangpyeong, central Korea. *Forest Science and Technology* **8**(1): 38-46.

Pinheiro J, Bates D, DebRoy S, Sarkar D, Heisterkamp S, Van Willigen B, Maintainer R. 2017. Package 'nlme'. *Linear and nonlinear mixed effects models, version* **3**(1).

Piper FI, Fajardo A, Hoch G. 2017. Single-provenance mature conifers show higher non-structural carbohydrate storage and reduced growth in a drier location. *Tree Physiology* **37**(8): 1001-1010.

Pittermann J, Choat B, Jansen S, Stuart SA, Lynn L, Dawson TE. 2010. The relationships between xylem safety and hydraulic efficiency in the Cupressaceae: the evolution of pit membrane form and function. *Plant physiology* **153**(4): 1919-1931.

Pittermann J, Sperry J. 2003. Tracheid diameter is the key trait determining the extent of freezing-induced embolism in conifers. *Tree Physiology* **23**(13): 907-914.

Pittermann J, Sperry JS, Hacke UG, Wheeler JK, Sikkema EH. 2005. Torus-margo pits help conifers compete with angiosperms. *Science* **310**(5756): 1924-1924.

Pittermann J, Sperry JS, Hacke UG, Wheeler JK, Sikkema EH. 2006a. Inter-tracheid pitting and the hydraulic efficiency of conifer wood: the role of tracheid allometry and cavitation protection. *American journal of botany* **93**(9): 1265-1273.

Pittermann J, Sperry JS, Wheeler JK, Hacke UG, Sikkema EH. 2006b. Mechanical reinforcement of tracheids compromises the hydraulic efficiency of conifer xylem. *Plant, Cell & Environment* **29**(8): 1618-1628.

Plaut JA, Yepez EA, Hill J, Pangle R, Sperry JS, Pockman WT, Mcdowell NG. 2012. Hydraulic limits preceding mortality in a piñon–juniper woodland under experimental drought. *Plant, Cell & Environment* **35**(9): 1601-1617.

Poorter L, Bongers F. 2006. Leaf traits are good predictors of plant performance across 53 rain forest species. *Ecology* **87**(7): 1733-1743.

Poorter L, Castilho CV, Schietti J, Oliveira RS, Costa FR. 2018. Can traits predict individual growth performance? A test in a hyperdiverse tropical forest. *New Phytologist* **219**(1): 109-121.

Poorter L, McDonald I, Alarcón A, Fichtler E, Licona JC, Peña-Claros M, Sterck F, Villegas Z, Sass-Klaassen U. 2010. The importance of wood traits and hydraulic conductance for the performance and life history strategies of 42 rainforest tree species. *New Phytologist* **185**(2): 481-492.

Poorter L, van der Sande MT, Arets EJ, Ascarrunz N, Enquist BJ, Finegan B, Licona JC, Martínez-Ramos M, Mazzei L, Meave JA. 2017. Biodiversity and climate determine the functioning of Neotropical forests. *Global ecology and biogeography* **26**(12): 1423-1434.

Poorter L, Wright SJ, Paz H, Ackerly DD, Condit R, Ibarra-Manríquez G, Harms KE, Licona J, Martinez-Ramos M, Mazer S. 2008. Are functional traits good predictors of demographic rates? Evidence from five neotropical forests. *Ecology* **89**(7): 1908-1920.

Puchi PF, Castagneri D, Rossi S, Carrer M. 2019. Wood anatomical traits in black spruce reveal latent water constraints on the boreal forest. *Global Change Biology*.

Puritch GS. 1973. Effect of water stress on photosynthesis, respiration, and transpiration of four *Abies* species. *Canadian Journal of Forest Research* **3**(2): 293-298.

Quero JL, Sterck FJ, Martínez-Vilalta J, Villar R. 2011. Water-use strategies of six co-existing Mediterranean woody species during a summer drought. *Oecologia* **166**(1): 45-57.

R Core Team. 2019. R: A Language and Environment for Statistical Computing. Vienna, Austria: R Foundation for Statistical Computing. Retrieved from: https://www. R-project. org/.

R Core Team 2020. R: a language and environment for statistical computing. Version 4.0. 2. Vienna, Austria.

Rahman MH, Kudo K, Yamagishi Y, Nakamura Y, Nakaba S, Begum S, Nugroho WD, Arakawa I, Kitin P, Funada R. 2020. Winter-spring temperature pattern is closely related to the onset of cambial reactivation in stems of the evergreen conifer Chamaecyparis pisifera. *Scientific Reports* **10**(1): 1-12.

Ramírez-Valiente JA, López R, Hipp AL, Aranda I. 2020. Correlated evolution of morphology, gas exchange, growth rates and hydraulics as a response to precipitation and temperature regimes in oaks (*Quercus*). *New Phytologist* **227**(3): 794-809.

Rathgeber CB, Rossi S, Bontemps J-D. 2011. Cambial activity related to tree size in a mature silver-fir plantation. *Annals of Botany* **108**(3): 429-438.

Reich PB. 2014. The world-wide 'fast–slow'plant economics spectrum: a traits manifesto. *Journal of Ecology* **102**(2): 275-301.

Reichgelt A, Sinke R. 2020. De toekomst van de fijnspar. *VAKBLAD natuur bos landschap* **165**: 16-17.

Revell LJ. 2012. phytools: an R package for phylogenetic comparative biology (and other things). *Methods in ecology and evolution* **3**(2): 217-223.

Rosas T, Mencuccini M, Barba J, Cochard H, Saura-Mas S, Martínez-Vilalta J. 2019. Adjustments and coordination of hydraulic, leaf and stem traits along a water availability gradient. *New Phytologist* **223**(2): 632-646.

Rosas Torrent T. 2019. *Integrating plant hydraulics into functional traits framework to understand plant adjustments along a water availability gradient*: Universitat Autònoma de Barcelona.

Roskilly B, Keeling E, Hood S, Giuggiola A, Sala A. 2019. Conflicting functional effects of xylem pit structure relate to the growth-longevity trade-off in a conifer species. *Proceedings of the National Academy of Sciences* **116**(30): 15282-15287.

Rosseel Y. 2012. Lavaan: An R package for structural equation modeling and more. Version 0.5–12 (BETA). *Journal of statistical software* **48**(2): 1-36.

Rossi S, Deslauriers A, Anfodillo T, Morin H, Saracino A, Motta R, Borghetti M. 2006. Conifers in cold environments synchronize maximum growth rate of tree-ring formation with day length. *New Phytologist* **170**(2): 301-310.

Rossi S, Deslauriers A, Griçar J, Seo JW, Rathgeber CB, Anfodillo T, Morin H, Levanic T, Oven P, Jalkanen R. 2008. Critical temperatures for xylogenesis in conifers of cold climates. *Global ecology and biogeography* **17**(6): 696-707.

Ryan MG, Phillips N, Bond BJ. 2006. The hydraulic limitation hypothesis revisited. *Plant, Cell & Environment* **29**(3): 367-381.

Sack L, Tyree MT 2005. Leaf hydraulics and its implications in plant structure and function. *Vascular transport in plants*: Elsevier, 93-114.

Sakschewski B, von Bloh W, Boit A, Rammig A, Kattge J, Poorter L, Peñuelas J, Thonicke K. 2015. Leaf and stem economics spectra drive diversity of functional plant traits in a dynamic global vegetation model. *Global Change Biology* **21**(7): 2711-2725.

Sala A, Piper F, Hoch G. 2010. Physiological mechanisms of drought-induced tree mortality are far from being resolved. *The New Phytologist* **186**(2): 274-281.

Sano Y 2016. Bordered pit structure and cavitation resistance in woody plants. *Secondary Xylem Biology*: Elsevier, 113-130.

Santarius KA. 1973. The protective effect of sugars on chloroplast membranes during temperature and water stress and its relationship to frost, desiccation and heat resistance. *Planta* **113**(2): 105-114.

Santiago LS, Goldstein G, Meinzer FC, Fisher JB, Machado K, Woodruff D, Jones T. 2004. Leaf photosynthetic traits scale with hydraulic conductivity and wood density in Panamanian forest canopy trees. *Oecologia* **140**(4): 543-550.

Saunders MR, Wagner RG. 2008. Height-diameter models with random coefficients and site variables for tree species of Central Maine. *Annals of Forest Science* **65**(2): 1-10.

Schippers P, Sterck F, Vlam M, Zuidema PA. 2015a. Tree growth variation in the tropical forest: understanding effects of temperature, rainfall and CO 2. *Global Change Biology* **21**(7): 2749-2761.

Schippers P, Vlam M, Zuidema PA, Sterck F. 2015b. Sapwood allocation in tropical trees: a test of hypotheses. *Functional plant biology* **42**(7): 697-709.

Schmid I, Kazda M. 2001. Vertical distribution and radial growth of coarse roots in pure and mixed stands of Fagus sylvatica and Picea abies. *Canadian Journal of Forest Research* **31**(3): 539-548.

Schmidt PA 1999. The diversity, phytogeography and ecology of spruces (*Picea*: Pinaceae) in Eurasia. *IV International Conifer Conference 615*. 189-201.

Schulte PJ, Hacke UG, Schoonmaker AL. 2015. Pit membrane structure is highly variable and accounts for a major resistance to water flow through tracheid pits in stems and roots of two boreal conifer species. *New Phytologist* **208**(1): 102-113.

Schwalm CR, Anderegg WR, Michalak AM, Fisher JB, Biondi F, Koch G, Litvak M, Ogle K, Shaw JD, Wolf A. 2017. Global patterns of drought recovery. *Nature* **548**(7666): 202-205.

Schwarz J, Skiadaresis G, Kohler M, Kunz J, Schnabel F, Vitali V, Bauhus J. 2020. Quantifying Growth Responses of Trees to Drought—a Critique of Commonly Used Resilience Indices and Recommendations for Future Studies. *Current Forestry Reports* **6**: 185-200.

Shestakova TA, Gutiérrez E, Kirdyanov AV, Camarero JJ, Génova M, Knorre AA, Linares JC, de Dios VR, Sánchez-Salguero R, Voltas J. 2016. Forests synchronize their growth in contrasting Eurasian regions in response to climate warming. *Proceedings of the National Academy of Sciences* **113**(3): 662-667.

Shipley B. 2000. A new inferential test for path models based on directed acyclic graphs. *Structural Equation Modeling* **7**(2): 206-218.

Shipley B, Vile D, Garnier É. 2006. From plant traits to plant communities: a statistical mechanistic approach to biodiversity. *Science* **314**(5800): 812-814.

Song Y, Sass-Klaassen U, Sterck F, Goudzwaard L, Akhmetzyanov L, Poorter L. 2021. Growth of 19 conifer species is highly sensitive to winter warming, spring frost and summer drought. *Annals of Botany* **128**(5): 545-557.

Sperry JS, Hacke UG, Pittermann J. 2006. Size and function in conifer tracheids and angiosperm vessels. *American journal of botany* **93**(10): 1490-1500.

Steppe K, Sterck F, Deslauriers A. 2015. Diel growth dynamics in tree stems: linking anatomy and ecophysiology. *Trends in plant science* **20**(6): 335-343.

Sterck F, Markesteijn L, Schieving F, Poorter L. 2011. Functional traits determine trade-offs and niches in a tropical forest community. *Proceedings of the National Academy of Sciences* **108**(51): 20627-20632.

Sterck F, Markesteijn L, Toledo M, Schieving F, Poorter L. 2014. Sapling performance along resource gradients drives tree species distributions within and across tropical forests. *Ecology* **95**(9): 2514-2525.

Sterck F, Poorter L, Schieving F. 2006. Leaf traits determine the growth-survival trade-off across rain forest tree species. *The American Naturalist* **167**(5): 758-765.
Sterck FJ, Martínez-Vilalta J, Mencuccini M, Cochard H, Gerrits P, Zweifel R, Herrero A, Korhonen JF, Llorens P, Nikinmaa E. 2012. Understanding trait interactions and their impacts on growth in Scots pine branches across Europe. *Functional Ecology* **26**(2): 541-549.
Sterck FJ, Schieving F. 2007. 3-D growth patterns of trees: effects of carbon economy, meristem activity, and selection. *Ecological Monographs* **77**(3): 405-420.
Sterck FJ, Zweifel R, Sass-Klaassen U, Chowdhury Q. 2008. Persisting soil drought reduces leaf specific conductivity in Scots pine (*Pinus sylvestris*) and pubescent oak (*Quercus pubescens*). *Tree Physiology* **28**(4): 529-536.
Takahashi K, Obata Y. 2014. Growth, allometry and shade tolerance of understory saplings of four subalpine conifers in central Japan. *Journal of plant research* **127**(2): 329-338.
Team RC 2019. R: a language and environment for statistical computing, version 3.0. 2. Vienna, Austria: R Foundation for Statistical Computing; 2013.
Thomas H, Gay A. 1987. Characterization of forages for drought resistance. *IBPGR Training Courses: Lecture Series* **1**: 29-35.
Thomas P, Polwart A. 2003. *Taxus baccata* L. *Journal of Ecology* **91**(3): 489-524.
Thornthwaite CW. 1948. An approach toward a rational classification of climate. *Geographical review* **38**(1): 55-94.
TNO-NITG. 2020. www.cinoloket.nl. Accessed January 2020.
Truettner C, Anderegg WR, Biondi F, Koch GW, Ogle K, Schwalm C, Litvak ME, Shaw JD, Ziaco E. 2018. Conifer radial growth response to recent seasonal warming and drought from the southwestern USA. *Forest Ecology and Management* **418**: 55-62.
Tyree MT, Ewers FW. 1991. The hydraulic architecture of trees and other woody plants. *New Phytologist* **119**(3): 345-360.
Urli M, Porté AJ, Cochard H, Guengant Y, Burlett R, Delzon S. 2013. Xylem embolism threshold for catastrophic hydraulic failure in angiosperm trees. *Tree Physiology* **33**(7): 672-683.
van der Sande MT, Poorter L, Schnitzer SA, Engelbrecht BM, Markesteijn L. 2019. The hydraulic efficiency–safety trade-off differs between lianas and trees. *Ecology* **100**(5): e02666.
van der Sande MT, Zuidema PA, Sterck F. 2015. Explaining biomass growth of tropical canopy trees: the importance of sapwood. *Oecologia* **177**(4): 1145-1155.
van der Wal A, Klein Gunnewiek PJ, Cornelissen JHC, Crowther TW, de Boer W. 2016. Patterns of natural fungal community assembly during initial decay of coniferous and broadleaf tree logs. *Ecosphere* **7**(7): e01393.
Vicente-Serrano SM, Beguería S, López-Moreno JI. 2010. A multiscalar drought index sensitive to global warming: the standardized precipitation evapotranspiration index. *Journal of climate* **23**(7): 1696-1718.
Violle C, Navas ML, Vile D, Kazakou E, Fortunel C, Hummel I, Garnier E. 2007. Let the concept of trait be functional! *Oikos* **116**(5): 882-892.
Vitali V, Büntgen U, Bauhus J. 2017. Silver fir and Douglas fir are more tolerant to extreme droughts than Norway spruce in south-western Germany. *Global Change Biology* **23**(12): 5108-5119.
Vitasse Y, Bottero A, Cailleret M, Bigler C, Fonti P, Gessler A, Lévesque M, Rohner B, Weber P, Rigling A. 2019. Contrasting resistance and resilience to extreme drought and late spring frost in five major European tree species. *Global Change Biology* **25**(11): 3781-3792.
Vitasse Y, Signarbieux C, Fu YH. 2018. Global warming leads to more uniform spring phenology across elevations. *Proceedings of the National Academy of Sciences* **115**(5): 1004-1008.
Vitra A, Lenz A, Vitasse Y. 2017. Frost hardening and dehardening potential in temperate trees from winter to budburst. *New Phytologist* **216**(1): 113-123.
Voltas J, Lucabaugh D, Chambel MR, Ferrio JP. 2015. Intraspecific variation in the use of water sources by the circum-Mediterranean conifer Pinus halepensis. *New Phytologist* **208**(4): 1031-1041.
Walker AP, De Kauwe MG, Bastos A, Belmecheri S, Georgiou K, Keeling R, McMahon SM, Medlyn BE, Moore DJ, Norby RJ. 2020. Integrating the evidence for a terrestrial carbon sink caused by increasing atmospheric CO2. *New Phytologist*.
Walters MB, Gerlach JP. 2013. Intraspecific growth and functional leaf trait responses to natural soil resource gradients for conifer species with contrasting leaf habit. *Tree Physiology* **33**(3): 297-310.
Webb SL, Scanga SE. 2001. Windstorm disturbance without patch dynamics: twelve years of change in a Minnesota forest. *Ecology* **82**(3): 893-897.
Weemstra M, Eilmann B, Sass-Klaassen UG, Sterck FJ. 2013. Summer droughts limit tree growth across 10 temperate species on a productive forest site. *Forest Ecology and Management* **306**: 142-149.
Weemstra M, Kiorapostolou N, van Ruijven J, Mommer L, de Vries J, Sterck F. 2020. The role of fine-root mass, specific root length and life span in tree performance: A whole-tree exploration. *Functional Ecology* **34**(3): 575-585.
Weemstra M, Mommer L, Visser EJ, van Ruijven J, Kuyper TW, Mohren GM, Sterck FJ. 2016. Towards a multidimensional root trait framework: a tree root review. *New Phytologist* **211**(4): 1159-1169.
West A, Hultine K, Jackson T, Ehleringer J. 2007. Differential summer water use by *Pinus edulis* and *Juniperus osteosperma* reflects contrasting hydraulic characteristics. *Tree Physiology* **27**(12): 1711-1720.
West A, Hultine K, Sperry J, Bush S, Ehleringer J. 2008. Transpiration and hydraulic strategies in a piñon–juniper woodland. *Ecological applications* **18**(4): 911-927.
Westoby M. 1998. A leaf-height-seed (LHS) plant ecology strategy scheme. *Plant and Soil* **199**(2): 213-227.

Westoby M, Falster DS, Moles AT, Vesk PA, Wright IJ. 2002. Plant ecological strategies: some leading dimensions of variation between species. *Annual review of ecology and systematics* **33**(1): 125-159.

Williams AP, Michaelsen J, Leavitt SW, Still CJ. 2010. Using tree rings to predict the response of tree growth to climate change in the continental United States during the twenty-first century. *Earth Interactions* **14**(19): 1-20.

Williams CM, Henry HA, Sinclair BJ. 2015. Cold truths: how winter drives responses of terrestrial organisms to climate change. *Biological Reviews* **90**(1): 214-235.

Willinge Gratama-Oudemans JJ. 1992. The arboretum of Schovenhorst, Putten, in the Netherlands. *Arboricultural Journal* **16**(3): 197-205.

Willson CJ, Manos PS, Jackson RB. 2008. Hydraulic traits are influenced by phylogenetic history in the drought-resistant, invasive genus *Juniperus* (Cupressaceae). *American journal of botany* **95**(3): 299-314.

Woodruff DR, Meinzer F, Lachenbruch B. 2008. Height-related trends in leaf xylem anatomy and shoot hydraulic characteristics in a tall conifer: safety versus efficiency in water transport. *New Phytologist* **180**(1): 90-99.

Wright I, Cannon K. 2001. Relationships between leaf lifespan and structural defences in a low-nutrient, sclerophyll flora. *Functional Ecology* **15**(3): 351-359.

Wright IJ, Reich PB, Cornelissen JH, Falster DS, Groom PK, Hikosaka K, Lee W, Lusk CH, Niinemets Ü, Oleksyn J. 2005. Modulation of leaf economic traits and trait relationships by climate. *Global ecology and biogeography* **14**(5): 411-421.

Wright IJ, Reich PB, Westoby M, Ackerly DD, Baruch Z, Bongers F, Cavender-Bares J, Chapin T, Cornelissen JH, Diemer M. 2004. The worldwide leaf economics spectrum. *Nature* **428**(6985): 821-827.

Wright SJ, Kitajima K, Kraft NJ, Reich PB, Wright IJ, Bunker DE, Condit R, Dalling JW, Davies SJ, Díaz S. 2010. Functional traits and the growth–mortality trade-off in tropical trees. *Ecology* **91**(12): 3664-3674.

Wullschleger SD, Hanson P, Todd D. 2001. Transpiration from a multi-species deciduous forest as estimated by xylem sap flow techniques. *Forest Ecology and Management* **143**(1-3): 205-213.

Xu Y-J, Röhrig E, Fölster H. 1997. Reaction of root systems of grand fir (*Abies grandis* Lindl.) and Norway spruce (*Picea abies* Karst.) to seasonal waterlogging. *Forest Ecology and Management* **93**(1-2): 9-19.

Yao GQ, Nie ZF, Turner NC, Li FM, Gao TP, Fang XW, Scoffoni C. 2021. Combined high leaf hydraulic safety and efficiency provides drought tolerance in Caragana species adapted to low mean annual precipitation. *New Phytologist* **229**(1): 230-244.

Yu H-W, He W-M. 2017. Negative legacy effects of rainfall and nitrogen amendment on leaf lifespan of steppe species. *Journal of Plant Ecology* **10**(5): 831-838.

Zang C, Hartl-Meier C, Dittmar C, Rothe A, Menzel A. 2014. Patterns of drought tolerance in major European temperate forest trees: climatic drivers and levels of variability. *Global Change Biology* **20**(12): 3767-3779.

Zanne AE, Tank DC, Cornwell WK, Eastman JM, Smith SA, FitzJohn RG, McGlinn DJ, O'Meara BC, Moles AT, Reich PB. 2014. Three keys to the radiation of angiosperms into freezing environments. *Nature* **506**(7486): 89-92.

Zargar A, Sadiq R, Naser B, Khan FI. 2011. A review of drought indices. *Environmental Reviews* **19**(NA): 333-349.

Zimmermann M 1983. Xylem structure and the ascent of sap, SpringerrV: Berlin.

Zohner CM, Mo L, Renner SS, Svenning J-C, Vitasse Y, Benito BM, Ordonez A, Baumgarten F, Bastin J-F, Sebald V. 2020. Late-spring frost risk between 1959 and 2017 decreased in North America but increased in Europe and Asia. *Proceedings of the National Academy of Sciences* **117**(22): 12192-12200.

Zweifel R, Etzold S, Sterck F, Gessler A, Anfodillo T, Mencuccini M, von Arx G, Lazzarin M, Haeni M, Feichtinger L. 2020. Determinants of legacy effects in pine trees–implications from an irrigation-stop experiment. *The New Phytologist* **227**(4): 1081.

Zweifel R, Sterck F. 2018. A conceptual tree model explaining legacy effects on stem growth. *Frontiers in Forests and Global Change* **1**: 9.

Summary

Summary

Climate and climate change affect plant species worldwide. This PhD dissertation aims to understand how climatic variation and species traits affect the growth of a wide range of 28 conifer specie. I studied the stem growth of conifer species planted in 1960's in a common garden experiment in the Netherlands and assessed growth sensitivity to climate variation and especially drought resilience, and its two underlying components, i.e., drought resistance (reduction in stem growth during a dry year) and drought recovery (a measure of achieving pre-drought growth rate). To identify possible mechanisms that can explain species differences in growth, I also measured 43 plant traits that are important for carbon, water, and nutrient use.

In **chapter 2**, a dendrochronological approach was used to assess the growth sensitivity of 19 conifer species to climatic variation. The growth of conifers was most negatively affected by summer drought (significantly for 89% of species), followed by spring frost (37%) and winter cold (32%). This implies that conifer species will lose productivity in a warmer and drier future climate during the growing season.

In **chapter 3**, I related drought resilience in stem growth to multiple dimensions of drought (timing, duration and severity), and addressed the possible underlying hydraulic mechanisms. Droughts led to 22% reduction in stem growth for 90% of species, but most species (80%) were resilient due to high recovery. Drought resistance decreased when droughts occurred early (significant for 65% of species), lasted longer (60%) or were more intense (55%). Surprisingly, hydraulic traits could not explain drought resilience of conifer species, perhaps because species avoid drought through other traits such as deep roots, leaf shedding or early leaf and cambial activity before summer drought. This chapter highlights the importance of addressing multiple dimensions of drought, i.e., timing, duration and severity to predict species responses to climate change.

The variation in growth and drought resistance might be determined by tracheids and pits since they could affect hydraulic safety and efficiency. In **chapter 4**, I assessed 1) the mechanisms underlying cavitation resistance and hydraulic conductivity, and 2) the phylogenetic signal of pits and tracheids across 28 conifer species. High cavitation resistance was determined by small pit size and strong pit sealing, which restrict air seeding, and are under strong phylogenetic control, whereas all hydraulic conductivity and tracheid traits were under weak phylogenetic control. Surprisingly, none of tracheid and pit traits could predict hydraulic conductivity, probably because species varied relatively little in hydraulic conductivity. Hydraulic conductivity only decreased with the cell wall thickness, probably due to the increased flow resistance between adjacent tracheids or reduced lumen area. In sum,

conifer species differ largely in cavitation resistance, the underlying traits, and hydraulic conductivity. They may therefore differ strongly in their climatic distribution and drought responses to climate change.

Relatively few studies have assessed how a comprehensive suite of traits affects the growth and drought resilience of conifer species. In **chapter 5**, I measured 43 functional traits for 28 conifer species and assessed how multiple leaf and stem traits were associated, and how these traits affected stem growth and drought resilience. Two trait spectra were found, reflecting a trade-off between hydraulic- and biomechanical safety versus hydraulic efficiency, and a trade-off between tough, long-lived tissues versus high carbon assimilation rate. Stem growth rate only increased with hydraulic efficiency (i.e., pit aperture and tracheid diameter), and drought resilience decreased with leaf lifespan. A longer leaf lifespan reduces drought recovery and resilience because of a reduced ability to replace drought-damaged tissues and track new climatic conditions with new, acclimated leaves. These insights may improve growth- and carbon cycling-related models and predict how trees respond to a drier future.

In sum, this thesis shows that 1) most conifer species have low resistance to early, prolonged and intense droughts, but they have a high recovery and are, therefore, highly resilient to drought; 2) small pit size and strong pit sealing capacity facilitate cavitation resistance, whereas none of the anatomical traits (except wall thickness) can explain hydraulic conductivity; 3) stem growth rate only increased with hydraulic efficiency (i.e., pit aperture diameter) and 4) drought resilience decreased with leaf lifespan rather than hydraulic traits. Conifer tree species can adopt multiple strategies of water or carbon use, which allows them to grow fast or be highly resilient to climatic variation.

Acknowledgements

Acknowledgments

“When life gives you lemons, make lemonade.’’ I have mastered making lemonade with the lemons with the help from people I have met during my academic journey.

My PhD journey started at the moment in 2017 when I contacted my promotor, Lourens Poorter. Wageningen University has been my dream university for ecology study since 2010, and I read many enlightening scientific papers written by Lourens, which encouraged me to pursue my PhD with him. Lourens, I felt very honored and excited when you replied to my email about writing a proposal. The following four years have proved that I made a good choice to do science with you. You are so patient and warm-hearted with me both in science and life. Being my scientific mentor, you always lead me in the right direction when I am lost in a difficult situation, and you are always helping me or recommending someone that I could turn to help. You are also the one who encourages me to talk with other people and expand my network. Lourens, you are for sure more than 100% a good supervisor! For research, you have taught me how to think and write logically and succinctly, and I will keep the things I have learned from you in my whole life. You are more than my scientific mentor to support my research, and you also set a good example to balance life and work. When I started my first year, you encouraged me to have holidays and enjoy the beautiful scenery in Europe, a combination of surprise and happiness, since I was not encouraged to have holidays in the former education systems. The funny thing is that my working efficiency highly depends on your timing of holidays. I can work more efficiently before your holidays and have my holidays when you have holidays, enabling me to work efficiently and live happily. You are also caring for others. I am grateful for inviting me for nice dinners when I wrote my thesis, which released my pressure and brought me lots of fun with you, Marielos, Franka and Sunny.

Similarly, I appreciate what you have done with my PhD project to my other promoter, Frank Sterck. You are the cool supervisor who likes to lock the door frequently, and I always try to find you according to the sound of the door. Although you were busy, you also very kindly helped me when I knocked on your door to ask questions for several minutes. You helped me contact people for hydraulic and photosynthetic measurements, enabling my project to go well. Frank, many thanks for giving nice comments and encouragement, helping me overcome difficulties, constructing scientific stories, and organizing a nice trip in Amsterdam. Frank and Lourens, you two showed me the importance of a good supervision team, which helps me to strengthen the base for my academic career and do science happily and efficiently. Words are powerless to express my gratitude. I will never forget what you have done.

Ute, many thanks for your help! You led me to the dendrochronological world and I learned a lot in the *Dendro* lab. You are more than the best welcome teacher in WUR, and also a superwoman full of energy. The *Dendro* lab also reminds me of all the wonderful

moments with Linar, Ellen and Leo. Linar, you are a cool Russian guy who can drink a lot of Vodka and a warm-hearted guy in the office who helps me a lot. Ellen, thank you for all your help in Dendro Lab. Leo, thank you so much for helping me in the field! Without your help, I could not finish my PhD. Leo, thank you for organizing all tour trips in botanical gardens, and the dinner with you and Paula.

In France I did part of my lab work, I thank Sylvain Delzon, Gaëlle Capdeville, Anne-Isabelle Gravel and Regis Burlett. Sylvain. You are so kind to host me and help me with making the beautiful curves. Gaëlle and Anne-Isabelle, you two helped me a lot with my measurements. I also thank a lot for the people who helped me a lot during my lab work and fieldwork: Aneglina, Chenxuan, Dainius, Jing, Lisa, Matteo, Manuel, Na, Qi, Shenglai, Tianjing, Weixuan, Xiaohan, Xiaqu, Yanjie, Zulin, Zexin, thanks to all of you!

Back to my "Femily" Group, these four years are precious and pleasant memory for me. For the people in Forest Ecology and Forest Management Group, I am grateful to all of you. Many thanks to the staff members (Douglas, Ellen, Frans, Frank, Francisca, Frits, Gert-Jan, Jan, Jente, Joke, Koen, Leo, Lourens, Maaike, Madelon, Marielos, Masha, Paul, Peter, Pieter and Ute). Douglas, Frans and Frits, thank you for creating a good working environment to balance life and work. Gert-Jan, Koen, Paul and Jan, thank you for your comments on my presentations or chapters. Jente, thank you for organizing Thursday Drinks. Joke, thank you for helping me a lot with all administrative issues. Madelon, thank you for inviting me for dinner at your big house in the forest. Pieter, thank you for organizing Journal Club. Maaike, thank you for sharing homemade brownie cakes during the coffee break. Masha, many thanks for helping me with statistical analysis and all the nice talks about science. Marielos, thank you for inviting me to assist in your course, during which I developed my communication skills, helped students, and learned to be an enthusiastic teacher from you. Marielos, I am also grateful for all your encouragement when I feel nervous and for organizing international dinners or some personal invitations in your place.

Thank you all PhD's (Alan, Alejandra, Ambra, Bárbara, Bo, Carolina B., Carolina L., Etienne, Federico, Heitor, Jazz, Johan, Jose, Juan Ignacio, Kathelyn, Linar, Lan, Laura, Louis, Marlene, Marco, Mart, Meike, Nicola, Pauline, Qi, Rens, Rodrigo, Shanshan, Sophie, Surya, Sylvana, Tomonari, Ursula, and Xiaohan), postdocs and visiting scholars (Aldicir, Andreia, Carlos, Catarina, Daisy, Danaë, Danju, Feng Xue, Martijn, Nathalia, Rafael, Richard, Teresa, Yajun and Zexin) in FEM. Qi and Shanshan, I greatly appreciate studying in the same group and having the same supervisors. Qi, Jingjing and Jiajia, thank you so much for the unlimited times of invitation for dinner, and I always enjoyed a lot the amazing food. Shanshan, I am grateful for your patience, kindness, and generosity. You are my best Chinese friend and colleague who cares a lot for other people and tries to make everyone comfortable, and I feel so lucky to have met you. My office mates (Alan, Marlene, Linar and Etienne), thank you for the jokes, humor, and also some complaints with the project. Alejandra, Meike and Sophie, thank you

for all the nice talks and laughter in our corridor. Bo, thank you for sharing the Chinese tea with me, which has released my homesickness. Rodrigo, thank you for helping me during my fieldwork and sharing Chinese food and Mexico tacos. José, thank you for helping me with statistical analysis and inviting me to big parties in your apartment. Linar (and Diana), Jazz, Federico, Xiaohan and Lan, thank you for having all the nice dinners with you. Ursula, thank you for sharing so much gossips and dinner with me. Laura, thank you for helping me a lot. You are always warm-hearted, kindness and willing to care for everybody, and you tell me to be relaxed and make my own choice when I meet difficulties.

I also thank all people I met in the Netherlands. Anna, Bart Kruijt, Bin Tuo, Biyao, Caifang, Changjun, Chengcheng, Chenhui, Chunfeng, Darrel, Erlinda, Frank L., Fred, Hongyu, Hua Li, Hui Jin, Ignas, Liting, Jiyao, Jin Wang, Judith, Keli, Kevin, Lei Deng, Ke Chen, Li Kang, Markus, Mengting, Mengying, Min Cai, Min Xu, Mingshan, Nana, Panpan, Patrick, Qinghua, Qi Zheng, Ronny, Selinrosja, Shenglai, Xiangyu, Xiaomei, Weixuan, Yale, Yanjie, Yingying, Ying Zhou, Zhe Zeng, and Zulin, thank you for meeting all of you and having lots of fun! *Nana*, thank you for your companion. I cherish every moment with you and you give me so many nice suggestions when I feel frustrated during my life. *Yanjie*, thank you for calming me down when I am nervous and you are the one who sets a very good example to work efficiently, live happily and keep curiosity for life. *Lei Deng*, thank you for your nice cooking and having a nice coffee time with you. *Min Cai*, thank you so much for giving comments on my thesis cover.

Thank you all PE&RC staff for providing scientific training. I especially thank Claudius van de Vijver, Lennart Suselbeek and Inka Bentum for organizing many creative training courses. Many thanks to Chinese government scholarships for financial support, providing me a chance to live and study in Wageningen and presume my Scientific career. I am grateful to Jop Klein and Els Ginkel for allowing me to do my research at Schovemhorst estate. Many thanks to Stichting Fonds of Schovemhorst, Stichting Fonds of Wageningen University and KNAW Fonds Ecologie for financial support on my PhD project.

I thank my friends in China, Rong, Bingshuang, Rentao, Yu, Yaqi and Shumin; you comforted me a lot when I felt homesick. Enrong Yan, Kailiang, Jiguang, Fuzheng, Ziyan, Mengmeng, Guiyao, thank you for discussing future careers and suggestions on making some nice figures. Jiguang, being my classmate since 2010, you have helped me a lot by advising on making some beautiful figures and checking the layout for my thesis. Finally, I am very grateful to my mom Guangzhen for unconditional love and support, who has supported me all my life and gives all her love to me. You are the person who makes what I am today. Mom, I love you so much!妈妈，永远爱您！

The PhD journey is full of companion, encouragement, gratitude, happiness, jokes, laughter, learning, love, sharing, support, and understanding.

Short Biography

Yanjun Song was born in November 13th, 1991 in Hubei, China. From 2010 to 2014, she studied Forestry (BSc) at Department of Forestry, Northwest A & F University (Shanxi Province, China). In 2014 she continued her education (MSc) at School of Ecological and Environmental Science, East China Normal University (Shanghai, China). In East China Normal University Enrong Yan guided her to the world of functional traits, and she was fascinated by the ecological world of traits and plant physiology. For her master thesis, she worked on the spectrum of plant form and function in two forest communities in Zhejiang Province of Eastern China. She finished her master's in 2017 and immediately continued her PhD research project with Lourens Poorter and Frank Sterck at Forest Ecology and Forest Management Group, Wageningen University and Research (Wageningen, the Netherlands). She carried out her PhD project to explore the difference of conifer species in functional traits, growth, and drought resilience. Her work offers novel insights for explaining the mechanisms of drought impacts on the growth and drought resilience of conifer species.

Publications

Published:

Y Song, F Sterck, U Sass-Klaassen, L Goudzwaard, L Akhmetzyanov, L Poorter (2021). Growth of 19 conifer species is highly sensitive to winter warming, spring frost and summer drought, *Annals of Botany*, 128(5): 545-557, https://doi.org/10.1093/aob/mcab090

Y Song, L Poorter, A Horsting, S Delzon, F Sterck (2021). Pit and tracheid anatomy explain hydraulic safety but not hydraulic efficiency of 28 conifer species. *Journal of Experimental Botany*, https://doi.org/10.1093/jxb/erab449

In advanced stage or submitted:

Y Song, F Sterck, U Sass-Klaassen, C Li, L Poorter (submitted). Drought resilience of conifer species decreases with early, prolonged and intense droughts and cannot be explained by hydraulic traits.

Y Song, F Sterck, X Zhou, C Li, Q Liu, B Kruijt, L Poorter (submitted). Drought resilience of conifer species is driven by leaf lifespan and not by hydraulic traits.

PE&RC Training and Education Statement

With the training and education activities listed below the PhD candidate has complied with the requirements set by the C.T. de Wit Graduate School for Production Ecology and Resource Conservation (PE&RC) which comprises of a minimum total of 32 ECTS (= 22 weeks of activities)

Review of literature (4.5 ECTS)

- How do functional traits affect the distribution of conifer tree species

Writing of project proposal (4.5 ECTS)

- Explaining conifer tree species distribution from underlying mechanisms

Post-graduate courses (9.3 ECTS)

- Structural equation modelling; WUR (2018)
- Wood anatomy & tree-ring ecology; Swiss Federal Institute for Forest, Snow and Landscape Research (WSL) (2019)
- Generalized linear models; WUR (2019)
- Mixed linear models; WUR (2019)
- Introduction to data science with R and R studio; WUR (2019)
- Forest management across Europe; WUR (2021)
- Swiss climate summer school; ETH Zurich (2021)

Laboratory training and working visits (4.2 ECTS)

- The measurements of cavitation resistance for conifer species; UMR BIOGECO, University of Bordeaux (2018)

Deficiency, refresh, brush-up courses (6 ECTS)

- Forest ecology and management; WUR (2018)

Competence strengthening / skills courses (2.1 ECTS)

- Scientific writing; WUR (2018)
- Career assessment; WUR (2021)

PE&RC Annual meetings, seminars and the PE&RC weekend (2.4 ECTS)

- PE&RC First year weekend (2017)
- Symposium root zone phenomics, physiology and ecology: creating space for the better half (2018)
- Symposium drought, plant hydraulic traits and vegetation modelling (2018)
- PE&RC Midterm year weekend (2019)
- PE&RC Day (2019)

Discussion groups / local seminars or scientific meetings (6.4 ECTS)

- Journal club; FEM (2017-2019)
- Seminar seed functional traits: from periphery to pinnacle; WUR (2018)
- Seminar responding to restoration challenges; WUR (2018)
- Symposium drought, plant hydraulic traits and vegetation modelling; WUR (2018)
- The strength of simplicity and the challenge of complexity: traits, trade-offs and scaling in an era of multiple global changes; WUR (2020)
- SKiPR meeting: studying photosynthesis of ecosystems through stable isotopes of carbon dioxide; WUR (2020)
- R Club; FEM (2020)
- International tree mortality network seminar series; WUR (2021)
- TRACE; online (2021)

International symposia, workshops and conferences (6.3 ECTS)

- Netherlands annual ecology meeting; Lunteren, the Netherlands (2018, 2019)
- Ecology Society of America (ESA); online (2020)
- Netherlands annual ecology meeting; online (2020)

Lecturing / supervision of practicals / tutorials (1.5 ECTS)

- Resource dynamics and sustainable utilization (2019-2021)
- Forest ecology and forest management (2020)

BSc / MSc thesis supervision (8 ECTS)

- Climate-growth relationships of six non-native conifer species from a common garden experiment in the Netherlands
- Physiology of conifer species is associated with pit pore anatomy but not with temperature and drought in their original distribution
- Functional trait spectra and correlations of 28 conifer species
- Productivity of ten non-native coniferous species at Schovenhorst Estate
- Internship

The research described in this thesis was financially supported by China Scholarship Council (CSC, No. 201706140106), KNAW Fonds Ecology under Grant number KNAWWF/87/19033, Oudemans Foundation from Landgoed Schovenhorst, and LEB fonds (2018-051C Song) from Wageningen University & Research.

Financial support from Wageningen University for printing this thesis is gratefully acknowledged.

Cover design:

Yanjun Song

Photography:

Yanjun Song

Printed:

ProefschriftMaken